Toward intracellular membrane Transport-Characterization of the Mitochondrial Carrier Family in Plants

Inaugural-Dissertation

zur Erlangung des Doktorgrades
der Mathematisch-Naturwissenschaftlichen Fakultät
der Heinrich-Heine-Universität Düsseldorf

vorgelegt von

Sarah Katharina Keßel-Vigelius

aus Düsseldorf

Düsseldorf, Oktober 2013

aus dem Institut für Biochemie der Pflanzen
der Heinrich-Heine-Universität Düsseldorf

Gedruckt mit der Genehmigung der
Mathematisch-Naturwissenschaftlichen Fakultät der
Heinrich-Heine-Universität Düsseldorf

Referent: Prof. Dr. A. P. M. Weber
Korreferent: Prof. Dr. Michael Feldbrügge

Tag der mündlichen Prüfung: 12.12.2013

Erklärung

Ich versichere an Eides Statt, dass ich die vorliegende Dissertation eigenständig und ohne unerlaubte Hilfe unter Beachtung der „Grundsätze zur Sicherung guter wissenschaftlicher Praxis“ an der Heinrich-Heine-Universität Düsseldorf angefertigt habe. Die Dissertation habe ich in der dieser oder in ähnlicher Form noch bei keiner anderen Institution eingereicht. Ich habe bisher keine erfolglosen Promotionsversuche unternommen.

Düsseldorf, den 28.10.2013

_____

Sarah K. Keßel-Vigelius

"On ne voit bien qu'avec le cœur.
L'essentiel est invisible pour les yeux."

Antoine de Saint-Exupéry

Meiner Familie
und all den anderen großartigen Menschen,
die mich bisher begleitet haben

CONTENTS

ABBREVIATIONS

AAC	Mitochondrial ATP/ADP carrier
ADP	Adenosine diphosphate
AMP	Adenosine monophosphate
ANT1	*Saccharomyces cerevisiae* peroxisomal ATP carrier
ATP	Adenosine triphosphate
ATPase	Adenosine triphosphatase
DIC	Dicarboxylate carrier
ER	Endoplasmic Reticulum
EYFP	Enhanced Yellow Fluorescent Protein
GFP	Green fluorescent protein
GUS	β-Glucuronidase
His-tag	Polyhistidine tag
HMM	Hidden-Markov model
i.e.	*id est*
Liposome	Artificial lipid vesicle
MC	Mitochondrial carrier
MCF	Mitochondrial carrier family
pH_{cyt},	Cytoplasmic pH
pHGFP	Modified ratiometric pHluorin, cytoplasmic
pHGFP-SKL	Peroxisomal targeted pHGFP sensor
pHluorin	pH sensitive GFP derivative
pH_{per}	Peroxisomal pH
PHT	Phosphate transporter (also termed MPT or PiC)
Pi	Inorganic phosphate
PNC	Peroxisomal adenine nucleotide carrier
PTS	Peroxisomal targeting signal
PXN	Peroxisomal NAD(H)/CoA carrier
$R_{405/488}$	Emission ratio at 405/488 nm
SDS	Sodium dodecyl sulfate
SDS-PAGE	SDS polyacrylamide gel electrophoresis
SIT	Inorganic sulfate transporter
SKL	Canonical peroxisomal targeting signal 1
TCA cycle	Tricarboxylic acid cycle
WGD	Whole-genome duplication
Δ*mir*Δ*pic*	Yeast mutated in the genes *MIR1* and *PIC2*

I. PREFACE

This thesis was divided into independent sections, written as manuscripts. *Manuscript 1* presents a screen to simultaneously scan 20 plant proteomes for uncharacterized Mitochondrial Carrier Family (MCF) members. *Manuscript 2* describes a detailed investigation of an inorganic sulfate transporter 1 (SIT1). *Manuscript 3* depicts a detailed biochemical and phenotypic analysis of the peroxisomal adenine nucleotide carriers 1 and 2 with respect to the connection of transport activity and intraperoxisomal pH. All manuscripts are presented as submission-ready versions. The *Addendum* of this thesis contains a study on the putative presence of peroxisomal ATPases sustaining a proton gradient across the membrane (VI.1), which was conducted as follow-up study on *Manuscript 3.* Secondly, an experiment is presented that examines the morphology of peroxisomes in *pnc1/2* mutants (VI.2). An individual outlook section follows every manuscript. Unit VII concludes *Manuscripts 1-3* and VI.1. Unit VIII contains two published reviews. *Manuscript 4* deals with the impact of plant peroxisomes on biotechnological applications and was published as Kessel-Vigelius et al., 2013, Plant Sci 210, 232-240. A technical review (*Manuscript 5*), describing Agrobacterium-mediated Arabidopsis transformation (Bernhardt et al., 2012, J Endocytobiosis Cell Res 22, 19-28) is presented.

II.1 SUMMARY

Pathways of plant metabolism are interconnected, which necessitates a broad repertoire of transport proteins, enabling the flux of energy, metabolic precursors, or end products across compartments (Lunn, 2007). A large family of metabolite transporters in plants is the mitochondrial carrier family (MCF) (Picault et al., 2004). MCF carriers are present in various organelles of the plant cell, including mitochondria, plastids, and peroxisomes (Haferkamp, 2007). They exhibit different substrate specificities, exchanging adenine nucleotides, amino acids, dicarboxylic acids, cofactors, phosphate and other metabolites across membranes. In Arabidopsis 58 MCF carriers are known, but only a quarter of them are characterized (Palmieri et al., 2011).

Mitochondrial carrier family proteins share a common threefold repetitive structure of 96 amino acids and a characteristic sequence motif, called mitochondrial energy signature (Picault et al., 2004). This repetitive sequence was used to simultaneously screen 20 plant proteomes for uncharacterized MCF carriers. Identified carriers were grouped into orthologous clusters according to their biochemical transport functions (*Manuscript 1*). In this screen we unexpectedly observed that the PHT3 family of mitochondrial phosphate transporters was split into two orthologous groups, although previous studies regarded the MCF carriers as one family of homologs (Picault et al., 2004). One orthologous group comprised PHT3;1 and PHT3;2, whereas the second group contained PHT3;3 (At2g17270). Since PHT3;3 was separated from the other PHT3 proteins, we hypothesized that this carriers displays a different function. Grouping exclusively with land plants and not with any algal, fungal or animal species, we hypothesized that PHT3;3 might have a function specific for plants.

The biochemical characterization of this carrier revealed a role of PHT3;3 in mitochondrial sulfate import (*Manuscript 2*). Hence, the carrier was termed inorganic sulfate transporter 1 (SIT1). Analyses of *sit1* T-DNA mutants revealed impairments in plant growth and development. Hence, an involvement of SIT1 in plant energy metabolism was hypothesized. We proposed that SIT1 and mitochondrial dicarboxylate carriers (DIC) might act in concert, shuttling dicarboxylic acids in exchange for sulfate. When SIT1 is absent, DIC carriers might import dicarboxylic acids and export phosphate instead of sulfate. Increased phosphate export could in turn cause decreased levels of mitochondrial ATP synthesis. Such an energy deprivation might lead to growth defects throughout all developmental stages as observed in *sit1* plants. However, the putative interplay of SIT1 and DIC carriers needs to be investigated in the future.

Regulation of cellular pH and establishment of proton gradients across membranes is crucial for plant metabolism and solute transport (Gjetting et al., 2012). We assessed the peroxisomal pH in different tissues, expressing a pH-sensitive green fluorescent protein in Arabidopsis peroxisomes. Measurements of the pH in these organelles revealed an acidic pH in etiolated shoot peroxisomes, whereas the matrix of root peroxisomes was alkaline (*Manuscript 3*). The results implied a functional

differentiation of peroxisomes in roots and in etiolated hypocotyl cells (Hayashi and Nishimura, 2003). In Arabidopsis, peroxisomes of hypocotyls are mainly involved in fatty acid β-oxidation. To elucidate if the cause for a peroxisomal acidification is linked to peroxisomal metabolism in this tissue, we examined the pH of hypocotyl peroxisomes in an Arabidopsis mutant deficient ATP import. Peroxisomal ATP supply is essential for fatty acid degradation and is mediated by the peroxisomal adenine nucleotide carriers 1 and 2 (PNC1, PNC2) (Linka et al., 2008). We hypothesized that either ATP import into peroxisomes is proton-compensated acidifying the peroxisomal lumen, or that β-oxidation and glyoxylate cycle influence the peroxisomal pH, as these metabolic processes release acids. Experiments demonstrated that the peroxisomal pH is not affected by β-oxidation and glyoxylate cycle, as lumenal pH of hypocotyl peroxisomes was not altered in mutants lacking PNC1 and PNC2. Additional studies were conducted to elucidate if peroxisomal proton pumps exist, which might control peroxisomal pH homeostasis and cause an acidification of the peroxisomal lumen (*Addendum*, VII.1). Preliminary experiments revealed that in the presence of the specific P-type ATPase inhibitor *ortho*-vanadate (Dröse and Altendorf, 1997), the acidic peroxisomal pH of hypocotyls almost reached wild-type level (pH 7.2). Further experiments are necessary to clearly determine if P-type ATPases regulate the pH of peroxisomes.

This thesis contributed to expand the knowledge of mitochondrial carrier family proteins in peroxisomes and mitochondria of plants, (i) developing a method to simultaneously identify MCF carriers in multiple plant proteomes, (ii) characterizing the mitochondrial sulfate transporter SIT1, (iii) analyzing the impact of the MCF members PNC1 and PNC2 involved in β-oxidation on peroxisomal pH, and (iv) elucidating the putative role of ATPases in peroxisomal pH maintenance.

References

Dröse, S., and Altendorf, K. (1997). Bafilomycins and concanamycins as inhibitors of V-ATPases and P-ATPases. J Exp Biol **200,** 1-8.

Gjetting, K.S.K., Ytting, C.K., Schulz, A., and Fuglsang, A.T. (2012). Live imaging of intra- and extracellular pH in plants using pHusion, a novel genetically encoded biosensor. J Exp Bot **63,** 3207-3218.

Haferkamp, I. (2007). The diverse members of the mitochondrial carrier family in plants. FEBS Lett **581,** 2375-2379.

Hayashi, M., and Nishimura, M. (2003). Entering a new era of research on plant peroxisomes. Curr Opin Plant Biol **6,** 577-582.

Linka, N., Theodoulou, F.L., Haslam, R.P., Linka, M., Napier, J.A., Neuhaus, H.E., and Weber, A.P.M. (2008). Peroxisomal ATP import is essential for seedling development in *Arabidopsis thaliana*. Plant Cell **20,** 3241-3257.

Lunn, J.E. (2007). Compartmentation in plant metabolism. J Exp Bot **58,** 35-47.

Palmieri, F., Pierri, C.L., De Grassi, A., Nunes-Nesi, A., and Fernie, A.R. (2011). Evolution, structure and function of mitochondrial carriers: a review with new insights. Plant J **66,** 161-181.

Picault, N., Hodges, M., Palmieri, L., and Palmieri, F. (2004). The growing family of mitochondrial carriers in Arabidopsis. Trends Plant Sci **9,** 138-146.

II.2 ZUSAMMENFASSUNG

Die Stoffwechselwege des pflanzlichen Metabolismus sind eng miteinander verbunden und über verschiedene Zellkompartimente verteilt. Dies erfordert ein großes Repertoire an Transportproteinen, die über Kompartimentgrenzen den Fluss von Energie, metabolischen Vorstufen, oder Endprodukten ermöglichen (Lunn, 2007). Eine bedeutende Familie pflanzlicher Transportproteine ist die MCF (mitochondrial carrier family) (Picault et al., 2004). Transporter dieser Klasse kommen in verschiedenen Pflanzenorganellen, wie Mitochondrien, Plastiden und Peroxisomen vor und verfügen über ein breites Substratspektrum. Sie transportieren Adeninnukleotide, Aminosäuren, Dikarbonsäuren, Phosphat oder andere Metabolite über Membranen. Das Genom von *Arabidopsis thaliana* kodiert 58 MCF Proteine, von denen aktuell lediglich ein Viertel charakterisiert ist (Palmieri et al., 2011).

Alle MCF-Transporter weisen eine dreifach repetitive Struktur, sowie ein charakteristisches Sequenzmotiv auf, welches als mitochondriale Energiesignatur bezeichnet wird (Picault et al., 2004). Diese repetitive Struktur wurde nachfolgend verwendet, um MCF-Mitglieder in 20 verschiedenen Pflanzenproteomen zu identifizieren. Die gefundenen Proteine wurden anhand ihrer biochemischen Transportfunktion in Orthologengruppen unterteilt (*Manuskript 1*). Anders als aus vorhergehenden Analysen zu erwarten war (Picault et al., 2004), divergierte die Familie mitochondrialer Phosphattransporter in zwei Orthologengruppen. Eine dieser Gruppen umfasste PHT3;1 und PHT3;2, die andere Gruppe enthielt PHT3;3. Es wurde postuliert, dass dieses Protein eine andere Transportfunktion aufweist, da es eine separate Gruppe bildete. Zudem wurde gezeigt, dass die Orthologengruppe mit PHT3;3 nur Sequenzen enthielt, die Landpflanzen zuzuordnen waren. Algen-, Pilz-, oder tierische Sequenzen wurden hingegen nicht gefunden. Daraufhin wurde angenommen, dass PHT3;3 eine pflanzenspezifische Funktion erfüllt.

Biochemische Untersuchungen von PHT3;3 zeigten, dass dieses Protein den Import von Sulfat in Mitochondrien bewerkstelligt (*Manuskript 2*). Folglich wurde PHT3;3 in SIT1 (inorganic sulfate transporter 1) umbenannt. Des Weiteren wurde die physiologische Rolle von SIT1 anhand von Arabidopsis Knockout-Pflanzen untersucht. Da diese Pflanzen stark in ihrer Entwicklung und ihrem Wachstum beeinträchtigt waren, wurde vermutet dass SIT1 und die mitochondrialen Dikarbonsäuretransporter (DIC) möglicherweise gekoppelt agieren, um Dikarbonsäuren im Austausch gegen Sulfat ins Mitochondrium zu importieren. Pflanzen, die SIT1 nicht exprimieren, tauschen möglicherweise mitochondriales Phosphat gegen Dikarbonsäuren aus. Dies könnte in Konsequenz zu einer geringeren ATP-Synthese in Mitochondrien führen, da weniger Phosphat zur Verfügung steht um Energie zu generieren. Solch eine Energieverarmung könnte die Wachstumsphänotypen bedingen, die in *sit1* Mutanten beobachtet wurden. Das mögliche Zusammenspiel von SIT1 und DIC wird zukünftig detaillierter untersucht werden.

Der Aufbau von Protonengradienten an Membranen und die Regulation des zellulären pH ist von entscheidender Bedeutung für den pflanzlichen Stoffwechsel und Metabolittransport (Gjetting et al., 2012). In dieser Arbeit wurde der peroxisomale pH anhand eines pH-sensitiven grün fluoreszierenden Proteins untersucht, welches in Peroxisomen unterschiedlicher Arabidopsisgewebe exprimiert wurde. Messungen zeigten, dass der pH in etioliertem Sprossgewebe sauer ist, während hingegen der pH in Wurzelperoxisomen alkalisch ist (*Manuskript 3*). Dieses Ergebnis impliziert eine funktionale Differenzierung von Wurzelperoxisomen und Sprossperoxisomen. Letztere bewerkstelligen hauptsächlich den Abbau von Fettsäuren mittels β-Oxidation und Glyoxylatzyklus (Hayashi and Nishimura, 2003). Um festzustellen, ob der saure pH in fettabbauenden Peroxisomen unmittelbar durch den Metabolismus bedingt wird, haben wir diesen in Hypokotylperoxisomen einer Arabidopsismutante untersucht, die ein defektes peroxisomales ATP-Importsystem aufweist. Die peroxisomale Zufuhr von ATP ist essentiell für den Abbau von Fettsäuren und erfolgt mittels der peroxisomalen Adeninnukleotidtransporter 1 und 2 (PNC1, PNC2) (Linka et al., 2008). Wir nahmen an, dass der Import von ATP entweder protonenkompensiert ist, was zur Ansäuerung des peroxisomalen Lumens führen könnte, oder dass β-Oxidation und der Glyoxylatzyklus selbst zu einer Erniedrigung des pH in Peroxisomen führen, da diese Stoffwechselwege Säuren freisetzen. Untersuchungen zeigten, dass β-Oxidation und Glyoxylatzyklus nicht für die pH Ansäuerung in Peroxisomen verantwortlich sind, da der peroxisomale pH in Arabidopsismutanten, die PNC1 und PNC2 nicht exprimieren, unverändert sauer war. Aufgrund dieser Ergebnisse wurde eine Folgestudie durchgeführt (*Addendum* VII.1). Diese zeigte, dass unter Gabe des spezifischen P-Typ ATPase Inhibitors *ortho*-Vanadat (Dröse and Altendorf, 1997) der pH in Hypokotylperoxisomen auf Wildtyplevel (pH 7.2) anstieg, was impliziert dass Peroxisomen über P-Typ ATPasen verfügen könnten. Ob diese ATPasen den peroxisomalen pH regulieren, wird in zukünftigen Experimenten untersucht werden.

Zusammenfassend hat diese Doktorarbeit dazu beigetragen das Wissen über die MCF Familie in pflanzlichen Mitochondrien und Peroxisomen zu vertiefen, indem (i) eine Methode entwickelt wurde effizient MCF Proteine in multiplen Pflanzenproteomen zu identifizieren. Zudem wurde (ii) der mitochondrialen Sulfattransporter SIT1 charakterisiert, (iii) der Einfluss der MCF Transportproteine PNC1 und PNC2 auf den peroxisomalen pH, sowie (iv) die Rolle von ATPasen in der Regulation des peroxisomalen pHs untersucht.

Referenzen

Dröse, S., and Altendorf, K. (1997). Bafilomycins and concanamycins as inhibitors of V-ATPases and P-ATPases. J Exp Biol **200,** 1-8.

Gjetting, K.S.K., Ytting, C.K., Schulz, A., and Fuglsang, A.T. (2012). Live imaging of intra- and extracellular pH in plants using pHusion, a novel genetically encoded biosensor. J Exp Bot **63,** 3207-3218.

Hayashi, M., and Nishimura, M. (2003). Entering a new era of research on plant peroxisomes. Curr Opin Plant Biol **6,** 577-582.

Linka, N., Theodoulou, F.L., Haslam, R.P., Linka, M., Napier, J.A., Neuhaus, H.E., and Weber, A.P.M. (2008). Peroxisomal ATP import is essential for seedling development in *Arabidopsis thaliana*. Plant Cell **20,** 3241-3257.

Lunn, J.E. (2007). Compartmentation in plant metabolism. J Exp Bot **58,** 35-47.

Palmieri, F., Pierri, C.L., De Grassi, A., Nunes-Nesi, A., and Fernie, A.R. (2011). Evolution, structure and function of mitochondrial carriers: a review with new insights. Plant J **66,** 161-181.

Picault, N., Hodges, M., Palmieri, L., and Palmieri, F. (2004). The growing family of mitochondrial carriers in Arabidopsis. Trends Plant Sci **9,** 138-146.

III. INTRODUCTION

Plant cells are highly compartmentalized

Plant cells evolved a complex metabolic network, which to some extend is unique. In comparison to fungi or animals, plants possess additional highly diversified cell compartments, such as plastids, vacuoles and cell walls. Metabolism is partitioned at a subcellular level, which allows a metabolic and biochemical speciation of the cell. Every such compartment houses a unique set of proteins enabling specific functions. Compartmentation allows metabolic pathways competing for same substrates to be operated and regulated at the same time in a single cell (Tegeder and Weber, 2006; Lunn, 2007).

Mitochondria and peroxisomes are important compartments in plants

Mitochondria are organelles 0.1-0.5 µm in diameter, which are surrounded by two membranes. They play a central role in cellular energy metabolism, synthesizing ATP from ADP by oxidative phosphorylation (Mackenzie and McIntosh, 1999; Logan, 2006). The mitochondrial tricarboxylic acid cycle provides reducing power for the respiratory electron chain, generating a proton motive force across the inner mitochondrial membrane. This proton gradient is coupled to ATP synthesis. In addition, mitochondria are involved in various other metabolic pathways, such as the biosynthesis of vitamin cofactors, nucleotides, amino acids, iron-sulfur clusters or lipids. Mitochondria also participate in carbon and nitrogen storage mobilization during germination (Logan, 2006).

Peroxisomes are small ubiquitous organelles about 1 µm in diameter and are surrounded by a single membrane (Hayashi and Nishimura, 2003). Compared to those of other organisms, peroxisomes of plants have highly specified functions. They play a central role in numerous metabolic and signaling pathways, including β-oxidation, senescence-associated processes, photorespiration, auxin and jasmonic acid biosynthesis, pathogen defense, biosynthesis of biotin and isoprenoids, as well as the metabolism of urate, polyamines, sulfite, or branched amino acids (Hu et al., 2012). Because peroxisomes host one or more reactions of several biosynthetic pathways, they have been attributed ‘organelles at the crossroads’ (Erdmann et al., 1997).

The metabolism of mitochondria and peroxisomes is highly diverse. To entirely understand how these organelles are integrated in plant metabolism, it is crucial to know how mitochondrial and peroxisomal pathways linked to other cell compartments and how this interplay is controlled (Lunn, 2007).

Plant cell compartmentation necessitates metabolite exchange

Multicompartmented pathways are connected by transport proteins, which facilitate a specific flux of solutes across a bilayer membrane, constituting a diffusion barrier for most solutes (Linka and Weber, 2010). Transporters regulate substrate partitioning, thus they sustain the complexity of metabolism (Tegeder and Weber, 2006). Membrane transport occurs in different modes. Channels

are selective pores and catalyze passive diffusion across the membrane. Pumps mediate a primary active transport, as they generate a gradient, such as a proton gradient. Primary active transport is energy consuming and thus is directly coupled to a source of energy, for example ATP hydrolysis (Schumacher, 2006). The free energy of the proton-electrochemical potential drives the transmembrane movement of a diverse range of solutes along this gradient (secondary active transport) (Forrest et al., 2011). Many carrier proteins are able to transport solutes against its concentration gradient and electrochemical potential. In the case of secondary active transport, solute exchange is coupled to protons or co-substrate ions (Barkla and Pantoja, 1996). During transport, carriers undergo a conformational change, exposing their substrate binding sites to the cytosol or to the matrix during catalysis (Jardetzky, 1966; Forrest et al., 2011). The substrate enters the carrier from the cytosolic side and is bound in the central cavity. Upon matrix conformation the carrier releases its substrate to the matrix side and the catalytic cycle continues (Palmieri et al., 2011). In comparison to channel-forming proteins, vectorial transport via carriers is many orders of magnitude slower, but therefore allows for tighter control. Important driving forces for transport across membranes are pH gradients (Rottensteiner and Theodoulou, 2006).

Subcellular pH in plants

The cellular pH is important to coordinate solute transport and biochemical reactions. An optimum of enzymatic functions depends on the maintenance of constant pH in particular cell compartments. Proton concentrations influence ionization of acidic or basic amino acid residues, and thereby affect protein solubility, structure and activity. That is, proton ion concentration influences transport activity (Orij et al., 2009; Gjetting et al., 2012). Proton pumps, such as H^+-Pyrophosphatases (PPases), vacuolar-type H^+-ATPases (V-ATPases) or plasma membrane-type ATPases (P-ATPases) establish proton gradients at cell compartments (Schumacher, 2006). Families of ATPases are distinguished by their transport mechanisms, structures and sensitivity toward specific inhibitors. Unlike their names might suggest, V-ATPases and P-ATPases are not only found at the plasma membrane or vacuole, but are present in the entire endomembrane system, mitochondria and chloroplasts (Dröse and Altendorf, 1997; Baxter et al., 2003; Heazlewood et al., 2004; Schumacher, 2006). Among the three types of proton-pumps known in plants, V-ATPases are most complex (Gaxiola et al., 2007). They are multi-subunit enzymes, consisting of eight subunits involved in ATP hydrolysis and six membrane-bound subunits required for proton translocation. In Arabidopsis, 27 genes encode for V-ATPases (Sze et al., 2002). P-ATPases are the major ion pumps in plants and fungi. The Arabidopsis genome encodes 46 P-ATPases (Baxter et al., 2003). They differ from V-ATPases, as they form a phosphorylated intermediate during catalysis (Axelsen and Palmgren, 2001). Whereas in V-ATPases multiple subunits form the holoenzyme, the functional unit of P-ATPases is monomeric (Sondergaard et al., 2004). All three types of ATPases are active transporters that utilize ATP as energy source to mediate the transport of protons. The established membrane potential

then energizes the transport of solutes against their electrochemical or concentration gradients (Krebs et al., 2010).

Determination of the intracellular pH in Arabidopsis

As knowledge of subcellular pH was limited, different methods have been developed to determine the intracellular pH of Arabidopsis *in vivo*. First studies applied nuclear magnetic resonance spectroscopy (^{31}P-NMR) to estimate the pH of apoplast and cytosol in higher plants. The resonance frequency of the nucleus of inorganic phosphate (Pi) in ^{31}P is strongly dependent on intracellular pH (Guern et al., 1991). Hence, non-invasive pH determination is feasible (Roberts et al., 1980; Nicolay et al., 1987). However, this technique faces major limitations, such as inaccurate pH measurements at acidic and alkaline pH, sensitivity to ionic compositions, and the large amount of material needed for this non-invasive technique impact experiments (Guern et al., 1991). Another method applied to determine local pH values in cells is loading compartments with pH-sensitive indicator dyes, such as BCECF (2′,7′-bis-2-carboxyethyl)-5-(and-6)-carboxyfluorescein) (Scott and Allen, 1999) or Oregon green (Fasano et al., 2001). Excitation at two different wavelengths yields fluorescence ratios, which are with the help of a calibration curve converted to pH values (Guern et al., 1991). As cell compartments are often inaccessible to chemical dyes or loading of the dye causes stress symptoms (Swanson et al., 2011), genetically encoded biosensors, such as pH-sensitive green fluorescent protein (GFP) probes were developed. Native forms of GFP are rather pH-insensitive, as their protein structures prevent the chromophores from an interaction with protons. However, various pH-sensitive sensors were engineered, which led to significant improvements in spatial or temporal resolution of pH measurements when compared to NMR-based studies (Choi et al., 2012). Using these probes, the proton ion concentrations of apoplast, cytosol and few organelles have been monitored in the model plant *Arabidopsis* (Miesenbock et al., 1998; Moseyko and Feldman, 2001; Gao et al., 2004; Shen et al., 2013).

The Mitochondrial Carrier Family

This thesis is focused on the Mitochondrial Carrier Family (MCF) in plants. The MCF is an important transporter class (TC 2.A.29), connecting parallel and interdependent pathways across compartments. Sequencing of plant genomes led to the discovery of various MCF members. These carriers are not only found in viridiplantae, but are highly conserved in a wide range of eukaryotic species. Their name might suggest that MCF members are exclusively located to mitochondria, however several carriers have been found in other organelles, *e.g* plastids, peroxisomes, endoplasmatic reticulum, and the plasma membrane (Bedhomme et al., 2005; Bouvier et al., 2006; Thuswaldner et al., 2007; Leroch et al., 2008; Linka et al., 2008; Rieder and Neuhaus, 2011; Bernhardt et al., 2012).

Substrate spectrum and transport modes of MCF proteins

First biochemical studies of mitochondrial carriers (MC) were conducted in animals, not in plants (Haferkamp, 2007). The MCF exhibits a broad spectrum of transport substrates that are variable in size and structure and are mostly negatively charged. MCFs facilitate a secondary active exchange of protons, nucleotides, carboxylic acids, keto acids, amino acids, and phosphate (Forrest et al., 2011; Palmieri et al., 2011). Most of the carriers are strict antiporters exchanging solutes in a 1:1 stoichiometry. However, few carriers mediate uniport or symport (Kunji, 2004; Bamber et al., 2007). Some carriers, such as ADP/ATP carriers are electrogenic, as their transport results in a net charge transfer (Gropp et al., 1999). Other carriers, for example the rat ornithine/citrulline carrier, facilitate an electroneutral exchange of substrates (Indiveri et al., 1997).

Structural features of MCF carriers

Despite their high diversity in transport substrates, MC proteins share common structural features, characteristic of this carrier class, but different from any other known transporter family. All carriers are nuclear-encoded and are about 30-40 kDa in size (Saraste and Walker, 1982; Aquila et al., 1985). Solving a high-resolution atomic structure of a MCF representative to 2.2 Å (Pebay-Peyroula et al., 2003) revealed a threefold repetitive structure of about 100 amino acids. Each of the three repeats comprises two α-helical transmembrane spans, which are connected by hydrophilic loops (Fig. 1). A conserved sequence motif called mitochondrial energy signature (Pfam-A domain PF00153) is detectable in odd numbered transmembrane spans and loops (Fig. 1). Apart from this motif, the sequences of MCF carriers are poorly conserved. MCF-mediated transport of metabolites is facilitated by salt bridge networks, which constitute the cytosolic and matrix gates and close the central cavity of the protein (Palmieri et al., 2011). MCFs can act as homodimers, or can form helical bundles, which form functional entity within membranes (Bamber et al., 2007; Kunji and Crichton, 2010).

On the evolution of mitochondrial carrier family proteins

The evolution of MCF carriers is not fully understood. It is believed that present-day MCF carriers arose from one ancestral sequence, which was further differentiated during evolution (Arco and Satrustegui, 2005). A basic module, encoding a two-transmembrane spanning protein might have existed that underwent two duplications and was then fused to one protein- the ancestor sequence of all MCFs (Haferkamp and Schmitz-Esser, 2012).

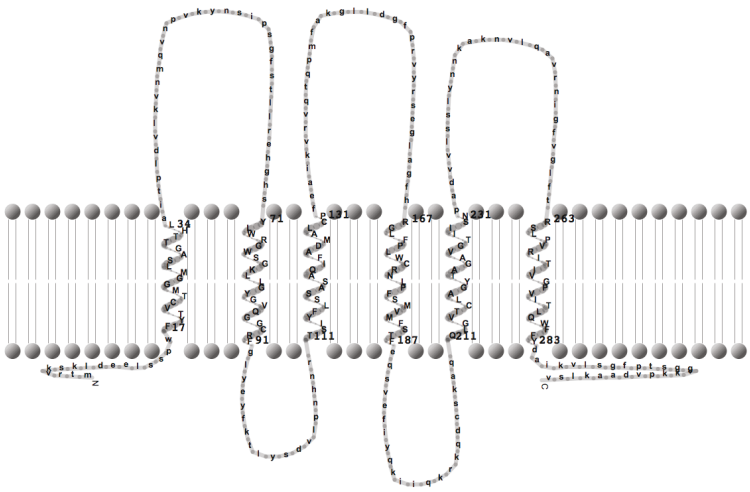

Fig. 1: Structural prediction of a classical *Arabidopsis* MCF transporter At2g17270.
PHT3;3 protein structure was predicted using the consensus sequence of Aramemnon v7.0 (Schwacke et al., 2003). Protein structure was graphically presented with TMRPres2D (Spyropoulos et al., 2004). Transmembrane helices (spiral structures) and transmembrane domain connecting loops (grey lines) are indicated.

Three scenarios, how MCF carriers were established, are possible: (i) MCFs have been introduced by the proteobacterial symbiont, (ii) by the archaebacterial host, or alternatively were (iii) newly invented (Palmieri et al., 2011; Haferkamp and Schmitz-Esser, 2012). Today the common understanding is that MCF carriers evolved when the mitochondrial organelle was established. It is proposed that the prototype MCF carrier was involved in mitochondrial energy transfer, as *e.g.* AAC carriers are. MCFs might have functionally differentiated before the separation of the three eukaryotic kingdoms. Given that, a minimal set of MCFs with different localization, transport properties and substrate specificities, which was the basis for present-day MCFs in eukaryotes, might have already existed in early protists (Haferkamp and Schmitz-Esser, 2012).

Green plants exhibit a high number of MCF carriers. Intra-genome comparisons revealed that the family of mitochondrial carriers was expanded by whole genome duplications and segmental duplications. Some MCF paralogs escaped large-scale gene losses, which often follow polyploidization events (Paterson et al., 2006). Nucleotide carriers are preferentially retained in angiosperms, indicating their transport function is of high importance for angiosperm evolution (Palmieri et al., 2011). This affirms the importance of MCF members, contributing to plant complexity and diversification (Palmieri et al., 2011).

Isolation and characterization of mitochondrial carrier family proteins

In early studies, six proteins were discovered in rat liver mitochondria that were purified and subjected to sequencing. These early studies revealed that the six proteins belonged to the same family, which was named MCF (Indiveri et al., 1992; Palmieri et al., 2011). In the following years, many carriers were identified, which shared the characteristic sequence features of this family. In candidate gene approaches, putative transport functions were predicted from genetic information, phylogenetic clustering and metabolic considerations (Picault et al., 2004; Haferkamp, 2007;

Haferkamp and Schmitz-Esser, 2012). In recent years, structural information on MCF carriers simplified the prediction of transport substrates. When aligning the threefold repeats of MCFs, symmetry-related amino acid triplets were discovered, located at the protein cavity. It was demonstrated that these conserved triplets relate to substrate specificity (Robinson et al., 2008; Palmieri et al., 2011).

The majority of mitochondrial carrier members are not characterized

Although the existence of a many MCF members and their putative substrates has been predicted in eukaryotic model organisms by bioinformatics, only a minor portion of MCs are biochemically characterized. In *Homo sapiens* a third of the MCs are described and about 50% of carriers are investigated in *Saccharomyces cerevisiae*. In *Arabidopsis thaliana* only a quarter of MCFs are functionally characterized (Palmieri et al., 2011; Haferkamp and Schmitz-Esser, 2012). In gene-to-function approaches, candidates were expressed in heterologous systems, reconstituted in lipid vesicles and subjected to *in vitro* transport assays testing various substrates (Picault et al., 2004). An alternative approach widely used is the complementation of auxotrophic phenotypes of yeast mutants (Catoni et al., 2003).

The mitochondrial ADP/ATP carrier- a prototype MCF

In eukaryotic mitochondria, energy in the form of ATP is generated and is sequestered to the cytosol from where it is distributed to other cellular compartments. The export of ATP in exchange for ADP is facilitated by the mitochondrial ADP/ATP carrier (AAC), which is a MCF member. A high membrane potential at the inner mitochondrial membrane controls the adenylate transport (Klingenberg, 2008). First attempts to unravel why mitochondria contain high levels of adenylates were performed with isolated mitochondria. At the same time silicon layer filtration established that the inner membrane of mitochondria constitutes a diffusion barrier. A separation of the $^{3}H_2O$ space and the ^{14}C-sucrose impermeable matrix space was demonstrated (Pfaff et al., 1965). Analyses revealed the existence of AAC, facilitating the export of ATP produced in across the inner mitochondrial membrane. First detailed characterizations of AAC were performed on protein isolated from rat liver mitochondria and bovine heart (Pfaff et al., 1969; Powell et al., 1989; Klingenberg, 2008). Based on sequence homology to the bovine AAC, yeast homologs were identified (Onishi et al., 1967; O'Malley et al., 1982), which were used as a platform to conveniently study structure-function relationships (Klingenberg, 2008). In *Arabidopsis*, three AAC isoforms (AAC1, AAC2, AAC3) are present. They were detected based on sequence homologies to mammalian and yeast AACs (Löytynoja and Milinkovitch, 2001; Haferkamp et al., 2002; Millar and Heazlewood, 2003). Studies revealed that AAC1 expression is high in all tissues, whereas AAC2 expression is only moderate. AAC3 is solely expressed in actively growing tissues. It is assumed that AAC1, due to its high abundance, acts in concert with the mitochondrial phosphate carrier PHT3;1 to regenerate ATP in Arabidopsis (Haferkamp, 2007). PHT3;1 (At5g14040) and its close homologs PHT3;2 (At3g48850) and PHT3;3 (At2g17270) appear to fuel mitochondrial with phosphate. It is assumed

that PHT proteins import phosphate either in a Pi/H^+ symport, a Pi/OH^- antiport mechanism, or as Pi homo-exchange (Liu et al., 2011). However, Arabidopsis PHT3 carriers are not characterized biochemically.

Adenine nucleotide carriers of the plant peroxisomal membrane

ATP, which is generated inside mitochondria, is exported to the cytosol by the mitochondrial ADP/ATP carrier (AAC). From there, ATP it is distributed to other cellular compartments, such as peroxisomes (Linka and Weber, 2010). Peroxisomes are surrounded by a single bilayer membrane and harbor several ATP-dependent reactions (Hu et al., 2012). As these organelles do not contain ATP generating mechanisms, the existence of ATP importing carriers in the peroxisomal membrane is essential. In a candidate gene approach three putative peroxisomal adenine nucleotide carriers of Arabidopsis peroxisomes were identified (At2g39970, At3g905290, At5g27520). These carriers belong to the MCF and share high sequence similarity with the *Saccharomyces cerevisiae* peroxisomal ATP carrier *ANT1*. Whereas At3g905290 and At5g27520 import ATP into peroxisomes (Linka et al., 2008), the third candidate At2g39970 imports NAD and CoA (Agrimi et al., 2012; Bernhardt et al., 2012). According to their functions, the carriers were termed peroxisomal adenine nucleotide carriers 1 and 2 (PNC1, PNC2) and peroxisomal NAD/CoA carrier (PXN). It was demonstrated biochemically that PNC proteins function as ATP transporters. They complement a yeast mutant deficient in the peroxisomal ATP transporter *ANT1*. Recombinant PNC proteins that were reconstituted into liposomes mediate a strict counter-exchange of ATP against ADP or AMP (Linka et al., 2008). The characterization of transgenic Arabidopsis RNA interference lines, which simultaneously suppress PNC1 and PNC2, revealed that these carriers are essential for seedling establishment during the pre-photoautotrophic growth phase. Mutant seedlings arrest early in establishment, which is caused by impaired peroxisomal ATP supply, leading to compromised lipolysis and ß-oxidation (Linka et al., 2008).

References

Agrimi, G., Russo, A., Pierri, C.L., and Palmieri, F. (2012). The peroxisomal NAD+ carrier of *Arabidopsis thaliana* transports coenzyme A and its derivatives. J Bioenerg Biomembranes **44,** 333-340.

Aquila, H., Link, T.A., and Klingenberg, M. (1985). The uncoupling protein from brown fat mitochondria is related to the mitochondrial ADP/ATP carrier. Analysis of sequence homologies and of folding of the protein in the membrane. EMBO J **4,** 2369.

Arco, A.D., and Satrustegui, J. (2005). New mitochondrial carriers: an overview. Cell Mol Life Sci **62,** 2204-2227.

Axelsen, K.B., and Palmgren, M.G. (2001). Inventory of the superfamily of P-type ion pumps in Arabidopsis. Plant Physiol **126,** 696-706.

Bamber, L., Harding, M., Monné, M., Slotboom, D.-J., and Kunji, E.R. (2007). The yeast mitochondrial ADP/ATP carrier functions as a monomer in mitochondrial membranes. Proc Natl Acad Sci U S A **104,** 10830-10834.

Barkla, B.J., and Pantoja, O. (1996). Physiology of ion transport across the tonoplast of higher plants. Annu Rev Plant Biol **47,** 159-184.

Baxter, I., Tchieu, J., Sussman, M.R., Boutry, M., Palmgren, M.G., Gribskov, M., Harper, J.F., and Axelsen, K.B. (2003). Genomic comparison of P-type ATPase ion pumps in Arabidopsis and rice. Plant Physiol **132,** 618-628.

Bedhomme, M., Hoffmann, M., McCarthy, E.A., Gambonnet, B., Moran, R.G., Rébeillé, F., and Ravanel, S. (2005). Folate metabolism in plants - An Arabidopsis homolog of the mammalian mitochondrial folate transporter mediates folate import into chloroplasts. J Biol Chem **280,** 34823-34831.

Bernhardt, K., Wilkinson, S., Weber, A.P.M., and Linka, N. (2012). A peroxisomal carrier delivers NAD($^{+}$) and contributes to optimal fatty acid degradation during storage oil mobilization. Plant J **69,** 1-13.

Bouvier, F., Linka, N., Isner, J.C., Mutterer, J., Weber, A.P., and Camara, B. (2006). Arabidopsis SAMT1 defines a plastid transporter regulating plastid biogenesis and plant development. Plant Cell **18,** 3088-3105.

Catoni, E., Desimone, M., Hilpert, M., Wipf, D., Kunze, R., Schneider, A., Flügge, U.I., Schumacher, K., and Frommer, W.B. (2003). Expression pattern of a nuclear encoded mitochondrial arginine-ornithine translocator gene from Arabidopsis. BMC Plant Biol **3,** 1.

Choi, W.G., Swanson, S.J., and Gilroy, S. (2012). High-resolution imaging of Ca^{2+}, redox status, ROS and pH using GFP biosensors. Plant J **70,** 118-128.

Dröse, S., and Altendorf, K. (1997). Bafilomycins and concanamycins as inhibitors of V-ATPases and P-ATPases. J Exp Biol **200,** 1-8.

Erdmann, R., Veenhuis, M., and Kunau, W.H. (1997). Peroxisomes: Organelles at the crossroads. Trends Cell Biol **7,** 400-407.

Fasano, J.M., Swanson, S.J., Blancaflor, E.B., Dowd, P.E., Kao, T.-h., and Gilroy, S. (2001). Changes in root cap pH are required for the gravity response of the Arabidopsis root. Plant Cell **13,** 907-921.

Forrest, L.R., Krämer, R., and Ziegler, C. (2011). The structural basis of secondary active transport mechanisms. Biochim Biophys Acta **1807,** 167-188.

Gao, D., Knight, M.R., Trewavas, A.J., Sattelmacher, B., and Plieth, C. (2004). Self-reporting Arabidopsis expressing pH and [Ca2+] indicators unveil ion dynamics in the cytoplasm and in the apoplast under abiotic stress. Plant Physiol **134,** 898-908.

Gaxiola, R.A., Palmgren, M.G., and Schumacher, K. (2007). Plant proton pumps. FEBS Lett **581,** 2204-2214.

Gjetting, K.S.K., Ytting, C.K., Schulz, A., and Fuglsang, A.T. (2012). Live imaging of intra- and extracellular pH in plants using pHusion, a novel genetically encoded biosensor. J Exp Bot **63,** 3207-3218.

Gropp, T., Brustovetsky, N., Klingenberg, M., Muller, V., Fendler, K., and Bamberg, E. (1999). Kinetics of electrogenic transport by the ADP/ATP carrier. Biophys J **77,** 714-726.

Guern, J., Felle, H., Mathieu, Y., and Kurkdjian, A. (1991). Regulation of intracellular pH in plant cells. Int Rev Cytol **127,** 1-1.

Haferkamp, I. (2007). The diverse members of the mitochondrial carrier family in plants. FEBS Lett **581,** 2375-2379.

Haferkamp, I., and Schmitz-Esser, S. (2012). The plant mitochondrial carrier family: functional and evolutionary aspects. Frontiers Plant Sci **3,** doi: 10.3389/fpls.2012.00002.

Haferkamp, I., Hackstein, J.H., Voncken, F.G., Schmit, G., and Tjaden, J. (2002). Functional integration of mitochondrial and hydrogenosomal ADP/ATP carriers in the *Escherichia coli* membrane reveals different biochemical characteristics for plants, mammals and anaerobic chytrids. Eur J Biochem **269,** 3172-3181.

Hayashi, M., and Nishimura, M. (2003). Entering a new era of research on plant peroxisomes. Curr Opin Plant Biol **6,** 577-582.

Heazlewood, J.L., Tonti-Filippini, J.S., Gout, A.M., Day, D.A., Whelan, J., and Millar, A.H. (2004). Experimental analysis of the Arabidopsis mitochondrial proteome highlights signaling and regulatory components, provides assessment of targeting prediction programs, and indicates plant-specific mitochondrial proteins. Plant Cell **16,** 241-256.

Hu, J., Baker, A., Bartel, B., Linka, N., Mullen, R.T., Reumann, S., and Zolman, B.K. (2012). Plant peroxisomes: biogenesis and function. Plant Cell **24,** 2279-2303.

Indiveri, C., Tonazzi, A., and Palmieri, F. (1992). Identification and purification of the ornithine/citrulline carrier from rat liver mitochondria. Eur J Biochem **207,** 449-454.

Indiveri, C., Tonazzi, A., Stipani, I., and Palmieri, F. (1997). The purified and reconstituted ornithine/citrulline carrier from rat liver mitochondria: electrical nature and coupling of the exchange reaction with H+ translocation. Biochem J **327,** 349-355.

Jardetzky, O. (1966). Simple allosteric model for membrane pumps. Nature **211,** 969-970.

Klingenberg, M. (2008). The ADP and ATP transport in mitochondria and its carrier. Biochim Biophys Acta **1778,** 1978-2021.

Krebs, M., Beyhl, D., Görlich, E., Al-Rasheid, K.A., Marten, I., Stierhof, Y.-D., Hedrich, R., and Schumacher, K. (2010). Arabidopsis V-ATPase activity at the tonoplast is required for efficient nutrient storage but not for sodium accumulation. Proc Natl Acad Sci U S A **107,** 3251-3256.

Kunji, E.R. (2004). The role and structure of mitochondrial carriers. FEBS Lett **564,** 239-244.

Kunji, E.R., and Crichton, P.G. (2010). Mitochondrial carriers function as monomers. Biochim Biophys Acta **1797,** 817-831.

Leroch, M., Neuhaus, H.E., Kirchberger, S., Zimmermann, S., Melzer, M., Gerhold, J., and Tjaden, J. (2008). Identification of a novel adenine nucleotide transporter in the endoplasmic reticulum of Arabidopsis. Plant Cell **20,** 438-451.

Linka, N., and Weber, A.P. (2010). Intracellular metabolite transporters in plants. Mol Plant **3,** 21-53.

Linka, N., Theodoulou, F.L., Haslam, R.P., Linka, M., Napier, J.A., Neuhaus, H.E., and Weber, A.P.M. (2008). Peroxisomal ATP import is essential for seedling development in *Arabidopsis thaliana*. Plant Cell **20,** 3241-3257.

Liu, F., Chang, X.-J., Ye, Y., Xie, W.-B., Wu, P., and Lian, X.-M. (2011). Comprehensive sequence and whole-life-cycle expression profile analysis of the phosphate transporter gene family in rice. Mol Plant **4,** 1105-1122.

Logan, D.C. (2006). The mitochondrial compartment. J Exp Bot **57,** 1225-1243.

Löytynoja, A., and Milinkovitch, M.C. (2001). Molecular phylogenetic analyses of the mitochondrial ADP-ATP carriers: The Plantae/Fungi/Metazoa trichotomy revisited. Proc Natl Acad Sci U S A **98,** 10202-10207.

Lunn, J.E. (2007). Compartmentation in plant metabolism. J Exp Bot **58,** 35-47.

Mackenzie, S., and McIntosh, L. (1999). Higher plant mitochondria. Plant Cell **11,** 571-586.

Miesenbock, G., De Angelis, D.A., and Rothman, J.E. (1998). Visualizing secretion and synaptic transmission with pH-sensitive green fluorescent proteins. Nature **394,** 192-195.

Millar, A.H., and Heazlewood, J.L. (2003). Genomic and proteomic analysis of mitochondrial carrier proteins in Arabidopsis. Plant Physiol **131,** 443-453.

Moseyko, N., and Feldman, L. (2001). Expression of pH-sensitive green fluorescent protein in *Arabidopsis thaliana*. Plant Cell Environ **24,** 557-563.

Nicolay, K., Veenhuis, M., Douma, A.C., and Harder, W. (1987). A 31P NMR study of the internal pH of yeast peroxisomes. Arch Microbiol **147,** 37-41.

O'Malley, K., Pratt, P., Robertson, J., Lilly, M., and Douglas, M. (1982). Selection of the nuclear gene for the mitochondrial adenine nucleotide translocator by genetic complementation of the op1 mutation in yeast. JBC **257,** 2097-2103.

Onishi, T., Kröger, A., Heldt, H., Pfaff, E., and Klingenberg, M. (1967). The response of the respiratory chain and adenine nucleotide system to oxidative phosphorylation in yeast mitochondria. Eur J Biochem **1,** 301-311.

Orij, R., Postmus, J., Ter Beek, A., Brul, S., and Smits, G.J. (2009). *In vivo* measurement of cytosolic and mitochondrial pH using a pH-sensitive GFP derivative in *Saccharomyces cerevisiae* reveals a relation between intracellular pH and growth. Microbiology **155,** 268-278.

Palmieri, F., Pierri, C.L., De Grassi, A., Nunes-Nesi, A., and Fernie, A.R. (2011). Evolution, structure and function of mitochondrial carriers: a review with new insights. Plant J **66,** 161-181.

Paterson, A.H., Chapman, B.A., Kissinger, J.C., Bowers, J.E., Feltus, F.A., and Estill, J.C. (2006). Many gene and domain families have convergent fates following independent whole-genome duplication events in Arabidopsis, Oryza, Saccharomyces and Tetraodon. Trends Gen **22,** 597-602.

Pebay-Peyroula, E., Dahout-Gonzalez, C., Kahn, R., Trezeguet, V., Lauquin, G.J., and Brandolin, G. (2003). Structure of mitochondrial ADP/ATP carrier in complex with carboxyatractyloside. Nature **426,** 39-44.

Pfaff, E., Klingenberg, M., and Heldt, H. (1965). Unspecific permeation and specific exchange of adenine nucleotides in liver mitochondria. Biochim Biophys Acta **104,** 312.

Pfaff, E., Heldt, H., and Klingenberg, M. (1969). Adenine nucleotide translocation of mitochondria. European J Biochem **10,** 484-493.

Picault, N., Hodges, M., Palmieri, L., and Palmieri, F. (2004). The growing family of mitochondrial carriers in Arabidopsis. Trends Plant Sci **9,** 138-146.

Powell, S.J., Medd, S.M., Runswick, M.J., and Walker, J.E. (1989). Two bovine genes for mitochondrial ADP/ATP translocase expressed differently in various tissues. Biochem **28,** 866-873.

Rieder, B., and Neuhaus, H.E. (2011). Identification of an Arabidopsis plasma membrane-located ATP transporter important for anther development. Plant Cell **23,** 1932-1944.

Roberts, J.K., Ray, P.M., Wade-Jardetzky, N., and Jardetzky, O. (1980). Estimation of cytoplasmic and vacuolar pH in higher plant cells by ^{31}P NMR. Nature **283,** 870-872.

Robinson, A.J., Overy, C., and Kunji, E.R. (2008). The mechanism of transport by mitochondrial carriers based on analysis of symmetry. Proc Natl Acad Sci U S A **105,** 17766-17771.

Rottensteiner, H., and Theodoulou, F.L. (2006). The ins and outs of peroxisomes: co-ordination of membrane transport and peroxisomal metabolism. Biochim Biophys Acta **1763,** 1527-1540.

Saraste, M., and Walker, J.E. (1982). Internal sequence repeats and the path of polypeptide in mitochondrial ADP/ATP translocase. FEBS Lett **144,** 250-254.

Schumacher, K. (2006). Endomembrane proton pumps: connecting membrane and vesicle transport. Curr Opin Plant Biol **9,** 595-600.

Schwacke, R., Schneider, A., van der Graaff, E., Fischer, K., Catoni, E., Desimone, M., Frommer, W.B., Flugge, U.I., and Kunze, R. (2003). ARAMEMNON, a novel database for Arabidopsis integral membrane proteins. Plant Physiol **131,** 16-26.

Scott, A.C., and Allen, N.S. (1999). Changes in cytosolic pH within Arabidopsis root columella cells play a key role in the early signaling pathway for root gravitropism. Plant Physiol **121,** 1291-1298.

Shen, J., Zeng, Y., Zhuang, X., Sun, L., Yao, X., Pimpl, P., and Jiang, L. (2013). Organelle pH in the Arabidopsis endomembrane system. Mol Plant **6,** 1419-1437.

Sondergaard, T.E., Schulz, A., and Palmgren, M.G. (2004). Energization of transport processes in plants. Roles of the plasma membrane H^+-ATPase. Plant Physiol **136,** 2475-2482.

Spyropoulos, I.C., Liakopoulos, T.D., Bagos, P.G., and Hamodrakas, S.J. (2004). TMRPres2D: high quality visual representation of transmembrane protein models. Bioinformatics **20,** 3258-3260.

Swanson, S., Choi, W.G., Chanoca, A., and Gilroy, S. (2011). *In vivo* imaging of Ca(2+), pH, and reactive oxygen species using fluorescent probes in **p**lants. Annu Rev Plant Biol **2010,** 18.

Sze, H., Schumacher, K., Müller, M.L., Padmanaban, S., and Taiz, L. (2002). A simple nomenclature for a complex proton pump: VHA genes encode the vacuolar $H(^{+})$-ATPase. Trends Plant Sci **7,** 157-161.

Tegeder, M., and Weber, A.P.M. (2006). Metabolite Transporters in the Control of Plant Primary Metabolism. In: Control of Primary Metabolism in Plants (Eds) W. C. Plaxton and M. T. McManus. (Blackwell Publishing Ltd), pp. 85-120.

Thuswaldner, S., Lagerstedt, J.O., Rojas-Stutz, M., Bouhidel, K., Der, C., Leborgne-Castel, N., Mishra, A., Marty, F., Schoefs, B., Adamska, I., Persson, B.L., and Spetea, C. (2007). Identification, expression, and functional analyses of a thylakoid ATP/ADP carrier from Arabidopsis. J Biol Chem **282,** 8848-8859.

IV. AIM OF THIS PHD THESIS

Intracellular membrane transport of solutes is important to understand how cellular metabolism is connected within the plant cell. The passage of metabolites across cellular boundaries is facilitated by specific transport proteins. Thus, they contribute to sustaining a functional metabolic network (Linka and Weber, 2010). The central focus of this thesis was to expand the knowledge of the mitochondrial carrier family (MCF) in plants. The objective was to characterize MCF members that have not yet been characterized in respect to their transport function, transport mode and *in planta* role.

In Arabidopsis, 58 MCF carriers are known, but only a quarter of them are biochemically investigated to date. MCF proteins in other plant species are largely unexplored (Palmieri et al., 2011). One goal of this thesis was to analyze the distribution of MCF carriers within the plant kingdom. For this, an unbiased large-scale screen was performed, searching multiple plant proteomes for additional uncharacterized MCF proteins (*Manuscript 1*). Isolated carriers were clustered in orthologous groups and their putative transport functions were assigned. This work explored the role of a MCF protein involved in sulfate transport. Hence, the MCF candidate was called SIT1 for inorganic sulfate transporter (*Manuscript 2*). As the MCF screen revealed a new plant-specific function for SIT1, the transport properties of recombinant protein were assessed by *in vitro* uptake studies. The physiological role of SIT1 in plants was investigated, examining growth phenotypes of homozygous T-DNA lines. The thesis further investigated the peroxisomal pH of different Arabidopsis tissues, as pH is an important factor to understand transport modes of solute carriers, such as MCF members (*Manuscript 3*). Stable transgenic Arabidopsis lines were established, expressing a pH-sensitive green fluorescent protein that was targeted to peroxisomes. Further, the impact of metabolism on peroxisomal pH was assessed.

In summary, this thesis addressed the following aspects: (i) large-scale identification of MCF proteins plants and distribution of functional classes of MCF orthologs within the plant kingdom, (ii) biochemical and physiological characterization of the MCF carrier SIT1 representing a sulfate transporter, (iii) investigation of the peroxisomal pH, tissue-specificity and impact of peroxisomal metabolism on pH.

References

Linka, N., and Weber, A.P.M. (2010). Intracellular metabolite transporters in plants. Mol Plant **3,** 21-53.

Palmieri, F., Pierri, C.L., De Grassi, A., Nunes-Nesi, A., and Fernie, A.R. (2011). Evolution, structure and function of mitochondrial carriers: a review with new insights. Plant J **66,** 161-181.

Picault, N., Hodges, M., Palmieri, L., and Palmieri, F. (2004). The growing family of mitochondrial carriers in Arabidopsis. Trends Plant Sci **9,** 138-146.

V. MANUSCRIPTS

Manuscript 1

Expanding the catalogue of mitochondrial carrier family proteins in plants

Sarah K. Kessel-Vigelius[1*], Anna R. Kersting[2], Christian Esser[2], Martin J. Lercher[2], Ilka Haferkamp[3], Andreas P.M. Weber[1], and Nicole Linka[1a]

[1]Plant Biochemistry, Heinrich-Heine University Düsseldorf, 40225 Düsseldorf, Germany;
[2]Bioinformatics, Heinrich-Heine University Düsseldorf, 40225 Düsseldorf, Germany;
[3]Plant Physiology, Technical University of Kaiserslautern, 67663 Kaiserslautern, Germany

*First author
[a]Corresponding author

Abstract

Solute transport is essential to connect intracellular metabolic networks across compartments, which are often surrounded by at least one bilayer membrane. As organellar borders constitute a diffusion barrier for metabolites, specific transport proteins are required to mediate flux of substrates. One class of transport proteins is the mitochondrial carrier family (MCF). In plants, members of this family are found in mitochondria, plastids, vacuoles, ER, Golgi and plasma membranes of almost all eukaryotes.

We performed a profile-based identification of MCF proteins in multiple genomes to expand the repertoire of these carriers in plants and to understand the evolution of this family. Our analysis substantiated that mitochondrial carrier family members were highly conserved in eukaryotes, whereas they did not occur in bacteria. An analysis of orthologous MCF proteins revealed, that congruent with previous phylogenetic approaches, MCFs formed distinct functional groups. In our analysis we found that within plants, Arabidopsis mitochondrial carrier family orthologs have specified and putatively evolved new plant-specific functions. Furthermore, we discovered that some functional MCF groups were apparently missing in rhodophytes and glaucophytes. For example, peroxisomal carrier proteins were only found in the green lineage.

Introduction

Mitochondria are plant organelles, involved in numerous multicompartmented metabolic pathways, such as photorespiration, nitrogen, or C1 metabolism (Mackenzie and McIntosh, 1999). These organelles are surrounded by two semi-permeable membranes, which constitute a diffusion barrier for most metabolites. This necessitates the presence of solute transport proteins facilitating exchange of intermediates for mitochondrial metabolism (Linka and Weber, 2010). A prominent class of transporters connecting mitochondrial metabolism with other compartments is the mitochondrial carrier family (MCF) (TC 2.A.29). MCF proteins are nuclear-encoded small carriers of 30-40 kDa, which are highly conserved in eukaryotes (Picault et al., 2004).

Although few MCF members have been biochemically characterized so far, it is already evident that they are highly diverse in their transport functions. They facilitate exchange of various substrates, such as nucleotides, carboxylic acids, keto acids, amino acids, and phosphate (Palmieri et al., 2011). Although most MCF proteins are strict antiporters, some carriers mediate uniport or symport (Kunji, 2004; Bamber et al., 2007). Their name might suggest that MCF members are exclusively located to mitochondria, however several carriers have been found in other organelles, *e.g* plastids, peroxisomes, ER, and the plasma membrane (Bedhomme et al., 2005; Bouvier et al., 2006; Thuswaldner et al., 2007; Leroch et al., 2008; Linka et al., 2008; Rieder and Neuhaus, 2011; Bernhardt et al., 2012b). For a long time, it was assumed that MCFs exclusively act as homo-dimers. Today, this view is challenged, because MCF carrier proteins can form helical bundle monomers that represent the functional entity within membranes in yeast.

Structural analyses of the first MCF carriers characterized, revealed common structural features (Saraste and Walker, 1982; Aquila et al., 1985), which are characteristic of this carrier class and distinct from any other known transporter family (Palmieri et al., 2011). MCFs share a threefold repetitive basic structure of about 100 amino acids. Each repeat comprises two α-helical transmembrane domains, connected by hydrophilic loops. Odd numbered transmembrane spans and loops contain a conserved sequence motif called mitochondrial energy signature (PF00153) (Palmieri et al., 2011). Apart from this motif, the conservation of MCF carriers on sequence level is comparably low.

The exact evolution of MCF carriers is still unknown. However, it is plausible that present-day MCF carriers arose from one universal basic module (Arco and Satrustegui, 2005). A pre-existing two-spanner gene fragment was tandem triplicated, fused and differentiated. Presumably, MCF carriers developed less than two billion years ago during the establishment of the mitochondrial organelle. MCFs may have been introduced by either the proteobacterial symbiont, or the archaebacterial host; alternatively they may have been newly invented (Palmieri et al., 2011; Haferkamp and Schmitz-Esser, 2012). Because mitochondrial generation of ATP is essential for life, the first MCF protein might have been involved in exporting ATP from the mitochondrial matrix. A second assumption is that the first MCF carrier exhibited a broad substrate spectrum and that speciation occurred later during eukaryote evolution. An alternative theory hypothesized that early protists already exhibited a basic set of MCF carriers with different transport properties, substrate specificities, and localization (Haferkamp and Schmitz-Esser, 2012).

The goal of this study was to gain insights into the evolution of the mitochondrial carrier family within the plant kingdom. For this, we first of all compiled a comprehensive catalogue of MCF carrier proteins in diverse plant and algal species. We combined Markov clustering of orthologs and paralogs with profile-specific identification tools to gain clusters of orthologous MCF carriers. We then performed an explorative analysis of Arabidopsis MCF homologs to generate a candidate gene list for biochemical analyses of transport functions.

A comprehensive view on MCF carriers and their evolution will contribute to understand the exceptional importance of transport proteins involved in the interplay of cellular metabolism across compartments.

Experimental procedures

Proteomes used in this study

To identify putative MCF carriers and to perform functional classifications, proteomes of the kingdoms plantae, fungi and animals were selected. Proteomes were first filtered for splice variants. Multiple splice variants were excluded, except the longest protein sequences. The following proteomes were used: *Arabidopsis lyrata* v1.0 (Hu et al., 2011), *Arabidopsis thaliana* v10 (Swarbreck et al., 2008), *Brassica rapa* v1.2 (Wang et al., 2011), *Capsella rubella* v1.0 (Slotte et al., 2013), *Carica papaya* v1.0 (Ming et al., 2008), *Citrus clementina* v1.0 (Talon and Gmitter, 2008),

Citrus sinensis v1.0 (Talon and Gmitter, 2008), *Cucumis sativus* v1.0 (Huang et al., 2009), *Eucalyptus grandis* v1.1 (Myburg et al., 2011), *Glycine max* v1.1 (Schmutz et al., 2010), *Lotus japonicus* v1.0 (Sato et al., 2008), *Manihot esculenta* v1.0, *Populus trichocarpa* v3.0 (Tuskan et al., 2006), *Ricinus communis* v1.0 (Chan et al., 2010), *Solanum tuberosum* v3.4 (Xu et al., 2011), *Vitis vinifera* v1.0 (Jaillon et al., 2007), *Brachypodium distachyon* v1.0 (Vogel et al., 2010), *Oryza sativa L. spp. japonica* v6.1 (Goff et al., 2002), *Sorghum bicolor* v1.4 (Paterson et al., 2009), *Zea mays* v2.0 (Hake and Walbot, 1980), *Physcomitrella patens* v1.6 (Rensing et al., 2008), *Selaginella moellendorffii* v1.0 (Banks et al., 2011), *Chlamydomonas reinhardtii* v5.3.1 (Merchant et al., 2007), *Micromonas pusilla CCMP1545* v3.0 (Worden et al., 2009), *Ostreococcus lucimarinus* v2.0 (Palenik et al., 2007), *Volvox carteri* v2.0 (Prochnik et al., 2010), *Cyanidioschyzon merolae* v1.0 (Nozaki et al., 2007), *Cyanophora paradoxa* (Price et al., 2012), *Hansenula polymorpha (Pichia angusta)* v2.0 (Ramezani‐Rad et al., 2003), *Saccharomyces cerevisiae* v1.0 (Giaever et al., 2002), *Ustilago maydis* (Kämper et al., 2006), *Mus musculus* v72.0 (Gregory et al., 2002), and *Homo sapiens* v72.0 (Venter et al., 2001). All plant genomes were downloaded from the Phytozome v9.1 database (http://www.phytozome.net) (Goodstein et al., 2012) with exception of the *Lotus japonicus* proteome, which was retrieved from the PLAZA database (http://bioinformatics.psb.ugent.be/plaza/) (Proost et al., 2009) and *Musa acuminata* proteome downloaded from Ensembl Plants v19 (http://plants.ensembl.org/) (D'Hont et al., 2012). *Cyanidioschyzon merolae* protein sequences were obtained from the *Cyanidioschyzon Merolae* Genome Project (http://merolae.biol.s.u-tokyo.ac.jp). *Cyanophora paradoxa* sequences were retrieved from the *Cyanophora paradoxa* Genome consortium (http://cyanophora.rutgers.edu/cyanophora/symposium.php). The *Ustilago maydis* and *Saccharomyces cerevisiae* proteome were downloaded from EnsemblFungi v19 (http://fungi.ensembl.org). The *Hansenula polymorpha* proteome was obtained from the JGI Genome Portal (http://genome.jgi.doe.gov/).

Further proteomes included were: *Ectocarpus siliculosus*, which was retrieved from the UniProtKB database release 2013_08 (http://www.uniprot.org/) (Schneider et al., 2009), *Neorickettsia risticii*, *Fluoribacter dumoffii, Legionella longbeachae, Legionella drancourtii,* and *Legionella pneumophila* proteomes and other bacterial proteomes, which were accessed via the NCBI Non-Redundant Database and RefSeq database (Pruitt et al., 2007). Cyanobacterial proteomes of *Nostoc* sp. PCC 7107 and *Anabaena* sp. PCC 7108 (Shih et al., 2013) were downloaded from JGI Genome Portal (http://genome.jgi.doe.gov/) (Grigoriev et al., 2012). The cyanobacterial proteomes of *Synechocystis* sp. PCC 6803, *Synechococcus* sp. WH 8102, *Synechococcus elongatus* PCC 6301, *Prochlorococcus marinus* str. MIT 9312, *Cyanothece* sp. ATCC 51142, *Nostoc punctiforme* ATCC 29133, *Chlorobium tepidum* TLS, *Trichodesmium erythraeum* IMS101, and *Arthrospira platensis* NIES-39 were obtained from the Cyanobase server (http://genome.microbedb.jp/CyanoBase) (Nakao et al., 2010).

Annotation of putative MCF carriers based on the Pfam-A model PF00153

For identification, we used the MCF-carrier specific Pfam-A signature motif PF00153 that was retrieved from Pfam (v27) at http://pfam.sanger.ac.uk (Finn et al., 2010). PF00153 was used as query to scan the protein database containing all eukaryotic proteomes with the *hmmsearch* tool of HMMER3.0 (http://hmmer.janelia.org/) (Eddy, 2011; Finn et al., 2011). Model specific score thresholding was applied. Specific bit score thresholds for PF00153 were obtained from Pfam (v27), which are more accurate than thresholding based only on statistical significance (Finn et al., 2011). Putative prokaryotic MCF carriers were identified with the online version of *hmmsearch* scanning NCBI NR and RefSeq databases for PF00153 and applying the taxonomy view (Pruitt et al., 2007).

Prediction of functional clusters with OrthoMCL

Clusters of orthologous and paralogous genes were calculated using the program OrthoMCL (http://www.orthomcl.org/) (Li et al., 2003). First, a Blastp all-vs-all comparison of the entire proteomes of 23 selected species was conducted (land plants, mosses, algae, fungi and mammals). Putative orthologs were identified by reciprocal best blast hits. Paralogs were classified as sequences of the same proteome that reciprocally had a higher similarity to each other than either was to any sequence of a different proteome (Li et al., 2003). Weighting was performed to calculate a similarity matrix to which Markov Clustering was applied (Enright et al., 2002). Clusters, containing sequences of at least two species, were saved in an output file of orthologs and recent paralogs. The output file was scanned for groups comprising at least one of the 58 Arabidopsis MCF carriers. The groups with Arabidopsis MCF proteins were selected and reverse-checked for the PF00153 motif characteristic of MCF carriers, as we expected that all proteins in the Arabidopsis MCF groups are also MCF carriers. The program HMMER was used to identify the PF00153 motif in MCF carrier groups established with OrthoMCL. Based on previous functional annotations of Arabidopsis MCF carriers (Palmieri et al., 2011; Haferkamp and Schmitz-Esser, 2012), we sorted the OrthoMCL MCF cluster according to their putative functions. We analyzed number and distribution of MCF carriers with the focus on plant species.

Results

Motif-based identification of MCF carriers in comparison to a reference dataset

Initial studies investigated the presence and evolution of MCF carriers in *Arabidopsis thaliana* (Picault et al., 2004; Haferkamp, 2007; Haferkamp and Schmitz-Esser, 2012), or within dicots, monocots and algae (Palmieri et al., 2011). Previous studies explored the relationship of MCF carriers by blasting a specific representative (pairwise method), extracting blast hits, assigning transmembrane domains and building phylogenetic trees (Picault et al., 2004; Haferkamp, 2007; Palmieri et al., 2011). In our analysis, we applied an alternative motif-based approach, solely identifying MCF carriers by a 96 amino acids long sequence motif (PX[D/E]XX[K/R]-(20-30 residues)-[D/E]GXXXX[W/Y/F][K/R]G) called mitochondrial energy transfer signature. This signature

was expressed as profile Hidden-Markov Model (HMM) PF00153, which was retrieved from the Pfam database (Finn et al., 2010). We applied HMMs, because residues in a functional sequence are subject to different selection pressures. Some positions are more conserved than others. Less conserved regions tolerate more insertions or deletion (Eddy, 1998). In contrast to standard multiple sequence alignments and pairwise methods, such as Blast, HMM models contain position-specific scoring information (Eddy, 1998). This study for the first time employed the application HMMER3.0 (Finn et al., 2011). As HMMER3.0 allowed the application of own target sequence databases, we filtered proteomes for splice variants first. We did so to improve the quality of our analysis, because in unfiltered genomes the probability exists that due to splice variants the same MCF carrier is recognized multiple times. Using this approach, we searched for putative MCF carriers within 29 publicly available plant proteomes, including 19 genomes of representatives from brown algae, fungi and mammals. In total we found 1366 MCF carriers. Protein sequences are listed in the supporting material.

We compared the number of MCF carriers identified with our method to an established set of MCF carriers (Picault et al., 2004; Haferkamp, 2007; Palmieri et al., 2011; Haferkamp and Schmitz-Esser, 2012) (Tab. 1). We examined a larger number of plant proteomes, *Homo sapiens*, and *Saccharomyces cerevisiae* and could show that the number of MCF carriers identified with our approach was in agreement with the reference dataset (Tab. 1). Slightly higher numbers of MCF carriers than in the reference set were found in *C. papaya*, *R. communis*, *B. distachyon*, *C. reinhardtii*, *O. lucimarinus*, and *H. sapiens*. Our analysis revealed a significantly higher number of MCFs in *S. bicolor* and *P. patens*. In case of *G. max*, *O. sativa* and *Z. mays* proteomes, the reference dataset contained a higher number of MCF carriers.

Tab. 1: Comparison of MCF carriers identified with HMMER3.0 with previously identified MCF proteins of a reference dataset.
Comparison of HMMER-identified MCF carriers with a reference dataset was obtained from Palmieri et al., 2011. Proteomes were screened for putative MCF carriers using the Pfam-A motif PF00153. Purple: 30-40 MCF carriers; blue: 40-50 MCF carriers; green: 50-70 MCF carriers; orange: >70 MCF carriers. The total number of genes was either retrieved from the database where the proteome was downloaded or from the original publications.

Species name	Classification	MCFs HMMER	MCFs Reference	Genes
Arabidopsis lyrata	Magnoliophyta Eudicots	66	66	32,670
Arabidopsis thaliana		58	58	33,602
Carica papaya		59	57	27,332
Cucumis sativus		61	61	32,528
Glycine max		94	125	54,174
Populus trichocarpa		91	91	41,377
Ricinus communis		66	65	31,221
Vitis vinifera		61	61	26,664
Brachypodium distachyon	Magnoliophyta Monocots	56	55	31,029
Oryza sativa		61	64	57,939
Sorghum bicolor		67	60	34,686
Zea mays		51	73	39,597
Physcomitrella patens	Embryophyta Bryophyta	98	93	38,354
Selaginella moellendorfii	Tracheophyta Lycophyta	60	60	34,914
Chlamydomonas reinhardtii	Chlorophyta	43	37	14,560
Ostreococcus lucimarinus		40	38	7,805
Saccharomyces cerevisiae	Fungi Ascomycetes	35	35	6,692
Homo sapiens	Animals Mammals	58	53	20,774

Distribution of MCF members within bacteria and brown algae

To get insights into the evolution of MCF carriers, we first screened bacterial proteomes from the NCBI Non-Redundant and RefSeq databases for the existence of MCF carriers with HMMER3.0 (Pruitt et al., 2007; Finn et al., 2011). We identified almost no MCF carriers in bacteria, except of few pathogenic *Neorickettsia* and *Legionella* species that were also found in a previous study (Dolezal et al., 2012) (Tab. S1). Cyanobacteria are basal to all plants, as photosynthetic eukaryotes descended from a single prokaryotic ancestor that acquired a photosynthetic cyanobacterium as endosymbiont (Bowman et al., 2007). We found that MCF proteins are absent in cyanobacteria. This indicated that MCFs developed later during eukaryotic evolution (Kunji, 2004) (Tab. S1). We then examined the phaeophycean alga *Ectocarpus siliculosus.* Brown algae are multicellular photosynthetic organisms that are only distantly related to green plants (Cock et al., 2010). We found *Ectocarpus* encoding for 60 MCF proteins (Tab. S1). In conclusion, our approach affirmed the idea that most bacteria do not contain MCF proteins, whereas MCFs are important and characteristic proteins of eukaryotes, including brown algae.

Distribution of MCF members within the plant kingdom

We continued to apply our approach to further plant and algal proteomes, which were not investigated previously and thus, expanded the list of MCF carriers (Tab. 2). Upon endosymbiosis

five main eukaryotic lineages evolved, one of which is the plant lineage. The plant lineage is divided into glaucophyta (freshwater algae), rhodophyta (red algae) and viridiplantae, including the group of chlorophyta (green algae) (Bowman et al., 2007) (Fig. 1).

Tab. 2: Identification of previously unknown MCF carriers in plants.
Proteomes were screened for putative MCF carriers using the Pfam-A motif PF00153. Purple: 30-40 MCF carriers; blue: 40-50 MCF carriers; green: 50-70 MCF carriers; orange: >70 MCF carriers. The total number of genes was either retrieved from the database where the proteome was downloaded or from the original publications.

Species name	Classification	MCFs	Genes
Cyanophora paradoxa	Glaucophyta	52	27,921
Cyanidioschyzon merolae	Rhodophyta	31	5,331
Micromonas pusilla	Chlorophyta	43	10,660
Volvox carteri		41	14,971
Musa acuminata	Magnoliophyta Monocots	114	36,519
Brassica rapa	Magnoliophyta Eudicots	95	41,018
Capsella rubella		61	26,521
Citrus clementina		63	33,929
Citrus sinensis		61	25,376
Eucalyptus grandis		76	36,376
Lotus japonicus		71	69,647
Manihot esculenta		83	47,000
Solanum tuberosum		59	51,472

In our analysis we identified MCF carriers within these major plant groups (Tab. 2, Fig. 1). The mitochondrial energy signature was present in 52 proteins of the glaucophyte *C. paradoxa* and in 31 proteins of the red alga *C. merolae.* The proteome of the unicellular green alga *M. pusilla* contained 43 MCF proteins. The multicellular green alga *V. carteri* encoded 41 MCFs. A major evolutionary step in plant history was the colonization of terrestrial landscapes. About 300 Myr years ago, gymnosperms and angiosperms (magnoliophyta) diverged. Within magnoliophyta, eudicots and monocots originated. We found that the monocot species *M. acuminata* exhibited 114 MCFs in its genome (Tab. 2). In eudicots, between 59 and 95 MCF carriers were identified. Our analysis revealed that with exception of the glaucophyte *C. paradoxa*, which has a large quantity of carriers, the number of MCFs increased along the branch leading to embryophytes. We experienced that *B. rapa* contained a high number or MCF carriers. The same was observed for previously identified MCFs in *G. max*, *P. trichocarpa* and *P. patens*.

Our results demonstrated that that the application of HMMs was valid to identify MCF carriers, because when compared to the reference dataset we robustly identified MCF carriers in our study. The distribution of the MCF within plants revealed that MCFs are conserved in greater presence, underlining the importance of this carrier class.

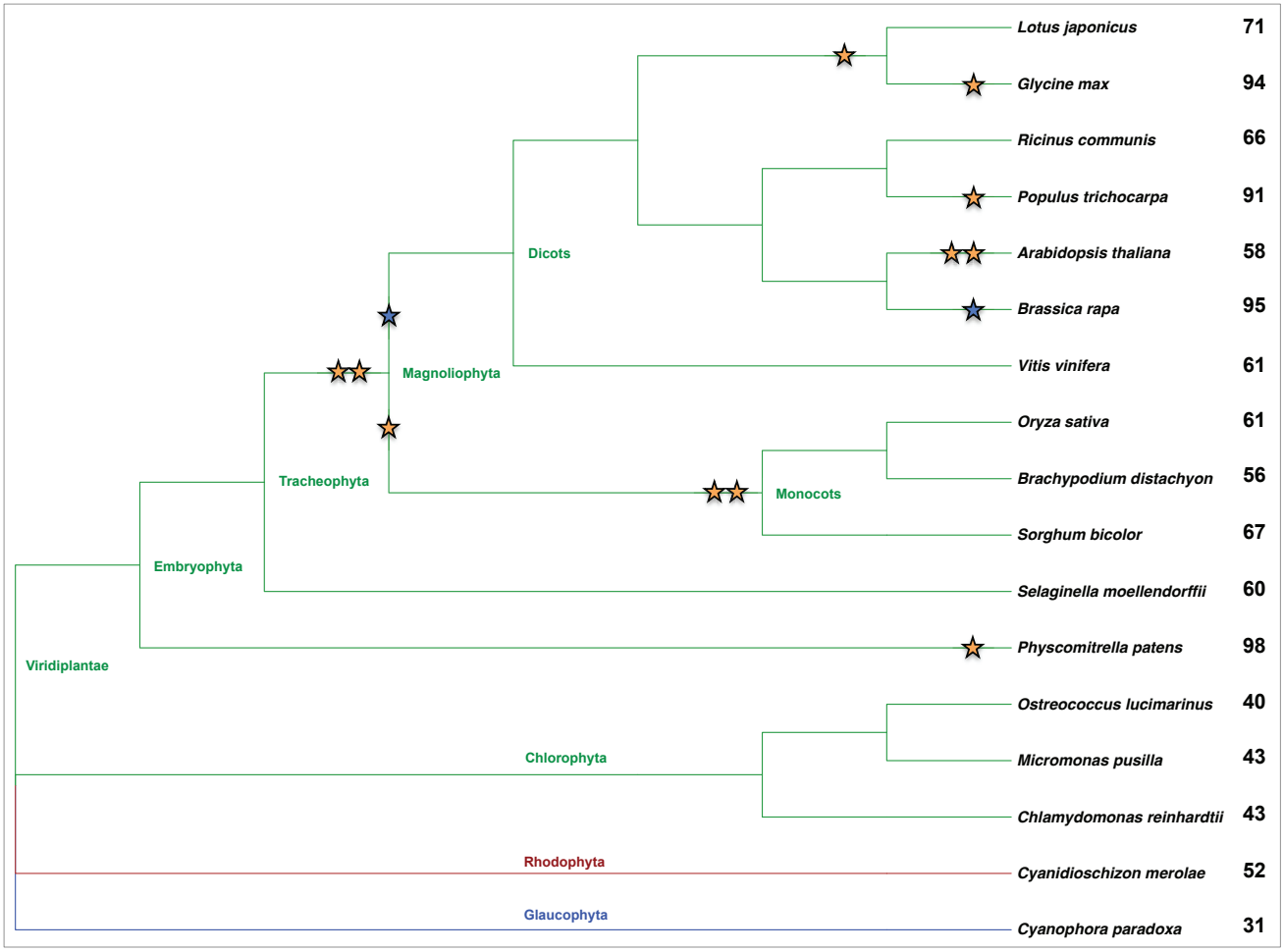

Fig. 1: Schematic phylogenetic tree of MCF carriers in primary photosynthetic eukaryotes.
Putative MCF carriers were identified from proteomes of primary photosynthetic eukaryotes by the Pfam-A motif PF00153. Species used for this analysis are schematically represented as unrooted phylogenetic tree, the number of MCF carriers is indicated at the leaves of the tree behind taxa names. Orange stars: whole genome duplication; blue stars: whole genome triplication. Information on genome duplications was taken from Van der Peer et al., 2009 and http://chibba.agtec.uga.edu/duplication/; Phylogenetic tree is a modified version of the phylogenetic tree of species at http://www.phytozome.net and http://bioinformatics.psb.ugent.be/plaza/. Branch lengths do not represent evolutionary time or nucleotide substitutions; position of stars is not meant to date polyploidization events.

MCF carriers constitute functional groups

We used a subset of 20 complete plant, fungal and animal proteomes and assigned putative functions to MCF carriers. We clustered proteins in orthologous and paralogous groups with OrthoMCL (Li et al., 2003). Groups of orthologs and paralogs were screened for the MCF motif PF00153 with HMMER3.0. Orthologous MCFs were classified in functional groups based on previously characterized MCF members (Haferkamp, 2007; Palmieri et al., 2011; Haferkamp and Schmitz-Esser, 2012).

We first extracted ortholog groups containing at least one of the 58 Arabidopsis MCF carriers (Tab. 3).

Tab. 3: Identification of functional MCF subgroups from *Arabidopsis thaliana* in other species.
OrthoMCL was used to identify orthologous genes in 20 proteomes. Groups of ortholog and paralog genes were computed with Markov clustering. All groups, which contained at least one Arabidopsis MCF carrier, were included. Based on a separation of Arabidopsis MCFs into functional clusters (Haferkamp and Schmitz-Esser, 2012), OrthoMCL groups were sorted correspondingly. Putative function and distribution of carriers are indicated below. Carriers, which were found in one OrthoMCL group, are listed together. Genes were annotated with TAIR10 and Aramemnon database.

Substrate	Identifier	Annotation	Angiosperms									Mosses		Chlorophytes		Rhod.	Glauc.	Fungi			Mammalia		
			Ath	Bdi	Bra	Gma	Lja	Osa	Rco	Sbi	Vvi	Ppa	Smo	Cre	Mpu	Cme	Cyp	Hpo	Sce	Uma	Hsa	Mmu	Sum
1. Nucleotides and Dinucleotides																							
ADP/ATP	AT3G08580.1, AT5G13490.1, AT4G28390.1	Putative mitochondrial adenylate translocator (AAC1; AAC2; AAC3)	3	1	3	7	2	2	3	1	1	6	4	1	1				3	1	1	1	41
	AT5G56450.1	Plasmamembrane-isoated adenine nucleotide transporter (PM-ANT1)	1	1	1	1	1	1	1	1	1	2	1			1	1				2	2	18
	AT5G17400.1	ER-located adenine nucleotide transporter (ER-ANT1)	1	1	2	2	1	1	2	1	1												12
	AT4G32400.1	Adenylate nucleotide uniporter (ABT1/pANT1)	1	2	2	4	2	2	1	2		3	2		1								22
	AT3G20240.1	MCF, adenine nucleotide carrier-like	1	3	1	2	1	2	1	3	1	1		1									16
	AT5G64970.1	MCF, adenine nucleotide carrier-like	1	1	1	1	1	1	2	1	3		1										15
	AT1G78180.1	MCF, adenine nucleotide carrier-like	1		1									1	1								2
	AT2G37890.1, AT3G53940.1, AT3G55640.1	MCFs, adenine nucleotide carrier-like	3	2	4	4	2	1	1	2	2	1	1										22
	AT4G01100.2	Adenine nucleotide transporter 1 (ADNT1)	1	1	2	6	2	1	2	1	2	1	1			2			1				27
	AT3G05290.1, AT5G27520.1	Peroxisomal adenine nucleotide carriers (AtPNC1; AtPNC2)	2	1	3	3	1		1	1	1	3	2					1		1			24
ATP-Mg/-Pi	AT5G61810.1, AT5G51050.1, AT4G07320.1	Putative mitochondrial ATP importers (AtAPC1, AtAPC2, AtAPC3)	3	1	4	7	1	1	2	2	2	2	1	1	1			1		2	2	2	34
	AT1G74240.1	Putative ATP-Mg/Pi carriers	1	1	1	1		1	1	1	1	1	1			1							13
PAP/CoA	AT5G01500.1, AT3G51870.1	Phosphoadenosine phosphosulfate carrier (AtPAPST1/TAAC; AtPAPST2)	2	2	2	2	1	1	1	1	1	2	1	1	2								18
	AT1G14560.1	Putative mitochondrial MtC-type coenzyme A transporter (AtCoAc1)	1	2	1	2	1	1	1	1	1	1	1	1	1			1	1	1	1	1	21
	AT4G28180.1, AT5G15640.1	Putative mitochondrial MtC-type coenzyme A transporter (AtCoAc2), MCF	2	2	3	5		2	2	2	1	1	1	1	1	1			1	1	1	1	27
Folate	AT5G66380.1	Mitochondrial folate transporter (AtFOLT1)	1	1	2	2	1	1	1	1	1	1	1	1	1	1	1	1	1	1	1	1	22
NAD	AT2G47490.1, AT1G25380.1	Putative NAD+ carrier proteins (ANDT1, ANDT2)	2	1	3	4	2	2	2	2	2	2	2	1	1	1	1	2	1	1	1	1	28
	AT2G39970.1	Putative peroxisomal NAD+ carrier (AtPXN)	1	1	1	2	1	1	1	1	1	4	1	1	1	1		1		1		1	20
Thiamine pyrophosphate	AT5G48970.1, AT3G21390.1	MCFs (homologous to ScTPC1)	2	1	2	4	2	1	1	1	1	1	1	1	1	1		1		1	1	1	24
2. Di-/Tricarboxylates, Keto acids																							
Dicarboxylic acids	AT2G22500.1, AT4G24570.1	Mitochondrial dicarboxylate carriers (AtDIC1, AtDIC2)	2	2	3	4	3	1	4	1	1	5	2					1	1	2	2	1	36
	AT5G09470.1	Mitochondrial dicarboxylate carrier (AtDIC3/AtPUMP6)	1		1																		2
Di-/Tricarboxylic acids	AT5G19760.1	Mitochondrial dicarboxylate/tricarboxylate carrier (AtDTC)	1	1	2	2	1	2	1	1	2	4	2	1	1	1	1			1		1	23
Succinate/fumarate	AT5G01340.1	Mitochondrial succinate/fumarate translocator (AtSFC1)	1	1	1	2	1	1	1	1	1	2	2	1	0	1	1	1	1	1	0		16
3. Amino acids																							
Basic amino acids	AT2G33820.1	Mitochondrial arginine-ornithine translocator (AtBAC1)	1	1	1	2	1	1	1	1	1	1	1	1	1								13
	AT1G79900.1	Mitochondrial arginine-ornithine translocator (AtBAC2)	1	1	1	4	1	1	1	1	1	1	1	1	1						2		22
Carnitine?	AT5G46800.1	Mitochondrial Carnitine Acyl Carrier-Like Protein (AtBOU)	1	2	2	4	3	1	1	1	1	2	1	3	1			1			2	2	37
S-Adenosylmethionine	AT4G39460.1, AT1G34065.1	S-adenosylmethionine transporters (AtSAMC1, AtSAMC2)	2	2	2	2	1	2	2	4	2	2	1	1	1	3	2	1	1	1	1	1	35
	AT2G35800.1	Putative calcium-dependent S-adenosyl methionine carrier (AtSAMTL)	1																				13
4. Phosphate																							
Phosphate	AT5G14040, AT3G48850	Mitochondrial phosphate transporters (AtPHT3;1, AtPHT3;2)	2	2	3	2	1	3	2	3	2	6	3	1	1	1		2	2	1	1	1	40
	AT2G17270	Putative Mitochondrial phosphate transporter (AtPHT3;3)	1	1	1	2		1	1	1	1	2	1										12
5. Other substrates																							
Uncoupling proteins	AT3G54110.1	Mitochondrial uncoupling protein (AtUCP1)	1	1	3	2	2	1	1	2	2	1	1	1	1					1	2	2	24
	AT5G58970.1	Mitochondrial uncoupling protein (AtUCP2)	1		1			1	1	1	1												3
	AT1G14140.1	Mitochondrial uncoupling protein (AtUCP4)	1	1	1	2	1	1	1	1	1	1	1	1	1	1	1			1	1	1	15
Mitoferrin/iron	AT1G07030.1, AT2G30160.1	MCFs (highly similar to HsMitoferrin 1, 2 and ScMRS3, 4)	2	1	3	2	1	1	2	1	1	1	4	1	1	1	1	2	1	2	2	1	31
	AT5G42130.1	Mitoferrin-like carrier (AtMFL1)	1	1	1	1		1	1	1	1	1	1			1	1						12
	AT4G27940.1, AT2G46320.1	Mitochondrial carrier protein (AtMTM1), MCF	2	1	3	4	1	1	2	1	2	2	1	1	1	1	1	1	1	1	2	2	31
6. Uncharacterized																							
	AT2G26360.1	Putative mitochondrial carrier protein	1		1																		2
	AT1G72820.1	Putative mitochondrial carrier protein	1	2	2	5	1	2	2	1	2	2	1										21
	AT4G15010.1	Putative mitochondrial carrier protein	1	1	1	2	1	1	1	1	1	1											11
	AT4G03115.1	Putative mitochondrial carrier protein	1	1	1	1		1	1	1	1			2	1								11
	AT5G26200.1	Putative mitochondrial carrier protein	1		1											1							3
	AT4G11440.1	Putative mitochondrial carrier protein	1	1	1	2	1	1	1	1	1	3	2	1	1	1	1	1	1	1	2	2	31
			58	49	78	106	36	50	53	47	47	74	47	25	27	17	11	17	22	17	27	25	14

The identified groups solely contained MCF carriers. Groups of homologs were regarded as functional units. The analysis demonstrated that both methods for MCF identification, established phylogenetic approaches or the OrthoMCL/HMMER approach, led to independent clades of MCFs, which contained only carriers with related functional properties (Picault et al., 2004; Haferkamp, 2007; Palmieri et al., 2011; Haferkamp and Schmitz-Esser, 2012). Based on previous functional annotations, we sorted OrthoMCL groups containing MCFs according to their putative function. We divided them into six functional classes, *i.e* protein clusters transporting nucleotides/dinucleotides, di-/tricarboxylates/keto acids, amino acids/carnitine, phosphate, or other substrates, and a class of proteins with unknown function (Tab. 3).

The carriers we included in our Arabidopsis-centric analysis were widely congruent with previous phylogenetic trees of Haferkamp and Palmieri. MCF members of most of functional classes were highly conserved within eukaryotes. However, the distribution of some MCF homolog groups within green, red and glaucophyte lineages was unexpected. We observed groups of orthologs that were restricted (i) to the green lineage, (ii) to angiosperms, or (iii) to land plants.

None of the peroxisomal MCF carriers was conserved in rhodophytes or glaucophytes. Moreover, also the peroxisomal NAD transporter (PXN, At2g39970) and adenine nucleotide carriers (PNC1, At3g05290; PNC2, At5g27520) were missing in these algal groups but existed in chlorophytes and viridiplantae. The same distribution was observed for mitochondrial adenylate translocators (AACs, At3g08580, At5g13490, At4g28390), orthologs of the dicarboxylate carrier DIC3 (At5g09470), and for proteins homologous to the succinate/fumarate carrier (At5g01340). Within the group of amino acid transporters, the mitochondrial arginine/ornithine translocators BAC1 and BAC2 (At2g33820, At1g79900) were green lineage-specific. Orthologs of the ER-located adenine nucleotide transporters (ER-ANT1, At5g17400) were restricted to angiosperms. The S-adenosyl methionine-like carrier SAMTL (At2g35800) was only present in land plants. Furthermore, the putative phosphate carrier PHT3;3 (At2g17270) was also restricted to land plants, whereas its close orthologs PHT3;1 and PHT3;2 (At5g14040, At3g48850) were universally conserved.

Discussion

In this study we scanned multiple plant proteomes in parallel for MCF carriers. A cluster analysis of MCF orthologs provided information about distributions of functional classes within the plant kingdom. First, we established a position-based approach involving Hidden-Markov models. Previous studies demonstrated that profile-based methods, involving information from a number of sequences, provide better results than pairwise methods (Maurer-Stroh et al., 2003; Sánchez-Pulido et al., 2003; Wistrand and Sonnhammer, 2005). Quantity and distribution of MCF carriers previously identified matched and hence supported our analysis (Tab. 1). In some cases, less MCF carriers were identified than in the reference dataset. We assumed that due to a filtering step we applied on proteomes, splice variants were removed and thereby the number of MCFs was reduced, as splice variants of the same carrier might have been recognized several times before. That the number of

MCFs slightly varied between analyses, might also be caused by different releases and qualities of proteomes (Shangguan et al., 2013). We demonstrated that our approach was valid to identify new MCF carriers in previously not investigated plants and algae. Before analyzing MCF carriers in the plant kingdom, we analyzed bacterial proteomes to gain a better view on general MCF evolution. So far, there is no evidence that MCF carriers developed in prokaryotes (Tab. S1). We found putative MCFs, which were moderately conserved in *Neorickettsia and Legionella*. Although it is widely accepted that the few sequences identified in prokaryotes are pseudogenes, acquired by horizontal gene transfer (Nakamura et al., 2004; Stael et al., 2011), the function of a MCF protein from the pathogen *L. pneumophila* was studied (Dolezal et al., 2012). The *L. pneumophila* MCF LncP is a mitochondrial ATP transporter that is homolog to yeast AAC. LncP is secreted during infection, is then incorporated into the host mitochondrial membrane. There, it serves to manipulate mitochondrial ATP transport, assisting the survival of the bacteria inside their host (Dolezal et al., 2012). This example challenged the notion that MCFs exclusively occur in eukaryotes.

We identified new MCFs in plants (Tab. 2) and found that MCFs are highly conserved in all plant lineages. Species, such as *B. rapa*, *G. max*, or *P. trichocarpa* encoded a high number of MCFs. These species underwent recent whole genome duplications (WGDs) (Cavalier-Smith, 2004; Keeling et al., 2005) (Fig. 1). WGDs are important driving forces for the evolution of organisms, as with the onset of polyploidization massive genome rearrangements occured. Genome duplications facilitate major leaps in evolution leading to diversification and speciation of organisms. However, gene loss or retention can differ dramatically between species depending on the selective forces (Adams and Wendel, 2005). In life history whole genome duplications occurred at least four times in plants (Van de Peer et al., 2009). Very recent genome duplications, or even triplications (3-5 myr years ago) occurred in *G. max*, *B. rapa*, *P. trichocarpa* and *M. acuminata* (Adams and Wendel, 2005; D'Hont et al., 2012). In *P. patens* a WGD happened after the angiosperm-moss split (65 myr years ago) (Rensing et al., 2007; Van de Peer et al., 2009). Vertebrates have undergone two ancient WGDs, in fungi there is evidence for one WGD. Fungal genomes in our analysis contained fewer MCFs than plants; the quantity of MCFs in animals was in the same range as in plants (Tab. 1, Tab. S1).

We combined OrthoMCL with profile HMM identification of MCFs as an alternative to a phylogenetic approach. We decided to use OrthoMCL, since computational costs of multiple sequence alignments and construction of phylogenetic trees, plus difficult interpretations of alignments and trees, exclude a phylogenetic approach for whole-genome comparisons in eukaryotes, or at least make it very difficult (Li et al., 2003). A functional Arabidopsis-centric classification revealed that with a higher developmental level in plants, higher speciation occurred and hence more MCF proteins and isoforms can be found (Tab. 3). Evolution, speciation and increasing number of MCF proteins probably correlate with the need of particularly land plants to metabolically adapt to constantly changing environmental conditions.

Adaptations specific to higher plants might be reflected within the PHT3 family of Arabidopsis that comprises the three mitochondrial carriers PHT3;1, PHT3;2 and PHT3;3, presumably facilitating the import of phosphate into mitochondria to fuel ATP synthesis (Poirier and Bucher, 2002). Heterologous complementation of a yeast mutant deficient in mitochondrial phosphate import revealed a phosphate transport capacity for PHT3;1 and PHT3;2, whereas this function could not be verified for PHT3;3 (Hamel et al., 2004). We observed that although in previous phylogenetic studies involving Arabidopsis MCF proteins, PHT3 proteins cluster together as one family of mitochondrial phosphate carriers (Picault et al., 2004), PHT3;3 constituted an orthologous group separate from PHT3;1 and PHT3;2. Whereas PHT3;1 and PHT3;2 proteins occurred in all kingdoms, the PHT3;3 orthologs appeared to be land plant specific. This might indicate a novel plant-specific role for this carrier, which needs to be investigated, assessing localization and biochemical function of PHT3;3 in comparison to PHT3;1 and PHT3;2.

It became evident that none of the peroxisomal MCF carriers of higher plants characterized to date existed in rhodophytes and glaucophytes. Neither orthologs of the peroxisomal NAD/CoA transporter PXN (Agrimi et al., 2012; Bernhardt et al., 2012b), nor of the adenine nucleotide transporters PNC1 and PNC2 (Arai et al., 2008; Linka et al., 2008) were detected. In land plants, PNC1, PNC2 and PXN are involved in fatty acid oxidation in peroxisomes (Arai et al., 2008; Linka et al., 2008; Bernhardt et al., 2012a). The role of peroxisomes in algae is generally less studied compared to land plants, and consequently the knowledge of degradation of fatty acids is also limited. Studies suggest that β-oxidation does not exclusively occur in peroxisomes of algae and that in some species enzymes of β-oxidation are exclusively located to mitochondria (Winkler et al., 1988). It is assumed that in the red alga *C. merolae*, which was included in our analysis, β-oxidation is a mitochondrial process. This might explain why PNC and PXN homologs are not required and hence were not identified in this specific alga (Gross, 1989). A determination of distinct transport features of PXN and PNC in green plants is required in the future.

The presence of a mitochondrial ATP exporter, such as the mitochondrial ATP/ADP carrier AAC is essential for all eukaryotic organisms with functional mitochondria (Haferkamp and Schmitz-Esser, 2012). However, our analysis revealed that AAC homologs were absent in rhodophytes and glaucophytes (Tab. 2). We assume that AAC-like proteins that are present in rhodophytes and glaucophytes, could mediate the export ATP from mitochondria. Besides AAC-like proteins, rhodophytes encode two ADNT1 homologs. These carriers might transport ATP in exchange with AMP or ADP. It was shown previously that the Arabidopsis carrier ADNT1 exports mitochondrial ATP, imports cytosolic AMP, but has also a low affinity for ADP (Palmieri et al., 2008). In contrast, glaucophytes contain two putative nucleotide carriers (PM-ANT1, FOLT1 homologs), which could be involved in mitochondrial energy passage. In conclusion, rhodophytes and glaucophytes might contain additional ATP carrier proteins that are different to AAC. These additional carriers might be good candidates for exporting ATP from algal mitochondria.

We observed a lower number of MCFs in algae then in higher plants (Tab. 2). This fact and the observation that homologs of essential transporters are absent in algae might indicate that MCF carriers of algae have a broad specificity, or are located to membranes of multiple organelles. During evolution plants gained a higher level of anatomical and metabolic complexity (Bowman et al., 2007; Lunn, 2007), which might have necessitated the existence of a larger repertoire of MCFs with distinct transport functions, differential expression and a high level of regulation. Future investigations of MCF carriers from chlorophytes to land plants will address the following aspects: (i) identification of the minimal set of MCF carriers, (ii) newly invented MCF carriers in plant evolution, and (iii) losses of MCF carrier groups in plant evolution.

We demonstrated that a profile-based identification of MCF carriers in multiple eukaryotic genomes is feasible. We confirmed that the MCF signature as it exists today is not contained in bacteria, undermining previous studies proposing that MCFs might have evolved later during evolution. Our analysis corroborated the view that MCFs are highly conserved within the plant kingdom, but that distinct functional groups might have evolved to new species-specific functions, as we demonstrated for groups of functional orthologous in plants. The distribution of MCF members within plant species and a characterization of plant-specific MCFs will aid to understand how plant mitochondria specified during evolution and will unravel how these organelles are interconnected within the metabolic network of the cell.

Supplemental material

Protein sequences can be found on a data medium attached to this thesis.

Tab. S1: Identification of previously unknown MCF carriers in a brown alga, fungi, animals and bacteria.
Proteomes were screened for putative MCF carriers using the Pfam-A motif PF00153. Purple: 30-40 MCF carriers; blue: 40-50 MCF carriers; green: 50-70 MCF carriers; orange: >70 MCF carriers. The total number of genes was either retrieved from the database where the proteome was downloaded or from the original publications.

Species name	Classification	MCFs	Genes
Ectocarpus siliculosus	Phaeophyta	60	16,256
Hansenula polymorpha	Fungi Ascomycetes	31	5,116
Ustilago maydis	Fungi Basidiomycetes	37	6,690
Mus musculus	Animals Mammals	53	23,139
Nostoc sp.	Cyanobacteria	0	7,432
Anabaena sp.		0	5,437
Synechocystis sp.		0	3,317
Synechococcus sp.		0	2,579
Prochlorococcus marinus		0	2,007
Cyanothece sp.		0	4,817
Chlorobium tepidum		0	2,310
Neorickettsia risticii	α-Proteobacteria	1	--
Legionella drancourtii	γ-Proteobacteria	1	--
Legionella longbeachae		3	--
Legionella pneumophila		5	--
Fluoribacter dumoffii		3	--

Acknowledgements

We acknowledge DFG-GRK 1525 for funding this research.

We thank Alisandra Denton, Plant Biochemistry, Heinrich-Heine University Düsseldorf for reading the manuscript. We thank the reviewers for reading and constructive criticism on our data.

References

Adams, K.L., and Wendel, J.F. (2005). Polyploidy and genome evolution in plants. Curr Opin Plant Biol **8,** 135-141.

Agrimi, G., Russo, A., Pierri, C.L., and Palmieri, F. (2012). The peroxisomal NAD^+ carrier of *Arabidopsis thaliana* transports coenzyme A and its derivatives. J Bioenerg Biomembrane **44,** 333-340.

Aquila, H., Link, T.A., and Klingenberg, M. (1985). The uncoupling protein from brown fat mitochondria is related to the mitochondrial ADP/ATP carrier. Analysis of sequence homologies and of folding of the protein in the membrane. EMBO J **4,** 2369.

Arai, Y., Hayashi, M., and Nishimura, M. (2008). Proteomic identification and characterization of a novel peroxisomal adenine nucleotide transporter supplying ATP for fatty acid beta-oxidation in soybean and Arabidopsis. Plant Cell **20,** 3227-3240.

Arco, A.D., and Satrustegui, J. (2005). New mitochondrial carriers: an overview. Cell Mol Life Sci **62,** 2204-2227.

Bamber, L., Harding, M., Monné, M., Slotboom, D.-J., and Kunji, E.R. (2007). The yeast mitochondrial ADP/ATP carrier functions as a monomer in mitochondrial membranes. Proc Natl Acad Sci U S A **104,** 10830-10834.

Banks, J.A., Nishiyama, T., Hasebe, M., Bowman, J.L., Gribskov, M., dePamphilis, C., Albert, V.A., Aono, N., Aoyama, T., and Ambrose, B.A. (2011). The Selaginella genome identifies genetic changes associated with the evolution of vascular plants. Science **332,** 960-963.

Bedhomme, M., Hoffmann, M., McCarthy, E.A., Gambonnet, B., Moran, R.G., Rébeillé, F., and Ravanel, S. (2005). Folate metabolism in plants - An Arabidopsis homolog of the mammalian mitochondrial folate transporter mediates folate import into chloroplasts. J Biol Chem **280,** 34823-34831.

Bernhardt, K., Wilkinson, S., Weber, A.P.M., and Linka, N. (2012a). A peroxisomal carrier delivers NAD^+ and contributes to optimal fatty acid degradation during storage oil mobilization. Plant J **69,** 1-13.

Bouvier, F., Linka, N., Isner, J.C., Mutterer, J., Weber, A.P., and Camara, B. (2006). Arabidopsis SAMT1 defines a plastid transporter regulating plastid biogenesis and plant development. Plant Cell **18,** 3088-3105.

Bowman, J.L., Floyd, S.K., and Sakakibara, K. (2007). Green genes - comparative genomics of the green branch of life. Cell **129,** 229-234.

Cavalier-Smith, T. (2004). Only six kingdoms of life. Proc Biol Sci **271,** 1251-1262.

Chan, A.P., Crabtree, J., Zhao, Q., Lorenzi, H., Orvis, J., Puiu, D., Melake-Berhan, A., Jones, K.M., Redman, J., and Chen, G. (2010). Draft genome sequence of the oilseed species Ricinus communis. Nat Biotechnol **28,** 951-956.

Cock, J.M., Sterck, L., Rouzé, P., Scornet, D., Allen, A.E., Amoutzias, G., Anthouard, V., Artiguenave, F., Aury, J.-M., and Badger, J.H. (2010). The Ectocarpus genome and the independent evolution of multicellularity in brown algae. Nature **465,** 617-621.

D'Hont, A., Denoeud, F., Aury, J.-M., Baurens, F.-C., Carreel, F., Garsmeur, O., Noel, B., Bocs, S., Droc, G., and Rouard, M. (2012). The banana (*Musa acuminata*) genome and the evolution of monocotyledonous plants. Nature **488,** 213-217.

Dolezal, P., Aili, M., Tong, J., Jiang, J.-H., Marobbio, C.M., fung Lee, S., Schuelein, R., Belluzzo, S., Binova, E., and Mousnier, A. (2012). *Legionella pneumophila* secretes a mitochondrial carrier protein during infection. PLoS Pathog **8,** e1002459.

Eddy, S.R. (1998). Profile hidden Markov models. Bioinformatics **14,** 755-763.

Eddy, S.R. (2011). Accelerated profile HMM searches. PLoS Comput Biol **7,** e1002195.

Enright, A.J., Van Dongen, S., and Ouzounis, C.A. (2002). An efficient algorithm for large-scale detection of protein families. Nucleic Acids Res **30,** 1575-1584.

Finn, R.D., Clements, J., and Eddy, S.R. (2011). HMMER web server: interactive sequence similarity searching. Nucleic Acids Res **39,** W29-W37.

Finn, R.D., Mistry, J., Tate, J., Coggill, P., Heger, A., Pollington, J.E., Gavin, O.L., Gunasekaran, P., Ceric, G., and Forslund, K. (2010). The Pfam protein families database. Nucleic Acids Res **38,** D211-D222.

Giaever, G., Chu, A.M., Ni, L., Connelly, C., Riles, L., Veronneau, S., Dow, S., Lucau-Danila, A., Anderson, K., and Andre, B. (2002). Functional profiling of the *Saccharomyces cerevisiae* genome. Nature **418,** 387-391.

Goff, S.A., Ricke, D., Lan, T.-H., Presting, G., Wang, R., Dunn, M., Glazebrook, J., Sessions, A., Oeller, P., and Varma, H. (2002). A draft sequence of the rice genome (*Oryza sativa* L. ssp. japonica). Science **296,** 92-100.

Goodstein, D.M., Shu, S., Howson, R., Neupane, R., Hayes, R.D., Fazo, J., Mitros, T., Dirks, W., Hellsten, U., and Putnam, N. (2012). Phytozome: a comparative platform for green plant genomics. Nucleic Acids Res **40,** D1178-D1186.

Gregory, S.G., Sekhon, M., Schein, J., Zhao, S., Osoegawa, K., Scott, C.E., Evans, R.S., Burridge, P.W., Cox, T.V., and Fox, C.A. (2002). A physical map of the mouse genome. Nature **418,** 743-750.

Grigoriev, I.V., Nordberg, H., Shabalov, I., Aerts, A., Cantor, M., Goodstein, D., Kuo, A., Minovitsky, S., Nikitin, R., and Ohm, R.A. (2012). The genome portal of the department of energy joint genome institute. Nucleic Acids Res **40,** D26-D32.

Gross, W. (1989). Intracellular localization of enzymes of fatty acid-β-oxidation in the alga *Cyanidium caldarium*. Plant Physiol **91,** 1476-1480.

Haferkamp, I. (2007). The diverse members of the mitochondrial carrier family in plants. FEBS Lett **581,** 2375-2379.

Haferkamp, I., and Schmitz-Esser, S. (2012). The plant mitochondrial carrier family: functional and evolutionary aspects. Frontiers Plant Sci **3,** doi: 10.3389/fpls.2012.00002.

Hake, S., and Walbot, V. (1980). The genome of Zea mays, its organization and homology to related grasses. Chromosoma **79,** 251-270.

Hamel, P., Saint-Georges, Y., de Pinto, B., Lachacinski, N., Altamura, N., and Dujardin, G. (2004). Redundancy in the function of mitochondrial phosphate transport in *Saccharomyces cerevisiae* and *Arabidopsis thaliana*. Mol Microbiol **51,** 307-317.

Hu, T.T., Pattyn, P., Bakker, E.G., Cao, J., Cheng, J.-F., Clark, R.M., Fahlgren, N., Fawcett, J.A., Grimwood, J., and Gundlach, H. (2011). *The Arabidopsis lyrata* genome sequence and the basis of rapid genome size change. Nat Genet **43,** 476-481.

Huang, S., Li, R., Zhang, Z., Li, L., Gu, X., Fan, W., Lucas, W.J., Wang, X., Xie, B., and Ni, P. (2009). The genome of the cucumber, *Cucumis sativus* L. Nat Genet **41,** 1275-1281.

Jaillon, O., Aury, J.-M., Noel, B., Policriti, A., Clepet, C., Casagrande, A., Choisne, N., Aubourg, S., Vitulo, N., and Jubin, C. (2007). The grapevine genome sequence suggests ancestral hexaploidization in major angiosperm phyla. Nature **449,** 463-467.

Kämper, J., Kahmann, R., Bölker, M., Ma, L.-J., Brefort, T., Saville, B.J., Banuett, F., Kronstad, J.W., Gold, S.E., and Müller, O. (2006). Insights from the genome of the biotrophic fungal plant pathogen *Ustilago maydis.* Nature **444,** 97-101.

Keeling, P.J., Burger, G., Durnford, D.G., Lang, B.F., Lee, R.W., Pearlman, R.E., Roger, A.J., and Gray, M.W. (2005). The tree of eukaryotes. Trends Ecol Evol **20,** 670-676.

Kunji, E.R. (2004). The role and structure of mitochondrial carriers. FEBS Lett **564,** 239-244.

Leroch, M., Neuhaus, H.E., Kirchberger, S., Zimmermann, S., Melzer, M., Gerhold, J., and Tjaden, J. (2008). Identification of a novel adenine nucleotide transporter in the endoplasmic reticulum of Arabidopsis. Plant Cell **20,** 438-451.

Li, L., Stoeckert, C.J., and Roos, D.S. (2003). OrthoMCL: identification of ortholog groups for eukaryotic genomes. Genome Res **13,** 2178-2189.

Linka, N., and Weber, A.P. (2010). Intracellular metabolite transporters in plants. Mol Plant **3,** 21-53.

Linka, N., Theodoulou, F.L., Haslam, R.P., Linka, M., Napier, J.A., Neuhaus, H.E., and Weber, A.P.M. (2008). Peroxisomal ATP import is essential for seedling development in *Arabidopsis thaliana*. Plant Cell **20,** 3241-3257.

Lunn, J.E. (2007). Compartmentation in plant metabolism. J Exp Bot **58,** 35-47.

Mackenzie, S., and McIntosh, L. (1999). Higher plant mitochondria. Plant Cell **11,** 571-586.

Maurer-Stroh, S., Dickens, N.J., Hughes-Davies, L., Kouzarides, T., Eisenhaber, F., and Ponting, C.P. (2003). The Tudor domain 'Royal Family': tudor, plant agenet, chromo, PWWP and MBT domains. Trends Biochem Sci **28,** 69-74.

Merchant, S.S., Prochnik, S.E., Vallon, O., Harris, E.H., Karpowicz, S.J., Witman, G.B., Terry, A., Salamov, A., Fritz-Laylin, L.K., and Maréchal-Drouard, L. (2007). The Chlamydomonas genome reveals the evolution of key animal and plant functions. Science **318,** 245-250.

Ming, R., Hou, S., Feng, Y., Yu, Q., Dionne-Laporte, A., Saw, J.H., Senin, P., Wang, W., Ly, B.V., and Lewis, K.L. (2008). The draft genome of the transgenic tropical fruit tree papaya (*Carica papaya* Linnaeus). Nature **452,** 991-996.

Myburg, A., Grattapaglia, D., Tuskan, G., Jenkins, J., Schmutz, J., Mizrachi, E., Hefer, C., Pappas, G., Sterck, L., Van De Peer, Y., Hayes, R., and Rokhsar, D. (2011). The Eucalyptus grandis Genome Project: Genome and transcriptome resources for comparative analysis of woody plant biology. BMC Proc **5,** I20.

Nakamura, Y., Itoh, T., Matsuda, H., and Gojobori, T. (2004). Biased biological functions of horizontally transferred genes in prokaryotic genomes. Nat Genet **36,** 760-766.

Nakao, M., Okamoto, S., Kohara, M., Fujishiro, T., Fujisawa, T., Sato, S., Tabata, S., Kaneko, T., and Nakamura, Y. (2010). CyanoBase: the cyanobacteria genome database update 2010. Nucleic Acids Res **38,** D379-D381.

Nozaki, H., Takano, H., Misumi, O., Terasawa, K., Matsuzaki, M., Maruyama, S., Nishida, K., Yagisawa, F., Yoshida, Y., and Fujiwara, T. (2007). A 100%-complete sequence reveals unusually simple genomic features in the hot-spring red alga *Cyanidioschyzon merolae*. BMC Biol **5,** 28.

Palenik, B., Grimwood, J., Aerts, A., Rouzé, P., Salamov, A., Putnam, N., Dupont, C., Jorgensen, R., Derelle, E., and Rombauts, S. (2007). The tiny eukaryote Ostreococcus provides genomic insights into the paradox of plankton speciation. Proc Natl Acad Sci U S A **104,** 7705-7710.

Palmieri, F., Pierri, C.L., De Grassi, A., Nunes-Nesi, A., and Fernie, A.R. (2011). Evolution, structure and function of mitochondrial carriers: a review with new insights. Plant J **66,** 161-181.

Palmieri, L., Santoro, A., Carrari, F., Blanco, E., Nunes-Nesi, A., Arrigoni, R., Genchi, F., Fernie, A.R., and Palmieri, F. (2008). Identification and characterization of ADNT1, a novel mitochondrial adenine nucleotide transporter from Arabidopsis. Plant Physiol **148,** 1797-1808.

Paterson, A.H., Bowers, J.E., Bruggmann, R., Dubchak, I., Grimwood, J., Gundlach, H., Haberer, G., Hellsten, U., Mitros, T., and Poliakov, A. (2009). The *Sorghum bicolor* genome and the diversification of grasses. Nature **457,** 551-556.

Picault, N., Hodges, M., Palmieri, L., and Palmieri, F. (2004). The growing family of mitochondrial carriers in Arabidopsis. Trends Plant Sci **9,** 138-146.

Poirier, Y., and Bucher, M. (2002). Phosphate transport and homeostasis in Arabidopsis. Arabidopsis Book **1,** e0024. doi: 10.1199/tab.0024.

Price, D.C., Chan, C.X., Yoon, H.S., Yang, E.C., Qiu, H., Weber, A.P., Schwacke, R., Gross, J., Blouin, N.A., and Lane, C. (2012*). Cyanophora paradoxa* genome elucidates origin of photosynthesis in algae and plants. Science **335,** 843-847.

Prochnik, S.E., Umen, J., Nedelcu, A.M., Hallmann, A., Miller, S.M., Nishii, I., Ferris, P., Kuo, A., Mitros, T., and Fritz-Laylin, L.K. (2010). Genomic analysis of organismal complexity in the multicellular green alga *Volvox carteri*. Science **329,** 223-226.

Proost, S., Van Bel, M., Sterck, L., Billiau, K., Van Parys, T., Van de Peer, Y., and Vandepoele, K. (2009). PLAZA: a comparative genomics resource to study gene and genome evolution in plants. Plant Cell **21,** 3718-3731.

Pruitt, K.D., Tatusova, T., and Maglott, D.R. (2007). NCBI reference sequences (RefSeq): a curated non-redundant sequence database of genomes, transcripts and proteins. Nucleic Acids Res **35,** D61-D65.

Ramezani‐Rad, M., Hollenberg, C.P., Lauber, J., Wedler, H., Griess, E., Wagner, C., Albermann, K., Hani, J., Piontek, M., and Dahlems, U. (2003). The Hansenula polymorpha (strain CBS4732) genome sequencing and analysis. FEMS yeast research **4,** 207-215.

Rensing, S.A., Ick, J., Fawcett, J.A., Lang, D., Zimmer, A., Van de Peer, Y., and Reski, R. (2007). An ancient genome duplication contributed to the abundance of metabolic genes in the moss *Physcomitrella patens*. BMC Evol Biol **7,** 130.

Rensing, S.A., Lang, D., Zimmer, A.D., Terry, A., Salamov, A., Shapiro, H., Nishiyama, T., Perroud, P.-F., Lindquist, E.A., and Kamisugi, Y. (2008). The Physcomitrella genome reveals evolutionary insights into the conquest of land by plants. Science **319,** 64-69.

Rieder, B., and Neuhaus, H.E. (2011). Identification of an Arabidopsis plasma membrane-located ATP transporter important for anther development. Plant Cell **23,** 1932-1944.

Sánchez-Pulido, L., Devos, D., Genevrois, S., Vicente, M., and Valencia, A. (2003). POTRA: a conserved domain in the FtsQ family and a class of β-barrel outer membrane proteins. Trends Biochem Sci **28,** 523-526.

Saraste, M., and Walker, J.E. (1982). Internal sequence repeats and the path of polypeptide in mitochondrial ADP/ATP translocase. FEBS Lett **144,** 250-254.

Sato, S., Nakamura, Y., Kaneko, T., Asamizu, E., Kato, T., Nakao, M., Sasamoto, S., Watanabe, A., Ono, A., and Kawashima, K. (2008). Genome structure of the legume, *Lotus japonicus*. DNA Res **15,** 227-239.

Schmutz, J., Cannon, S.B., Schlueter, J., Ma, J., Mitros, T., Nelson, W., Hyten, D.L., Song, Q., Thelen, J.J., and Cheng, J. (2010). Genome sequence of the palaeopolyploid soybean. Nature **463,** 178-183.

Schneider, M., Lane, L., Boutet, E., Lieberherr, D., Tognolli, M., Bougueleret, L., and Bairoch, A. (2009). The UniProtKB/Swiss-Prot knowledgebase and its plant proteome annotation program. J Proteomics **72,** 567-573.

Shangguan, L., Han, J., Kayesh, E., Sun, X., Zhang, C., Pervaiz, T., Wen, X., and Fang, J. (2013). Evaluation of Genome Sequencing Quality in Selected Plant Species Using Expressed Sequence Tags. PloS ONE **8,** e69890.

Shih, P.M., Wu, D., Latifi, A., Axen, S.D., Fewer, D.P., Talla, E., Calteau, A., Cai, F., de Marsac, N.T., and Rippka, R. (2013). Improving the coverage of the cyanobacterial phylum using diversity-driven genome sequencing. Proc Natl Acad Sci U S A **110,** 1053-1058.

Slotte, T., Hazzouri, K.M., Ågren, J.A., Koenig, D., Maumus, F., Guo, Y.-L., Steige, K., Platts, A.E., Escobar, J.S., and Newman, L.K. (2013). The *Capsella rubella* genome and the genomic consequences of rapid mating system evolution. Nat Genet **45,** 831-835.

Stael, S., Rocha, A.G., Robinson, A.J., Kmiecik, P., Vothknecht, U.C., and Teige, M. (2011). Arabidopsis calcium-binding mitochondrial carrier proteins as potential facilitators of mitochondrial ATP-import and plastid SAM-import. FEBS Lett **585,** 3935-3940.

Swarbreck, D., Wilks, C., Lamesch, P., Berardini, T.Z., Garcia-Hernandez, M., Foerster, H., Li, D., Meyer, T., Muller, R., and Ploetz, L. (2008). The Arabidopsis Information Resource (TAIR): gene structure and function annotation. Nucleic Acids Res **36,** D1009-D1014.

Talon, M., and Gmitter, F.G. (2008). Citrus genomics. International Journal of Plant Genomics **2008**.

Thuswaldner, S., Lagerstedt, J.O., Rojas-Stutz, M., Bouhidel, K., Der, C., Leborgne-Castel, N., Mishra, A., Marty, F., Schoefs, B., Adamska, I., Persson, B.L., and Spetea, C. (2007). Identification, expression, and functional analyses of a thylakoid ATP/ADP carrier from Arabidopsis. J Biol Chem **282,** 8848-8859.

Tuskan, G.A., Difazio, S., Jansson, S., Bohlmann, J., Grigoriev, I., Hellsten, U., Putnam, N., Ralph, S., Rombauts, S., and Salamov, A. (2006). The genome of black cottonwood, *Populus trichocarpa* (Torr. & Gray). Science **313,** 1596-1604.

Van de Peer, Y., Maere, S., and Meyer, A. (2009). The evolutionary significance of ancient genome duplications. Nature Rev Genet **10,** 725-732.

Venter, J.C., Adams, M.D., Myers, E.W., Li, P.W., Mural, R.J., Sutton, G.G., Smith, H.O., Yandell, M., Evans, C.A., and Holt, R.A. (2001). The sequence of the human genome. Science **291,** 1304-1351.

Vogel, J.P., Garvin, D.F., Mockler, T.C., Schmutz, J., Rokhsar, D., Bevan, M.W., Barry, K., Lucas, S., Harmon-Smith, M., and Lail, K. (2010). Genome sequencing and analysis of the model grass Brachypodium distachyon. Nature **463,** 763-768.

Wang, X., Wang, H., Wang, J., Sun, R., Wu, J., Liu, S., Bai, Y., Mun, J.-H., Bancroft, I., and Cheng, F. (2011). The genome of the mesopolyploid crop species Brassica rapa. Nature genetics **43,** 1035-1039.

Winkler, U., Säftel, W., and Stabenau, H. (1988). β-oxidation of fatty acids in algae: localization of thiolase and acyl-CoA oxidizing enzymes in three different organisms. Planta **175,** 91-98.

Wistrand, M., and Sonnhammer, E.L. (2005). Improved profile HMM performance by assessment of critical algorithmic features in SAM and HMMER. BMC bioinformatics **6,** 99.

Worden, A.Z., Lee, J.-H., Mock, T., Rouzé, P., Simmons, M.P., Aerts, A.L., Allen, A.E., Cuvelier, M.L., Derelle, E., and Everett, M.V. (2009). Green evolution and dynamic adaptations revealed by genomes of the marine picoeukaryotes Micromonas. Science **324,** 268-272.

Xu, X., Pan, S., Cheng, S., Zhang, B., Mu, D., Ni, P., Zhang, G., Yang, S., Li, R., and Wang, J. (2011). Genome sequence and analysis of the tuber crop potato. Nature **475,** 189-195.

Contribution of the authors to manuscript 1

S.K.-V. wrote the manuscript and performed all analyses. **A.R.K.**, **C.E.** and **M.L.** supervised bioinformatics analyses and were involved in drafting the manuscript. **I.H.** participated in discussions and corrected the manuscript. **N.L.**, and **A.P.M.W.** participated in scientific discussions and assisted in drafting this manuscript. **N.L.** designed the research.

Outlook

Investigation of PHT3;3 in Arabidopsis

The identification of Arabidopsis MCF orthologs revealed that PHT3;3 clustered separately from PHT3;1 and PHT3;2. PHT3;3 was only present in embryophytes, whereas the other PHT3 proteins were universally conserved.

We aim to study the role of PHT3;3 in Arabidopsis, performing biochemical studies to unravel the substrate of PHT3;3 and analyzing mutant plants lacking PHT3;3 to study the impact *in planta*. We will express recombinant PHT3;1 and PHT3;3 proteins in yeast, isolate yeast membranes and reconstitute them into artificial lipid vesicles. First, we will assess whether the carriers are able to mediate a phosphate homoexchange, as yeast complementation studies suggested that PHT3 carriers are phosphate transporters (Hamel et al., 2004). If so, we expect recombinant PHT3;1 and PHT3;3 protein to mediate phosphate uptake. But as PHT3;3 seems to fulfill a different function and is land plant specific, we expect the carrier not to be a major phosphate transporter. Thus, we will test if PHT3;3 transport another substrate required in mitochondria, of which the transporters is unknown.

Arabidopsis mutants devoid of PHT3;3 will elucidate the impact of this carrier in plants. If the carrier has a unique function, we assume to observe growth phenotypes in Arabidopsis. If no phenotypes become obvious, the plants will be subjected to metabolite profiling assessing metabolic phenotypes. Promoter-GUS constructs will be created, observing tissue-specific promoter activity in plants.

Detailed characterization of the roles of PNC1 and PNC2 in Arabidopsis

We observed that peroxisomal MCF members, such as PNC1 and PNC2 are not present in red algae and glaucophytes. So far, PNC carriers were solely investigated in adenine nucleotide transport (Linka et al., 2008). We plan to perform a detailed biochemical characterization to explore the full substrate spectrum of PNC carriers. This might provide insights why PNC carriers are only found in green algae and plants. We plan to establish a double knockout line for PNC1 and PNC2 to further explore *in planta* functions of both carriers besides supplying ATP for fatty acid degradation. In this respect, transport modes will be studied. The yeast homolog of PNC1 and PNC2 exhibits a proton-coupled electroneutral import of ATP into peroxisomes (Lasorsa et al., 2004). Thus, it is likely that Arabidopsis PNCs also co-transport protons. We propose that under conditions where PNCs are strongly required, such as the degradation of fatty acids for seedling establishment (Linka et al., 2008), increased proton import could result in an acidification of the peroxisomal lumen. This, we will analyze determining the peroxisomal pH in wildtype and the double mutant line using a pH-sensitive green fluorescent protein biosensor (Moseyko and Feldman, 2001; Gao et al., 2004; Schulte et al., 2006; Shen et al., 2013). The peroxisomal pH in different plant tissues has not been studied before.

The role of AAC in rhodophytes and glaucophytes

Our analysis revealed the absence of direct AAC homologs in rhodophytes and glaucophytes. However, it is believed that in all eukaryotic organisms, which contain fully functional mitochondria, the existence of a mitochondrial ATP exporter is essential. It is proposed that the primary MCF transporter was an AAC transporter involved in mitochondrial energy passage (Haferkamp and Schmitz-Esser, 2012), thus we hypothesize that also red algae and glaucophytes are depending on mitochondrial ATP transport presumably facilitated by AACs. Nevertheless, certain AAC-like proteins are present, which could take over the function of AACs. Rhodophytes for example encode two ADNT1 proteins, which might export ATP against AMP. It was shown previously that the Arabidopsis ADNT1, which mediates the export of mitochondrial ATP against cytosolic AMP, exhibits also a low affinity for ADP (Palmieri et al., 2008). In contrast, glaucophytes contain only two putative nucleotide carriers (PM-ANT1, FOLT1 homologs). It might be interesting to analyze if these two proteins are dual-targeted.

We are interested in unraveling ATP transport in red algae and glaucophytes, isolating membranes of the glaucophyte *Cyanophora paradoxa* and the rhodophyte *Cyanidioschyzon merolae*. We will measure ATP exchange over these membranes in (i) untreated samples and (ii) in samples treated with the specific AAC inhibitor bongrekic acid (BKA) (Fiore et al., 1998). Analyses will reveal whether ATP exchange occurs and if this exchange is mediated by AACs, hence can be inhibited by BKA treatment. If ATP exchange is detectable and is not inhibited by BKA, we will try to identify the nature of the putative non-AAC ATP transporter. Finally, we intend to biochemically characterize the putative nucleotide carrier identified in our screen reconstituting recombinant proteins and performing *in vitro* uptake studies.

References

Fiore, C., Trezeguet, V., Le Saux, A., Roux, P., Schwimmer, C., Dianoux, A., Noel, F., Lauquin, G.-M., Brandolin, G., and Vignais, P. (1998). The mitochondrial ADP/ATP carrier: structural, physiological and pathological aspects. Biochimie **80,** 137-150.

Gao, D., Knight, M.R., Trewavas, A.J., Sattelmacher, B., and Plieth, C. (2004). Self-reporting Arabidopsis expressing pH and [Ca^{2+}] indicators unveil ion dynamics in the cytoplasm and in the apoplast under abiotic stress. Plant Physiol **134,** 898-908.

Haferkamp, I., and Schmitz-Esser, S. (2012). The plant mitochondrial carrier family: functional and evolutionary aspects. Front Plant Sci **3,** doi: 10.3389/fpls.2012.00002.

Hamel, P., Saint-Georges, Y., de Pinto, B., Lachacinski, N., Altamura, N., and Dujardin, G. (2004). Redundancy in the function of mitochondrial phosphate transport in *Saccharomyces cerevisiae* and *Arabidopsis thaliana*. Mol Microbiol **51,** 307-317.

Lasorsa, F.M., Scarcia, P., Erdmann, R., Palmieri, F., Rottensteiner, H., and Palmieri, L. (2004). The yeast peroxisomal adenine nucleotide transporter: characterization of two transport modes and involvement in DeltapH formation across peroxisomal membranes. Biochem J **381,** 581-585.

Linka, N., Theodoulou, F.L., Haslam, R.P., Linka, M., Napier, J.A., Neuhaus, H.E., and Weber, A.P. (2008). Peroxisomal ATP import is essential for seedling development in *Arabidopsis thaliana*. Plant Cell **20,** 3241-3257.

Moseyko, N., and Feldman, L. (2001). Expression of pH‐sensitive green fluorescent protein in *Arabidopsis thaliana*. Plant Cell Environ **24,** 557-563.

Palmieri, L., Santoro, A., Carrari, F., Blanco, E., Nunes-Nesi, A., Arrigoni, R., Genchi, F., Fernie, A.R., and Palmieri, F. (2008). Identification and characterization of ADNT1, a novel mitochondrial adenine nucleotide transporter from Arabidopsis. Plant Physiol **148,** 1797-1808.

Schulte, A., Lorenzen, I., Bottcher, M., and Plieth, C. (2006). A novel fluorescent pH probe for expression in plants. Plant Methods **2,** 7.

Shen, J., Zeng, Y., Zhuang, X., Sun, L., Yao, X., Pimpl, P., and Jiang, L. (2013). Organelle pH in the Arabidopsis endomembrane system. Mol Plant **6,** 1419-1437.

Manuscript 2

A plant-specific carrier involved in mitochondrial sulfate transport

Sarah K. Kessel-Vigelius[1*], Ilka Haferkamp[2], Christian Esser[3], Rüdiger Simon[4], Jianping Hu[5], Andreas P.M. Weber[1], and Nicole Linka[1a]

[1]Plant Biochemistry, Heinrich-Heine University Düsseldorf, 40225 Düsseldorf, Germany;
[2]Plant Physiology, Technical University of Kaiserslautern, 67663 Kaiserslautern, Germany;
[3]Bioinformatics, Heinrich-Heine University Düsseldorf, 40225 Düsseldorf, Germany;
[4]Plant Developmental Genetics, Heinrich-Heine University Düsseldorf, 40225 Düsseldorf, Germany;
[5]Department of Energy, Plant Research Laboratory, Michigan State University, East Lansing, Michigan-48823, USA

*First author
[a]Corresponding author

Abstract

Plant metabolism is interconnected across several compartments, which are surrounded by at least one lipid bilayer membrane. These organellar borders, such as the mitochondrial inner membrane, constitute a diffusion barrier for metabolites. Thus, specific solute carrier proteins are essential to regulate metabolite fluxes over membranes. Despite their significance for plant metabolism, the knowledge of carrier proteins is far from complete.

A family of three mitochondrial phosphate transport proteins (PHT3) in *Arabidopsis* was found to fuel mitochondrial ATP synthesis with inorganic phosphate. Our studies revealed that one PHT3 member shared less sequence identity with the Arabidopsis PHT3 proteins, as well as with known mitochondrial phosphate carriers from other species. This carrier exclusively clustered with land plant species, whereas the branch with other PHT3 proteins comprised fungi, algae and embryophytes, indicating a new plant-specific transport function in Arabidopsis, which differs from the other PHT3 carriers.

In vitro uptake assay with recombinant protein revealed that this unique transporter prefers inorganic sulfate as substrate instead of phosphate. Based on our biochemical data we named this carrier protein SIT1 for inorganic sulfate transporter. Plants lacking *SIT1* transcript showed decelerated plant growth, delayed germination and abnormal seed development, which might indicate an essential role of SIT1in these processes. Here we discuss a putative link between SIT1-mediated sulfate transport and the replenishment of the TCA cycle with dicarboxylic acids.

Introduction

Mitochondria are ubiquitous organelles of the plant cell involved in numerous complex biochemical processes, such as cellular energy supply via tricarboxylic acid cycle and oxidative phosphorylation. The tricarboxylic acid cycle provides reducing equivalents, which are fed into the electron transport chain to drive the synthesis of ATP from ADP and inorganic phosphate (Pi) (Fernie et al., 2004; Bowsher et al., 2007). Besides respiration, these organelles play an essential role in nitrogen and sulfur assimilation, photorespiration, crassulacean acid metabolism, C_4 photosynthesis and C_1 metabolism (Mackenzie and McIntosh, 1999; Fernie et al., 2004; Palmieri et al., 2011).

These metabolic activities require balanced fluxes of metabolites between mitochondria and other compartments, since numerous mitochondrial pathways are multi-compartmented. A tight intra-organeller connection exists between mitochondria, plastids, peroxisomes and the cytosol (Mackenzie and McIntosh, 1999; Scott et al., 2007). To supply mitochondrial metabolism with intermediates, transport proteins are required to mediate the flux of solutes across both mitochondrial membranes. The outer mitochondrial membrane contains voltage-dependent anion channels, allowing the free diffusion of solutes up to 4-5 kDa, whereas the inner membrane constitutes a selective barrier, containing a diverse set of specific carrier proteins (Linka and Weber, 2010).

A large quantity of inner mitochondrial membrane proteins, such as the ADP/ATP carrier, the adenine nucleotide carrier, or the dicarboxylate carrier belong to a class of transporters called mitochondrial carrier family (MCF) (Haferkamp, 2007; Palmieri et al., 2008a; Palmieri et al., 2008b). Features of this transporter class are a molecular mass of 30-40 kDa, six transmembrane spans, the tripartite structure of homologous domains and a characteristic amino acid sequence motif (Haferkamp and Schmitz-Esser, 2012). The majority of MCF carriers localizes to mitochondria, but transporters of this class are also found in membranes of other compartments (Bedhomme et al., 2005; Bouvier et al., 2006; Thuswaldner et al., 2007; Kirchberger et al., 2008; Leroch et al., 2008; Linka et al., 2008; Bernhardt et al., 2012a). In Arabidopsis, only a quarter of MCF proteins are functionally characterized to date (Palmieri et al., 2011). However, the numerous metabolic functions of mitochondria require the presence of additional, yet uncharacterized solute transporters.

One essential transport step at the mitochondrial membrane is Pi import to fuel ATP synthesis. MCF transporters facilitate the uptake of Pi into the mitochondrial matrix. In *Saccharomyces cerevisiae* two MCF members Pic2p (YER053c) and Mir1p (YJR077c) enable the Pi supply of mitochondria. It was shown that the absence of both carriers disrupts mitochondrial Pi import and consequently leads to drastic phenotypes. A yeast double mutant deficient in Mir1p and Pic2p (Δ*mir*Δ*pic*) is not able to grow on non-fermentable carbon sources, because it does not generate ATP via respiration, as Pi availability in the mitochondrial matrix is drastically limited (Zara et al., 1996; Hamel et al., 2004). This indicates that Pic2p and Mir1p are functionally redundant. Expression analyses revealed Pic2p as minor isoform. It is less abundant than Mir1p under standard conditions, but is highly expressed at high temperatures (Hamel et al., 2004). A recent study identified Pic2p as copper transporter (Vest et al., 2013). Nevertheless, both genes need to be deleted to fully abolish mitochondrial phosphate import.

In plants, Pi import into mitochondria is presumably facilitated by members of the PHT3 family (Poirier and Bucher, 2002), which in other reports is termed AT (Hamel et al., 2004), MPT (Zhu et al., 2012) or PiC family (Linka and Weber, 2010). The Arabidopsis PHT3 family comprises three genes: PHT3;1 (At5g14040), PHT3;2 (At3g48850) and PHT3;3 (At2g17270) (Poirier and Bucher, 2002; Picault et al., 2004). It is assumed that PHT proteins, like their mammalian counterparts (Stappen and Kramer, 1994; Wohlrab and Briggs, 1994), import phosphate either in a Pi/H^+ symport, a Pi/OH^- antiport mechanism, or as Pi homo-exchange (Liu et al., 2011). However, little is known about their *in vivo* roles (Chen et al., 2008).

Yeast complementation studies revealed a Pi transport capacity for PHT3;1 and PHT3;2, whereas this function could not be verified for PHT3;3 (Hamel et al., 2004). When expressed in the Δ*mir*Δ*pic* yeast mutant, PHT3;1 and PHT3;2, but not PHT3;3 restored phosphate transport activities (Hamel et al., 2004). This implies that (1) PHT3;3 displays a different transport function, (2) PHT3;3 is not functionally expressed in yeast, or (3) PHT3;3 is not targeted to yeast mitochondria. The reason for an unsuccessful complementation with PHT3;3 was not further investigated by Hamel

and colleagues. However, it needs to be solved to understand the role of PHT3;3 in Arabidopsis. Several indications imply a unique function for PHT3;3 different to the other PHT3 proteins. The predicted transmembrane topology of PHT3;3 varies from PHT3;1 and PHT3;2 (Zhu et al., 2012). Furthermore, PHT3;3 exhibits a distinct gene expression pattern in Arabidopsis that differs from that of PHT3;1 and PHT3;2 (Zhu et al., 2012). Due to its biochemical function characterized in this study, we named PHT3;3 hereafter inorganic sulfate transporter 1 (SIT1).

Our study provides evidences that SIT1 does not represent a major phosphate transporter, but instead fulfills a novel plant-specific function in mitochondria. Phylogenetic analyses revealed that SIT1 exhibits basic features of a mitochondrial phosphate transporter, but shows lowest identity with mitochondrial phosphate transporters from other species, such as yeast or mammals. We found that SIT1 specifically groups with land plant species, whereas the PHT3;1 and PHT3;2 containing clade of the phylogenetic tree comprises fungal, algal and higher plant species. *In vitro* uptake experiments with recombinant SIT1 protein demonstrated a higher preference for sulfate than for phosphate. Studies with an Arabidopsis mutant deficient in SIT1 showed phenotypic abnormalities, including impaired germination, late flowering, or misshaped embryos, indicating a putative role in plant development. We hypothesize that SIT1 acts as a sulfate importer that might metabolically interacts with other MCF carriers such as mitochondrial DIC transporters specific for dicarboxylic acid/sulfate exchange.

Experimental procedures

Materials

Chemicals and reagents were purchased from Sigma-Aldrich (http://www.sigmaaldrich.com), Promega (http://www.promega.com) and Bio-Rad (http://www.bio-rad.com/). Enzymes and molecular reagents for recombinant DNA techniques were obtained from New England Biolabs (http://www.neb.com), Thermo Fisher Scientific (http://www.thermoscientificbio.com/fermentas/), and Qiagen (http://www.qiagen.com). Plant growth media and plant agar were purchased from Duchefa BV.

Cloning procedures

In silico DNA sequences for cloning were downloaded from the Aramemnon webserver (http://aramemnon.uni-koeln.de) and Saccharomyces Genome Database (http://www.yeastgenome.org/). Cloning was performed according to standard molecular techniques (Sambrook et al., 1989). Sequences were verified by DNA sequencing (GATC Biotech, http://www.gatc-biotech.com). Primers were synthesized by Sigma-Aldrich. The sequences of all primers generated for this study are listed in the supplementary data table S1.

Plant material and growth conditions

Wildtype *Arabidopsis thaliana* (ecotype Columbia) was obtained from the European Arabidopsis Stock Centre (NASC) at the University of Nottingham (http://arabidopsis.info). The *sit1-1*T-DNA line

(GK432A12) was obtained from Gabi-Kat consortium at the University of Bielefeld (http://www.gabi-kat.de).The homozygous *sit1-2*T-DNA line (SAIL591_H09) was provided by Dr. Ilka Haferkamp, University of Kaiserslautern.

Seeds were surface-sterilized, stratified for 2 d at 4°C and then germinated on half-strength MS plates, solidified with 0.8% (w/v) plant agar. For further analyses plants were transferred to soil after 14 d on agar plates and incubated under long-day conditions with 16 h light/ 8 h dark cycles at 22°C/18°C, 100 µmol m^{-2} s^{-1} and about 70% humidity unless stated otherwise. Arabidopsis wild-type plants were stably transformed using a modified floral dip protocol (Zhang et al., 2006; Bernhardt et al., 2012b). Transgenic plants were selected on appropriate antibiotics MS plates.

Isolation of T-DNA insertion line GK432A12

The T-DNA line *sit1-1* was screened with PCR-based methods to identify homozygous lines for *sit1-1.* A gene-specific primer combination SV179/SV180 and a gene/T-DNA junction primer combination SV180/P52 were used.

Reverse transcriptase-polymerase chain reaction (RT-PCR)

To analyze transcript levels in the *sit1-1* mutant, RNA was isolated from rosette leaf material according to the protocol published by (Chomczynski and Sacchi, 1987). cDNA synthesis was performed using the SuperScript II Reverse Transcriptase (Promega). SIT1 was amplified using the primers SV80 and SV82. The *ACT7* gene was amplified as cDNA quality control with P67 and P68.

Phenotypic observations of mutants

Wildtype and mutant were germinated on half-strength MS agar plates and transferred to soil. After six weeks plants were photographed.

Early seedling development assay

Wildtype and *sit1* seeds were surface sterilized and germinated on half-strength MS agar plates. After 6 d seedlings (N = 250) were counted and developmental phenotypes were documented according to the four given stages. I: Radicle not emerged; II: Radicle emerged; III: Cotyledons expanded, IV: Cotyledons fully expanded/true green leaves. Stages I and II were classified as germination, stages II and IV as early plant establishment.

Root growth analysis

Root growth of *sit1* was analyzed, growing seedlings vertically on 0.5 x MS agar plates under long day conditions. After 12 days root lengths were measured and analyzed with Macbiophotonics ImageJ (www.macbiophotonics.ca/imagej).

Seed analysis and chloral hydrate clearing

To analyze seed morphology, siliques were split longitudinally along their natural dehiscence under a dissecting microscope. The valves were separated to examine the seeds. Chloral hydrate clearing was performed to make seed embryos visible, without removing the seed coat. Siliques or seeds

were incubated in a chloral hydrate/glycerol/water solution (8:1:2, w/v/v) over night at room temperature. The chloral hydrate solution was replaced with 70% (v/v) ethanol for microscopy. Embryos were observed with phase-contrast microscopy (Eclipse Ti, Nikon) or a dissecting microscope (SMZ1500, Nikon).

Flowering time analysis

To measure growth retardation of the *sit1* mutant in comparison to wildtype, the onset of flowering was monitored in *sit1* and wildtype. Flowering time was determined under long days for 25 plants per line. Rosette and cauline leaves were counted on plants, which had bolted and had an inflorescence of 6-10 cm.

GUS assay

A promoter::β-glucuronidase (GUS) assay was performed to examine SIT1 promoter activity in Arabidopsis. A construct (pSV158) was generated fusing a 1121-kb *SIT1* promoter to the GUS gene (Jefferson et al., 1987) in the vector pMDC163 (Curtis and Grossniklaus, 2003). The promoter was amplified with Gateway primers SV87/SV88 by standard proof-reading PCR. The PCR fragment was subcloned in pDONOR207 and finally introduced into pMDC163 by Gateway cloning. Tissue samples or seedlings (10 d-old) were collected and stained with GUS solution (0.1 M NaH_2PO_4 (pH 7.0), 10 mM Na-EDTA, 0.5 mM $K_3[Fe(CN)_6]$, 0.5 mM $K_4[Fe(CN)_6]$ x $3H_2O$, 0.1% Triton X-100, 1 mM X-Gluc). Tissues were incubated in GUS staining solution three times for 5 min under vacuum and stored at 37°C until the staining became visible. The GUS stain was fixed for 10 min at 65°C in fixation solution (50% (v/v) ethanol, 5% (v/v) glacial acetic acid, 3.7% (v/v) formaldehyde). Chlorophyll was removed with 80% (v/v) ethanol solution for 10-30 min at 65°C. GUS-stained tissues were observed under a dissecting microscope (Stemi2000C with AxioCam ICc3 camera and a cold light source KLI500, Carl Zeiss).

Transient expression of SIT1 YFP-fusions in N. benthamiana

A EYFP-fusion construct was generated and expressed in tobacco to visualize the subcellular localization of SIT1. The coding sequence of SIT1 was amplified with SV80 and SV81 and subcloned into pDONOR207. For expression SIT1 was recombined into pGW-YFP (pSV126) or YFP-pGW (pSV129) (Reumann et al., 2009). Tobacco leaves were co-infiltrated with the expression construct and a peroxisomal marker CFP-PTS1. After 3 days expression was examined with a confocal microscope (LSM 510 Meta, Carl Zeiss).

Protein biochemistry

Protein analysis via SDS-PAGE and immunoblot analysis was performed according to standard protocols (Hause et al., 2003). For immunodetection, either an α-polyhistidine HPR-conjugated mouse IgG1 antibody (MACS molecular, http://www.miltenyibiotec.com), or a monoclonal α-pentahistidine mouse antibody (Qiagen)/ alkaline phosphatase-conjugated anti-mouse IgG

(Promega) was used. Protein concentrations were determined in a bichinonic acid assay (Thermo Fisher Scientific, http://www.thermofisher.com).

Recombinant protein expression in yeast

SIT1 and the two PHT3 proteins from Arabidopsis were recombinantly expressed in yeast. The corresponding coding sequences were amplified by standard PCR methods using the following att-primers: SV28/SV29 (PHT3;1), SV77/SV78 (PHT3;2), SV80/SV81 (SIT1). Via Gateway cloning entry clones in pDONOR 207 were generated. For C-terminal His-tag fusion of the target proteins, the three entry clones were recombined into pYES-DEST52 (Invitrogen). The resulting expression vectors for PHT3;1 (pSV17b), PHT3;2 (pSV107) and SIT1 (pSV108) were transformed into the yeast strain FGY217 (genotype: MATα ura3-52 lys2Δ201 pep4Δ (Kota et al., 2007). Yeast cells were transformed according to standard protocols for lithium acetate/PEG transformation (Gietz and Schiestl, 2007).

The protocol for recombinant protein expression was adapted from (Drew et al., 2008). A single yeast colony was inoculated in 150 mL yeast nitrogen base (YNB) with 2% glucose (w/v), but without uracil (YNB -ura; 0.67% (w/v) YNB, 0.1% (w/v) adenine, arginine, cysteine, leucine, lysine, threonine, tryptophan, 0.05% (w/v) aspartic acid, histidine, serine, isoleucine, phenylalanine, methioine, proline, tyrosine, valine). The cells were grown over night in an orbital shaker at 30°C and 280 rpm. The overnight culture was diluted to an OD_{600} of 0.12 in 500 mL YNB –ura supplied with 0.1% (w/v) glucose. At an OD_{600} of 0.6 protein expression was induced by adding 2% (w/v) galactose. Yeast cells were harvested by centrifugation (10 min at 4,000 x*g*) after 22 h of incubation at 30°C and 280 rpm. Until further processing, the cells were stored at -80°C after decanting the supernatant and snap-freezing the pellet.

Isolation of yeast membranes

Yeast pellets were re-suspended in CR buffer (50 mM Tris-HCl (pH 7.6), 1 mM EDTA, 0.6 M sorbitol) supplied with cOmplete ULTRA protease inhibitor (Roche, http://www.roche.de). Yeast cells (1g cells/ 3 mL CRB) were broken in a heavy-duty cell disruptor (Constant Systems Ltd., http://www.constantsystems.com) at incremental pressures of 25, 30, 32 and 35 kpsi for four passes at 4°C. Unbroken cells and cell debris were removed by centrifugation at 10,000 x*g* for 10 min. The supernatant was transferred in ultra-clear polyallomer tubes. Membranes were enriched by ultracentrifugation at 100,000 x*g* for 45 min at 4°C. The yeast pellets were re-suspended in MR buffer (20 mM Tris-HCl (pH 7.6), 1 mM $CaCl_2$ and 0.6 M sucrose) and stored at -80°C.

Generation of the ΔmirΔpic double yeast mutants by mating

The two single knockout yeast lines Δ*mir* (accession: Y06897; phenotype: BY4742; Mat α; his3D1; leu2D0; lys2D0; ura3D0; YER053c::kanMX4) and Δ*pic* (accession: Y10188; phenotype: BY4741; Mat a; his3D1; leu2D0; lys2D0; ura3D0; YJR077c::kanMX4) were ordered at Euroscarf (http://web.uni-frankfurt.de/fb15/mikro/euroscarf/index.html).

The double mutant Δ*mir*Δ*pic* was generated by mating *mir*Δ and *pic*Δ (Treco and Winston, 2001). Sporulation was induced in liquid sporulation medium (1% (w/v) potassium acetate, 0.05% (w/v) zinc acetate). Spores released from ascii by zymolase treatment (1 mg/mL) were dispersed by sonication (75% output power, 30 s, two cycles). Spores were plated on YNB –methionine –lysine + 0.2 mg/mL G418 (Sigma-Aldrich) (Treco and Winston, 2001) and randomly selected for the growth phenotype on glycerol reported in (Hamel et al., 2004). All stages of yeast mutant generations were investigated by light microscopy (Eclipse Ti, Nikon). Double mutants were isolated. To analyze yeast chromosomal DNA, cell walls were digested with lyticase (60 U/mL in 0.5 M NaPi. pH 7.0) for 30 min at 30°C and DNA was released after boiling the digested cells for 10 min. Cell debris were removed by centrifugation. Gene deletions were confirmed by PCR analysis.

Complementation assay and localization studies in ΔmirΔpic

To complement the Δ*mir*Δ*pic* mutant, protein constructs without affinity tag were generated. The coding sequences of the Arabidopsis PHT3 proteins, SIT1 and the yeast phosphate carrier *MIR1* were amplified by standard PCR, fusing Gateway attachments to both sites of the genes (PHT3;1, SV28/SV30; PHT3;2, SV77/SV79; SIT1, SV80/82; *MIR1*, SV156/SV170). Amplicons were recombined into pDONOR207 and subsequently introduced into the expression vector pRS426-GPD-ccdB (Addgene) via Gateway cloning. The expression clones pSV135 (PHT3;1), pSV138 (PHT3;2), pSV141 (SIT1), and pSV185 (*MIR1*) were transformed into Δ*mir*Δ*pic* (Gietz and Schiestl, 2007). Yeast cells were grown for 3 days on YNB –uracil supplemented with 2% (v/v) ethanol and G418 (0.2 mg/mL) as selective agent.

A C-terminal EYFP-fusion was used to localize SIT1 and Mir1p as mitochondrial control in yeast. Corresponding gateway constructs, pSV142 and pSV148, were generated and transformed into Δ*mir*Δ*pic*. Yeast cells were grown at 30°C in liquid culture over night (YNB- ura +G418). Cells were harvested by centrifugation for 5 min at 3,000 rpm. Cells were washed with wash buffer (25 mM Hepes-KOH (pH 7.3), 10 mM $MgCl_2$) before they were stained with 50 µM MitoTracker Red CMXRos (Invitrogen) for 10 min at room temperature. To remove residual Mito Tracker dye cells were washed with wash buffer twice. Yeast cells were immobilized on poly-L-Lysine (Sigma) coated microscope slides for confocal microscopy. Analysis of yeast cells was performed with a confocal laser scanning microscope LSM 510 Meta (Carl Zeiss). The x63/1.4 Oil DIC objective was chosen, pixel time was set to 1.27 µs and the pinhole was set to 100 µm. MitoTracker Red-labeled mitochondria were excited at 561 nm, fluorescence emission was detected with a 575-nm to 615-nm band pass filter. SIT1 and Mir1p proteins fused to EYFP were excited at 488 nm, emission was recorded with a 505-nm to 550-nm band-pass filter.

Reconstitution and transport activity assays in liposomes

Yeast membranes were reconstituted into L-α-phosphatidylcholine/cardiolipin liposomes (95:5) by freeze-thaw-sonication procedure for *in vitro* uptake studies (Kasahara and Hinkle, 1976; Palmieri et al., 1995).

Proteoliposomes were either preloaded with 30 mM $H_2PO_4^-$, 30 mM K_2SO_4, or produced without pre-loading (negative control). Counter-exchange substrate, which was not incorporated into proteoliposomes during reconstitution, was removed with gel filtration on Sephadex G-25M columns (GE Healthcare, http://www.gehealthcare.com).

Transport assays were started by adding 0.3 mM [^{32}P]-phosphoric acid or 0.3 mM [^{35}S]-sulphuric acid (Hartmann Analytic, http://www.hartmann-analytic.de/). The uptake reaction was terminated passing proteoliposomes over Dowex AG1-X8 anion-exchange columns, binding the non-incorporated radiolabelled phosphate or sulfate by chromatography. The incorporated radiolabeled compounds were analyzed by liquid scintillation counting. Data fitting was performed with GraphPad Prism 5.0 software (GraphPad, http://www.graphpad.com).

To test the activity of SIT1, a sulfate efflux experiment was designed. Homo-exchange of 30 mM $sulfate_{in}$/ 0.3 mM $sulfate_{out}$ was followed over time. After 32 min 200 mM K_2SO_4 was added externally to induce possible efflux of radiolabelled sulfate out of the proteoliposomes. Competitive inhibition assays were set up as sulfate homo-exchange transport assay (30 mM $K_2SO_{4\ in}$/0.3 mM $K_2SO_{4\ out}$). After 5 min 1.5 mM competition substrate was added.

Phylogenetic analysis of putative PHT3 carriers

Proteomic information for tree analysis was retrieved from Ensembl Genome Database (http://www.ensembl.org) whenever possible (Needleman and Wunsch, 1970). Following archaeplastida species were included: *Arabidopsis thaliana*, *Brachypodium distachyon, Brassica rapa, Glycine max, Lotus japonicus, Ricinus communis, Vitis vinifera, Oryza sativa japonica, Sorghum bicolor, Physcomitrella patens, Selaginella moellendorffii, Chlamydomonas reinhardtii, Cyanidioschyzon merolae, Cyanophora paradoxa, Micromonas pusilla CCMP 1545.* Following fungal species were included: *Saccharomyces cerevisiae, Hansenula polymorpha, Ustilago maydis.* As animal species we integrated *Mus musculus* and *Homo sapiens.* The *Lotus japonicus* proteome was downloaded from the PLAZA database (http://bioinformatics.psb.ugent.be/plaza/) (Arimura et al., 2008). *Cyanidioschyzon merolae* protein sequences were obtained from the *Cyanidioschyzon merolae* Genome Project (http://merolae.biol.s.u-tokyo.ac.jp) (Fernie et al., 2004). The *U. maydis* proteome was downloaded from the MIPS FTP server (ftp://ftpmips.gsf.de/ustilago/Umaydis_valid/Umaydis_valid_orf_prot_121009) (Bowsher and Tobin, 2001). If proteomes contained splice variants, they were filtered for the longest splice variant, which was kept.

Orthologous protein sequences were grouped with the OrthoMCL algorithm to group species-specific gene families (Scott et al., 2007). A phylogenetic tree was constructed from sequences of clusters containing putative PHT3 members with RAxML (Nakamori et al., 2002). Nonparametric bootstrapping with 100 replicates was performed. The phylogenetic tree was visualized with Fig Tree (http://tree.bio.ed.ac.uk/software/figtree/). A global sequence alignment was

performed on the basis of the Needleman-Wunsch algorithm. The alignment matrix obtained was plotted in R.

Domain mapping and architecture of PHT3 carriers

To gain deeper structural insights, PHT3 carriers were screened for Pfam-A domains with the *hmmscan* mode of HMMER3.0. The carrier sequences were used as query against the Pfam-A database (Eddy, 2011). A database was created with HMMER, compressing and indexing the flatfiles for scanning. For Pfam-A domains the model-defined gathering threshold was used (Ekman et al., 2007; Finn et al., 2011). Pfam-A per-domain outputs were combined and searched for overlapping domains. The longest domain was kept and the shorter was neglected (Kersting et al., 2012). Visualization of domain occurrence and arrangements was performed with DoMosaics (http://domosaics.net/) (Moore and Bornberg-Bauer, 2012; Moore et al., 2013). Likely false positive fragmentary domain assignments with an E-value $>10^{-6}$ were removed.

Results

Phylogenetic analyses reveal a unique position for Arabidopsis SIT1

In phylogenetic analyses of the mitochondrial carrier family from Arabidopsis, SIT1 encoded by At2g17270 forms a subcluster with the two phosphate carriers PHT3;1 (At5g14040) and PHT3;2 (At3g48850) (Picault et al., 2004). To unravel the relationship of Arabidopsis SIT1 to PHT3 proteins in more detail, we screened for putative homologs in various primary photosynthetic plants, fungi and animals. We calculated an unrooted phylogenetic tree, which revealed the existence of 55 carriers in the proteomes of 21 eukaryotic organisms (Tab. S1). All proteomes contained at least one to a maximum of eight homologous proteins.

A phylogenetic analysis of the putative PHT3 proteins revealed two major clades, one covering PHT3;1 and PHT3;2 proteins (clade A), and a second composed of SIT1 and its homologs (clade B) (Fig. 1). Clade A was constituted of subclades comprising algal and fungal sequences (clade C). The PHT3;1/PHT3;2 clade branched off from the fungal subclade and was closely related to human and mouse sequences, which split off from the fungal clade separately. The SIT1 branch was exclusively formed by embryophytic proteins, *i.e*. mosses and higher plant species, whereas no algal, mammalian or fungal sequences were included.

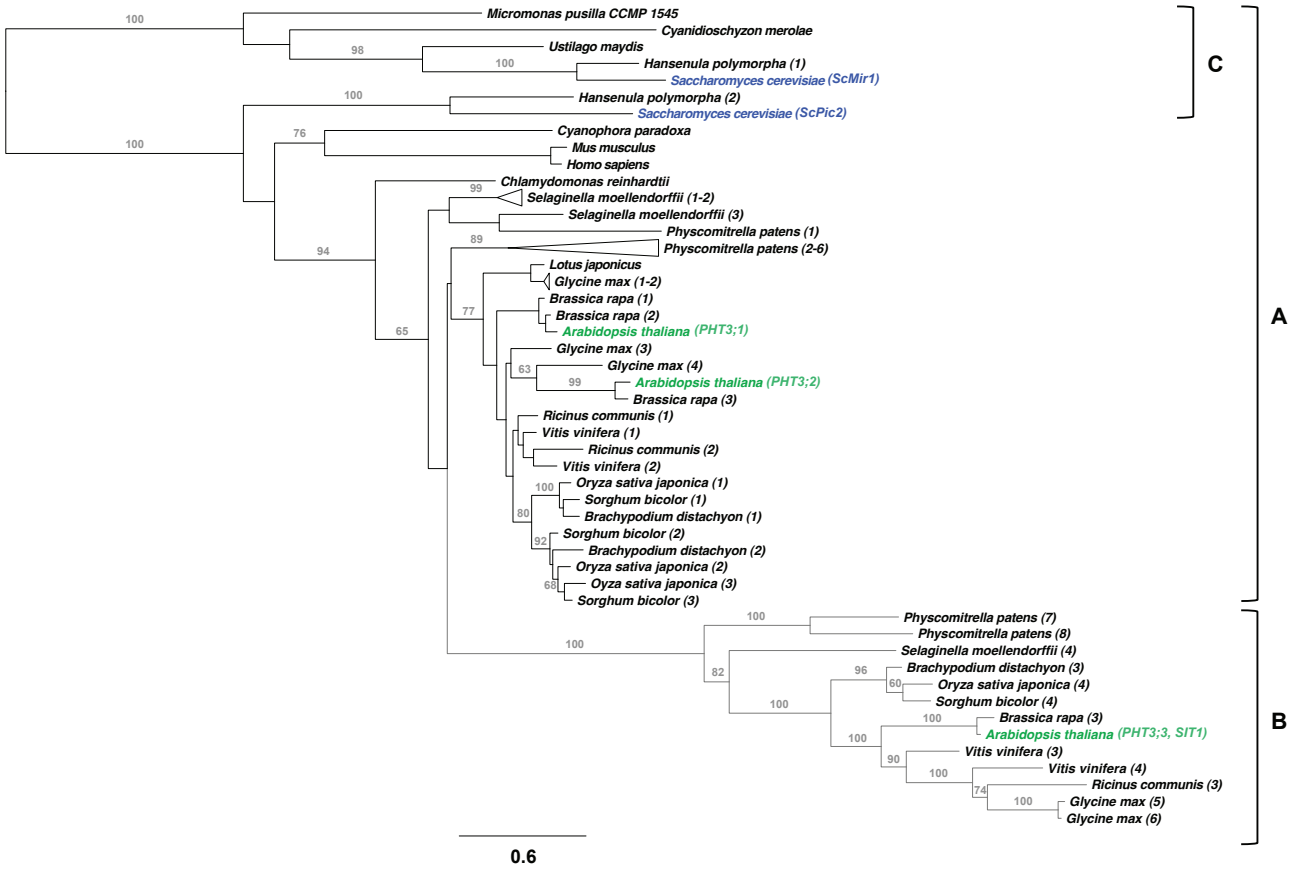

Fig. 1: Phylogenetic tree of PHT3;1, PHT3;2 and SIT1 proteins in archaeplastida, fungi and animals.
Numbers above branches indicate RAxML calculated bootstraps. Only bootstrap values ≥ 60% are shown. Branch lengths are proportional to the number of substitutions per site (see scale bar). The names of the *Arabidopsis* proteins used for the query are indicated in green. *Saccharomyces cerevisiae* orthologs are indicated in blue. If more than one gene/species is depicted in the tree, the genes are numbered from top to bottom. Triangles indicate collapsed clades. PHT3;3 is also referred to as SIT1 in this paper.

To investigate the global sequence identity of all carriers isolated from the phylogenetic tree, we performed a global sequence alignment based on the Needleman-Wunsch algorithm (Needleman and Wunsch, 1970). In global alignments sequences are aligned across their entire length including gap positions, whereas local alignments only align certain regions of arbitrary length, without any penalty for gaps (Chenna et al., 2003). To visualize the obtained results, a graph was generated depicting the percentages of sequence identity of amino acids plotted against each other in a color-coded scale from 0% (white) to 100% (red). White lines were used to separate clusters (Fig. 2).

The plot reflected the results gained from the phylogenetic tree. The global alignment plot contained two large clusters and two small sequence clusters, which match the clades of the phylogenetic tree (Fig. 1). It became evident that PHT3;1 and PHT3;2 share a higher level of global identity (70%) with each other, than with SIT1 (40-50%). Moreover, SIT1 shared higher identity with sequences of cluster B (55-99%) than with the largest cluster A, containing PHT3;1 and PHT3;2 (40-90%). Finally, SIT1 was less identical to mammalian and fungal sequences than PHT3;1 and PHT3;2.

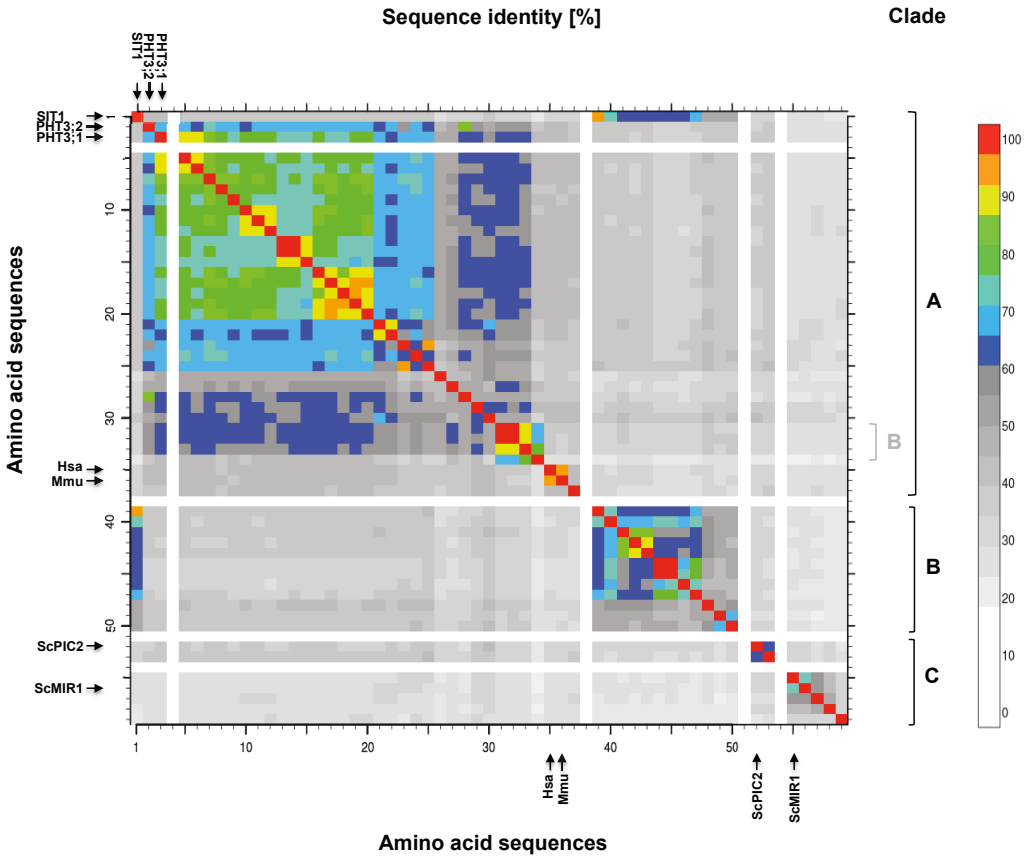

Fig. 2: Plot of global sequence alignments of PHT3;1, PHT3;2 and SIT1 proteins in archaeplastida, fungi and animals.
Global sequence alignment analysis was performed using the Needleman-Wunsch alignment algorithm. The color scale indicates the level of global sequence identity (white, 0% to red, 100%) from low to high. White lines in plot are cluster separators. The three Arabidopsis proteins are indicated above, as well as the orthologs from human (Hsa), mouse (Mmu) and yeast (*MIR1* and *PIC2*). The clades of the phylogenetic tree (Fig. 1) are marked on the right.

As phylogeny revealed a unique position for SIT1, we examined if protein domains differed between SIT1 and the other PHT3 proteins. Domains are regions in proteins, which are considered the units of function, structure and evolution (Moore et al., 2008; Kersting et al., 2012). Proteins are known to evolve to new functions or specificities by domain fusion, recombination, loss, exchange, or differentiation of existing domains (Björklund et al., 2005). In plants, roughly 50% of proteins are covered by domain annotations (Kersting et al., 2012). We screened PHT3 carriers for Pfam-A domains with the *hmmscan* mode of HMMER3.0 (Finn et al., 2010; Eddy, 2011; Finn et al., 2011). PHT3 carrier sequences contain three repeats of the mitochondrial carrier family-specific domain PF00153, which consists mainly of the specific sequence motif PX[D/E]XX[K/R]-(20-30 residues)-[D/E]GXXXX[W/Y/F][K/R]G (Palmieri et al., 2011). Whereas positions of PF00153 domains were largely identical in PHT3;1 and PHT3;2, domain positioning differed in SIT1. This difference was caused by the lack of the longer N-terminal stretch preceding the first transmembrane domain, which was present in PHT3;1 and PHT3;2, but absent in SIT1 (Fig. S1). This N-terminal sequence extension contained the mitochondrial target signal. In sum, we did not identify any additional Pfam-

A domains in SIT1, all proteins exhibit three repeats of the MCF carrier sequence motif PF00153.

The phylogenetic analysis suggested that SIT1 proteins represent a subfamily distinct from the group of PHT3;1 and PHT3;2 proteins that was newly established in land plants. Thus, we assumed that in the course land plant evolution speciation of SIT1 might have occurred. However, on protein level we did not observe significant differences in domain occurrence or architecture that might explain considerable speciation of SIT1.

SIT1 does not complement a mutant deficient in mitochondrial phosphate transport, although it localized to yeast mitochondria

First we addressed the question, whether SIT1 was functionally redundant to PHT3;1 and PHT3;2, or whether SIT1 had a unique transport function (Takabatake et al., 1999; Hamel et al., 2004). We expressed the Arabidopsis proteins in a yeast mutant deficient in the mitochondrial Pi carriers Pic2p (YER053c) and Mir1p (YJR077c). Although the lack of Mir1p was sufficient to abolish Pi import into mitochondria, we generated a double mutant (Δ*mir*Δ*pic*) (Hamel et al., 2004; Vest et al., 2013). We mated a *mir1*-null and *pic2*-null strain and performed a random spore selection to identify a double mutant. The deletion of *PIC2* and *MIR1* was confirmed by PCR analysis, amplifying full-length gene products. No PCR product was detectable for *PIC2* and *MIR1*, confirming a complete gene-knockout in the Δ*mir*Δ*pic* mutant. Moreover, the kanMX insertion cassettes, abolishing *PIC2* and *MIR1* gene expression, were detected (Fig. S2). As described in Hamel *et al*., 2004 the yeast double mutant was not able to grow on non-fermentable carbon sources (Fig. 3A).

We performed a heterologous complementation assay expressing the Arabidopsis proteins in the yeast double mutant under the control of a constitutive promoter. We analyzed the growth of the corresponding Δ*mir*Δ*pic* mutant on plates with ethanol as sole carbon source. It was previously shown that the lack of both *PIC2* and *MIR1* led to growth defects on non-fermentable carbon sources, such as glycerol or ethanol (Zara et al., 1996; Hamel et al., 2004). Only if the Pi import function of the mutant is restored, ATP can be generated via oxidative phosphorylation. After a diauxic shift of Δ*mir*Δ*pic* expressing the Arabidopsis proteins to ethanol-containing medium, the transformants were grown for 3 d at 30°C. Our complementation assay revealed, that PHT3;1 and PHT3;2 complemented Δ*mir*Δ*pic*, whereas SIT1 only partially rescued the double mutant phenotype. As expected, untransformed Δ*mir*Δ*pic*, as well as the empty vector control did not grow on ethanol plates. The expression of *MIR1* in the Δ*mir*Δ*pic* background fully restored growth (Fig. 3A).

A prerequisite for functional complementation is that the heterologous SIT1 is targeted to mitochondria in the Δ*mir*Δ*pic* mutant. To verify this we performed localization experiments via fluorescence microscopy (Fig. 3B). An EYFP-tagged SIT1 was expressed in Δ*mir*Δ*pic* cells, which were stained with the mitochondria-specific dye MitoTracker Red. The presence of both EYFP fusion proteins was verified by immunodetection (Fig. S2). Confocal microscopy revealed that SIT1-EYFP co-localized with mitochondria in yeast (Fig. 3B, middle column). The pattern and distribution

of fluorescence signal matched the fluorescence pattern of Mir1p-EYFP (Fig. 3B, left column). As negative control, yeast mitochondria were stained with MitoTracker in the absence of EYFP-fused protein (Fig. 3B, right column).

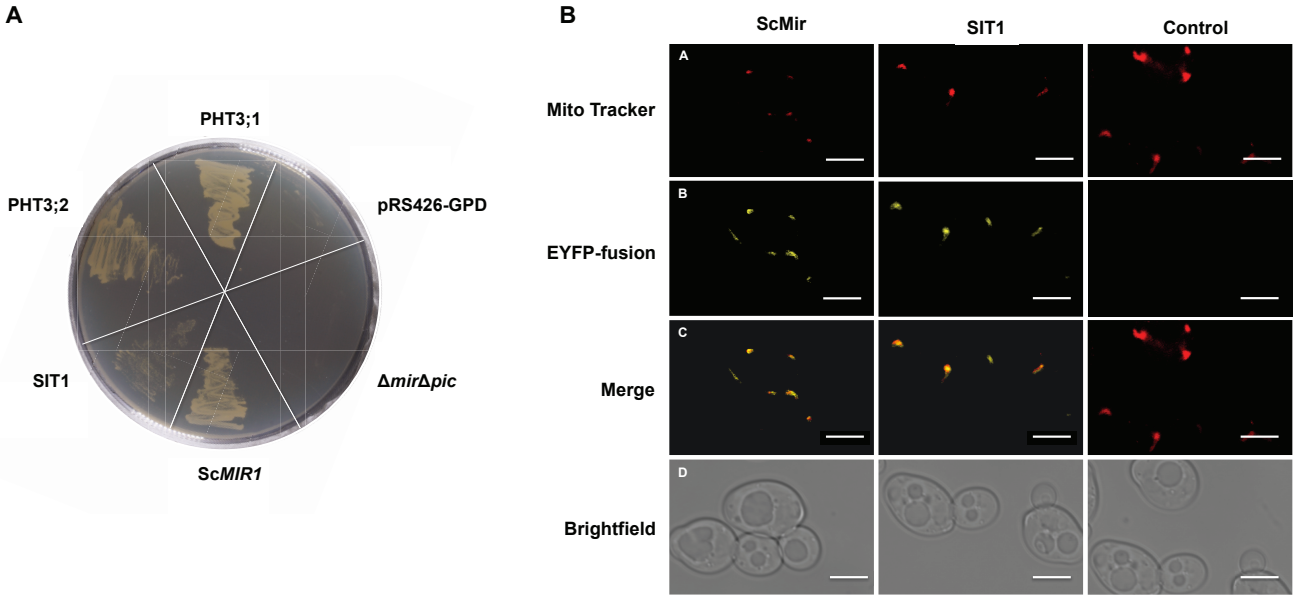

Fig. 3: SIT1, which is targeted to mitochondria in yeast, does not rescue the Δ*mir*Δ*pic* phenotype.
A: Complementation of the yeast mutant Δ*mir*Δ*pic* lacking mitochondrial phosphate transport. Mutants were complemented with the Arabidopsis PHT3;1, PHT3;2 and SIT1 proteins. As positive control the mutant phenotype was reverted expressing the endogenous yeast phosphate carrier *MIR1* constitutively. As negative control the empty vector pRS426-GPD was expressed. The assay was performed on selective medium with ethanol as carbon source. B: Confocal images from Δ*mir*Δ*pic* cells expressing the Arabidopsis SIT1 protein (second column), and the endogenous yeast protein Mir1p. For co-localization yeast cells were stained with MitoTracker Red (A). Proteins were tagged with EYFP at the C-terminus (B). Merged (C) and bright field images (D) are shown. Yeast cells only stained with the mitochondrial dye (A) were used as control (last column). Bar = 5 µm.

We concluded that PHT3;3 is not a major mitochondrial Pi transporter, as it did not complement Δ*mir*Δ*pic* to the same level as PHT3;1 and PHT3;2. Although SIT1 was targeted to yeast mitochondria, we cannot rule out that the protein was inactive or only poorly active in yeast.

SIT1 exhibits low phosphate import capacity

To investigate a possible Pi transport function of SIT1, we performed *in vitro* uptake assays with recombinant SIT1 protein in comparison to the mitochondrial phosphate carrier PHT3;1, we expressed the corresponding proteins with a C-terminal histidine affinity tag in the *S. cerevisiae* FGY217 strain (Kota et al., 2007). As demonstrated in Figure 4A, the synthesis of PHT3;1-His and SIT1-His was validated by immunoblot analysis with an anti-His antibody. Immunoblot detection revealed a single protein band at the sizes of 44 kDa, and 39kDa for PHT3;1-His and SIT1-His, respectively. Yeast membranes containing either recombinant PHT3;1-His or SIT1-His were reconstituted into liposomes by freeze-thaw-sonication procedure (Kasahara and Hinkle, 1976; Palmieri et al., 1995). We used membranes from wildtype yeast cells as controls, which did not heterologously express any of these proteins. This enabled us to estimate the background activity of yeast endogenous phosphate carriers. Uptake of 0.3 mM radiolabelled [^{32}P]-phosphoric acid in

liposomes pre-loaded with 30 mM unlabeled phosphate was determined (Fig. 4B-C). Liposomes consisted of a mixture of L-α-phosphatidylcholine and cardiolipin. Because PHT3;1 mediated transport is cardiolipin-dependent (Fig. S4), we prepared liposomes with cardiolipin. Cardiolipin interacts with MCF transporters and thus is required for transport in reconstituted lipid vesicles (Kolbe et al., 1981; Kadenbach et al., 1982; Klingenberg, 2009).

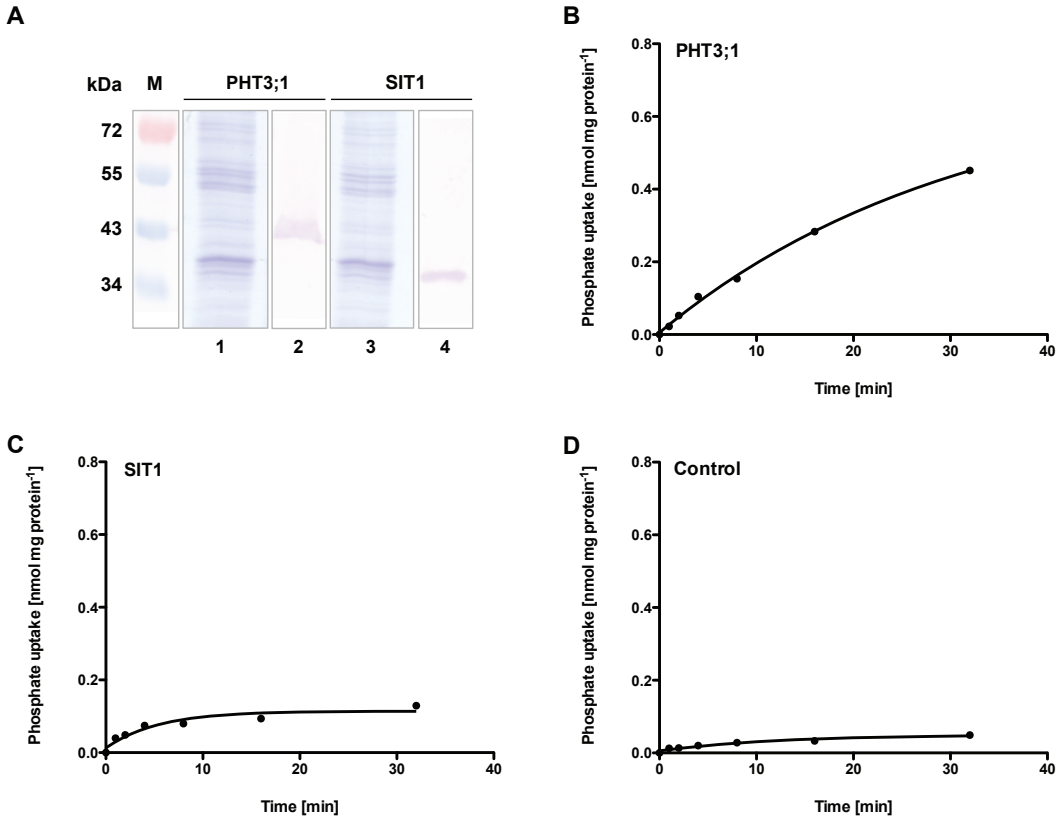

Fig. 4: SIT1 mediates a marginal uptake of phosphate *in vitro.*
A: Coomassie-stained SDS-PAGE gel (lane 1 and 3) and immunoblot analysis (lane 2 und 4) of PHT3;1-His (44 kDa) and SIT1–His (39 kDa) verifies expression in yeast. Proteins were detected with an anti-His antibody; M, protein marker. B-D: For time-dependent *in vitro* phosphate uptakes yeast membranes were isolated and reconstituted into liposomes pre-loaded 30 mM internal phosphate. The uptake of radiolabelled 0.25 mM [^{32}P]-phosphate was determined as technical replicates; B: PHT3;1-His, C: SIT1-His, D: Empty vector control, pYES2.

We observed a significant Pi import into liposomes when Pi was present as counter-exchange substrate (Fig. 4B-D). The homoexchange of Pi mediated by PHT3;1 proteoliposomes followed a first order kinetics and reached a maximum uptake rate of 0.4 nmol mg protein^{-1} (Fig. 4B). SIT1 did also exchange low levels of Pi across the liposomal membrane. Its maximum uptake capacity was around 3-fold lower compared to PHT3;1 (0.13nmol mg protein^{-1}, Fig. 4C). In sum, SIT1-mediated a phosphate exchange that only marginally exceeded background activity (0.05 nmol mg protein^{-1}, Fig. 4D).

Our results confirmed that we were able to functionally express SIT1 protein in yeast. We hypothesized that the rate of Pi uptake by SIT1 was not sufficient to complement the yeast mutant phenotype. Hence, we assumed that Pi was not the favored substrate of SIT1.

SIT1 accepts sulfate as substrate

We tested whether SIT1 was able to transport sulfate, because this compound is similar to phosphate in molecular structure and its two negative charges. We reconstituted yeast membranes expressing SIT1 and measured the uptake of 0.3 mM radiolabelled [^{32}S]-sulfate into liposomes pre-loaded with 30 mM unlabeled sulfate (Fig. 5).

Our *in vitro* studies revealed that SIT1-His mediated a sulfate/sulfate exchange with a maximum uptake rate at 32 min of 0.7 nmol mg protein^{-1} (Fig. 5A). Compared to the uptake of phosphate, SIT1 exchanged sulfate with higher preference (Fig. 4C). Recombinant PHT3;1 was also tested for sulfate transport (Fig. 5B). We observed that sulfate was taken up, but to far lesser extent (0.3 nmol mg protein^{-1}). The maximum uptakes rates of PHT3;1 did not differ between sulfate and phosphate (Fig. 4B, 5B), demonstrating that this carrier did not highly discriminate between the two substrates. In the absence of overexpressed proteins only marginal background activities, caused by endogenous carriers could be measured (0.04 nmol mg protein^{-1}) (Fig. 5C).

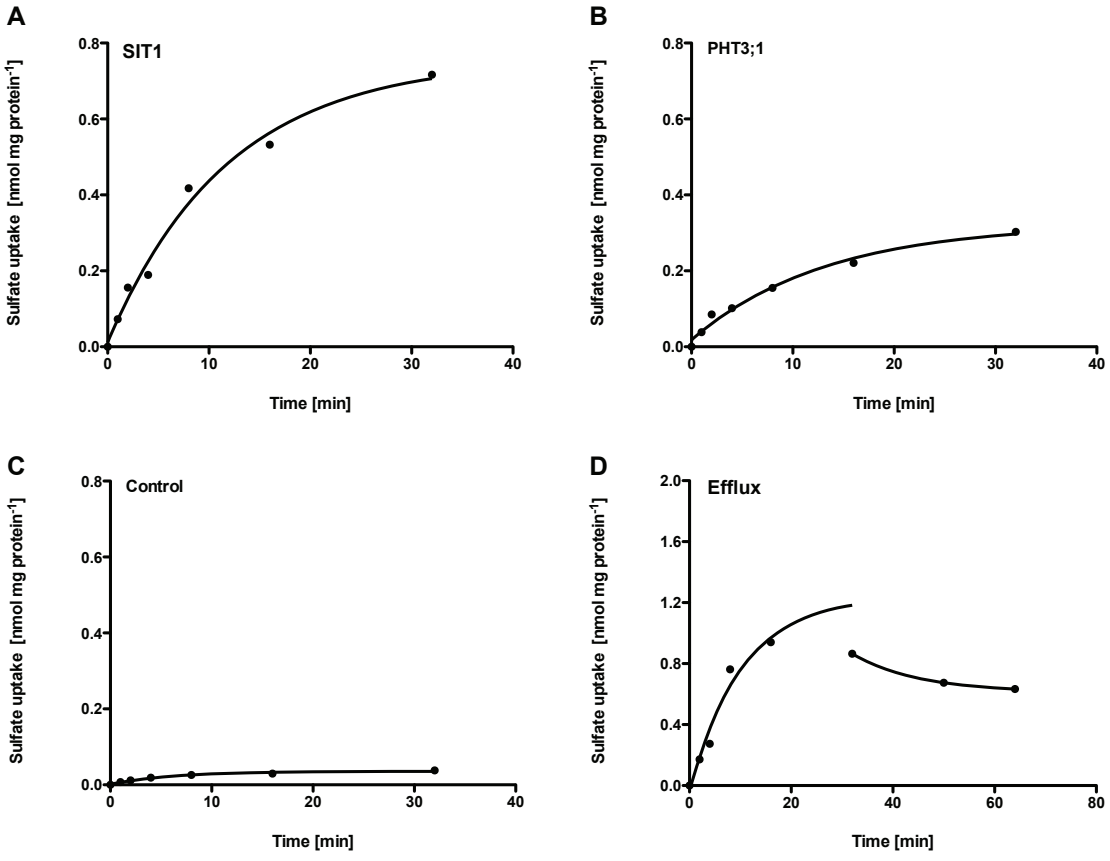

Fig. 5: SIT1 mediates an active time-dependent sulfate homoexchange *in vitro*.
For time-dependent sulfate uptakes yeast membranes were isolated and reconstituted into liposomes pre-loaded with internal 30 mM sulfate. The time-courses of radiolabelled 0.3 mM [^{35}S]-sulfate were measured as technical replicates; A: SIT1-His, B: PHT3;1-His, C: Empty vector control.
D: Sulfate efflux studies; yeast membranes over-expressing recombinant SIT1-His protein were isolated and reconstituted into liposomes pre-loaded internal sulfate (30 mM). The time-course of radiolabelled [^{35}S]-sulfate (0.3 mM) uptake was determined. After 32 min 300 mM additional sulfate was added externally to promote the efflux of [^{35}S]-sulfate from liposomes.

As additional proof, we confirmed that sulfate was in fact imported into liposomes via SIT1 (Fig. 5D). We performed efflux experiments measuring the export of radioactive-labeled sulfate from liposomes against unlabeled external sulfate (Palmieri et al., 1995). After 32 min uptake of labeled sulfate, we offered a 10-fold higher external concentration of unlabeled sulfate. This caused significant efflux of intra liposomal sulfate out of SIT1 liposomes. The internal sulfate concentration of SIT1 proteoliposomes decreased from 0.94 nmol mg protein^{-1} to 0.63 nmol mg protein^{-1} after 64 min. The fact that high amounts of external non-labeled sulfate stimulated efflux of internal radioactivity indicated that SIT1 acts in a counter exchange mode.

To identify possible further substrates of SIT1, we performed competition experiments using mitochondrial metabolites, including sulfate, adenosine-5'-phosphosulfate, sulfide, sulfite, phosphate, thiaminepyrophosphate, adenosine 3′, 5′-diphosphate, adenosine 3′-phosphate 5′-phosphosulfate, adenosine diphosphate, guanosinediphosphate, malate; glutamate, arginine, cysteine, orotate, and acetate. We determined sulfate uptake into SIT1 liposomes preloaded with 30 mM sulfate in the presence of a 5-fold excess of externally competing substrates. Sulfate/sulfate exchange rates in the absence of any competitor were set to 100% and competition reactions were calculated relative to it (Fig. 6).

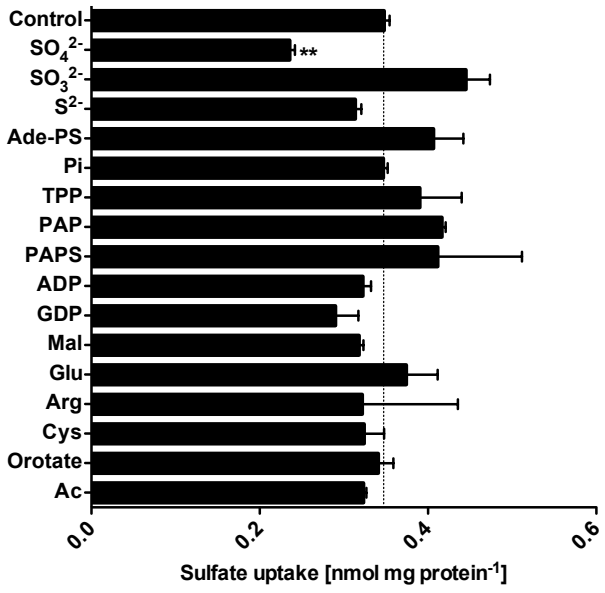

Fig. 6: SIT1-mediated sulfate homo-exchange cannot be competed by any of the counter-exchange substrates tested.
The influence on putatively competing substrates on sulfate homoexchange was determined. Liposomes were preloaded with 30 mM unlabeled sulfate and reconstituted with recombinant SIT1-His protein. Uptake experiments were initiated with 0.3 mM [^{35}S]-sulfate. After 5 min 1.5 mM of various substrates was offered externally and the influence on sulfate homoexchange, reflected by radiolabelled sulfate incorporated, was determined. Ade-PS: Adenosine-5'-phosphosulfate; SO_3^{2-}: Sulfite; S^{2-}: Sulfide; Pi: Phosphate; TPP: Thiaminepyrophosphate; PAP: Adenosine 3′,5′ -diphosphate; PAPS: Adenosine 3′ -phosphate 5′ -phosphosulfate; ADP: Adenosine diphosphate; GDP: Guanosine diphosphate; Mal: Malate; Glu: Glutamate; Arg: Arginine; Cys: Cysteine; Ac: Acetate. The data represent arithmetic means ± SEs of three technical replicates of two independent experiments; ** p = 0.002.

We demonstrated that none of the substrates tested did significantly reduce the sulfate/sulfate exchange activity of SIT1. Only excess amounts of sulfate inhibited the uptake of

labeled substrate. Notably, the addition of Pi did not significantly compete for an uptake of labeled sulfate (Fig. 6).

In sum, we could demonstrate that SIT1 preferentially exchanged sulfate. Thus, we assumed that SIT1 is a sulfate transporter, whereas PHT3;1 mediated phosphate transport. Competition experiments did not reveal another counter-exchange substrate for SIT1 besides sulfate. Efflux studies elucidated that SIT1-mediated sulfate exchange was active transport.

SIT1 is localized to mitochondria in plants

The subcellular localization of a protein is important information to understand its *in vivo* role. SIT1 is predicted to be located in mitochondria or peroxisomes based on the subcellular localization predictions in the Aramemnon (http://aramemnon.botanik.uni-koeln.de) and SUBA database (http://suba.plantenergy.uwa.edu.au/) (Schwacke et al., 2003; Heazlewood et al., 2007). A clear mitochondrial localization prediction was not found, because SIT1 in contrast to PHT3;1 and PNT3;2 lacked an N-terminal sequence extension containing the mitochondrial targeting information.

To experimentally investigate the targeting of SIT1, we conducted co-localization studies using fluorescence microscopy to analyze the SIT1 targeting. The coding sequence of SIT1 was fused to an N- and C-terminal EYFP and was transiently expressed in tobacco (Fig. 7). A peroxisomal marker protein, CFP tagged with the peroxisomal targeting signal 1 (PTS1), was co-expressed. The resulting fluorescence signals of both, SIT1-EYFP and EYFP- SIT1, did not merge those of CFP-PTS1, implying that SIT1 was not targeted to peroxisomes (Fig. 7C). The peroxisomal marker and the SIT1 fusion constructs exhibited a punctate pattern, which correlated to the distribution and size of peroxisomes and mitochondria in the cell. The diameter of the signal emerging from the peroxisomal control was significantly larger than the signal of SIT1 fusions, which related well to the size difference of peroxisomes (1-2 µm) and mitochondria (0.5-1 µm) (Arimura et al., 2008; Mitsuya et al., 2010). Thus, we propose that SIT1 is located to mitochondria in plants, as it has been shown for yeast (Fig. 3B).

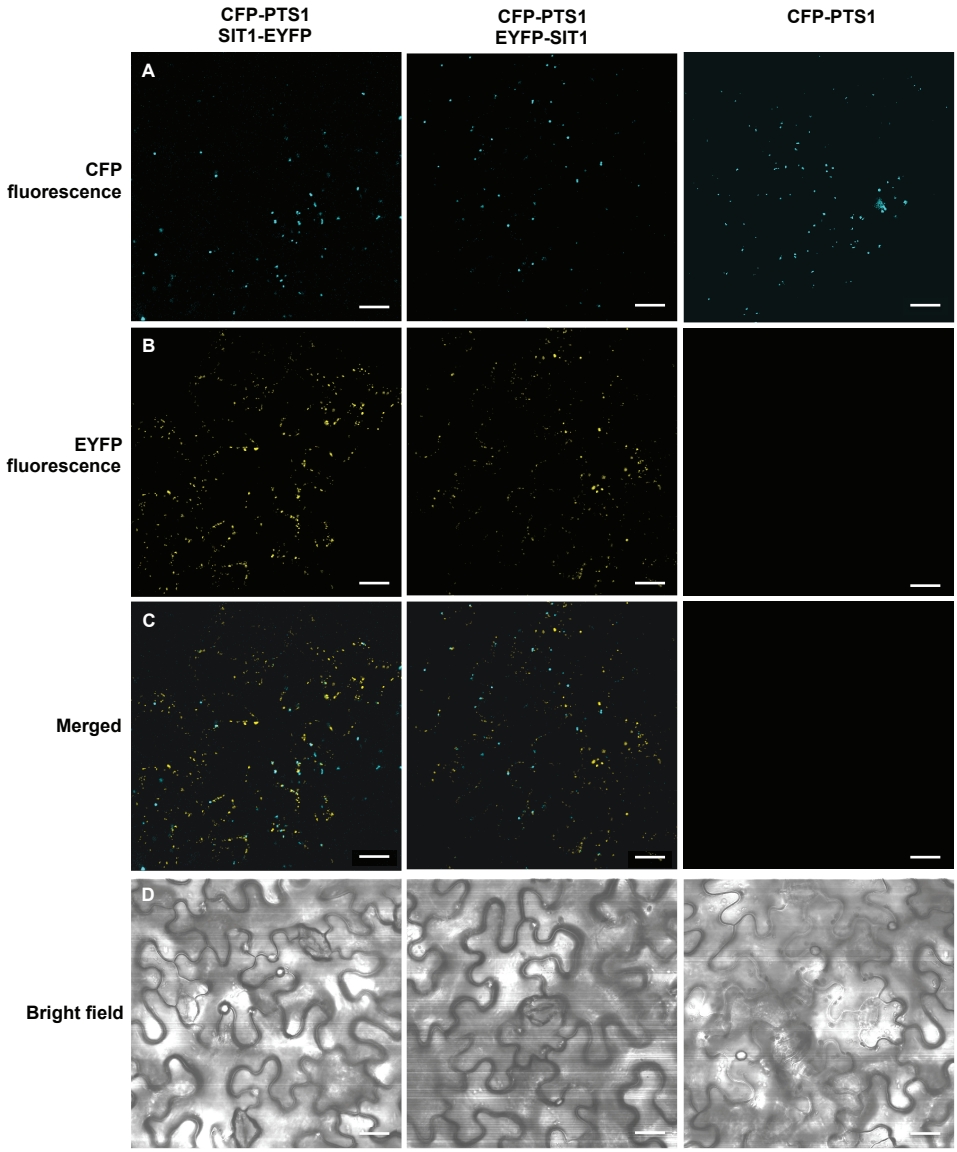

Fig. 7: SIT1 is localized to mitochondria in plants.
Confocal images from leaf epidermal cells of tobacco plants transiently co-expressing the peroxisomal organelle marker CFP-PTS1 and the EYFP-tagged SIT1 proteins. SIT1 was either tagged with EYFP at the C-terminus (SIT1-EYFP, first column), or tagged at its N-terminus (EYFP- SIT1, middle column). (A), CFP fluorescence, (B) EYFP fluorescence, (C) Merged images and (D) bright field images. Tobacco plants expressing only the peroxisomal marker were used as control (third column). Bar = 20 µm.

SIT1 is ubiquitously expressed, but higher transcript levels are found in flowers and apex tissues.

To get insights into the physiological role of SIT1, we examined the publicly available expression database Arabidopsis eFP browser (Winter et al., 2007). We observed that *SIT1* was ubiquitously expressed, but higher mRNA levels were found in flower tissues, especially carpels, shoot apex, and seeds, and in apex tissues (Fig. 8A).

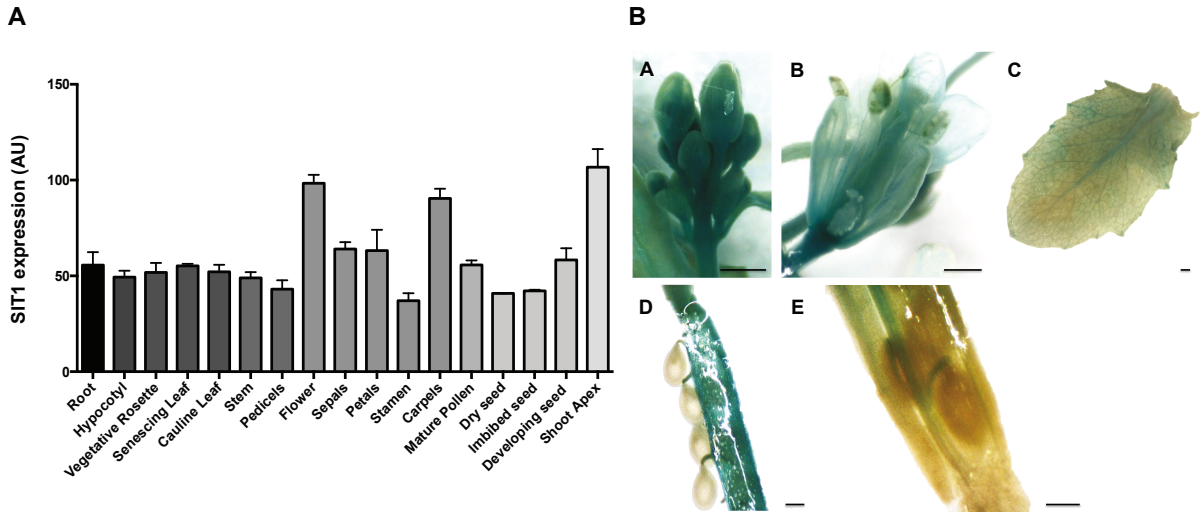

Fig. 8: SIT1 is ubiquitously expressed, but stronger in apex and flower tissues.
A: Detailed tissue-specific expression of *SIT1.* Tissue-specific *SIT1* expression data was taken from the eFP browser. Expression is given as mean fluorescence units (AU) ± SD. B: GUS staining of the SIT1 promoter activity in flower buds (A), flowers (B), leaves (C), siliques (D, E), and seeds (E). Tissues were taken from six week-old plants. Bar = relative arbitrary units.

Promotor-GUS studies were performed to unravel tissue-specific *SIT1* abundances. We analyzed transgenic Arabidopsis plants expressing the SIT1 promoter fused to the GUS gene. Tissue of six week-old seedlings was stained and promoter activity was analyzed in flowers, leaves, siliques and seeds (Fig. 8B). Flower buds and pedicels of different developmental stages were strongly stained (Fig. 8B, A). Intense staining was also detected in sepals, petals and carpels, whereas lesser staining was found in carpels and stamens (Fig. 8B, B). Almost no staining was observed, in leaves, except for major veins, minor veins and hydathodes (Fig. 8B, C). In siliques, only valves and funiculi were strongly stained (Fig. 8B, D). No pronounced promoter activity was detected in ovules (Fig. 8B, E). In other organs of the plant, GUS staining was hardly or not detectable. In sum, *SIT1* was apparently expressed throughout various plant tissues. GUS staining was only observed in tissues, where the carrier was highly expressed, which agreed widely with microarray data. Due to low promoter activities, GUS staining could not be detected in other Arabidopsis tissues.

Germination and early seedling establishment are arrested in sit1-1.

To investigate the function of SIT1 in plants, we established a T-DNA insertion line GK432A12 (*sit1-1*). In this mutant plant the T-DNA was inserted in the 5'-UTR, 176 bases upstream of the start methionine of SIT1 coding sequence (Fig. S5, A). This T-DNA integration led to an absence of transcript in homozygous *sit1-1* plants. No *SIT1* transcript was detected by RT-PCR analysis (Fig. S5, B). We obtained a second T-DNA insertion line SAIL591_H09 (*sit1-2)* of the same ecotype for phenotypic studies (Dr. Ilka Haferkamp, University of Kaiserslautern). The T-DNA in *sit1-2* was inserted at about the same position as in *sit1-1.*

To find out if a loss of SIT1 affects early stages of plant development, we examined germination efficiency and seedling establishment in both *sit1* mutant lines. Seeds were placed on MS agar plates and after six days seedling development was classified according to the given stages: (I) Radicle not emerged, (II) radicle emerged, (III) cotyledons expanded, (IV) cotyledons fully expanded and green. We observed a strong deceleration in early seedling growth for *sit1-1*, which was less pronounced in *sit1-2* (Fig. 9).

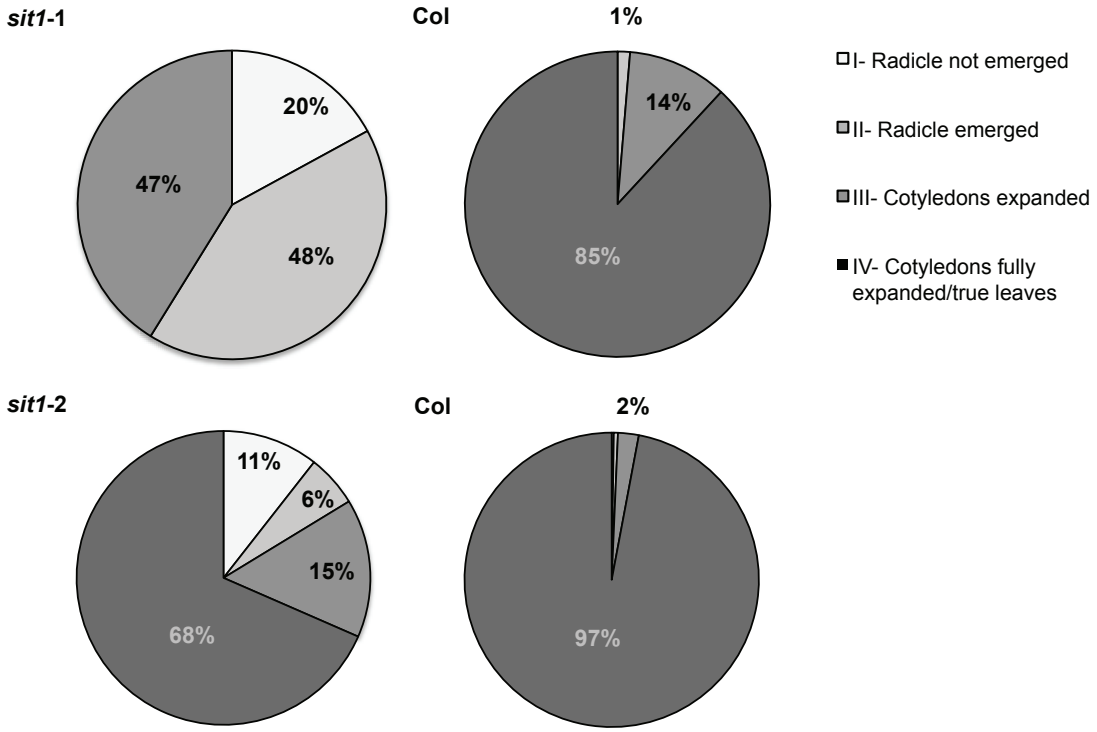

Fig. 9: Development is retarded in *sit1* mutant plants.
A: Germination and early seedling establishment assay. Wildtype and mutant seedlings were grown for 6 d on half-strength MS medium. Development of the seedlings was observed and divided into for different stages I-IV; Germination: I- radicle not emerged, II- radicle emerged; Early seedling development: III- cotyledons expanded, IV- cotyledons fully expanded/true green leaves. *sit-1*: N=250 seedlings/line, 2 technical replicates; *sit-2*: N=500.

Whereas 85% of wildtype seedlings exhibited fully developed cotyledons and first true leaves within six days, the *sit1-1* mutant did not reach this stage of development. The majority of mutant plants had an emerged radicle (48%) or cotyledons, which were not fully developed at this stage (47%). In 20% of the mutants the radicle did not even become visible. In contrast, all wildtype seeds germinated, 1% of seedlings had an emerged radicle and 14% exhibited cotyledons, which were not green. In case of *sit1-2,* 68% of seedlings had fully developed cotyledons, between 6% and 16% of seedlings arrested in stages I to III. The *sit1-2* wildtype developed comparably to the wildtype of *sit1-1* (Fig. 9).

We analyzed whether the impaired germination was associated to defects in seed filling or seed development. To evaluate embryonic defects in *sit1*-1, siliques were opened and ovules were cleared with chloral hydrate. Clearing allowed an observation of embryos, without removing integuments or seed coats (Fig. 10A, 3-5). Besides spontaneous abortions, which can be observed

in wildtype, *sit1*-1mutants exhibited a significantly higher number of defective seeds per silique (Fig. 10B). The frequency of misshaped embryos was 18 times higher in the mutant when compared to wildtype. Embryos were arrested in different stages, *e.g.* globular or heart stage (Fig. 10A, 3, 10A, 5). However, most embryos were fully developed (Fig. 10A, 4). Taken together, a higher number of embryos in *sit1*-1 were undeveloped, implying that SIT1 might be essential for seed development.

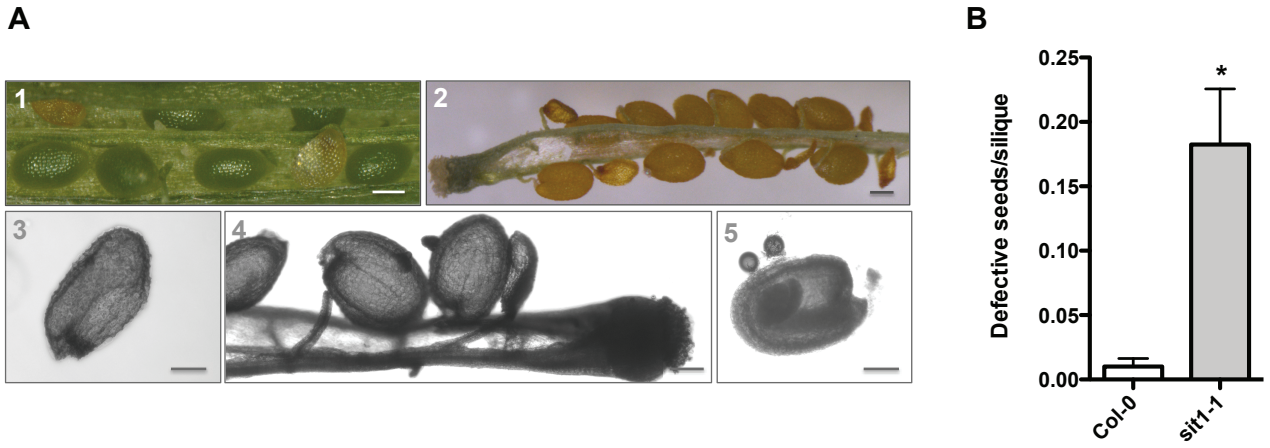

Fig. 10: Seeds are defective in *sit1-1* mutant plants.
Analysis of seeds in *sit1*. Siliques of the *sit1-1* mutant were opened and examined with light microscopy. To visualize embryos in seeds, the seeds were cleared with chloral hydrate (lower row). Bar = 50 µM (left). C: The number of abnormal seeds/siliques was counted in the six-week old *sit1-1* mutants (filled bar) and wildtype (open bar) (right). N = 50; *p = 0.04.

Arabidopsis plants lacking SIT1 are retarded in growth

For further phenotypic analyses we grew wildtype, *sit1-1* and *sit1-2* plants under long-day conditions. Compared to wildtype, both T-DNA insertion lines showed retardations in growth (Fig. 11A, 11C). The growth phenotype slightly varied between plants. Some plants almost grew wildtype-like, whereas others were stunted in growth. In addition, root growth was shorter but less consistent in *sit1-1*. On average the primary root length of twelve days-old seedlings was shorter in *sit1-1*, but the mutant had more lateral roots than wildtype (Fig. S6). Although *SIT1* was significantly expressed in flowers, floral organs were not obviously altered in mutant plants. However, we observed a delayed onset of flowering. The number of leaves on plants, which started to bolt, was significantly higher for both *sit1* mutant lines than for wildtype. Quantification of leaves is an established measure for flowering time and thus a marker of development, since a correlation between the number of days until flowering and the number of leaves exists (Koornneef et al., 1991). The wildtype exhibited about 25 leaves, whereas on average *sit1-1* had 32 and *sit1-2* had 35 leaves when starting to flower (Fig. 11B, D). Our phenotypic analyses of the *sit1* mutants revealed retardation in plant growth and a prolonged transition to flowering.

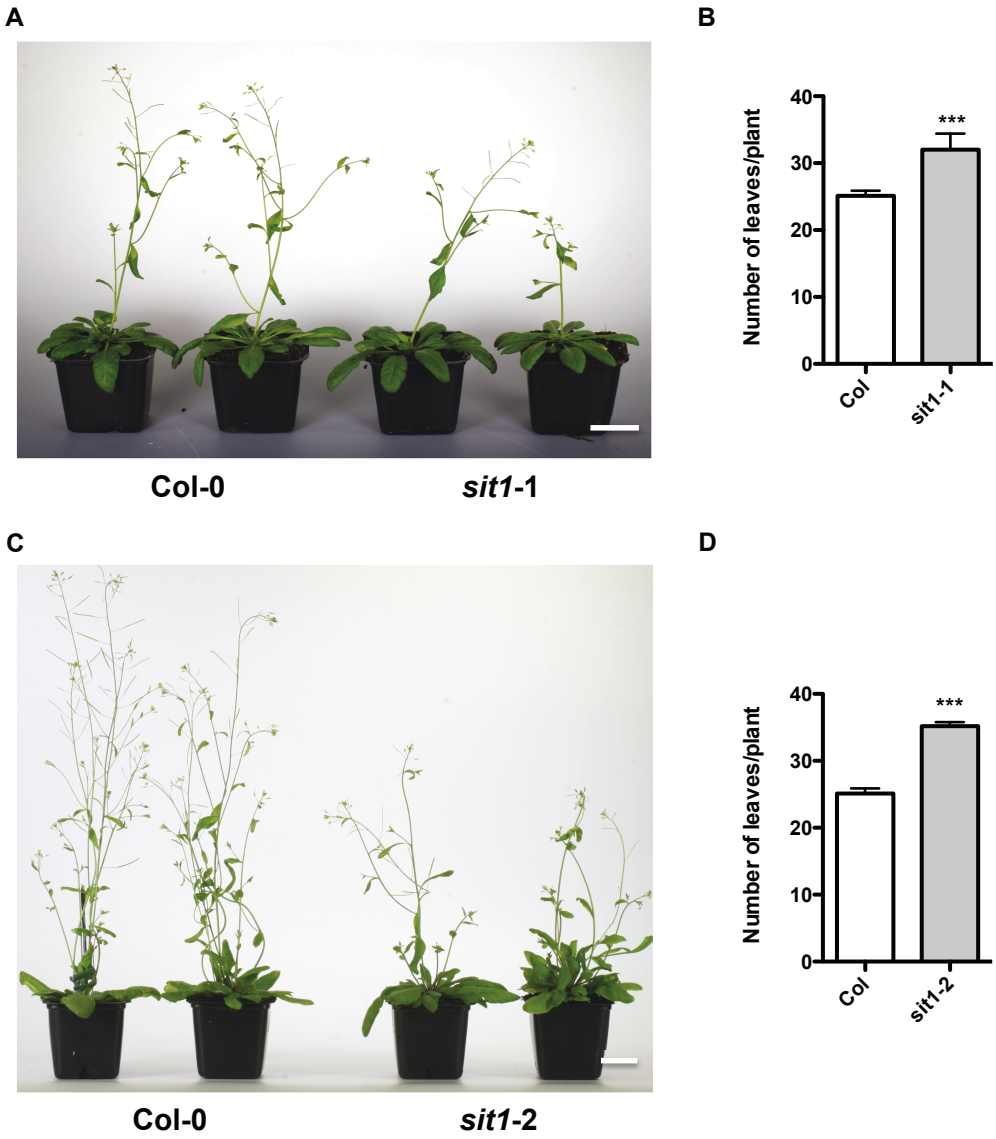

Fig. 11: Phenotypic analysis of adult *sit1* mutant lines.
A: Phenotypic growth of *sit1-1* mutants (left). Wildtype and mutant were grown for six weeks under a long day conditions (16h-light/8-h dark), bar = 1 cm; B: To analyze flowering time cauline and rosette leaves were counted (right). N = 24; ****p* = 0.0008; C: Phenotypic growth of *sit1 -2* mutants. Wildtype and *sit1-2* mutant were grown for eight weeks under a long day conditions (16h-light/8-h dark), scale bar = 1 cm; D: To analyze flowering time cauline and rosette leaves were counted (right). N = 24; ****p* = 0.0001.

Discussion

In this study, we demonstrated that SIT1 represents a mitochondrial sulfate transporter, which is specific for embryophytes. Former studies annotated this protein as phosphate transporter, because its protein sequence clustered together with the mitochondrial phosphate carriers PHT3;1 and PHT3;2 (Picault et al., 2004). In our phylogenetic analyses we included 21 proteomes from plant, animal and fungal kingdoms to cover various species with different features. This sequence-based analysis revealed a clear separation of SIT1 from other PHT3s in different clusters (Fig. 1 and 2). SIT1 branched off from the clade of mitochondrial phosphate carriers and formed an autonomous subgroup exclusively established by homologs from embryophytes. The annotation of protein domains and architecture did not indicate pronounced functional differences between SIT1 and PHT3;1, or PHT3;2 (Fig. S1). However, on single amino acid level, PHT3 sequence comparisons revealed that key residues responsible for phosphate transport activity in mammalian and yeast Pi carriers were not conserved in SIT1, but in PHT3;1 and PHT3;2 (Dolce et al., 1994; Phelps et al., 1996; Zhu et al., 2012). The SIT1 protein displayed amino acid transitions of cysteine to valine at position 44 and of glutamic acid to glutamine at position 126 instead (Dolce et al., 1994; Phelps et al., 1996). Additionally, analyses of the 3D-structure of SIT1 revealed a more distinct loop region preceding the fifth transmembrane domain (Zhu et al., 2012). Directed mutagenesis of SIT1 residues will determine if these structural changes are responsible for the functional diversity of SIT1 compared to PHT3;1 and PHT3;2.

Specific transport capacities of SIT1 became evident when we complemented a yeast mutant deficient in mitochondrial Pi uptake (Fig. 3A). In contrast to PHT3;1 and PHT3;2, SIT1 was not able to fully restore the yeast growth phenotype, although it was targeted to mitochondria (Fig. 3B). Since we observed low phosphate transport activity for SIT1 *in vitro* (Fig. 4C), we anticipated that it only transported basal levels of phosphate into yeast mitochondria, leading to partial complementation. Consequently we investigated, whether SIT1 preferred another transport substrate to phosphate. Uptake experiments with recombinant proteins revealed that SIT1 specifically catalyzed an active sulfate exchange, indicating that SIT1 prefers sulfate instead of phosphate as transport substrate. In comparison, PHT3;1 did not discriminate between sulfate and phosphate (Fig. 5). Based on our efflux experiments we excluded an artificial sulfate transport of SIT1, because the SIT1-mediated sulfate import was reversible (Fig. 5). Competitive inhibition experiments, however, did not reveal another putative *in vivo* substrate for SIT1, as only sulfate competed for the substrate-binding site in SIT1 (Fig. 6). We hypothesize that SIT1 mediates sulfate import in a proton-coupled manner or as exchange against hydroxyl ions (Fig. 12A). This transport mode is proposed for the mitochondrial phosphate transporters PHT3;1 and PHT3;2, although they catalyze a Pi/Pi exchange *in vitro* (Pratt et al., 1991; Stappen and Kramer, 1994; Liu et al., 2011), and is also demonstrated for the tonoplast sulfate transporter SULTR4 (Kataoka et al., 2004). We assume that due to a coupling to protons or hydroxyl ions, which was not tested with our

experimental setup, it might be possible that no other exchange substrate was identified. Whether SIT1 mediates such a transport mode will be tested biochemically (Takabatake et al., 1999; Nakamori et al., 2002).

Subcellular localization studies demonstrated that SIT1 was targeted to mitochondria (Fig. 7). Surprisingly, fusing an EYFP-tag to the amino terminus of SIT1 did not disrupt mitochondrial targeting, although it is known that the mitochondrial targeting peptide resides in the N-terminal parts of proteins (Heazlewood et al., 2004). Fusing fluorescent tags to the amino terminus of mitochondrial proteins can disturb mitochondrial import and can lead to an accumulation of proteins in the cytosol. As localization studies indicated, that the N-terminal EYFP tag fused to SIT1 only partially masked targeting information and the protein was still located to mitochondria, we hypothesized that SIT1 presumably exhibits internal signals, directing the protein to the mitochondrial membrane, as demonstrated for the mitochondrial ADP/ATP carriers from plants (Dyall et al., 2004). Since SIT1 is located to mitochondria and transports sulfate, the role of a sulfate import system of plant mitochondria needs to be investigated. Previous studies demonstrated that DIC carriers import dicarboxylic acids, *i.e.* oxaloacetate and malate into mitochondria (Palmieri et al., 2008a). These dicarboxylic acids can replenish the TCA cycle and prevent impairments of this essential pathway (Palmieri et al., 2008a). Kinetic studies with recombinant DIC proteins from Arabidopsis revealed that the preferred counter-exchange substrate for dicarboxylic acids is sulfate, but also phosphate can serve as counterexchange substrate (Palmieri et al., 2008a). Such an exchange-mode necessitates the presence of sulfate in the mitochondrial matrix. Thus, we assume that SIT1 plays a role in preloading the mitochondria with sulfate for the replenishment of the TCA cycle with dicarboxylic acids (Fig. 12A). A loss of SIT1 in Arabidopsis led to mutants with impaired growth and development. We hypothesize that mitochondrial sulfate is not available in the absence of SIT1. Under these circumstances, we hypothesize that DIC carriers import dicarboxylic acids against phosphate (Fig. 12B).

An increased export of Pi might deplete mitochondria with Pi and in consequence negatively affect mitochondrial ATP synthesis. Such a proposed energy deprivation would lead to growth defects throughout all developmental stages as observed for the *sit1* mutant. Mutants devoid of SIT1 are impaired in germination and post-germinative growth (Fig. 9). The growth defect persisted in adult plants (Fig. 11). Additionally, we observed a late-flowering phenotype in mutants, which might be associated to elevated contents of soluble sugars and decreased starch accumulation in these plant lines (Dr. Ilka Haferkamp, personal communication). High soluble sugar levels in sink organs, such as flowers, siliques and seeds indicate that plants cannot efficiently use these carbohydrates for storage reserve accumulation, as biosynthesis of starch and fatty acids depend on the provision of ATP (Vigeolas et al., 2004). Hence, low ATP levels lead to less storage reserve accumulation, which might affect seed filling and leads to defective *sit1* seeds.

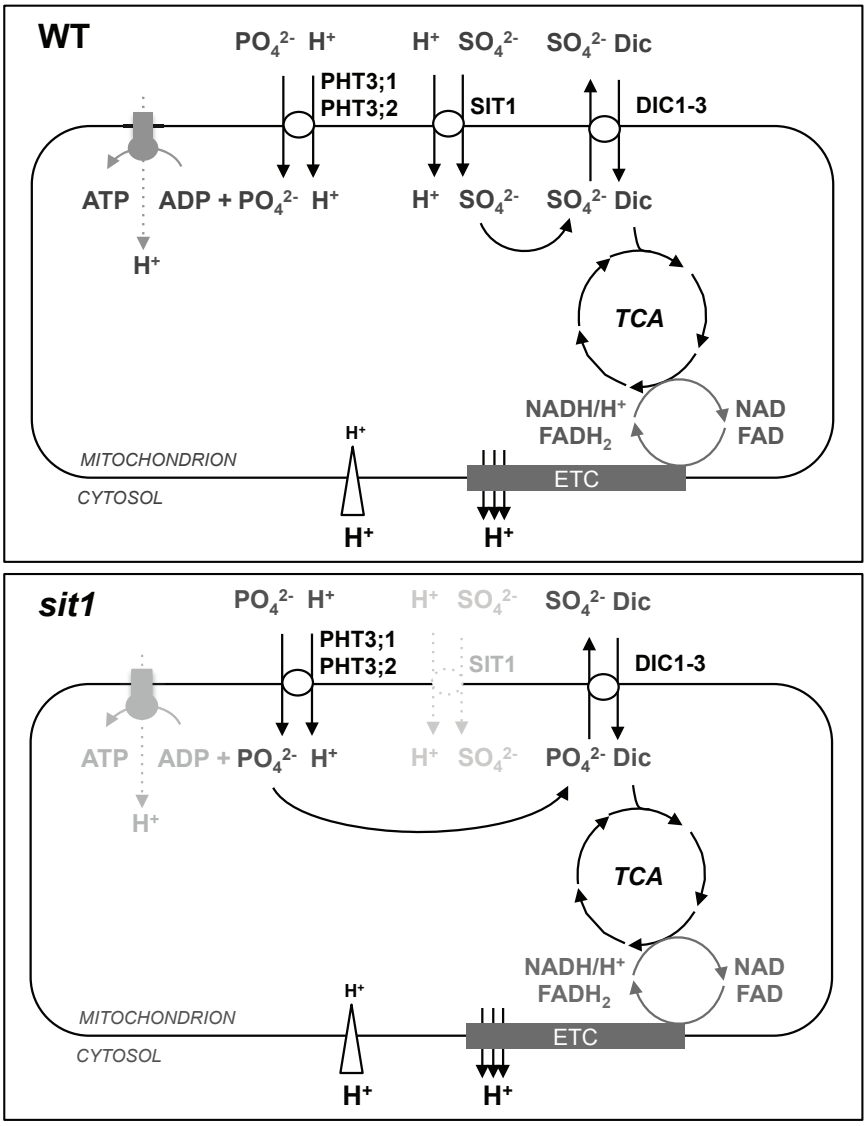

Fig. 12: SIT1 provides sulfate as counter-exchange substrate for DIC, which imports dicarboxylic acids to replenish the TCA cycle.
WT: SIT imports sulfate (SO_4^{2-}) as symport with protons (H^+) to provide a counter-exchange for DIC, which imports dicarboxylic acids (Dic) to replenish the tricarboxylic acid cycle (TCA). The phosphate (PO_4^{2-}) imported by PHT3;1 and PHT3;2 fuels ATP synthesis, which in concert the mitochondrial electron transport chain (ETC) generates a proton gradient across the membrane.
sit1: When SIT1 is absent, DIC imports Dic against PO_4^{2-}. The competition of PO_4^{2-} between DIC ATP synthesis leads to diminished ATP levels. The plants suffer from energy deprivation.

However, to which extent a loss of SIT1 leads to defects in embryo maturation or seed filling remains to be tested. The mutants will be subjected to detailed analyses measuring lipid- and starch contents of developing seeds (Kang and Rawsthorne, 1994; Li et al., 2006).

In line with our mutant phenotype, SIT1 was highly expressed in torpedo-staged embryos (Willmann et al., 2011). Embryos follow a pattern of cell divisions, which are grouped into different stages: pre-globular, globular, transition, heart, torpedo, bent green cotyledons and mature embryo. In the torpedo phase, embryos turn green and accumulate storage products, pattering and tissue development is completed at this stage. As *SIT1* expression is absent in torpedo-staged embryos, we assume that this defect impacts storage product levels, influencing embryonic maturation, dormancy and germination (Willmann et al., 2011). Although the cytosolic energy pool is depleted in

sit1 mutants, plants are viable and fertile. We assume in greening seeds low levels of photosynthesis and Rubisco activity, uncoupled from the Calvin Cycle, provide energy for storage product synthesis. Rubisco, together with enzymes of the Oxidative Pentose Phosphate Pathway, very efficiently converts carbohydrates to acetyl-CoA via pentose phosphate (Schwender et al., 2004). This bypass might explain a comparably mild effect of a depleted cytosolic energy pool on *sit1* mutants.

The fact that SIT1 expression seems to be less significant for earlier embryonic stages could explain why *sit1* seedlings do not show any organ defects, because until the heart stage patterning and setting of tissue types and axes of the embryo is completed (Jenik et al., 2007; Willmann et al., 2011). Examinations of mRNA expression patterns *of SIT1* and GUS staining analyses revealed the highest expression in flowers and meristems, tissues that give rise to growth, development and reproduction. However, no visible defects were observed in flowers. In other tissues SIT1 promoter activity was not detectable, because only tissues with high activity could be stained. In tissues without staining *SIT1* expression was low.

We assume that due to its unique biochemical function and involvement in land plant-specific pathways, SIT1 has a unique function in higher plants. Embryophytes have a highly compartmented complex metabolic network (Lunn, 2007), which differs from algae, fungi and animals. Higher plants have a highly developed energy metabolism, which is dominated by photosynthesis. There, energy metabolism tightly cooperates between the chloroplast and the rest of the cell (Paul and Foyer, 2001). However, the exact reason of specificity needs to be investigated in the future.

Our study elucidated that the SIT1 is a mitochondrial carrier, which is functionally diverse from its closest relatives PHT3;1 and PHT3;2. It prefers sulfate instead of phosphate as a transport substrate. We propose that intra-mitochondrial sulfate, which is provided by SIT1, might act as an important counter-exchange substrate for the import of dicarboxylic acids, mediated by DIC transporters. Physiological studies of *sit1* mutants imply an impact of the carrier on plant energy metabolism.

Supplemental Material

Supplemental Figures

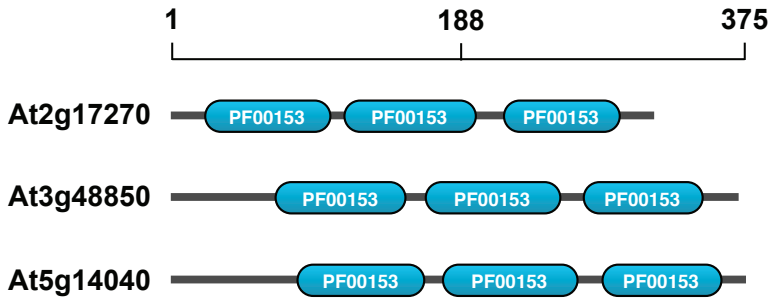

Fig. S1: Domain architecture of Arabidopsis PHT3 carriers.
Pfam-A domains of all Arabidopsis MCF carriers were annotated. The arrangements of the only domain found (PF00153) in PHT3 carriers are depicted. Arabidopsis identifiers belonging to the specific domain arrangement are indicated. Amino acid positions are indicated above domain architectures. Domain positions PF00153 (aa): 22-103, 111-196, 213-288 (At2g17270, SIT1); 67-151, 163-250; 264-341 (At3g48850, PHT3;2); 81-163, 174-261, 276-353 (At5g14040, PHT3;1).

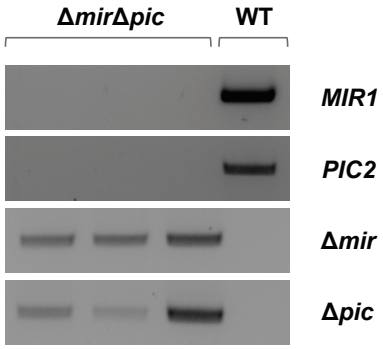

Fig. S2: *MIR1* and *PIC2* are absent in the generated Δ*mir*Δ*pic yeast* mutant.
A PCR analysis was performed to verify that full-length gene products of *MIR1* and *PIC2* are absent in Δ*mir*Δ*pic*. Three different mutants and the respective wildtype BY4742 were analyzed. To detect the gene products for MIR1 and PIC2 primers SV55/SV56 (3047 bp) and SV57/SV60 (1866 bp) were used. The gene/kanMX cassette junction primers for Δ*mir* and Δ*pic* were SV55/P78 (531 bp) and SV57/P78 (486 bp). DNA was stained with ethidium bromide.

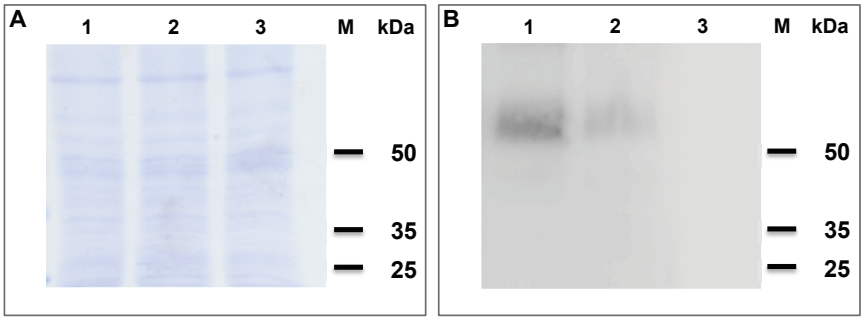

Fig. S3: SIT1-EYFP and Mir1p-EYFP are expressed in the Δ*mir*Δ*pic* mutant.
A: Coomassie-stained SDS-PAGE to detect SIT1-EYFP (lane 1), Mir1p-EYFP (lane 2) and the empty vector control 426GPD-ccdB-EYFP (lane 3). M, marker. B: Immunoblot analysis detects SIT1-EYFP (lane 1), Mir1p-EYFP (lane 2), and empty vector control (lane 3). For detection an anti-GFP antibody was used. Expected protein sizes for SIT1-EYFP 62 kDa and Mir1p-EYFP 63 kDa. M, marker.

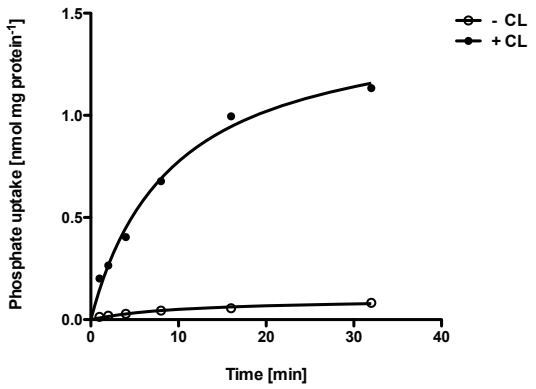

Fig. S4: PHT3;1 is stimulated by the addition of cardiolipin to the liposomal lipid mixture.
PHT3;1 protein was expressed in the *S. cerevisiae* FGY217 strain. Yeast membranes were isolated and reconstituted into liposomes pre-loaded with 30 mM phosphate, which either contained 5% (w/v) of cardiolipin (filled circles) or no cardiolipin (open circles). The incorporation of radiolabelled 0.25 mM [^{32}P]-phosphate into proteoliposomes was determined over time.

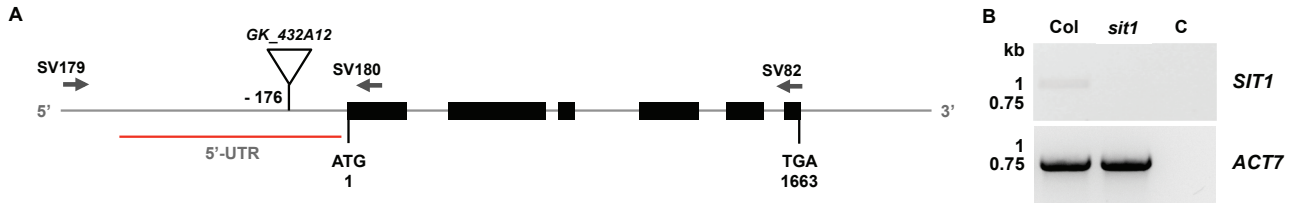

Fig. S5: Characterization of T-DNA insertion line GK432A12 (*sit1-1*).
A: Schematic drawing of positioning of T-DNA (GK_432A12) in the *sit1-1* mutant. The filled boxes represent the six exons of the SIT1 gene, the lines mark the intron regions; the 5'-UTR is marked in red. Start (ATG) and stop (TGA) of the gene are indicated. B: Wildtype and *sit1-1* were grown for six-weeks. In RT-PCR cDNA was transcribed from total leaf RNA. For PCR analysis of transcript abundance cDNA specific primers flanking the SIT1 coding sequence were used and primers amplifying the ACT7 cDNA. The expected product size for SIT1 is 994 bp, the product size of ACT7 is 740 bp. PCR products were stained with ethidium bromide.

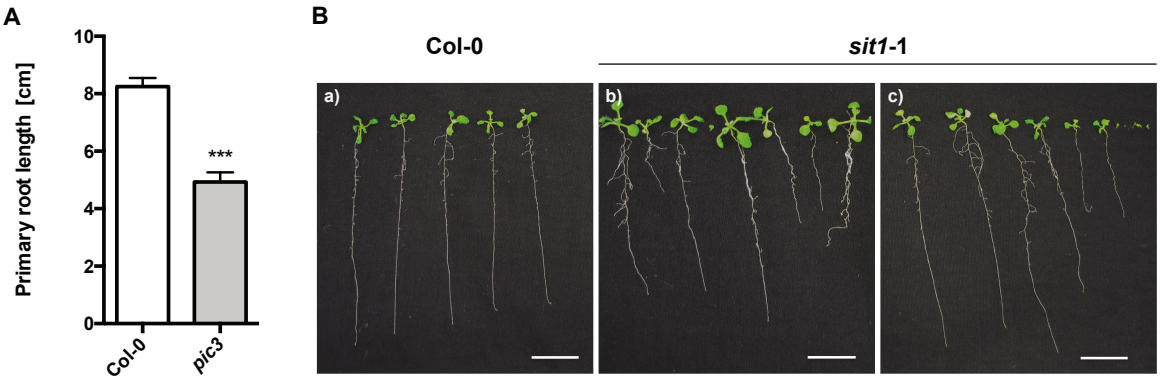

Fig. S6: Primary root growth is arrested in *sit1-1*.
A: Primary root length of wildtype (open bar) and mutant (filled bar). N = 50 seedlings/line; ***p = 0.001. B: Wildtype (a) and the mutant seedlings (b, c) were grown for 12 d on half-strength MS medium. Bar = 1 cm.

Supplemental sequences

Tab. S1: Protein sequences of Fig. 1 in FASTA format

>Cyanidioschyzon_merolae_CMT361CT
MLVRFSQLVTWSQTPMVTALQQRKDNGGSNCGVDQVLRAAPSTLPTVWGALGGRPATLVA
CSADENPTFGTYLKFALAGAICCSVTHSAVVPVDVVKTRLQLSDKYHGMTHAARTIVKEE
GALALLTGLSPTAVGYFLQGWFKFGLYEYFKRLYSSLAGPEAAEKGRFGIWLAAGGTAEF
FADLALCPLEATRIRLVSQPTFASSLPEAFGKLISNEGLRGLYAGLFPILLKQIPYTMAK
FAVFEAASEFIYRTLERMGKPKADMRDSTKLLISLNSGIFAGICAAVVSQPADTVLSVIN
KSRVTGSIAEATFRIIRELGPRGLFRGLGARAIMVGSLTAGQFFIYDGLKQLLGVAPVHK
KEVAPLVGSAAQPASVAARAQQSQ
>Homo_sapiens_ENSG00000075415
MFSSVAHLARANPFNTPHLQLVHDGLGDLRSSSPGPTGQPRRPRNLAAAAVEEQYSCDYG
SGRFFILCGLGGIISCGTTHTALVPLDLVKCRMQVDPQKYKGIFNGFSVTLKEDGVRGLA
KGWAPTFLGYSMQGLCKFGFYEVFKVLYSNMLGEENTYLWRTSLYLAASASAEFFADIAL
APMEAAKVRIQTQPGYANTLRDAAPKMYKEEGLKAFYKGVAPLWMRQIPYTMMKFACFER
TVEALYKFVVPKPRSECSKPEQLVVTFVAGYIAGVFCAIVSHPADSVVSVLNKEKGSSAS
LVLKRLGFKGVWKGLFARIIMIGTLTALQWFIYDSVKVYFRLPRPPPPEMPESLKKKLGL
TQ*
>Oryza_sativa_01_LOC_Os04g37600.1
MAVVSESSRKALLPSFLYAAPAASSSPSFAAAAAVGVRGVPAPSLAGPAVWARSPREPAG
KIEMYSPAFYAACTAGGIASCGLTHMTVTPLDLVKCNMQIDPAKYKSISSGFGVLLKEQG
ARGFFRGWVPTLLGYSAQGACKFGFYEFFKKYYSDIAGPEYAAKYKTLIYLAGSASAEVI
ADIALCPMEAVKVRVQTQPGFARGLSDGLPKFVKAEGYAGLYKGIVPLWGRQIPYTMMKF
ASFETVVEMIYKYAIPAPKSECSKPLQLGVSFAGGYIAGVFCAIVSHPADNLVSFLNNAK
GATVGDAVNKLGMWGLFTRGLPLRIVMIGTLTGAQWGLYDAFKVMVGLPTTGGVAPTPAK
*
>Oryza_sativa_02_LOC_Os02g52860.1
MALSDRSRESLLPSFLYTSSAARSFATGATRFPSPVSPASPAPGAVGGGAPISIQAPREK
IEMYSPAFYAACTAGGIASCGLTHMAVTPLDLVKCNMQIDPAKYKSITSGFGVLLKEQGP
RGFFRGWVPTLLGYSAQGACKFGFYEFFKKYYSDIAGPEYAQKYKTLIYLAGSASAEVIA
DVALCPFEAVKVRVQTQPGFARGLSDGLPKFVRSEGALGLYKGIVPLWGRQIPYTMMKFA
SFETIVEMIYKHAVPVPKSECSKSFQLGISFAGGYIAGVFCAIVSHPADNLVSFLNNAKG
ATVGDAVKKLGLWGLFTRGLPLRIVMIGTLTGAQWGIYDAFKVMVGLPTTGGVTPAPGAA
EKALQASA*
>Oryza_sativa_04_LOC_Os09g38100.1
MPEMGARGGEAGAARVANGGGGGGTGGMRLFSPEYYALCTGGGMLAAGATHLAITPLDVL
KVNMQVNPMKYNSIFSGLNILVKEEGASSLWRGWAGKFFGYGFQGGCKFGLYEYFKKKYS
DVLVDRNKSTIYFISSASAQIIADVALCPFESVKVRVQTQPMFAKGLIDGFPRVYATEGL
SGFYKGLLPLWGRNLPFSMLMFSTFEHTVDILYRNVIQKKKEDCSTMQQLGATCLAGYIS
GAVGTVVSNPADNIVSSLYNKKAKNIIDAVKSIGFRGLFTRSLPVRITLVGPVITMQWFF
YDTIKILTGLPTSGGLPRELEEV*
>Oryza_sativa_03_LOC_Os06g10810.1
MALSDRSRESLLPSFLYSTAGARPYTAGGGGAAFRLPAAAAPGGVGGGAPIEIQAPREKI
EMYSPAFYAACTAGGIASCGLTHMAVTPLDLVKCNMQIDPAKYKSITSGFGILAKEQGVR
GFFRGWVPTLLGYSAQGACKFGFYEFFKKYYSDIAGPEYAQKYKTLIYLAGSASAEVIAD
VALCPFEAVKVRVQTQPGFARGLGDGLPKFIKSEGALGLYKGIVPLWGRQIPYTMMKFAS
FETIVEQIYKHAVPVPKSECSKSFQLGISFAGGYIAGVFCAIVSHPADNLVSFLNNAKGA
TVGDAVKKLGLWGLFTRGLPLRIVMIGTLTGAQWGIYDAFKVMVGLPTTGGVTPAPSTSD
AGLKAVSA*
>Selaginella_moellendorffii_02_118858
MLRPGGERKNAPPVSADGQRGGFFIPAASEPGKIPLYSAEFYAACTAGGILSCGLTHTFV
TPLDIVKCNMQIDPKKYKSIGTGFSIIKQEQGPKGLFKGWGPTLIGYSAQGACKFGLYEF
FKKFYADMVGEEVAHDYKTFVYLAGSASAEFFADIALCPFEAIKVRVQTKPGFANGLRDG
FSKFVAQEGYGGLYKGLAPLWGRQIPYTMMKFACFEGTVEALYKYVVPVPKEKCSKLTQL
EVSFAAGYIAGIFCAVVSHPADNLVSFLNSTKGGTVGDAIKKMGLVGLMTRGLPLRIVMV
GTLTGAQWGIYDAFKVFVGL*

>Selaginella_moellendorffii_03_166544
MALEDCRRSSALPSFLYKSKGFKAPAPAPAINGGGGGALQSSRFLIPSPDESKKIAMYSP
EFYAACTVGGILSCGLTHTAVTPLDMVKCNMQIDPAKYRSIGSGFGVLYKEAGPKGLFKG
WVPTLFGYSAQGAFKFGLYEFFKKYYSDLAGEENAYKYKTFIYLAGSASAEFFADIALCP
MEAVKVRVQTKPGFANGLLDGLPKITRAEGVPGLYRGLVPLWGRQIPYTMMKFACFEATV
EALYKYVIPKPKDECSKVEQLGVSFGGGYIAGIFCAIVSHPADNLVSFLNNTKDATIGQA
VKSMGPVALFTRGLPLRIVMIGTLTGAQWGIYDAFKVFVGLPTSGGVSKAPEQLTTPLPL
PSA*
>Selaginella_moellendorffii_04_445447
MDAIQWGPEEIALFSSKYYAACFAGGLLSAGTTHFLVTPFDNLKVNMQVHPAKYSGGILS
GFGVLWKERGPTGLWRGWGGKLYGYGAQGACKFSLYEFFKHRYCDAAGPENSATYRTPIY
FAASACAQMIADVVLCPFESIKVRLQAQPGFAKGLIDGFPKVYSAERLPGLYRGLLPLWS
RNIPFAMLMFTSFEHSVDLIYRNVVKKPRSECSTTTTLLVTCGAAYISGITGTVVSNPAD
NVISSLYNKGGTVVQAIKRIGLVGLFTRSLPLRIALVGPVVTMQWFIYDSVKVSIGLPTS
GGTYVEEESSAS*
>Selaginella_moellendorffii_01_270420
MALEDSRSSTLPSFLYKSKGFKAPAPAIPINGQSSSRFLIPSPDETRKIAMYSPEFYAAC
TVGGALCCGLTHMAMTPLDVVKCNMQIDPAKYKSTASGFGTLYREAGPKGLFKGWVPTLL
GYSAQGAFKYGLYEFFKKYYSDLAGAENAYKYKTFIYLAGSFSSEFFADIALCPMEAVKV
RVQTKPGFANGLLDGLPKITRAEGVAGLYRGLVPLWGRQIPYTMMKFTCFEATVEALYKN
VVPKPKDECSKVEQLGVSFAGGYIAGIFCALVSHPADNLVSFLNNTKDATVGQAVKSMGL
VALVTRGLPLRIVMIGTLTGAQWVIYDAFKVFVGLPTTGGVSKAPEELTTPLPLPTA*
>Arabidopsis_thaliana_PHT3;3_SIT1_AT2G17270.1
MTRVKSKLDEELSSPWFYTVCTMGGMLSAGTTHLAITPLDVLKVNMQVNPVKYNSIPSGF
STLLREHGHSYLWRGWSGKLLGYGVQGGCRFGLYEYFKTLYSDVLPNHNRTSIYFLSSAS
AQIFADMALCPFEAIKVRVQTQPMFAKGLLDGFPRVYRSEGLAGFHRGLFPLWCRNLPFS
MVMFSTFEQSVEFIYQKIIQKRKQDCSKAQQLGVTCLAGYTAGAVGTIISNPADVVLSSL
YNNKAKNVLQAVRNIGFVGLFTRSLPVRITIVGPVITLQWFFYDAIKVLSGFPTSGGVKK
PVDAAKLSV
>Arabidopsis_thaliana_PHT3;1_AT5G14040.1
MESPKNSLIPSFLYSSSSSPRSFLLDQVLNSNSNAAFEKSPSPAPRSSPTSMISRKNFLI
ASPTEPGKGIEMYSPAFYAACTFGGILSCGLTHMTVTPLDLVKCNMQIDPAKYKSISSGF
GILLKEQGVKGFFRGWVPTLLGYSAQGACKFGFYEYFKKTYSDLAGPEYTAKYKTLIYLA
GSASAEIIADIALCPFEAVKVRVQTQPGFARGMSDGFPKFIKSEGYGGLYKGLAPLWGRQ
IPYTMMKFASFETIVEMIYKYAIPNPKSECSKGLQLGVSFAGGYVAGVFCAIVSHPADNL
VSFLNNAKGATVGDAVKKIGMVGLFTRGLPLRIVMIGTLTGAQWGLYDAFKVFVGLPTTG
GVAPAPAIAATEAKA
>Arabidopsis_thaliana_PHT3;2_AT3G48850.1
MSDSSRSLIPSFLYSSDHRLFQATTMSTHLKSQPLISPTNSSVSSNGTSFAIATPNEKVE
MYSPAYFAACTVAGMLSCGITHTAITPLDVIKCNMQIDPLKYKNITSAFKTTIKEQGLKG
FTRGWSPTLLGYSAQGAFKYGLYEYAKKYYSDIVGPEYAAKYKTLIYLAGSASAEIVADV
ALCPMEAVKVRVQTQPGFARGLSDGLPKIIKSEGFRGLHKGLVPLWGRQIPYTMMKFATF
ENTVELIYKKVMPTPKEECSKPVQLGVSFAGGYIAGIFCAIISHPADNLVSFLNNSKGAT
VADAVKRLGLWGMLTRGLPLRIFMIGTLTGAQWVIYDAVKVLAGLPTTGGASPATALAPS
VSA
>Cyanophora_paradoxa_Cypa6539
MTTLFANALHLRSLQPALAAPSLDKKVSPIYIPSVVEPAKRALIPSAIELYTPKYYYNCA
IGGALACGLTHTAIVPLDLVNPKEYASIGDGFKKVVAAEGAAGLAGGWLPTLIGYSLQGT
CKFGFYELFKKLYADAVGEENAHAYRTYLYLAASASAEVIADAALCPMEAVKVRMQTKPG
FPLALGPAMSLIMKEEGLNGFYKGLAPLWMRQIPYTMVKFASFEKTVEFIYNFLGGNRAD
YSKVQQLGITFAAGYWADYVVSQLNKNPGSSVGGILSEAGLSGVWRGLGARIIMIGTLTG
LQWFIYDYFKVMVGLPTTGAAPAKK*
>Lotus_japonicus_LJ4G031270
MAPSLVPGFLYSSKTLSQLDSSINTNHGLPPLSTTSSIGSHSSSPSPQGRSPMIPSPKEG
IPLFSPAYYAACSAGGVFSCGLTHMAVTPLDLVKCNMQIDPLKYKSITSGFGVLLKEQGA
KGFFRGWVPTLFGYSAQGACKFGFYEFFKKYYSDLAGPENAAKYKTFIYLAGSASAEVIA
DVALCPMEAVKVRVQTQPGFARGLSDGLPKFVKADGVAGLYKGLVPLWGRQIPYTMMKFA
SFETIVEMIYKQVIPTPKEQCSKNKQLGVSFAAGYIAGVLCAIVSHPADNLVSFLNNAKG
ATVGDAVKKIGVVGLFTRGLPLRIVMIGTLTGAQWGLYDSFKVFVGLPTTGGSAPAPVK
>Physcomitrella_patens_02_Pp1s308_15V6.1

MEPAMDTTGRRSLFPDYLYTSRAVFQPQNSCVAATNNTGVFAQHSSRPGTSSPYLLPKLL
PIRTAGPPSPASPTITIPSGDESNRIQMYSMEYFLACGLGGLLCCGLTHTAVTPIDVVKC
NMQIAPKKYTGVLGGFQLVVREEGVRGLWRGWAPTFVGYCIQGAGKYGFYEYFKKQYSDA
VGTENATRYKTAVFLGASFSAEFLADLGLCPFEAVKVRVQTQPGFARGLSDGLPKLIASD
GFAGLYKGLVPLWGRQIPYTMMKFATFESTVEALYTHLVPVPKSECSKQTQLGVSFTAGY
IAGIACAIISHPADNLVSFLNNAKGATVSQAVQEMGVTALLTRGLPLRIFMIGTLTGAQW
GIYDSFKVFVGFPTSGSSGDNDTEARVEH*
>Physcomitrella_patens_01_Pp1s233_41V6.1
MTASENQGLLPDYLYRSRGALSALVGIAGVSTSSPCGSRRRSTLGLAQVHDDVFRQFRSG
TCFDERVGSTGRSTGRDGLGKFMIPGISETRQIPLHTGEFYAYCAFGGVLSCGITHTGVT
PLDIVKCNMQIDPGKYEFIGSGFKLIMADQGLKGLYKGWGPTLIGYSLQGACKFGLYEYF
KHMYAEMAGEPFATDHKSLVFLAGSASAEFVADIALCPFEAIKVRVQTQPGYAKGLTDGM
SKFLATEGFTGLYAGIVPLWGRQIPYTMMKFTSFEATVDALYAHVVPVPKKECSKGYQLG
VSFAAGYIAGVLCAVVSHPADNLVSYLNCKKGASIRQAISDIGMFNLFTRGLPLRIFMIG
TLTGAQWGLYDSFKVYVGL*
>Physcomitrella_patens_03_Pp1s2_600V6.1
MIFAEKRTPTVPAFLYSIEARRTGISALPSLFQTLTTEASSNVAPAYTSSSLFKQVASAA
KTSTGVASSVMVPSPSEPGKIVMFSGEYYRACAVGGMMCCGLTHMGVTPIDVVKCNMQIA
PEKYKSISSGFSLLVKEQGAVGLVRGWVPTLMGYSVQGACKYGFYEYFKKTYSDMAGAED
AKRFKTLIYLGASASAEVIADVGLCPFEAVKVRVQTNPGFAKGIMDGMPKLIASDGVGGL
FKGLVPLWCRQIPYTMMKFATFESTVEAIYKYAVPVPKSEVSSGTQLGISFTAGYIAGVA
CAVISHPADNLVSFLNKSKEATVSGAVKQMGVKALFTRGLPLRIIMIGTLTGAQWGIYDS
FKVFVGLPTTGGVVEEPRKLA*
>Pp1s2_605V6.1
MAADPKTRTLVAARSLELIATHEFLGEMPNPPPPLPLQNPTSSIIALFHSILTTQLSLCS
DCSFRASTSPNAQCFHPRQELRCLITLFYWFRVAESCLVDLVCKRERSELILQLPAVMAF
AEKCTPMVPAFLYSTVARRTGISALPSLFQTMTTEASSNVAPAYTSSSLFKQVASAAKTS
TGVASSVMVPSPSEPGKIVMFSGEYYRACAVGGMMCCGLTHMGVTPIDVVKCNMQIAPEK
YKSISSGFSLLVKEQGAVGLVRGWVPTLMGYSVQGACKYGFYEYFKKTYSDMAGAEDAKR
FKTLIYLGASASAEVIADVGLCPFEAVKVRVQTNPGFAKGIMDGMPKLIASDGVGGLFKG
LVPLWCRQIPYTMMKFATFESTVEAIYKYAVPVPKSEVSSGTQLGISFTAGYIAGVACAV
ISHPADNLVSFLNKSKEATVSGAVKQMGVKALFTRGLPLRIIMIGTLTGAQWGIYDSFKV
FVGLPTTGGVVEEPRKLA*
>Physcomitrella_patens_07_Pp1s134_72V6.1
MVGQASLFVGSNRVEREPEVTWDAQIRANKLELFTSKYYAACAVGGMISAGSVHLLITPL
DMLKVNMQANPLKYRSIMSGFGIVYREQGIGGIWKGWSSKLFGYGAQGACKFGLYEYFKK
FYADLAGPEFTKENKTAIFAAGSLSAQVIADVALNPFESVKVKVQTGYAKGLVDGFPRLY
RAEGLAGLYRGLPLLWGRNIPFSVLMFSTFEHSVDFLYKNVLQRPKNDCSRIQQLGITCM
AGYMSGVTGTIISNPADILITTVNKNRKLSMVQAAKRIGVTGLFTRSLPLRIMIVGPMAT
AQWLCYDTLKVLVGLPTSGGIEQFVEVD*
>Physcomitrella_patens_08_Pp1s5_438V6.1
MEQTWVPQMPTTKLELFSNKYYAACALSGMISTGSVHLLVTPFDMLKVNMQANPRKYKSI
VKSFGIIYSEQGLKGIWKGWGSKLCGYSAQGAFKFGLYEYFKKFYSDVAGTDYIRLNKTS
IYVASSLSAQIIADTALCPFESIKVRVQTGYAKGLTDGLPKVYRAEGLTGLYKGLVSLWG
RNLPFAVLMFSTFEHSVDFLYGNIIHKPKNECSMGVQLGVTCMAGYMSGVAGTIISNPAD
NMITAINKRKGLSYVQAAKSIGLVGLFTRSLPLRVMLVGPLVTAQWFCYDSMKVLVGLPT
SGGVEHLISDQDGL*
>Physcomitrella_patens_06_Pp1s61_90V6.1
MVFAEKRTSMVPEFLYSTKTARSGISAPKSLFQALTAEASSNAAPAYTASSLFKQVAGAA
RTPAGVASPFMVPSASERKIVMFSGEYYRACAVGGMLCCGLTHMGVTPIDVVKCNMQIAP
EKYKSISGGFSLIVKEHGVVGLFRGWVPTLLGYSVQGACKYGFYEYFKKTYSDMAGPENA
KKYKTVIYLAGSASAEVIADVGLCAFEAVKVRVQTNPGFAKGLSDGMPKLIASDGVKGLF
KGLVPLWGRQIPYTMMKFATFESTVEAIYKYAVPVPKSEVSSSSQLGISFTAGYIAGVAC
AIISHPADNLVSFLNKSKDATVKQAIDQMGLKALFTRGLPLRIIMIGTLTGAQWGIYDSF
KVFVGLPTTGGVVEEPKKE*
>Physcomitrella_patens_05_Pp1s61_113V6.1
MVFAEKRTSMVPEFLYSTKTARSGISASKSLFQALTAEASSHAAPAYTASSLFKQVAGAA
RTPAGVASPLMVPSASERKIVMFSGEYYRACAVGGMLCCGLTHMGVTPIDVVKCNMQIAP
EKYKSISGGFSLIVKEHGVVGLFRGWVPTLLGYSVQGACKYGFYEYFKKTYSDMAGPENA
KKYKTVIYLAGSASAEVIADVGLCAFEAVKVRVQTNPGFAKGLSDGMPKLIASDGVKGLF

KGLVPLWGRQIPYTMMKFATFESTVEAIYKYAVPVPKSEVSSSSQLGISFTAGYIAGVAC
AIISHPADNLVSFLNKSKDATVKQAIDQMGLKALFTRGLPLRIIMIGTLTGAQWGIYDSF
KVFVGLPTTGGVVEEPKK*
>Brachypodium_distachyon_03_Bradi4g37420.1
MGSRGGGGTSGAEAPRRSGRGGAGGMRLFSPEYYALCAGGGMLAAGTTHLAITPLDVLKV
NMQVNPMKYNTIFSGLSVLVKEEGVSSLWRGWGGKLFGYGAQGGCKFGLYEYFKKQYSDV
LVDSNRSTIFFLSSASAQIIADVALCPFESVKVRVQTQPMFAKGLVDGFPRVYAAEGLSG
FYRGLLPLWGRNLPFSMLMFSTFEHTVGFLYQKVIQKKKEDCSTAQQLGATCLAGYISGA
VGTVVSNPADNIVSSLYNKKAKNIIHAVKSIGLRGLFTRSLPIRITLVGPVVTMQWFFYD
SIKILTGLPPSGGLPRELEEANT*
>Brachypodium_distachyon_01_Bradi5g11740.1
MAVSESSRNALLPSFLYAVPAAATSPFSSAAGVAGSGLVVPSSAAVATRPAVWARAPSEP
SGKIEMYSPAFYAACTAGGIASCGLTHMTVTPLDLVKCNMQIDPAKYKSISSGFGVLLKE
QGARGFFRGWVPTLIGYSGQGACKFGFYEFFKKYYSDIAGPEYAAKYKTLIYLAGSASAE
VIADIALCPMEAVKVRVQTQPGFARGLSDGLPKFVKAEGYAGLYKGIVPLWGRQIPYTMM
KFASFETIVEMIYKYAIPAPKSECSKSLQLGVSFAGGYVAGVFCAIVSHPADNLVSFLNN
AQGGTVGDAVKKLGLWGLFTRGLPLRIVMIGTLTGAQWGIYDAFKVMVGLPTTGGAAPPP
AAAGEQLKA*
>Brachypodium_distachyon_02_Bradi3g57890.1
MALSDLSRESLLPSFLYTSTAARSFAGASRFPSSSSPQAPSFGGGSAGGRKPFSLQAPNE
KIEMYSPAFYAACTAGGIASCGLTHMAVTPLDLVKCNMQIDPAKYKSISSGFGVLLKEQG
ARGFFRGWVPTLLGYSAQGACKFGFYEFFKKTYSDMAGPENALKYKTLIYLAGSASAEVI
ADIALCPFEAVKVRVQTQPGFARGLSDGLPKFIKAEGAGGLYKGIVPLWGRQIPYTMMKF
ASFETIVELIYKHAVPVPKSECSKPFQLGISFAGGYIAGVFCAIVSHPADNLVSFLNNAK
GATMGDAVKKIGVLGLFTRGLPLRIVMIGTLTGAQWGIYDAFKVMVGLPTTGGVAPAPPV
EAAPVA*
>Chlamydomonas_reinhardtii_Cre03.g172300.t1.2
MAPQTSPMVSAALATMQPKQEQQPAVPALSSALNTGILGKMVAASATEVAPRKIELYSSE
YYWTCALGGVASCGLTHMGVTPLDVVKCNIQTNPAKYKGISTGFRVLVAEQGAAGLFKGW
VPTLLGYSAQGACKFGLYEYFKKTYADMAGEEVAKKYQSAIFLAGSASAEFFADIALCPF
EAVKVKVQTVPGFAKGLSDGLPKFVAQEGWGGLFKGIKPLWGRQIPYTMMKFGAFENTVQ
AIYKYAMPKPKSECSKGEQLGVSFAAGYIAGVFCAVVSHPADNLVSKLNAQKGATVGDIV
KEMGWYALFTRGLGLRIIMIGTLTGLQWGIYDAFKVSMGLPTTGSVEEKKK*
>28592.m000281
MVTLEQPLRIKEDCHYKAAAGYYGICAVSGMLSAGTTHLAMTPLDVLKVNMQVNPVKYSS
IYSCFTAILREQGPSAFWRGWAGKLIGYGVQGGCRFGFYEYFKSLYSDVLDNSNRNLVFF
MSSASAEIFANLGLCPFEAIKVRVQAQPHFAKGLLDGFPRLYASEGFLGFYRGLVPLLAR
SLPFSIVMFSTFEHSADFLYRTVIQRRKEDCSKSQQLGVTCLAGYAAGSVGSFVSNPADN
IVSCLYNRKADSLLLAIKKIGFSNLLTRSLPIRIMLVGPAVTLQWLFYDTIKVFSGLPAS
GEVRTEVETDRAN
>Ricinus communis_01_30131.m006856
MGFSDSSKQSLIPSFLYSSSSSSKTLTLSKLLHSNQQSPSPSLMRKSSGNFVIPAPSEPG
KIEMYSPAFYAACTAGGILSCGLTHMTVTPLDLVKCNMQIDPAKYKSISSGFGILLKEQG
VRGFFRGWVPTLLGYSAQGACKFGFYEFFKKYYSDIAGPEHAAKYKTLIYLAGSASAEVI
ADVALCPFEAVKVRVQTQPGFARGLSDGLPKFVKSEGALGLYKGIVPLWGRQIPYTMMKF
ASFETIVEMIYKHAIPTPKDQCSKSLQLGVSFAGGYVAGVFCAIVSHPADNLVSFLNNAK
GATVGDAVKKLGLWGLFTRGLPLRIVMIGTLTGAQWGIYDAFKVFVGLPTTGGVAPAAPA
AELAKA
>Ricinus communis_02_30147.m014426
MAISAKSSQSLIPDFLYSSNFDLDASPDAKYGLYRSSFVSKSLPSNVGGGAVSRNFVIPA
PKEKIEMYSPAFYAACTAGGTFSCGLTHMAVTPLDLVKCNMQINPAKYKSISSGFGILLK
EQGIKGFFRGWVPTLLGYSAQGACKYGFYEFFKKYYSDIAGPEYAAKYKTLIYLAGSASA
EIIADVVLCPMEAVKVRVQTQPGFARGLADGMPKFIRSEGYAGLYKGLVPLWGRQIPYTM
MKFASFETIVEQIYKHAIPTPKDQCSNSLQLGVSFAGGYIAGVFCAIVSHPADNLVSFLN
NAKGATAGDAIKQLGLWGLFTRGLPLRIVMIGTLTGTQWGIYDAFKVFVGLPTSGGAPPP
AAAKA
>Ustilago_maydis_UM05105
MATFTERFTKGTYPIHSVAEAIKPGPQGVDLYSRFFLAGALCCSLTHGAVTPIDVVKTRI
QLEPTVYNKGMIGGFRQVIAKEGAGALLTGLGPTVLGYFLQGGFKFGGYELFKKILVSQM
DNDTAVKNRMAIYLGASAIAEFFADIALCPLEATRIRLVSQPTFANGLAPAFLKIAREEG

LGGFYAGFGPILFKQIPYNMAKFATMEVVLEKAIQAYGKPKSELSGGEATFLNLGSGLIA
GFAAATISQPADTLLSKINKQKALPGETITGRITKMAGELGVRGLFGGLTTRLVMVGSIT
AGQFGIYGELKKALGATNTVEISKA*
>Brassica_rapa_01_Bra023446
MESSKNSLIPSFLYSSSSSPRSVLLDQVINSNSNAAFQSPNLEKNSPSPSPKTMASRKNF
LIASPTEPGKGIEMYSRDFYAACTVGGILSCGLTHMAVTPLDLVKCNMQIDPAKYKSISS
GFGILLKEQGVRGFFRGWVPTLLGYSAQGACKFGFYEFFKKYYSDLAGPEFAAKYKTLIY
LAGSASAEVIADVALCPFEAVKVRIQTQPGFARGMSDGFPKFVKSEGYGGLYKGLAPLWG
RQIPYTMMKFASFETIVEMIYKYAIPNPKHECSKGLQLGVSFAGGYVAGVFCAIVSHPAD
NLVSFLNNAKGATVGDAVKKIGMVGLFTRGLPLRIVMIGTLTGAQWGLYDAFKVFVGLPT
TGGVTPAPAAKA*
>Brassica_rapa_02_Bra008784
METPKTSSLIPSFLYSSSPRSILEKSPSPAARSSPATMVSRKSFLIASPTEPGKGIEMYS
PAFYAACTFGGVLSCGLTHMTVTPLDLVKCNMQIDPAKYKSISSGFGILLKEQGVKGFFR
GWVPTLLGYSAQGACKFGFYEFFKKYYSDLAGPEFAAKYKTLIYLAGSASAEVIADVALC
PFEAVKVRVQTQPGFARGMSDGFPKFVKSEGYGGLYKGLAPLWGRQIPYTMMKFASFETI
VEMIYKYAIPNPKHECSKGLQLGVSFAGGYVAGVFCAIVSHPADNLVSFLNNAKGATVGD
AVKKIGMVGLFTRGLPLRIVMIGTLTGAQWGLYDAFKVFVGLPTTGGVTPAPVIAAAEA*
>Brassica_rapa_04_Bra019570
MSDSSRSLIPSFLYSSDHRLFQLHEPAMNMTQRKAQPSRSLKTSSVSSNGPSFAIPAPNE
KVELYSPAYFAACTVGGMLSCGVTHTAVTPLDVLKCNMQVKLLNQNCLVLLLAELILRIN
IFEPYSKAMYVIDPSKYKNITSAFKTTIKEQGLKGFTRGWSPTLIGYSAQGAFKYGLYEY
AKKYYSDIVGPENAAKYKTLIYLAGSASAEIVADVALCPMEAVKVRVQTQPGFARGLSDG
LPKIIRSEGVRGLFKGLVPLWGRQIPYTMMKFATFENTVELIYKKVIPTPKEECSEPVQL
GVSFAGGYIAGIFCAVISHPADNLVSFLNNSKGATVSDAVKRLGLLGMFTRGLPLRIFMI
GTLTGAQWVIYDAVKVLAGLPTTGGASPATALAPAVSA*
>Brassica_rapa_03_Bra009654
MTSVKRKLDDELSSPWFYTVCTMGGMLSAGTTHLAITPLDVLKVNMQVNPVKYNSIPSGF
STLLREHGHSYLWRGWSGKLLGYGVQGGCRFGLYEYFKTLYSNVLPNNNRTSLYFLSSAS
AQIFADMALCPFEAIKVRVQTQPLFAKGLLDGFPRVYRNEGLAGFHRGLFPLWCRNLPFS
MVMFSTFEQSVEFIYKNIIQKRKQDCSKSQQLGVTCLAGYTAGAVGTIISNPADVVVSSL
YNNKAKNVLQAVRNIGLVGLFTRSLPVRITIVGPVITLQWFFYDAIKVLSGFPTSGGVEK
PVDATKLAV*
>Glycine_max_05_Glyma11g09300.1
MVMEGRICEELTPRYYALCAIGGMLSAGTTHLAITPFDVLKVNMQVHPIKYYSISSCFTT
LLREQGPSVLWKGWTGKFFGYGAQGGCRFGLYEYFKEVYSNVLVDQNRSFVFFLSSASAE
VFANVALCPFEAVKVRVQAQTCFAKGLYDGFPKLYASEGTRGFYRGLIPLLGRNIPFSMV
MFSTFEHSVDFLYRNVVKRKKEDCSIGQQLGVTCLAGYAAGSVGSFISNPADNIVSSLYN
RKADSLALAIRNIGLANLFTRSLPIRMLLVGPSITLQWFFYDTIKILGGMSTSGGVRTDM
RGNGAG*
>Glycine_max_02_Glyma08g01190.1
MAPSDQSRHSLVPGFLYSSKTLSHLNNNTNHELPPSSSPQGGTNTKSPMILSPKEGIRMF
SPAYYAACSAGGIFSCGLTHMAVTPLDLVKCNMQIDPVKYKNITSGFGVLLKEQGAKGFF
KGWVPTLLGYSAQGACKFGFYEFFKKYYSDLAGPENAIKYKTIIYLAGSASAEVIADVAL
CPMEAVKVRVQTQPGFARGLSDGLPKFIKADGVSGLYKGLVPLWGRQIPYTMMKFASFET
IVEKIYKYAIPTPKEQCSKTMQLGVSFAAGYIAGVLCAIVSHPADNLVSFLNNAKGATIG
DAVNKIGVVGLFTRGLPLRIVMIGTLTGAQWGLYDSFKVFVGLPTTGGSTPAPVK*
>Glycine_max_01_Glyma05g38480.1
MAPSDQSHHSLVPGFLYSSKTLSHLNNNTNHGLPPSSSIASSSLPQGRTKSPMILSPKEG
IRMFSPAYYAACSAGGIFSCGLTHMAVTPLDLVKCNMQIDPVKYKNITSGFGVLLKEQGA
KGFFKGWVPTLLGYSAQGACKFGFYEFFKKYYSDLAGPENAIKYKTIIYLAGSASAEVIA
DVALCPMEAVKVRVQTQPGFARGLSDGLPKFIKADGVSGLYKGLVPLWGRQIPYTMMKFA
SFETIVEKIYKYAIPTPKEQCSKTKQLGVSFAAGYIAGVLCAIVSHPADNLVSFLNNAKG
ATVGDAVKKIGVVGLFTRGLPLRIVMIGTLTGAQWGLYDSFKVFVGLPTTGGSAPAPVR*
>Glycine_max_06_Glyma01g36120.1
MVMEGRICEELKPRYYALCAIGGMLSAGTTHLAITPFDVLKVNMQVHPIKYYSISSCFTS
LLREQGPSVLWKGWTGKFFGYGAQGGCRFGLYEYFKEVYSNVLVDQNRSFVFFLSSASAE
VFANVALCPFEAVKVRVQAQPCFAKGLYDGFPKLYASEGTRGFYRGLIPLLGRNIPFSMV
MFSTFEHSVDFLYRNVVKRKKEDCSIGQQLGVTCLAGYAAGSVGSFISNPADNIVSSLYN
RKADSLALAIRNIGLANLFTRSLPIRMLLVGPSITLQWFFYDTIKILGGMPTSGEVRTDV

RGDGAG*
>Glycine_max_03_Glyma19g27380.2
MALPDSSSRRNSLIPSFIYSSSSKTLPLHHMLNTASAAAAAAPSPPPANLDAGSRGLMIP
SPSESRKIELYSPAFYAACTAGGILSCGLTHMTVTPLDLVKCNMQIDPAKYKSISSGFGV
LLKEQGFRGFFRGWVPTLLGYSAQGACKFGFYEFFKKYYSDIAGPEYASKYKTLIYLAGS
ASAEVIADIALCPFEAVKVRVQTQPGFARGLSDGLPKFVRSEGTLGLYKGLVPLWGRQIP
YTMMKFASFETIVELIYKHAIPTPKNECTKSLQLGVSFAGGYVAGVLCAIVSHPADNLVS
FLNNAKGATVGDAVKKLGLWGLFTRGLPLRIVMIGTLTGAQWGIYDAFKVFVGLPTTGGP
APAAAPAPGSELAKA*
>Glycine_max_04_Glyma16g26240.1
MAPVDSDTLGRHSLIPSYLYSSPSPQKKKMEASSFAIHSPRENRNIEMFSPSFYAACTVG
GSLSCGPTHTGITPLDVVKCNIQIDPVKYKNTSTGFGVMFEEQGLRGFFRGWGPTLVGYS
AQGAFKYGFYEFFKKYYSDIAGPEYATKYKTLIYLAGSASAELIAGVALCPFEAVKVRVQ
TQPGFARGLADGLPKLVRTEGVSGLYKGIVPLWGRQVPYTMMKFASYENIVEMIYKHAIP
KPKYECSNSLQLGVSIVSGYMAGILCATVSHPADNLVSFLNNSKGATVGDAVKKLGLWGL
FTRGLPLRILMVGTLTGAQWGIYDSFKVFVGLPTTGGVAPAAVLAPASAA*
>Micromonas_pusilla_MicpuC2.estExt_Genewise1.C_170191
MAASGKAEYGLDYFLKGALAGGICCSITHGALTPVDVVKTRMQLEPTKYTGMISGFNKVI
AEEGAGALLTGLGPTAFGYFVQGWFKFGGVEYFKIQAAQSMTEQQTWDNRNSIYLGASAA
AEFIADIFLCPLEATRIRLVSNPTYADSMLGCMAKMVKEEGVIGAFYSGFGPILAKQVPY
TMAKFAVQGATAEKIYDSLGKTPKEMSSGENISVSLASGVVAGVTAAIISHPADTLLSKI
NKAGAGGSGGMFSRLANIAAETGLVKLCTQGLAARCVMIGTLTAGQFGIFDIVMNAVGAS
KFHFHDPSKGDH*
>Sorghum_bicolor_04_Sb02g032310.1
MGDAEAASRVGRRGAAAAAGMRVFSPEYYALCAGGGMLAAGATHLAITPLDVLKVNMQVN
PMKYNSIFSGLNVLVKEEGPSSLWRGWGGKFVGYGVQGGCRFGLYEYFKKRYSDMLVDSN
KSTIYFLSSASAQIIADVALCPFESVKVRVQTQPMFAKGLVDGFPRVYATEGLSGFYRGL
LPLWGRNLPFSMLMFSAFEHTVDFLYQKVIQKKKEDCSTIQQLGATCVAGYISGAVGTVV
SNPADNIVSSLYNKKAENIIHAVKSIGFRNLFTRSLPIRIALVGPVISMQWFFYDTIKIL
TGLPPSGGLPRELEEVNI*
>Sorghum_bicolor_02_Sb04g034260.1
MALSDRSRESLLPSFLYSSSARSFAATGAAAARLPVSAPAPAAAGAGGRVPFSIQAPSEK
IEMYSPAFYAACTAGGIASCGLTHMAVTPLDLVKCNMQIDPAKYKSISSGFGVLLKEQGA
RGFFRGWVPTLLGYSAQGACKFGFYEFFKKYYSDIAGPEYAQKYKTLIYLAGSASAEVIA
DVALCPFEAVKVRVQTQPGFARGLSDGLPKFVRSEGALGLYKGIVPLWGRQIPYTMMKFA
SFETIVELIYKHAVPVPKSECSKTTQLGISFAGGYIAGVFCAIVSHPADNLVSFLNNAKG
ATVGDAVKKLGLWGLFTRGLPLRIVMIGTLTGAQWGIYDAFKVMVGLPTTGGPAPAAVAA
PAAEAESKASA*
>Sorghum_bicolor_01_Sb06g018210.1
MAVSESSRNALLPSFLYAAPAAASPFAAAASVGGRTVAAPSAAAAARPAIWARAPSEPGR
RIEMYSPAFYAACTAGGVASCGLTHMTVTPLDLVKCNMQIDPAKYKSITSGFGVLLKEQG
PKGFFRGWVPTLLGYSAQGACKFGFYEFFKKYYSDIAGPEYAAKYKTLIYLAGSASAELI
ADIALCPMEAVKVRVQTQPGFARGLSDGLPKFVKAEGYSGLYKGIVPLWGRQIPYTMMKF
ASFETVVEMIYKYAIPAPKNECSKNLQLGVSFAGGYIAGVFCAIVSHPADNLVSFLNNAK
GATVGDAVKKIGLVGLFTRGLPLRIVMIGTLTGAQWGIYDAFKVMVGLPTTGGAAPTPAA
TKA*
>Sorghum_bicolor_03_Sb10g007010.1
MALSDRSRESLLPSFLYSPAATRSFAGASRFPASPAAAAASAPSVAGGGALPFTIQAPNE
KIEMYSPAFYAACTAGGIASCGLTHMAVTPLDLVKCNMQIDPAKYKSISSGFGILAKEQG
VRGFFRGWVPTLLGYSAQGACKFGFYEFFKKYYSDIAGPEYAQKYKTLIYLAGSASAEVI
ADVALCPFEAVKVRVQTQPGFARGLSDGLPKFIKSEGALGLYKGIVPLWGRQIPYTMMKF
ASFETIVELIYKHAVPVPKSECSKPFQLGISFAGGYIAGVFCAIVSHPADNLVSFLNNAK
GATVGDAVKKLGLWGLFTRGLPLRIVMIGTLTGAQWGIYDAFKVMVGLPTTGGVTPAPAP
ATEEAALKASA*
>Hansenula_polymorpha_01_fgenesh1_kg.7_#_18_#_isotig00782
MASTYQTPNYTVSDYAKFALAGAIGCGVTHGSMTPIDVVKTRIQLEPTVYNTGMIGSFKK
VVANEGAGALLTGLGPTVLGYSLQGAFKFGGYELFKKTFIDSLGYQTAVQYKDAIYIGSA
AIAEFFADIALCPLEATRIRLVSQPTFANGLIGGFARILREEGVGSFYNGFTPILFKQIP
YNIAKFLTYERASQAIYSFVTTPKDQLSSTAVTGINLGAGVIAGCMAAVVSQPADTLLSK
VNKTKKAPGQSTVGLLAQLARELGVRGSFTGLSTRLVMVGTLTSLQFALYGSIKGALGCP

PAVELGAGGH*
>Hansenula_polymorpha_02_estExt_fgenesh1_pg2.C_70310
MSSDKIELYSSKYYIACATGGFLACAPTHSGVLPLDLVKCRLQVKPGLYKGNLDGIKSII
KTEGLRKVFTGIGPTFIGYGLQGSGKYGFYEVFKKKYSDFFGVSNAYVYMLASASAEFLA
DIALCPFESMKVKIQTTLPPNPVVGLYSNLYSGLVPLWFRQIPYTCVKFTSFEKIVELIY
ASFLTKPKEQYSKIQQTGVSFAGGYVAGIFCALVSHPADVMVSLINNESGKGESMLSAVG
RIYKRIGFSGLWNGLGARIVMIGTLTGFQWLIYDSFKVSVGLPTTGH*
>Mus musculus_ENSMUSG00000061904
MFSSVAHLARANPFNAPHLQLVHDGLSGPRSPPAPPRRSRHLAAAAVEEQYSCEYGSGRF
FLLCGLGGIISCGTTHTALVPLDLIKCRMQVDPQKYKGIFNGFSITLKEDGVRGLAKGWA
PTLIGYSMQGLCKFGFYEVFKALYSNILGEENTYLWRTSLYLASSASAEFFADIALAPME
AAKVRIQTQPGYANTLREAVPKMYKEEGLNAFYKGVAPLWMRQIPYTMMKFACFERTVEA
LYKFVVPKPRSECTKAEQLVVTFVAGYIAGVFCAIVSHPADSVVSVLNKEKGSTASQVLQ
RLGFRGVWKGLFARIIMIGTLTALQWFIYDSVKVYFRLPRPPPPEMPESLKKKLGLTE*
>Saccharomyces_cerevisiae_MIR1_YJR077C
MSVSAAPAIPQYSVSDYMKFALAGAIGCGSTHSSMVPIDVVKTRIQLEPTVYNKGMVGSF
KQIIAGEGAGALLTGFGPTLLGYSIQGAFKFGGYEVFKKFFIDNLGYDTASRYKNSVYMG
SAAMAEFLADIALCPLEATRIRLVSQPQFANGLVGGFSRILKEEGIGSFYSGFTPILFKQ
IPYNIAKFLVFERASEFYYGFAGPKEKLSSTSTTLLNLLSGLTAGLAAAIVSQPADTLLS
KVNKTKKAPGQSTVGLLAQLAKQLGFFGSFAGLPTRLVMVGTLTSLQFGIYGSLKSTLGC
PPTIEIGGGGH*
>Saccharomyces_cerevisiae_PIC2_YER053C
MESNKQPRKIQLYTKEFYATCTLGGIIACGPTHSSITPLDLVKCRLQVNPKLYTSNLQGF
RKIIANEGWKKVYTGFGATFVGYSLQGAGKYGGYEYFKHLYSSWLSPGVTVYLMASATAE
FLADIMLCPFEAIKVKQQTTMPPFCNNVVDGWKKMYAESGGMKAFYKGIVPLWCRQIPYT
MCKFTSFEKIVQKIYSVLPKKKEEMNALQQISVSFVGGYLAGILCAAVSHPADVMVSKIN
SERKANESMSVASKRIYQKIGFTGLWNGLMVRIVMIGTLTSFQWLIYDSFKAYVGLPTTG
*
>Vitis_vinifera_02_GSVIVT01008630001
MAVTPLDLVKCNMQIDPTKYKSISSGFGVLLKEQGVKGFFRGWVPTLLGYSAQGACKYGF
YEFFKKYYSDIAGPEYATKYKILIYLAGSASAEIIADVALCPMEAVKVRVQTQPGFARGL
SDGLPKFVKSEGALGLYKGLVPLWGRQIPYTMMKFASFETIVEMLYKYAIPTPKEQCSKS
LQLGVSFAGGYVAGILCAIVSHPADNLVSFLNNAKGATVGDAVKNLGLWGLFTRGLPLRI
VMIGTLTGAQWGIYDTFKVFVGLPTTGGVTPAPAATVPAKV*
>Vitis_vinifera_04_GSVIVT01022311001
MRGVEERRECGELTPGPGYFWVCTIGGMLSAGTTHVAITPLDVLKVNMQVYPIKYNTISS
CFITLLREQGPSAFWRGWATKFFGYGVQGGFRFGLYEYFKKLYSDVLVDHNRSFIFFASS
ASAEVLANVALCPFEAVKVRVQAQPHFAKGLLDGFPKLYASEGLYGFYRGLVPLWGRNLP
FSMIMFSTFEHSVDFLYRNVIHRRKEDCSRVQQLGVTCLAGCAAGSVASLITNPADNIVA
SLYNRKADSLLLAVKKIGLMNLFTRSLPIRIILVGPVVTLQWLVYDTIKVLSGLPTSGEV
LTDKEVNKKV*
>Vitis_vinifera_03_GSVIVT01023867001
MMRVEGRAYQELSPSYYGICTVGGMLSAGTIHLAITPLDVLKVNMQVNPIKYNSITSGLN
TLWKEQGPSALWRGWSGKLFGYGVQGGCKFGLYEYFKRIYSDVLVDQNRSVIFFVSSASA
QVFADVALCPFEAVKVRVQTQPHFAKGLADGFPKLYATEGLSGFYKGLFPLWGRNLPFSM
TMFSTFEHSIDFIYDNIIQKKKEDCSVAQQLGVTCLAGYAAGAFGTLISNPADNIVSSLY
NKNAENVLQAAKNIGFANLFTRSLPLRITFVGPVVTLQWFFYDTIKVLSGFPTSGGPVRH
IEEADRSA*
>Vitis_vinifera_01_GSVIVT01033005001
MAVTPLDLVKCNMQIDPAKYKSISSGFGVLLKEQGVRGFFRGWVPTLLGYSAQGACKFGF
YEFFKKYYSDIAGPEYAAKYKTLIYLAGSASAEVIADVALCPMEAVKVRVQTQPGFARGL
SDGFPKFVKSEGALGLYKGIVPLWGRQIPYTMMKFASFETIVEMLYKYAIPTPKDQCSKT
LQLGVSFAGGYVAGVFCAIVSHPADNLVSFLNNAKGATVGDAVKNLGLWGLFTRGLPLRI
VMIGTLTGAQWGLYDAFKVFVGLPTTGGIAPAPPAPTTSELAKA*

Tab. S2: Primers used in this study

Primer	Sequence (5'-3')
SV28	GGGGACAAGTTTGTACAAAAAAGCAGGCTCCACCATGGAATCTCCGAA
SV29	GGGGACCACTTTGTACAAGAAAGCTGGGTCGGCTTTGGCTTCAGTAGCTG
SV30	GGGGACCACTTTGTACAAGAAAGCTGGGTTTAGGCTTTGGCTTCAGTAGCT
SV55	CTTTCCTCTAGTCTTTTGTCGAATG
SV56	AATATGTTACTGCGATGAAATGGAT
SV57	TTTGATATAAATACAGCGGGACCTA
SV60	ATGAAAATAACTTTGGTCAAACAGC
SV77	GGGGACAAGTTTGTACAAAAAAGCAGGCTCCACCATGTCTGACTCAAGCAGATCG
SV78	GGGGACCACTTTGTACAAGAAAGCTGGGTCTGCACTTACAGATGGAGCAAG
SV79	GGGGACCACTTTGTACAAGAAAGCTGGGTCTTATGCACTTACAGATGGAGCAAG
SV80	GGGGACAAGTTTGTACAAAAAAGCAGGCTCCACCATGACAAGAGTCAAGAGTAAACTAGAC
SV81	GGGGACCACTTTGTACAAGAAAGCTGGGTCCACTGATAATTTAGCTGCATCCA
SV82	GGGGACCACTTTGTACAAGAAAGCTGGGTCTCACACTGATAATTTAGCTGCATCC
SV87	GGGGACAAGTTTGTACAAAAAAGCAGGCTTCTTTGTGTGCTGTTTGATTATGTT
SV88	GGGGACCACTTTGTACAAGAAAGCTGGGTGAATGATCGATCCTCATTGACTG
SV156	GGGGACAAGTTTGTACAAAAAAGCAGGCTCCATGTCTGTGTCTGCTGCTCCT
SV170	GGGGACCACTTTGTACAAGAAAGCTGGGTCCTAATGACCACCACCACCAA
SV179	TCATTGGAGAGAAGATGGTGG
SV180	TTATAGCCAAATGGGTTGTTCC
P52	CCCATTTGGACGTGAATGTAGACAC
P67	TTCAATGTCCCTGCCATGTA
P68	TGAACAATCGATGGACCTGA
P78	CTGCAGCGAGGAGCCGTAAT

Acknowledgements

We acknowledge DFG-GRK 1525 for funding this research. We gratefully thank Dr. Christian Eßer at the Bioinformatics Institute, Heinrich-Heine University Düsseldorf for his expert contribution to this paper supporting phylogenetic analyses and global sequence alignments of PHT3 carriers. We also thank Prof. Dr. Michael Feldbrügge at the Institute of Microbiology, Heinrich-Heine University for scientific discussions. We acknowledge Alisandra Denton, Plant Biochemistry, Heinrich-Heine University Düsseldorf for reading this manuscript. We thank the reviewers for carefully reading this manuscript and constructive criticism on our data.

References

Arimura, S.-i., Fujimoto, M., Doniwa, Y., Kadoya, N., Nakazono, M., Sakamoto, W., and Tsutsumi, N. (2008). Arabidopsis ELONGATED MITOCHONDRIA1 Is Required for Localization of DYNAMIN-RELATED PROTEIN3A to Mitochondrial Fission Sites. Plant Cell **20,** 1555-1566.

Bedhomme, M., Hoffmann, M., McCarthy, E.A., Gambonnet, B., Moran, R.G., Rébeillé, F., and Ravanel, S. (2005). Folate metabolism in plants- An Arabidopsis homolog of the mammalian mitochondrial folate transporter mediates folate import into chloroplasts. J Biol Chem **280,** 34823-34831.

Bernhardt, K., Wilkinson, S., Weber, A.P.M., and Linka, N. (2012a). A peroxisomal carrier delivers NAD($^+$) and contributes to optimal fatty acid degradation during storage oil mobilization. Plant J **69,** 1-13.

Bernhardt, K., Vigelius, S.K., Wiese, J., Linka, N., and Weber, A.P.M. (2012b). Agrobacterium-mediated *Arabidopsis thaliana* transformation: an overview of T-DNA binary vectors, floral dip and screening for homozygous lines. J Endocytobiosis Cell Res **22,** 19-28.

Björklund, Å.K., Ekman, D., Light, S., Frey-Skött, J., and Elofsson, A. (2005). Domain rearrangements in protein evolution. J Mol Biol **353,** 911-923.

Bouvier, F., Linka, N., Isner, J.C., Mutterer, J., Weber, A.P., and Camara, B. (2006). Arabidopsis SAMT1 defines a plastid transporter regulating plastid biogenesis and plant development. Plant Cell **18,** 3088-3105.

Bowsher, C.G., and Tobin, A.K. (2001). Compartmentation of metabolism within mitochondria and plastids. J Exp Bot **52,** 513-527.

Bowsher, C.G., Lacey, A.E., Hanke, G.T., Clarkson, D.T., Saker, L.R., Stulen, I., and Emes, M.J. (2007). The effect of Glc6P uptake and its subsequent oxidation within pea root plastids on nitrite reduction and glutamate synthesis. J Exp Bot **58,** 1109-1118.

Chen, Y.F., Wang, Y., and Wu, W.H. (2008). Membrane transporters for nitrogen, phosphate and potassium uptake in plants. J Integr Plant Biol **50,** 835-848.

Chenna, R., Sugawara, H., Koike, T., Lopez, R., Gibson, T.J., Higgins, D.G., and Thompson, J.D. (2003). Multiple sequence alignment with the Clustal series of programs. Nucleic Acids Res **31,** 3497-3500.

Chomczynski, P., and Sacchi, N. (1987). Single-step method of RNA isolation by acid guanidinium thiocyanate-phenol-chloroform extraction. Anal Biochem **162,** 156-159.

Curtis, M.D., and Grossniklaus, U. (2003). A gateway cloning vector set for high-throughput functional analysis of genes *in planta*. Plant Physiol **133,** 462-469.

Dolce, V., Iacobazzi, V., Palmieri, F., and Walker, J.E. (1994). The sequences of human and bovine genes of the phosphate carrier from mitochondria contain evidence of alternatively spliced forms JBC **269,** 10451-10460.

Drew, D., Newstead, S., Sonoda, Y., Kim, H., von Heijne, G., and Iwata, S. (2008). GFP-based optimization scheme for the overexpression and purification of eukaryotic membrane proteins in *Saccharomyces cerevisiae*. Nat Protoc **3,** 784-798.

Dyall, S.D., Brown, M.T., and Johnson, P.J. (2004). Ancient invasions: from endosymbionts to organelles. Science **304,** 253-257.

Eddy, S.R. (2011). Accelerated profile HMM searches. PLoS computational biology **7,** e1002195.

Ekman, D., Björklund, Å.K., and Elofsson, A. (2007). Quantification of the elevated rate of domain rearrangements in metazoa. J Mol Biol **372,** 1337-1348.

Fernie, A.R., Carrari, F., and Sweetlove, L.J. (2004). Respiratory metabolism: glycolysis, the TCA cycle and mitochondrial electron transport. Curr Opin Plant Biol **7,** 254-261.

Finn, R.D., Clements, J., and Eddy, S.R. (2011). HMMER web server: interactive sequence similarity searching. Nucleic Acids Res **39,** W29-W37.

Finn, R.D., Mistry, J., Tate, J., Coggill, P., Heger, A., Pollington, J.E., Gavin, O.L., Gunasekaran, P., Ceric, G., and Forslund, K. (2010). The Pfam protein families database. Nucleic Acids Res **38,** D211-D222.

Gietz, R.D., and Schiestl, R.H. (2007). Frozen competent yeast cells that can be transformed with high efficiency using the LiAc/SS carrier DNA/PEG method. Nat Protoc **2,** 1-4.

Haferkamp, I. (2007). The diverse members of the mitochondrial carrier family in plants. FEBS Lett **581,** 2375-2379.

Haferkamp, I., and Schmitz-Esser, S. (2012). The plant mitochondrial carrier family: functional and evolutionary aspects. Front Plant Sci **3,** doi: 10.3389/fpls.2012.00002.

Hamel, P., Saint-Georges, Y., de Pinto, B., Lachacinski, N., Altamura, N., and Dujardin, G. (2004). Redundancy in the function of mitochondrial phosphate transport in *Saccharomyces cerevisiae* and *Arabidopsis thaliana*. Mol Microbiol **51,** 307-317.

Hause, B., Hause, G., Kutter, C., Miersch, O., and Wasternack, C. (2003). Enzymes of jasmonate biosynthesis occur in tomato sieve elements. Plant Cell Physiol **44,** 643-648.

Heazlewood, J.L., Verboom, R.E., Tonti-Filippini, J., Small, I., and Millar, A.H. (2007). SUBA: the Arabidopsis Subcellular Database. Nucleic Acids Res **35,** D213-218.

Heazlewood, J.L., Tonti-Filippini, J.S., Gout, A.M., Day, D.A., Whelan, J., and Millar, A.H. (2004). Experimental analysis of the Arabidopsis mitochondrial proteome highlights signaling and regulatory components, provides assessment of targeting prediction programs, and indicates plant-specific mitochondrial proteins. Plant Cell **16,** 241-256.

Jefferson, R.A., Kavanagh, T.A., and Bevan, M.W. (1987). GUS fusions: beta-glucuronidase as a sensitive and versatile gene fusion marker in higher plants. EMBO J **6,** 3901-3907.

Jenik, P.D., Gillmor, C.S., and Lukowitz, W. (2007). Embryonic patterning in *Arabidopsis thaliana*. Annu Rev Cell Dev Biol. **23,** 207-236.

Kadenbach, B., Mende, P., Kolbe, H.V., Stipani, I., and Palmieri, F. (1982). The mitochondrial phosphate carrier has an essential requirement for cardiolipin. FEBS Lett **139,** 109-112.

Kang, F., and Rawsthorne, S. (1994). Starch and fatty-acid synthesis in plastids from developing embryos of oilseed rape (Brassica-Napus L). Plant J **6,** 795-805.

Kasahara, M., and Hinkle, P.C. (1976). Reconstitution of D-glucose transport catalyzed by a protein-fraction from human erythrocytes in sonicated liposomes. Proc Natl Acad Sci U S A **73,** 396-400.

Kataoka, T., Watanabe-Takahashi, A., Hayashi, N., Ohnishi, M., Mimura, T., Buchner, P., Hawkesford, M.J., Yamaya, T., and Takahashi, H. (2004). Vacuolar sulfate transporters are essential determinants controlling internal distribution of sulfate in Arabidopsis. Plant Cell **16,** 2693-2704.

Kersting, A.R., Bornberg-Bauer, E., Moore, A.D., and Grath, S. (2012). Dynamics and adaptive benefits of protein domain emergence and arrangements during plant genome evolution. Genome Biol Evol **4,** 316-329.

Kirchberger, S., Tjaden, J., and Neuhaus, H.E. (2008). Characterization of the Arabidopsis Brittle1 transport protein and impact of reduced activity on plant metabolism. Plant J **56,** 51-63.

Klingenberg, M. (2009). Cardiolipin and mitochondrial carriers. Biochim Biophys Acta **1788,** 2048-2058.

Kolbe, H.V., Bottrich, J., Genchi, G., Palmieri, F., and Kadenbach, B. (1981). Isolation and reconstitution of the phosphate-transport system from pig heart mitochondria. FEBS Lett **124,** 265-269.

Koornneef, M., Hanhart, C.J., and Veen, J.H. (1991). A genetic and physiological analysis of late flowering mutants in *Arabidopsis thaliana*. Mol Gen Genet **229,** 57-66.

Kota, J., Gilstring, C.F., and Ljungdahl, P.O. (2007). Membrane chaperone Shr3 assists in folding amino acid permeases preventing precocious ERAD. J Cell Biol **176,** 617-628.

Leroch, M., Neuhaus, H.E., Kirchberger, S., Zimmermann, S., Melzer, M., Gerhold, J., and Tjaden, J. (2008). Identification of a novel adenine nucleotide transporter in the endoplasmic reticulum of Arabidopsis. Plant Cell **20,** 438-451.

Li, Y., Beisson, F., Pollard, M., and Ohlrogge, J. (2006). Oil content of Arabidopsis seeds: the influence of seed anatomy, light and plant-to-plant variation. Phytochemistry **67,** 904-915.

Linka, N., and Weber, A.P. (2010). Intracellular metabolite transporters in plants. Mol Plant **3,** 21-53.

Linka, N., Theodoulou, F.L., Haslam, R.P., Linka, M., Napier, J.A., Neuhaus, H.E., and Weber, A.P. (2008). Peroxisomal ATP import is essential for seedling development in *Arabidopsis thaliana*. Plant Cell **20,** 3241-3257.

Liu, F., Chang, X.-J., Ye, Y., Xie, W.-B., Wu, P., and Lian, X.-M. (2011). Comprehensive sequence and whole-life-cycle expression profile analysis of the phosphate transporter gene family in rice. Mol Plant **4,** 1105-1122.

Lunn, J.E. (2007). Compartmentation in plant metabolism. J Exp Bot **58,** 35-47.

Mackenzie, S., and McIntosh, L. (1999). Higher plant mitochondria. Plant Cell **11,** 571-586.

Mitsuya, S., El-Shami, M., Sparkes, I.A., Charlton, W.L., Lousa Cde, M., Johnson, B., and Baker, A. (2010). Salt stress causes peroxisome proliferation, but inducing peroxisome proliferation does not improve NaCl tolerance in *Arabidopsis thaliana*. PLoS ONE **5,** e9408.

Moore, A.D., and Bornberg-Bauer, E. (2012). The dynamics and evolutionary potential of domain loss and emergence. Mol Biol Evol **29,** 787-796.

Moore, A.D., Björklund, Å.K., Ekman, D., Bornberg-Bauer, E., and Elofsson, A. (2008). Arrangements in the modular evolution of proteins. Trends Biochem Sci **33,** 444-451.

Moore, A.D., Grath, S., Schüler, A., Huylmans, A., and Bornberg-Bauer, E. (2013). Quantification and functional analysis of modular protein evolution in a dense phylogenetic tree. Biochim Biophys Acta **5,** 898-907.

Nakamori, K., Takabatake, R., Umehara, Y., Kouchi, H., Izui, K., and Hata, S. (2002). Cloning, functional expression, and mutational analysis of a cDNA for *Lotus japonicus* mitochondrial phosphate transporter. Plant Cell Physiol **43,** 1250-1253.

Needleman, S.B., and Wunsch, C.D. (1970). A general method applicable to the search for similarities in the amino acid sequence of two proteins. J Mol Biol **48,** 443-453.

Palmieri, F., Indiveri, C., Bisaccia, F., and Iacobazzi, V. (1995). Mitochondrial metabolite carrier proteins: purification, reconstitution, and transport studies. Methods Enzymol **260,** 349-369.

Palmieri, F., Pierri, C.L., De Grassi, A., Nunes-Nesi, A., and Fernie, A.R. (2011). Evolution, structure and function of mitochondrial carriers: a review with new insights. Plant J **66,** 161-181.

Palmieri, L., Picault, N., Arrigoni, R., Besin, E., Palmieri, F., and Hodges, M. (2008a). Molecular identification of three *Arabidopsis thaliana* mitochondrial dicarboxylate carrier isoforms: organ distribution, bacterial expression, reconstitution into liposomes and functional characterization. Biochem J **410,** 621-629.

Palmieri, L., Santoro, A., Carrari, F., Blanco, E., Nunes-Nesi, A., Arrigoni, R., Genchi, F., Fernie, A.R., and Palmieri, F. (2008b). Identification and characterization of ADNT1, a novel mitochondrial adenine nucleotide transporter from Arabidopsis. Plant Physiol **148,** 1797-1808.

Paul, M.J., and Foyer, C.H. (2001). Sink regulation of photosynthesis. J Exp Bot **52,** 1383-1400.

Phelps, A., Briggs, C., Mincone, L., and Wohlrab, H. (1996). Mitochondrial phosphate transport protein. Replacements of glutamic, aspartic, and histidine residues affect transport and protein conformation and point to a coupled proton transport path. Biochem **35,** 10757-10762.

Picault, N., Hodges, M., Palmieri, L., and Palmieri, F. (2004). The growing family of mitochondrial carriers in Arabidopsis. Trends Plant Sci **9,** 138-146.

Poirier, Y., and Bucher, M. (2002). Phosphate transport and homeostasis in Arabidopsis. Arabidopsis Book **1,** e0024. doi: 10.1199/tab.0024.

Pratt, R.D., Ferreira, G.C., and Pedersen, P.L. (1991). Mitochondrial phosphate transport. Import of the H^+/Pi symporter and role of the presequence. J Biol Chem **266,** 1276-1280.

Reumann, S., Quan, S., Aung, K., Yang, P.F., Manandhar-Shrestha, K., Holbrook, D., Linka, N., Switzenberg, R., Wilkerson, C.G., Weber, A.P.M., Olsen, L.J., and Hu, J.P. (2009). In-depth proteome analysis of Arabidopsis leaf peroxisomes combined with *in vivo* subcellular targeting verification indicates novel metabolic and regulatory functions of peroxisomes. Plant Physiol **150,** 125-143.

Sambrook, J., Russell, D.W., and Russell, D.W. (1989). Molecular cloning: a laboratory manual, 3rd edn. (Cold Spring Harbor Laboratory Press).

Schwacke, R., Schneider, A., van der Graaff, E., Fischer, K., Catoni, E., Desimone, M., Frommer, W.B., Flugge, U.I., and Kunze, R. (2003). ARAMEMNON, a novel database for Arabidopsis integral membrane proteins. Plant Physiol **131,** 16-26.

Schwender, J., Goffman, F., Ohlrogge, J.B., and Shachar-Hill, Y. (2004). Rubisco without the Calvin cycle improves the carbon efficiency of developing green seeds. Nature **432,** 779-782.

Scott, I., Sparkes, I.A., and Logan, D.C. (2007). The missing link: inter-organellar connections in mitochondria and peroxisomes? Trends Plant Sci **12,** 380-381.

Stappen, R., and Kramer, R. (1994). Kinetic mechanism of phosphate/phosphate and phosphate/OH^- antiports catalyzed by reconstituted phosphate carrier from beef heart mitochondria. J Biol Chem **269,** 11240-11246.

Takabatake, R., Hata, S., Taniguchi, M., Kouchi, H., Sugiyama, T., and Izui, K. (1999). Isolation and characterization of cDNAs encoding mitochondrial phosphate transporters in soybean, maize, rice, and Arabidopis. Plant Mol Biol **40,** 479-486.

Thuswaldner, S., Lagerstedt, J.O., Rojas-Stutz, M., Bouhidel, K., Der, C., Leborgne-Castel, N., Mishra, A., Marty, F., Schoefs, B., Adamska, I., Persson, B.L., and Spetea, C. (2007). Identification, expression, and functional analyses of a thylakoid ATP/ADP carrier from Arabidopsis. J Biol Chem **282,** 8848-8859.

Treco, D.A., and Winston, F. (2001). Growth and Manipulation of Yeast. In: Curr Protoc Mol Biol, (John Wiley & Sons, Inc), doi: 10.1002/0471142727.mb1302s19.

Vest, K.E., Leary, S.C., Winge, D.R., and Cobine, P.A. (2013). Copper Import into the Mitochondrial Matrix in *Saccharomyces cerevisiae* Is mediated by Pic2, a Mitochondrial Carrier Family Protein. JBC **288,** 23884-23892.

Vigeolas, H., Möhlmann, T., Martini, N., Neuhaus, H.E., and Geigenberger, P. (2004). Embryo-specific reduction of ADP-Glc pyrophosphorylase leads to an inhibition of starch synthesis and a delay in oil accumulation in developing seeds of oilseed rape. Plant Physiol **136,** 2676-2686.

Willmann, M.R., Mehalick, A.J., Packer, R.L., and Jenik, P.D. (2011). MicroRNAs regulate the timing of embryo maturation in Arabidopsis. Plant Physiol **155,** 1871-1884.

Winter, D., Vinegar, B., Nahal, H., Ammar, R., Wilson, G.V., and Provart, N.J. (2007). An "electronic fluorescent pictograph" browser for exploring and analyzing large-scale biological data sets. PLoS ONE **2,** e718.

Wohlrab, H., and Briggs, C. (1994). Yeast mitochondrial phosphate transport protein expressed in *Escherichia coli*. Site-directed mutations at threonine-43 and at a similar location in the second tandem repeat (isoleucine-141). Biochemistry **33,** 9371-9375.

Zara, V., Dietmeier, K., Palmisano, A., Vozza, A., Rassow, J., Palmieri, F., and Pfanner, N. (1996). Yeast mitochondria lacking the phosphate carrier/p32 are blocked in phosphate transport but can import preproteins after regeneration of a membrane potential. Mol Cell Biol **16,** 6524-6531.

Zhang, X., Henriques, R., Lin, S.S., Niu, Q.W., and Chua, N.H. (2006). Agrobacterium-mediated transformation of Arabidopsis thaliana using the floral dip method. Nat Protoc **1,** 641-646.

Zhu, W., Miao, Q., Sun, D., Yang, G., Wu, C., Huang, J., and Zheng, C. (2012). The mitochondrial phosphate transporters modulate plant responses to salt stress via affecting ATP and gibberellin metabolism in *Arabidopsis thaliana*. PLoS ONE **7,** e43530.

Contribution of the authors to manuscript 2

S.K.-V. wrote the manuscript and performed all experiments. **I.H.** donated the T-DNA line SAIL_591_H09 and was actively involved in developing the hypothesis of a connection of SIT1 and DIC carriers. **C.E.** assisted with the phylogenetic analysis of PHT3 carriers and performed the analysis for figure 2. **R.S.** helped to analyze siliques and embryos of *sit* mutants. **N.L.**, **A.P.M.W.** and **J.H** participated in scientific discussions and assisted in drafting this manuscript. **N.L.** designed the research.

Outlook

Biochemical studies to assess SIT1 substrate specificity

To confirm the transport capacity of SIT1 for sulfate, kinetic constants have to be measured to determine the specificity of the carrier for sulfate. It is of interest to determine the transport mode of SIT1, *i.e.* to test if the carrier facilitates uniport or symport with protons.

Site-directed mutagenesis of SIT1 and its impact on substrate specificity

Comparisons of protein sequences revealed that key residues responsible for PHT3-mediated phosphate transport activity in mammals and yeast are not conserved in Arabidopsis SIT1, but in PHT3;1 and PHT3;2 (Dolce et al., 1994; Phelps et al., 1996; Zhu et al., 2012). We proposed that these amino acid changes cause the functional diversity of SIT1. We applied site-directed mutagenesis of the SIT1 sequence, converting the key residues back to the situation in PHT3;1 and PHT3;2. Three constructs were generated: (i) Valine was transformed to cysteine at position 44, (ii) glutamine was converted to glutamic acid at position 126, (iii) a combination of (i) and (ii). Heterologous complementation of Δ*mir*Δ*pic* will be repeated involving the initial constructs used and the mutated forms of SIT1. It will be examined, whether mutated SIT1 leads to full complementation of the yeast mutant, as it was observed for PHT3;1 and PHT3;2 (Hamel et al., 2004). Complementation will indicate if one amino acid change in SIT1 is responsible to shift the substrate specificity from phosphate to sulfate.

On the physiological role of SIT1 in Arabidopsis

We aim to extend the physiological studies with *sit1* mutants to understand the role of this putative sulfate carrier in plant mitochondria. Preliminary phenotypic assays detected growth defects in *sit1* Arabidopsis mutants. These experiments will be repeated to exclude possible artifacts caused by growth conditions or inconsistent ages of seed stocks. The observations we made on growth arrests in seedlings and adult plants in both lines will be verified in a larger scale. A *sit1* line over-expressing SIT1 under the control of a ubiquitin promoter was generated. Plants will be analyzed, if growth arrests can be complemented. We expect that an overexpression of SIT1 in the *sit1* background will rescue growth defects, which were observed in loss of function lines.

We proposed that SIT1 and dicarboxylate carriers (DIC) act in concert to mediate a constant replenishment of tricarboxylic acid cycle (TCA) intermediates, which helps to maintain constant rates of respiration. The TCA cycle produces reducing equivalents to generate energy through the respiratory chain. Plants devoid of SIT1 might suffer of lower cellular energy levels, as DIC carriers would then use phosphate supplied by PHT3;1 and PHT3;2 as counter-exchange substrate for the import of dicarboxylic acids. In consequence, less phosphate would be available for ATP synthesis. To examine our hypothesis, we will measure intracellular ATP levels in whole-cell extracts and in isolated mitochondria.

Investigation of seed defects

Seed development is a complex process comprising three phases: embryogenesis, seed filling, and maturation. Seed filling is marked by massive synthesis of storage reserves, such as proteins, starch, and oils, which are then deposited (Hajduch et al., 2010). An abortion of SIT1 led to seed defects in *sit1*-1. Analyses of seed and embryo morphologies will be repeated with the second T-DNA line *sit1*-2. A determination of fatty acid composition and oil content in mutant lines and wildtype will be conducted to uncover putative impacts of a SIT1 loss on seed embryogenesis or filling. We propose that *sit1* mutants suffer of lower ATP levels, which might affect storage reserve deposition. It is also possible that lower energy contents affect embryogenesis, leading to seeds with an aberrant morphology.

In the same context starch levels of Arabidopsis mutant and wildtype seeds will be determined. Starch is an indicator for seed filling, as seeds of in oilseed-storing plants, which exhibit low oil levels, starch synthesis is also reduced (Focks and Benning, 1998; Vigeolas et al., 2004).

Studies on physiology and expression to examine a putative interplay of SIT1 and DIC carriers

The proposed interplay of SIT1 and DIC will be tested by phenotypic investigations of *sit1* mutants and of *dic* mutants. We will generate a set of mutants, *i.e* a *dic1*/*dic2* Arabidopsis mutant and a *dic1*/*dic2*/*sit1* triple mutant. These mutants will be compared to *sit1* mutants in various experiments. Germination, growth behavior and metabolite profiles will be investigated. Mass-spectrometry will provide information on energy status and metabolites. In preliminary experiments *sit1-2* mutants exhibited high levels of soluble sugars. We will repeat these analyses, involving the second *sit1* line, the *dic* double mutant and triple mutant. A comparative analysis determining TCA cycle and resulting respiration activity is planned. With a Clark electrode oxygen levels in a suspension containing isolated Arabidopsis mitochondria of wildtype and all mutants will be measured. Oxidative phosphorylation, which comprises TCA cycle and respiratory chain, requires oxygen to produce ATP. When the TCA cycle is slowed down due to a lack of intermediates, we assume that the respiration rate will decrease. A profile of TCA cycle intermediates could be determined by mass spectrometry. To shed light on a putative connection between SIT1 and DIC, we will compare *SIT1* and *DIC* transcripts in the mutants and wildtype by qRT-PCR.

References

Dolce, V., Iacobazzi, V., Palmieri, F., and Walker, J.E. (1994). The sequences of human and bovine genes of the phosphate carrier from mitochondria contain evidence of alternatively spliced forms. J Biol Chem **269,** 10451-10460.

Focks, N., and Benning, C. (1998). wrinkled1: A novel, low-seed-oil mutant of Arabidopsis with a deficiency in the seed-specific regulation of carbohydrate metabolism. Plant Physiol **118,** 91-101.

Hajduch, M., Hearne, L.B., Miernyk, J.A., Casteel, J.E., Joshi, T., Agrawal, G.K., Song, Z., Zhou, M., Xu, D., and Thelen, J.J. (2010). Systems analysis of seed filling in Arabidopsis: using general linear modeling to assess concordance of transcript and protein expression. Plant Physiol **152,** 2078-2087.

Hamel, P., Saint-Georges, Y., de Pinto, B., Lachacinski, N., Altamura, N., and Dujardin, G. (2004). Redundancy in the function of mitochondrial phosphate transport in *Saccharomyces cerevisiae* and *Arabidopsis thaliana*. Mol Microbiol **51,** 307-317.

Phelps, A., Briggs, C., Mincone, L., and Wohlrab, H. (1996). Mitochondrial phosphate transport protein. Replacements of glutamic, aspartic, and histidine residues affect transport and protein conformation and point to a coupled proton transport path. Biochem **35,** 10757-10762.

Vigeolas, H., Möhlmann, T., Martini, N., Neuhaus, H.E., and Geigenberger, P. (2004). Embryo-specific reduction of ADP-Glc pyrophosphorylase leads to an inhibition of starch synthesis and a delay in oil accumulation in developing seeds of oilseed rape. Plant Physiol **136,** 2676-2686.

Zhu, W., Miao, Q., Sun, D., Yang, G., Wu, C., Huang, J., and Zheng, C. (2012). The mitochondrial phosphate transporters modulate plant responses to salt stress via affecting ATP and gibberellin metabolism in *Arabidopsis thaliana*. PLoS ONE **7,** e43530.

Manuscript 3

The peroxisomal pH in Arabidopsis is acidic in storage oil mobilization

Sarah K. Kessel-Vigelius[1*], Melanie Krebs[3], J. Lennart Charton[1], Hendrik Wolff[1], Jianping Hu[2], Karin Schumacher[3], Andreas P.M. Weber[1], and Nicole Linka[1a]

[1]Institute of Plant Biochemistry, Heinrich-Heine University Düsseldorf, 40225 Düsseldorf Germany;
[2]Department of Energy Plant Research Laboratory, Michigan State University, East Lansing, Michigan-48823, USA;
[3]Department of Developmental Biology, Centre for Organismal Studies, University of Heidelberg, 69120 Heidelberg, Germany

*First author
[a]Corresponding author

Abstract

Regulation of pH and establishment of proton gradients across membranes is crucial for plant metabolism, solute transport, growth and development. In this study, we chose a non-invasive method to analyse the tissue-specific pH of plant peroxisomes, using a pH-sensitive fluorescent protein sensor. A modified version of pH-sensitive green fluorescent protein was expressed in the cytosol and peroxisomes of stable transgenic Arabidopsis lines. With confocal laser scanning microscopy we determined the cytosolic and peroxisomal pH in roots and non-green shoots, measuring the ratio of fluorescence intensity at two different excitation wavelengths. Our analyses revealed a proton gradient at the peroxisomal membrane, which varied for different plant tissues. We observed an acidic pH in peroxisomes of etiolated shoot tissue, whereas the matrix of root peroxisomes was alkaline. These findings point to a functional differentiation of peroxisomes in root and in etiolated hypocotyl cells. Since Arabidopsis is a seed oil storing-plant, peroxisomes of hypocotyls are mainly involved in fatty acid degradation via β-oxidation during storage oil mobilization. To elucidate the cause for the peroxisomal acidification, we examined the pH of hypocotyl peroxisomes in an Arabidopsis mutant deficient in β-oxidation due to impaired ATP import. We hypothesized that either ATP import into peroxisomes is proton-compensated and thus the peroxisomal lumen is acidified, or that β-oxidation and glyoxylate cycle, as they release acids, influence the peroxisomal pH. Our analyses revealed that β-oxidation did not directly affect the luminal pH of peroxisomes. Although β-oxidation and glyoxylate cycle was compromised in the Arabidopsis mutant, the peroxisomal pH remained unchanged.

Introduction

Plant peroxisomes play a pivotal role in numerous metabolic processes, including lipid mobilization via β-oxidation and glyoxylate cycle, photorespiration, phytohormone biosynthesis, pathogen defense, and amino acid catabolism. They contain a prospective repertoire of enzymes, which depends on the tissue-specific function (Hu et al., 2012). In cotyledons or hypocotyls of pre-photoautotrophic seedlings and senescing tissues, peroxisomes mainly convert lipids to carbohydrates via β-oxidation and glyoxylate cycle to drive seedling growth (Pracharoenwattana and Smith, 2008). In leaves, the primary role of peroxisomes is photorespiration. In this pathway glycolate is converted to glycine and serine to glycerate (Reumann and Weber, 2006). Both fatty acid degradation and photorespiration are examples of a spatial and temporal coordination of metabolism in various cellular compartments, as enzymatic reactions are distributed over peroxisomes and other cell compartment, such as mitochondria, plastids and cytosol (Graham, 2008; Hu et al., 2012). This necessitates the transport of intermediates and cofactors across the peroxisomal membrane, which is facilitated by specified carrier proteins. To date, only few metabolite transport proteins have been characterized in plant peroxisomes (Linka and Esser, 2012).

The pH of a particular cell compartment is important for optimal enzymatic functions and solute transport. The proton (H^+) concentration determines ionization of acidic or basic amino acid residues and influences protein solubility and structure and thus regulates protein functionality (Orij et al., 2009; Gjetting et al., 2012). In addition, a proton ion gradient across the membrane is an important driving force of proton-coupled metabolite transport (Rottensteiner and Theodoulou, 2006). A pH gradient is also required for metabolite trapping in organelles, such as vacuoles where protonation determines the flux of solutes (Martinoia et al., 2007).

In this study we investigated the peroxisomal pH in different plant tissues to gain a more comprehensive picture about transport processes and metabolism of plant peroxisomes. In the past, the *in vivo* peroxisomal pH was studied in diverse eukaryotic organisms with different methods and sensors. Pioneering studies took advantage of nuclear magnetic resonance (NMR) spectroscopy to estimate the pH of apoplast and cytosol in higher plants (Roberts et al., 1980; Nicolay et al., 1987). The pH of these compartments was examined by loading pH-sensitive indicator dyes, such as BCECF (2′,7′-bis-2-carboxyethyl)-5-(and-6)-carboxyfluorescein) (Scott and Allen, 1999) or Oregon green (Fasano et al., 2001). Because organelles are often difficult to load or are inaccessible to chemical dyes, genetically encoded biosensors, such as pH-sensitive GFP variants, were developed to study the intraorganellar pH. Using this novel tool, the proton concentrations of apoplast, cytosol and organelles were monitored in the model plant *Arabidopsis thaliana* (Miesenbock et al., 1998; Moseyko and Feldman, 2001; Gao et al., 2004; Shen et al., 2013).

The pH of the peroxisomal matrix is still a matter of debate in mammals and yeast. In animals and yeasts both an acidic pH, (Lasorsa et al., 2004; Nicolay et al., 1987; van der Klei et al., 2006), as well as an alkaline pH (Dansen et al., 2000; van Roermund et al., 2004) were reported. Another study concluded that the pH of human fibroblasts and chinese hamster ovary cells adapts to the cytosolic pH and thus is near neutral (Jankowski et al., 2001). In plants, the pH of the peroxisomal matrix and the existence of a proton gradient across the peroxisomal membrane have been only transiently determined in Arabidopsis leaf protoplasts (Shen et al., 2013).

However, how peroxisomal pH is maintained or how a proton gradient across the peroxisomal membrane is generated remains to be solved. Proton-dependent metabolite transport processes could influence the H^+ concentration inside the peroxisomal lumen, as it was postulated for yeast peroxisomes (Lasorsa et al., 2004; van Roermund et al., 2004). The peroxisomal ATP carrier from *Saccharomyces cerevisiae* Ant1p co-transports protons into the peroxisomal lumen to compensate the electrogenic exchange of $ATP^{(4-)}$ and $AMP^{(2-)}$ (Lasorsa et al., 2004). The peroxisomal import of ATP is required for activation of fatty acids prior to enter β-oxidation. The co-transport of protons with each molecule of ATP mediated by Ant1p causes an acidification of the organellar lumen, especially under conditions when a high turnover of fatty acids occurs. This implies that peroxisomal metabolism could have an impact on lumenal pH.

In this study, we established stable transgenic Arabidopsis lines expressing a cytoplasmic or peroxisomal-targeted pH-sensitive green fluorescent protein called pHGFP under the control of the constitutive Arabidopsis promoter *UBIQUITIN10* (Norris et al., 1993; Grefen et al., 2010). The reporter protein has an adjusted codon usage and optimized solubility in Arabidopsis to minimize non-specific effects caused by sensor concentration, distribution or illumination (Schulte et al., 2006). Confocal laser scanning microscopy (CLSM) was used to investigate cytoplasmic and peroxisomal pH in root cells as well as in hypocotyl cells of etiolated seedlings. Thus, our experiments complement the study of Shen et al., 2013, which analyzed the peroxisomal pH in leaves transiently. In contrast to an alkaline pH of root peroxisomes, we observed that the peroxisomal matrix of hypocotyl cells was acidic. To address why peroxisomal lumen is acidified in a tissue that is involved storage-oil mobilization, we tested if ATP import into peroxisomes is proton-compensated, leading to an acidic matrix, as it is described for yeast peroxisomes (Lasorsa et al., 2004). Alternatively, we analysed the role of β-oxidation and glyoxylate cycle, as these processes release acids, which in turn could cause an acidification of the peroxisomal pH.

Our study contributes to gain a broader view on the peroxisomal pH of plants, which significantly influences enzyme activities and solute transport processes and thus controls peroxisomal metabolism.

Experimental procedures

Materials

Chemicals and reagents were obtained from Sigma-Aldrich (http://www.sigmaaldrich.com), Promega (http://www.promega.com) and Bio-Rad (http://www.bio-rad.com/). Enzymes and molecular reagents for recombinant DNA techniques were purchased from New England Biolabs (http://www.neb.com), Thermo Fisher Scientific (http://www.thermoscientificbio.com/fermentas/), and Qiagen (http://www.qiagen.com). Plant growth media and plant agar were obtained from Duchefa BV and Caisson Laboratories Inc.

Cloning procedures

Cloning was performed according to standard molecular techniques (Sambrook et al., 1989). Sequences were verified by DNA sequencing (GATC Biotech, http://www.gatc-biotech.com).

To generate stable transgenic plants expressing a cytoplasmic pHGFP sensor, the plant binary vector pUTKan-pHGFP was constructed. A 661 bp fragment from the *UBQ10* promoter (Norris et al., 1993) was amplified by standard PCR methods using the primer combination UBQ10-*Kpn*I-Fwd (5'-AAGGTACCCGACGAGTCAGTAATAAACGGCG-3') and UBQ10-*Kpn*I-Rev (5'-GATGGTACCCGCACTCGAGCTGTTAATCAG-3'). To obtain pUTKan the UBQ10 fragment was subcloned into pJET1.2 (Thermo Fisher Scientific) followed by excision and insertion into the vector backbone of pTKan (Krebs et al., 2012) via the introduced *Kpn*I sites. pUTKan was digested with *Pst*I and a 741 bp fragment, encoding *pHGFP*, was obtained by cutting pHGFP-SP (Moseyko and

Feldman, 2001) with *BamH*I and *Sac*I. The overhanging 5'- and 3'-termini of the respective fragments were blunted and finally ligated to obtain pUTKan-pHGFP.

A peroxisomal pHGFP variant was generated fusing the tripeptide SKL at the C terminus of the sensor (Reumann, 2004). pHGFP was amplified from the cytoplasmic pUTKan-pHGFP clone using the forward primer pHGFP–*BamH*I-Fwd (5'-CACACGGATCCACCATGAGTAAAGGAGAAGAACTTTTCAC-3') and the reverse primer pHGFP-SKL-*Sal*I-Rev (5'- CACACGTCGACTCAGAGTTTGGATTTGTATAGTTCATCCAT-3'). The PCR product was subcloned into pGEM-T Easy (Promega). The excised product was then introduced into the pUTKan binary vector via *BamH*I and *Sal*I, resulting in pHGFP-SKL. All final constructs were sequenced before transformed into *Arabidopsis*.

For protein expression and *in vitro* uptake assays, AtPNC1 (At3g05290) and AtPNC2 (At5g27520) sequences were downloaded from the Aramemnon database (http://aramemnon.uni-koeln.de). The sequences without stop codon were amplified from Arabidopsis cDNA (AtPNC1, AtPNC2) and fused to a C-terminal HA tag (YPYDVPDYAYPYDVPDYA) by standard PCR reactions. The HA-tagged products were subcloned into pJET1.2 (Thermo Fisher Scientific). For cloning into pET16b the following forward primer T7-Fwd (5'- TAATACGACTCACTATAGGG-3') was used for all three constructs. For PNC1 the reverse primer PNC1-HA-*BamHI*-Rev (5'-CACACGGATCCTTAAGCGTAATCCGGAACATCGTATGGGTAAGGACTTCTTAACTTACCCTTTG TG-3') was used, for PNC2 the reverse primer PNC2-HA-*BamHI*-Rev (5'-CACACGGATCCTTAAGCGTAATCCGGAACATCGTATGGGTATGGACTTTTCAATCTAGCCTTTG-3') was chosen. After excision from pJET, the PCR products were ligated into pET16b.

Plant material and growth conditions

Wildtype *Arabidopsis thaliana* (ecotype Columbia), *pnc1* (SAIL_303H02) and *pnc2* (SALK_014579) were obtained from the European Arabidopsis Stock Centre (NASC) at the University of Nottingham (http://arabidopsis.info). Homozygous lines were established in Linka et al., 2008. The *pex14* T-DNA line (SALK_007441) was originally obtained from ABRC at Ohio State University. The *pnc1/2* double mutant was generated crossing *pnc1* and *pnc2* T-DNA lines (Kopriva, 2006). Seeds were surface-sterilized and stratified for 2 d at 4°C.

Arabidopsis wildtype plants were stably transformed with pHGFP and pHGFP-SKL using a modified floral dip protocol (Bernhardt et al., 2012; Zhang et al., 2006). For both pH sensor constructs, transgenic plants were selected on 50 µg $µl^{-1}$ kanamycin. For pH measurements, homozygous lines exhibiting similar expression levels and constant expression pattern of pHGFP were chosen.

For pH analysis seedlings were grown on 0.5x MS in the presence of 1% (w/v) sucrose (pH 5.8), solidified with 0.45% (w/v) phyto agar for 5 d at 22°C, 70% humidity under constant illumination (100 µmol m^{-2} s^{-1}, plates were covered with one layer of mesh). For other physiological studies the

seedlings were grown for 5 d in short day conditions (16 h light/ 8 h dark cycles, 100 µmol m^{-2} $s^{-}1$, 22°C/18°C, 70% humidity).

Etiolated seedlings were grown in darkness for 5 d at 22°C covering the plates with aluminum foil. A 12 h light pulse was given to induce germination.

Analysis of sucrose-dependent seedling establishment

Seedling establishment of *pnc1*, *pnc2* and *pnc1/2* was analyzed growing etiolated seedlings vertically on 0.5x MS agar plates with or without 1% (w/v) external sucrose. After 5 days hypocotyl length was measured and analyzed with Macbiophotonics ImageJ (www.macbiophotonics.ca/imagej).

Staining of oil droplets

The lipophilic dye Nile Red (Invitrogen, http://www.invitrogen.com/) was used to stain lipid bodies in *pnc* mutants and wildtype hypocotyls as described in (Linka et al., 2008). After 5 d of growth staining was performed for 5 minutes. Images were taken at a LSM510 Meta confocal laser scanning microscope (Zeiss, http://www.zeiss.de/) at 488 nm excitation and 530-600 nm emission. Image processing was performed with the LSM Image Browser 4.2 software (Zeiss) and MBF ImageJ.

2,4-DB Assay

To study the sensitivity to 2,4-D and 2,4-DB, seedlings were grown either in short days or in darkness on 0.5x MS agar plates with or without (i) 0.8 µM 2,4-DB, (ii) 0.23 µM 2,4-D, or (iii) 17 mM ethanol (control). Stocks 2,4-D and 2,4-DB were prepared in 100% (v/v) ethanol.

Confocal laser scanning microscopy for pH studies and imaging processing

The pH in cytosol and peroxisomes was examined using a LSM 510 Meta ConfoCor3 Laser Scanning Microscope (Zeiss) or a Leica TCS SP5II Laser Scanning Confocal Microscope (Leica). The Zeiss microscope was equipped with a C-Apochromat 63x/1.2 W Korr UV-VIS-IR objective (correction 0.17). On the Leica microscope a HCX PL APO x 63 water immersion objective was used.

The ratiometric GFP was sequentially excited at 405 nm and 488 nm. The emitted light was detected at 500 nm to 520 nm. In addition a bright field image was taken. The detection pinhole size was set to 3.59 Airy units in all experiments. To determine the maximum dynamic range of the pH sensor, gain and offset settings were adjusted to the brightest signal at pH 6.0 and 9.0. Images with more than 40% saturated fluorescence areas were omitted from analysis. Images were taken with the AxioVision 4.8 (Zeiss) or LAS AF Lite (Leica) software. Images were processed with Mac Biophotonics ImageJ software (http://www.macbiophotonics.ca/downloads.htm). After background subtraction by thresholding, integrated pixel densities were determined. The pixel intensity ratios were calculated in Microsoft Excel 2010 (http://office.microsoft.com/de-de/excel/) dividing the values of the 405-nm images by the values of the 488-nm images. The peroxisomal or cytosolic pH was

calculated using the Origin 8.5 software (http://www.originlab.de/) and plotted in GraphPad Prism 5.04 (http://www.graphpad.com/prism/).

In situ calibration and intracellular pH measurements

To determine the pH of peroxisomes and cytosol, *in situ* calibration of pHGFP and pHGFP-SKL was performed. The calibration buffers were composed of 50 mM ammonium acetate, and either (i) 50 mM 2-(N-morpholino)ethanesulfonic acid (MES) (pH 6.0), or (ii) 50 mM HEPES (pH 7.0 to 9.0). The pH of the buffers was adjusted with 1 M 1,3 bis(tris(hydroxymethyl)methylamino)propane (BTP). 5-d old seedlings were incubated in calibration buffers for 30 minutes at room temperature. Imaging for calibration was performed in the presence of the calibration buffers. The means of all 405/488 nm fluorescence intensity ratios ($R_{405/488}$) per pH step were calculated and plotted against the pH value of the buffer. The calibration curves obtained were fitted in GraphPad Prism 5.04 with a Boltzmann fit, which generates a sigmoidal curve. Calibrations were repeated at least three times with ≥ 15 seedlings per pH step.

For pH measurements seedlings were kept in 0.5x MS liquid medium supplemented with 1% (w/v) sucrose (pH 5.8). At least 15 images were taken and each experiment was repeated three times.

Protein expression in an E.coli-based cell-free system

As template for protein expression plasmid DNA was used, which was isolated with a PureYield™ Plasmid Miniprep System kit (Promega). Proteins were expressed recombinantly using the PURExpress® *In Vitro* Protein Synthesis Kit (New England Biolabs). The standard protocol was modified by adding 1% (w/v) L-α-phosphatidylcholine liposomes and 0.04% (w/v) Brij-35 to the protein synthesis reaction (Nozawa et al., 2007).

Protein biochemistry

Protein analysis via SDS-PAGE and immunoblot analysis was performed according to standard protocols (Sambrook et al., 1989). For immunodetection, a monoclonal α-HA/Peroxidase (HPR)-conjugated rat IgG1 antibody was used (Roche, http://www.roche.de). Protein concentrations were determined in a bichinonic acid assay (Thermo Fisher Scientific).

Protein reconstitution and liposome transport assays

For uptake studies proteins were reconstituted into L-α-phosphatidylcholine liposomes, which were either preloaded with 30 mM ATP or without pre-loading (negative control) by freeze-thaw procedure (Kasahara and Hinkle, 1976). Transport assays were started by adding 200 µM radiolabelled [α-^{32}P]ATP (Hartmann Analytic, http://www.hartmann-analytic.de/). Assays were terminated by passing proteoliposomes over Dowex AG1-X8 anion-exchange columns, binding the non-incorporated ATP. The incorporated radiolabeled ATP was analyzed by liquid scintillation counting. Data fitting was performed in GraphPad Prism 5.0 software (GraphPad, http://www.graphpad.com).

Results

Expression of a pH-sensitive GFP in Arabidopsis peroxisomes

We determined the lumenal pH of peroxisomes (pH_{per}) in Arabidopsis, stably expressing a ratiometric pH-sensitive GFP sensor in this cell compartment (Moseyko and Feldman, 2001). The ectopic expression of the sensor was driven by the Arabidopsis *UBIQUITIN10* (*UBQ10*) promoter (Norris et al., 1993). This promoter confers a medium strength but uniform gene expression throughout all developmental stages and in all plant tissues (Geldner et al., 2009; Grefen et al., 2010; Krebs et al., 2012). To target the pH-sensitive GFP to peroxisomes, a Type 1 Peroxisomal Targeting Signal (PTS1) consisting of three amino acids (serine (S)-lysine (K)-leucine (L)), was fused at the C-terminus of the fluorescent protein (Gould et al., 1989). The fusion protein is referred to as pHGFP-SKL. Such a SKL-fusion is common method in plants used to directly target heterologous proteins, such as fluorescence sensors, to peroxisomes (Mano et al., 2002). Additionally, we established a pH sensor without any targeting signal (pHGFP), which was expressed in the cytosol of Arabidopsis. We determined the cytosolic pH to validate the method we applied to determine the *in vivo* pH of peroxisomes. Thus, the cytosolic pH served as reference for the peroxisomal pH we determined, because the cytosolic pH of stably transformed Arabidopsis lines was measured earlier (Moseyko and Feldman, 2001). Both pHGFP and pHGFP-SKL were transformed to Arabidopsis. Plants homozygous for the sensor constructs were selected on kanamycin. We obtained four independent peroxisomal lines (pHGFP-SKL1-4) and three independent cytosolic lines (pHGFP1-3).

As standard growth conditions for our assays we cultivated sterile-grown seedlings for five days on half-strength MS agar plates supplied with sucrose. At this stage, cotyledons were fully expanded and the seedlings were photosynthetically active. In this study two different tissue types, roots and etiolated shoots were examined. Roots were grown exposed to light to maximize root biomass. Establishment of the photosynthetic apparatus of the plant is promoted in light. Photosynthesis-derived sucrose is transported from cotyledons to sink organs, such as roots, which leads to rapid root elongation (Nagel et al., 2006). To gain hypocotyl material, the seedlings were grown in complete darkness, which induces hypocotyl elongation. In the absence of light, root growth is repressed and skotomorphogenesis is stimulated (Gendreau et al., 1997).

To confirm the ectopic expression of the cytosolic and peroxisomal pHGFP reporter, transgenic Arabidopsis lines were subjected to confocal microscopy. The fluorescence pattern of pHGFP and pHGFP-SKL was analyzed in peroxisomes and cytosol of both tissues (Fig. 1). The pH-sensitive GFP was sequentially excited at 405 nm and 488 nm. Fluorescence emission was detected at 500 to 520 nm. The peroxisomal pH sensor pHGFP-SKL showed a punctate pattern, characteristic of the shape and size of peroxisomes (Mano et al., 2002), whereas pHGFP was localized diffusely to the edges and boundaries of the cells, which is characteristic of a cytoplasmic localization (Moseyko and Feldman, 2001) (Fig. 1).

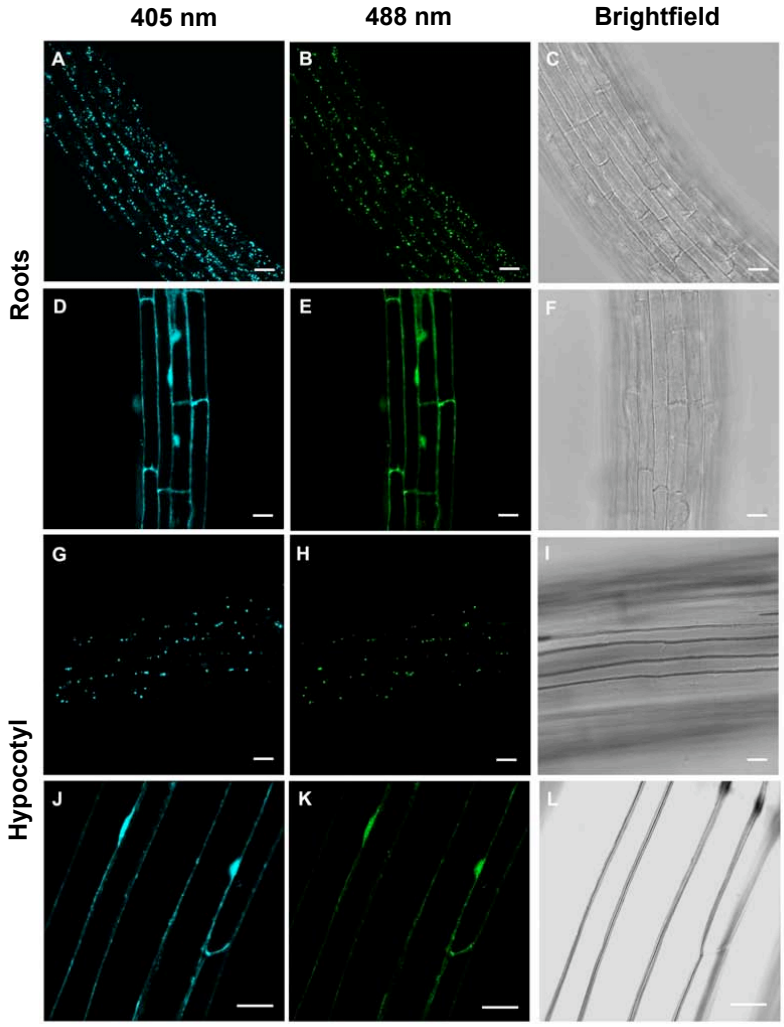

Fig. 1: Ectopic expression of pHGFP and pHGFP-SKL in Arabidopsis.
The fluorescence of root and hypocotyl cells expressing pHGFP-SKL (A-C, G-I) and pHGFP (D-F, J-L) was recorded by confocal microscopy. The pH sensitive GFP was excited with 405 nm (A, D, G, J) and 488 nm (B, E, H, K). A bright field image (C, F, I, L) was taken to verify the intactness of the imaged shoot tissue. Bars = 20 µm.

Our results showed that pHGFP and pHGFP-SKL were targeted to the expected cell compartments. The fluorescence signal was uniform and of satisfying intensity for ratiometric pH imaging.

In situ calibration to calculate the intracellular pH of cytosol and peroxisomes

For accurate pH measurements, *in situ* calibration was performed with the peroxisomal pHGFP-SKL and the cytosolic control pHGFP in roots and etiolated hypocotyls (Overly et al., 1995). For root pH measurements, Arabidopsis seedlings were grown in light, whereas for hypocotyl pH measurements seedlings were grown in complete darkness. These conditions were chosen to yield a maximum of plant material for the respective experiments.

The pH-sensitive GFP was excited at 405 nm and 488 nm; emission was detected at 500 to 520 nm for calibration. Pixel densities were measured and noise levels were reduced. Ratio values ($R_{405/488}$) of pHGFP and its peroxisomal variant were calculated. Ratios were plotted against the

calibration buffer pH. Calibration buffers contained ammonium acetate, because weak acids and bases, such as ammonium acetate, increase plasma membrane permeability and lead to an equilibration of internal and external pH to those of calibration buffers. Ammonium acetate uncouples the pH gradient across a membrane (Kell et al., 1981; Moseyko and Feldman, 2001; Pollard et al., 1979).

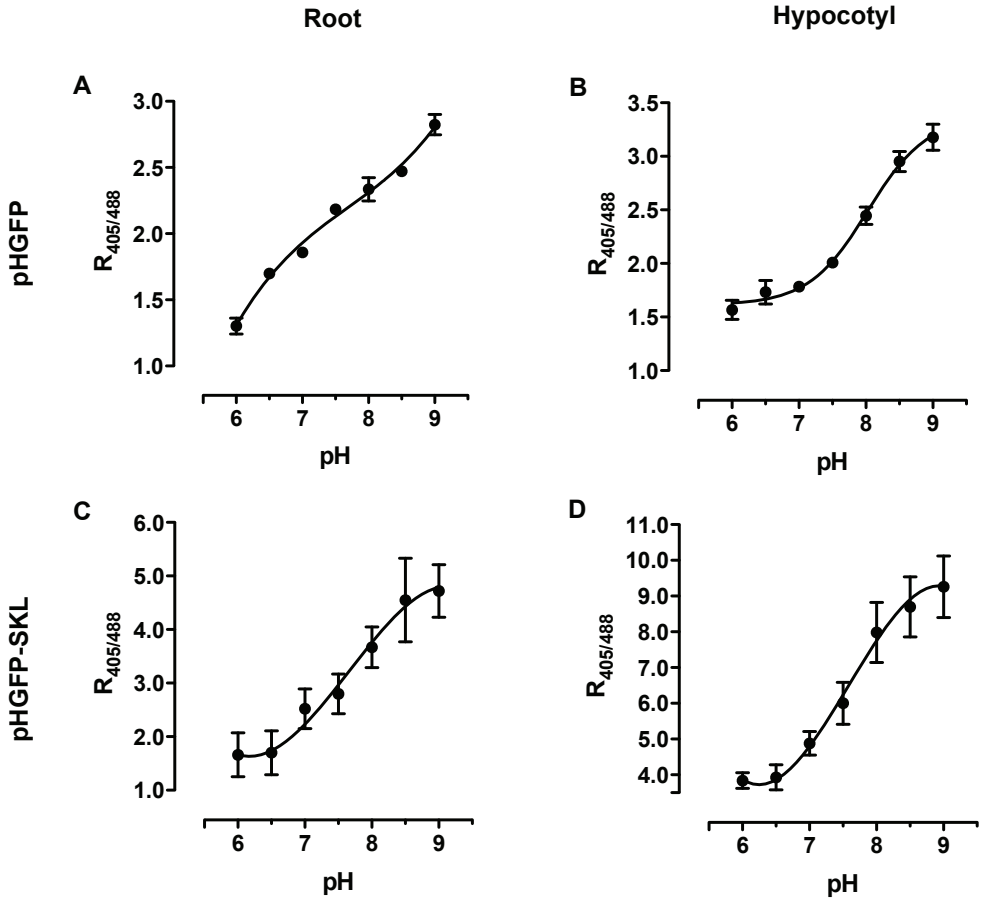

Fig. 2: *In situ* calibration curves to determine cytosolic and peroxisomal pH in roots and hypocotyl in Arabidopsis seedlings.
To determine pH_{per} and $pH_{cyt,}$ calibration curves were recorded in roots (A, C) and shoots (B, D) of Arabidopsis seedlings treated with ammonium acetate containing pH buffers. Panels A and B depict the calibrations for pHGFP, panels C, D for pHGFP-SKL. Data points are given as means ± SEM. N ≥ 15 per pH step.

In Figure 2 calibration curves for both pH_{cyt} (upper panel) and pH_{per} (lower panel) in roots (A, C) and hypocotyls (B, D) are depicted. The sensors responded over the pH range from 6.0 to 9.0 with a reversible $R_{405/488}$, which was progressively quenched at low pH. A clear midpoint was detectable in all graphs, which followed a sigmoidal curve shape (Fig. 2). This is characteristic of systems with a chemical equilibrium. A second calibration method was used to validate loading of peroxisomes with pH buffer. The alternative technique using the ionophore nigericin instead of ammonium acetate led to comparative calibration results (Fig. S2). In following studies calibration was performed with ammonium acetate. We favored ammonium acetate over nigericin, because it is

not toxic to the cell and does not lead high levels of background fluorescence (Moseyko and Feldman, 2001).

The data demonstrated that calibration could be performed for both sensors as expected. The sensors reacted dynamically over the chosen pH range. Calibration could be successfully performed to determine the peroxisomal pH in hypocotyls and roots precisely.

Influence of light on cytosolic pH

We analyzed the impact of light on root pH, because light-induced pH changes are a common mechanism in plants (Guern et al., 1991; Bethmann et al., 1998). As roots are not exposed to light under natural conditions, we analyzed if the artificial growth conditions chosen to maximize root biomass impacted root pH. First, the cytosolic pH in root cells of 5-day-old seedlings grown in the presence of sucrose in continuous light was analyzed (Fig. 3, open bar).

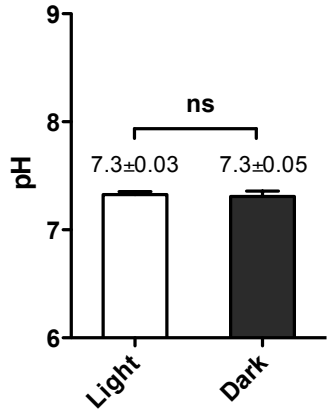

Fig. 3: Comparison of cytosolic pH in Arabidopsis roots grown under continuous light or in complete darkness. Cytosolic pH was measured in 5-d old roots grown in continuous light (open bar) or complete darkness (grey bar). The pH was calculated from one representative line for pHGFP and pHGFP-SKL. Values are given as mean pH values. Error bars represent SEMs. ns, $P = 0.7445$.

Measurements of pH were steadily performed *in situ*, keeping seedlings in liquid MS medium. Sequential images of thirty seedlings per experiment were taken. The analysis of three independent pHGFP1-3 lines revealed a mean pH_{Cyt} of 7.3 ± 0.03 (Tab. S2, Fig. 3). This pH value resembled the results obtained for the root cytosolic pH in Arabidopsis earlier (Moseyko and Feldman, 2001). To mimic natural growth conditions, we grew roots for five days in the presence of sucrose under constant darkness. Root biomass was significantly reduced, compared to light-grown seedlings. We determined the pH_{Cyt} of root cells and as 7.3 ± 0.03 (Fig. 3, filled bar). This value did not diverge from the root pH_{cyt} of plants grown in constant illumination (Fig. 3).

In conclusion, our experiments demonstrated that light did not influence the root cytosolic pH. In both light-grown and dark-grown roots of 5-d old seedlings the average pH_{Cyt} was 7.3. Because light did not alter pH, roots were always grown on MS medium with sucrose under illumination and hypocotyls in darkness. Since our measurements of the cytosolic root pH were in line with previous studies, Arabidopsis lines expressing the cytosolic pHGFP reporter were used as reference for peroxisomal pH measurements.

Measurements of the peroxisomal pH in different tissues

Since peroxisomes have tissue-specific functions (Pracharoenwattana and Smith, 2008), we investigated whether the peroxisomal pH was altered in different plant tissues. Therefore, we measured the peroxisomal pH in roots and hypocotyls of 5-day-old seedlings grown on MS medium in the presence of sucrose. Root peroxisomes of pHGFP-SKL lines grown in constant light exhibited an alkaline pH (Fig. 4, Tab. S2).

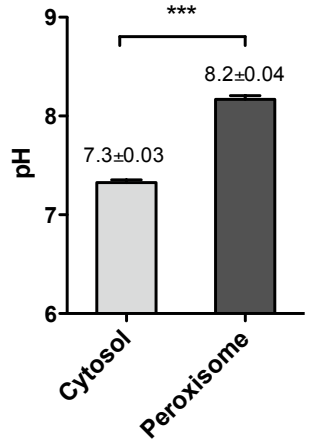

Fig. 4: Investigation of the peroxisomal pH in Arabidopsis roots.
Cytosolic pH (light grey) was calculated from three independent control lines expressing pHGFP. Peroxisomal pH (dark grey) was calculated from four independent lines expressing pHGFP-SKL. For pH analysis plants were grown on ½ MS supplemented with sucrose for 5 d in continuous light. Values are given as mean pH values. Error bars represent SEMs. ****P* < 0.0001.

The average peroxisomal pH of 8.2 ± 0.04 was significantly higher than that of the cytosol (pH = 7.3 ± 0.03). This result was consistent with the alkaline pH determined transiently in leaf peroxisomes (Shen et al., 2013). Interestingly, we detected that hypocotyl cells of pHGFP-SKL seedlings cultivated in complete darkness exhibited an average peroxisomal pH of 6.3 ± 0.03, whereas the cytosolic pH in hypocotyls was unaltered (pH = 7.3 ± 0.03, Tab. S2, Fig. 5).

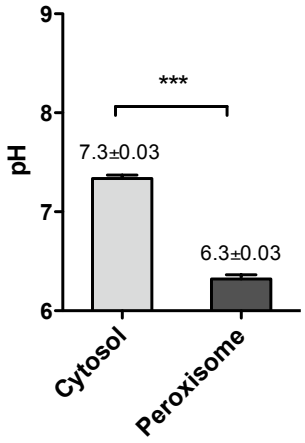

Fig. 5: The peroxisomal pH in Arabidopsis hypocotyls is acidic.
Cytosolic pH (light grey) was calculated from three independent control lines expressing pHGFP. Peroxisomal pH (dark grey) was calculated from four independent lines expressing pHGFP-SKL. For pH analysis plants were grown on ½ MS supplemented with sucrose for 5 d in constant darkness. Values are given as mean pH values. Error bars represent SEMs. ****P* < 0.0001.

Our analysis indicated that the peroxisomal pH drastically varied in different plant tissues. In contrast to peroxisomes from roots and leaves, the peroxisomal matrix was acidic in peroxisomes involved in storage-oil mobilization.

Sucrose does not alter the peroxisomal pH

Seedlings were grown in the presence of sucrose in continuous darkness to promote skotomorphogenesis. Sucrose is known to function as an important signaling molecule that regulates genes involved in photosynthesis, metabolic and developmental processes (Sheen et al., 1999; Rook et al., 2001).

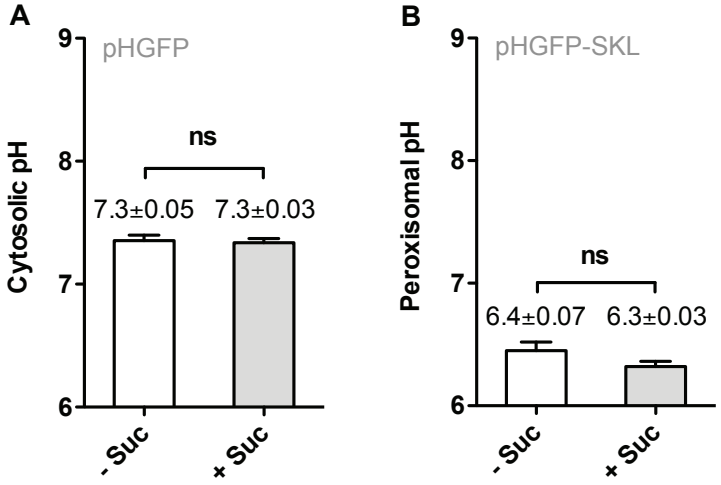

Fig. 6: Comparison of pH in Arabidopsis hypocotyls grown in the absence or presence of sucrose.
Cytosolic and peroxisomal pH values were determined in 5-d old seedlings grown in complete darkness in the absence (white bars), or presence of 1% (w/v) sucrose (grey bars). The pH was calculated from one representative line for pHGFP (A) and pHGFP-SKL (B). Values are given as mean pH values. Error bars represent SEMs. Cytosolic pH, $P = 0.7681$, ns; peroxisomal pH, $P = 0.1069$, ns

To exclude that an external supply of sucrose affects the pH of peroxisomes, we tested if the peroxisomal pH of pHGFP-SKL hypocotyls was altered in the absence of sucrose. Without sucrose 5-day-old pHGFP-SKL1 seedlings were less developed when compared to seedlings of the same age grown on sucrose-containing medium. However, the peroxisomal pH did not differ significantly between pHGFP-SKL1 plants grown in the presence (grey bars) or absence of sucrose (white bars) (Fig. 6). The peroxisomal pH was 6.4±0.07 in plants grown without sucrose or 6.3±0.03 in plants grown on sucrose-containing medium. Cytosolic pH of hypocotyl cells was determined in both experimental conditions as control. In the absence of sucrose the cytosolic pH was 7.3±0.05, plants grown on plates with sucrose exhibited a pH of 7.3±0.03 (Fig. 6). Hence, exogenous sucrose had no effect on peroxisomal pH in etiolated Arabidopsis seedlings.

ATP import into plant peroxisomes is not proton-coupled

Previous work in *S. cerevisiae* indicated that the peroxisomal ATP transporter Ant1p is involved in the formation of a proton gradient across the peroxisomal membrane. *In vitro* uptake studies with recombinant protein demonstrated that the yeast carrier imports ATP together with protons in

exchange for AMP. This leads to an acidification of the peroxisomal lumen (Lasorsa et al., 2004). Hence, we investigated whether the Arabidopsis adenine nucleotide transport proteins 1 and 2 (PNC1 and PNC2, (Linka et al., 2008) catalyze a proton-coupled ATP import *in vitro*.

We expressed PNC1 and PNC2 fused to an HA-affinity tag using a cell-free *E.coli*-based expression system (Fig. 7). Even in cell-free systems the expression of membrane proteins often leads to the formation of protein aggregates, which are unfavorable as aggregated proteins are often misfolded (Nozawa et al., 2007). The standard protocol for *E. coli* cell-free expression was modified, including a detergent (Brij-35) and liposomes, which enable native protein folding during translation (Nozawa et al., 2007). To test how these additives influence protein expression and activity, translation reactions were prepared without additives (Fig. 7, 1), with Brij-35 (Fig. 7, 2), or with liposomes and Brij-35 (Fig. 7, 3).

The presence of PNC1-HA and PNC2-HA proteins was confirmed by immunoblotting with an anti-HA antibody. The calculated molecular masses of the HA-tagged proteins were 36.6 kDa for PNC1 and 36.2 kDa for PNC2. The empty vector pET16b was expressed as negative control. In contrast to the Coomassie-stained SDS gels (Fig. 7, upper panel) where no distinct protein bands corresponding to PNC1 and PNC2 were observable, the immunoblot revealed specific signals for PNC1-HA and PNC2-HA, A, but not for the control pET16b (Fig. 7, lower panel). Protein signals corresponded to the molecular masses expected for the three carriers. Bands below 35 kDa in PNC1 samples were most likely caused by protein degradation. On protein expression level, no differences were observed between the three expression conditions. Protein translation of PNCs was neither inhibited, nor enhanced by Brij-35 and liposomes.

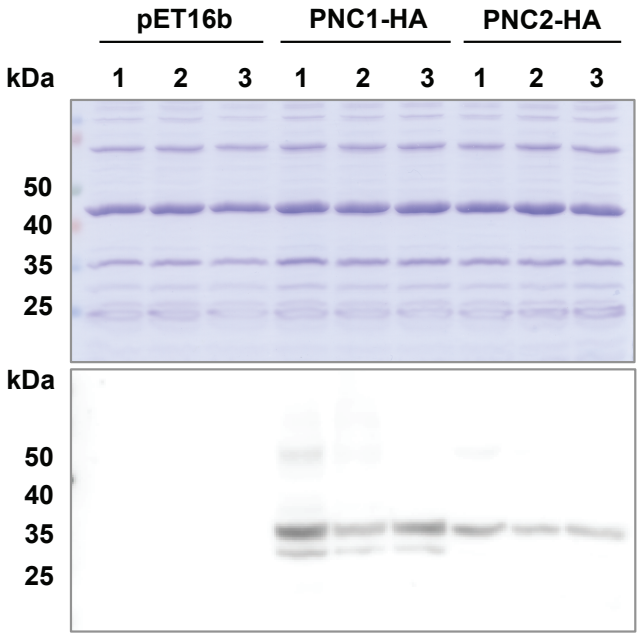

Fig. 7: Detection of PNC1-HA and PNC2-HA proteins expressed *in vitro*.
SDS-PAGE (upper part) and immunoblot detection (lower part) of pET16b (empty vector), PNC1-HA and PNC2-HA expressed in an *E.coli* cell-free system. Expression was performed without additives (1), in the presence of Brij-35 (2), and with Brij-35 and liposomes (3). The expected molecular mass of the carriers is 35 kDa.

To test the co-translational association of cell-free expressed proteins with liposomes, we performed floating experiments (Nozawa et al., 2007) (Fig. 8). Cell-free expression batches containing synthesized PNC2-HA proteins translated in the presence or absence of liposomes were loaded on a discontinuous sucrose density gradient. Ultracentrifugation was applied to fractionate cell-free expression components, non-integrated PNC2-HA protein and proteoliposomes. Eight fractions were collected from top to bottom of the gradient and were assayed for PNC2-HA protein abundance (Fig. 8).

Due to a higher density of PNC2-HA protein incorporated into liposomes, we expected that the majority of PNC2-HA protein signal would be detected in lower gradient fractions when liposomes are present. Without liposomes, we expected PNC2-HA to be present in all gradient fractions with a tendency towards top fractions. When PNC2-HA was translated in the absence of liposomes, most protein was found in fractions 1 and 2 with decreasing abundance in lower fractions. Almost no signal was detected in the bottom fraction (Fig. 8, A). In contrast, most PNC2-HA protein when translated in the presence of liposomes led to a shift towards lower gradient fractions. The maximum protein amount was found in fraction 5 (Fig. 8, B).

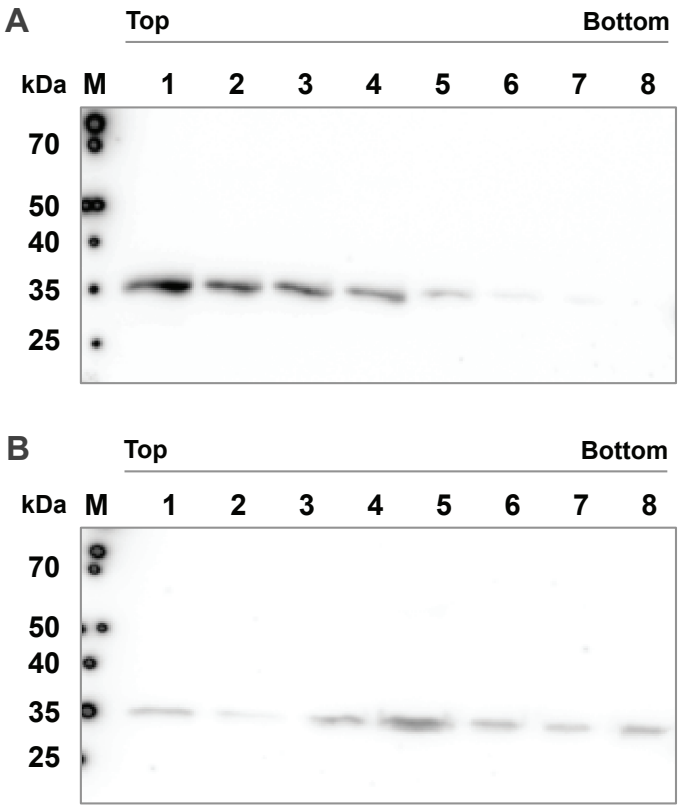

Fig. 8: PNC2-HA protein is integrated into liposomes during translation.
PNC2-HA was expressed cell-free in the presence of Brij-35 (0.04%, w/v). Expression was performed in the presence (A) or absence (B) of liposomes (1%, w/v). Proteins were separated on a discontinuous sucrose gradient. From top to bottom of the gradient eight fractions (1-8) were isolated. Presence of PNC2-HA protein was verified by immunoblotting using an anti HA-antibody. The expected molecular mass of PNC2 is 35.2 kDa.

This experiment indicated that PNC2-HA was successfully integrated into liposomes during translation, as the protein signal migrated to lower fractions when liposomes were present in the translation batch.

To analyze if the addition of Brij-35 and liposomes impacts the activity of recombinant PNC2-HA, proteins were reconstituted in liposomes for *in vitro* uptake experiments (Kasahara and Hinkle, 1976). Proteoliposomes were pre-loaded with 10 mM ATP and 200 µM radiolabelled [α^{32}-P]ATP was offered externally. Uptake rates of the ATP homoexchange mediated by PNC2-HA were measured over time comparing different expression conditions. As negative control PNC2 proteoliposomes reconstituted without pre-loading were produced. When PNC proteoliposomes did not contain a counterexchange substrate, an import of radiolabelled ATP was not possible, because PNC carriers act as strict antiporters (Linka et al., 2008) (Fig. 9). The ATP homoexchange capacity of PNC2-HA translated in the absence of additives led to inactive protein. Negligible uptake rates were observed for PNC2-HA and the negative control (Fig. 9, A). PNC2-HA was also not active when expressed in the presence of Brij-35 only. A marginal internal ATP concentration of 3 nmol ATP mg protein^{-1} was measured in both the PNC2-HA sample and the negative control after 64 minutes (Fig. 9, B). Only when both liposomes and Brij-35 were added, PNC2-HA transport activity was stimulated. The homoexchange of ATP followed a first order kinetics and maximum uptake of 223 nmol ATP mg protein^{-1} (Fig. 9, C).

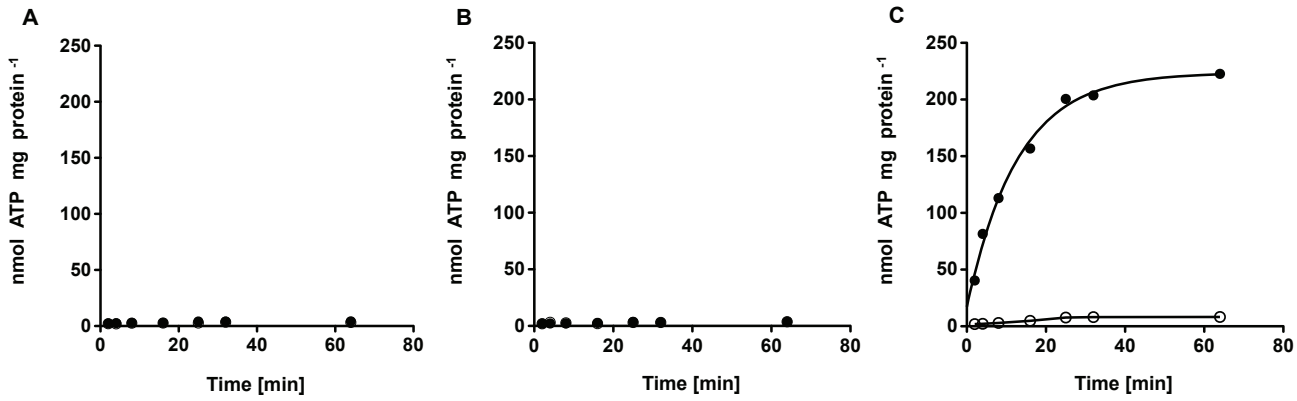

Fig. 9: PNC2-HA exhibited ATP counterexchange activity if expressed in the presence of liposomes and a detergent.
To test the efficiency of different expression conditions, PNC2-HA was expressed without additives (A), in the presence of Brij-35 (0.04%, w/v) (B), or in the presence of Brij-35 and liposomes (1%, w/v) (C). Time-dependent ATP uptake assays (200 µM) were performed to test the activity of PNC2-HA, reconstituted in liposomes preloaded with 10 mM ATP.

After establishing optimal expression and uptake conditions, all *E.coli* cell-free translation processes were performed in the presence of lipid vesicles and Brij-35 as a detergent, ensuring solubility of the synthesized protein and its direct functional integration into liposomes. Adding detergents and lipid vesicles stimulated protein activity.

To validate if PNC1 was also functionally expressed, protein was expressed in the presence of liposomes and Brij-35 and then reconstituted into liposomes pre-loaded with ATP. Time-dependent uptake experiments with [α^{32}-P]ATP confirmed the activity of PNC1 (Fig. 10, A) and PNC2 (Fig. 10,

B). The carriers facilitated an active ATP counter-exchange (Fig. 10, filled symbols). PNC1 reached a maximum internal concentration of 35 nmol ATP mg protein^{-1}, PNC2 accumulated 200 nmol ATP mg protein^{-1}. Only marginal ATP exchange was observed in control samples without pre-loading (Fig. 10, open symbols).

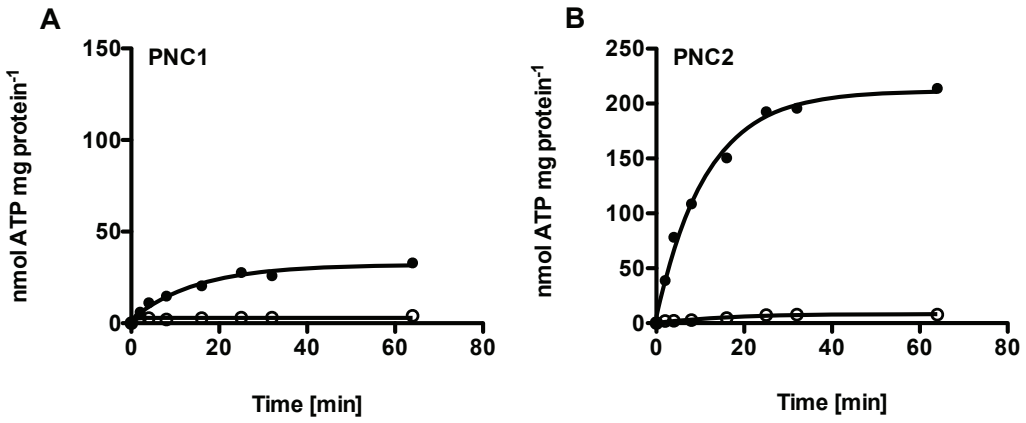

Fig. 10: Time-dependent uptake studies of recombinant PNC1 and PNC2 protein reconstituted in liposomes.
PNC1 and PNC2 proteins were expressed in an *E.coli*-based *in vitro* system under modified conditions. Recombinant protein was reconstituted in liposomes pre-loaded with internal 10 mM ATP or no substrate (negative control). The uptake of radiolabelled ATP (200 µM ^{32}P-ATP) mediated by PNC1 (A) and PNC2 (B) was followed over time.

Since we established the expression of functional proteins, we assessed whether PNC1 and PNC2 catalyze a proton-compensated ATP import. Therefore, we performed *in vitro* ATP uptake experiments into AMP preloaded liposomes in the presence of varying internal and external pH to promote a proton-coupled driving force at the liposomal membrane. Proteoliposomes were prepared with (i) an outwards-directed proton gradient (pH 6.0$_{in}$/pH 7.0$_{out}$), (ii) no pH gradient (pH 7.0$_{in}$/pH 7.0$_{out}$), or (iii) an inwards-directed gradient (pH 8.0$_{in}$/pH 7.0$_{out}$) (Fig. 11, top to bottom).

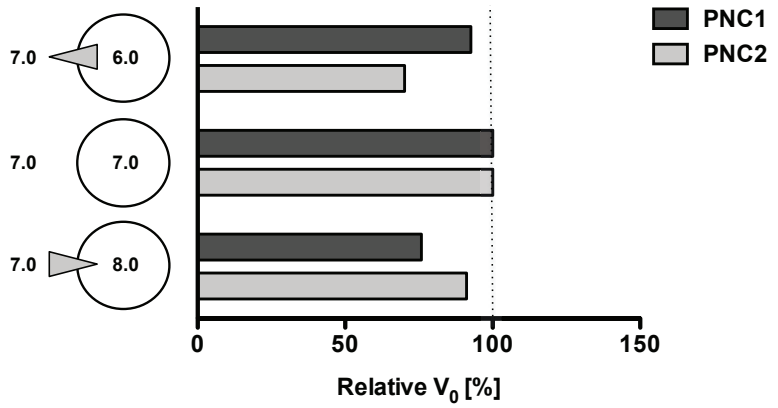

Fig. 11: A proton gradient across the liposomal bilayer does not stimulate the time-dependent uptake of ATP mediated by PNC1 and PNC2.
Recombinant PNC1 (dark grey) and PNC2 (grey) proteins were expressed and reconstituted in liposomes pre-loaded with 10 mM AMP. The initial velocities of the uptake of 200 µM radiolabelled ATP into liposomes with an outwards directed proton gradient (pH 6.0 inside, pH 7.0 outside), no proton gradient (pH 7.0 inside, pH 7.0 outside, used as reference for calculation), or an inwards directed proton gradient (pH 8.0 inside, pH 7.0 outside) was followed over time. Data is presented as initial velocity of the ATP/AMP exchange of three technical replicates, ns = P >0.05.

Relative initial velocities of time-dependent uptake of 200 µM [^{32}P]-ATP into liposomes in the presence of 10 mM AMP were calculated relative to the ATP/AMP exchange at equal pH. The experiment revealed that a proton gradient did not stimulate the uptake of ATP into PNC1 and PNC2 proteoliposomes significantly (Fig. 11). As a pH gradient did not influence uptake mediated by the carriers, we concluded that in Arabidopsis hypocotyls the exchange of adenine nucleotides mediated by PNC1 and PNC2 was not proton-compensated. Thus, PNC carriers seemed not to be directly responsible for an acidification of the peroxisomal lumen.

The pnc1/2 double mutant is strongly compromised in β-oxidation

To study if a high flux of fatty acids through β-oxidation and glyoxylate cycle leads to an acidification of the peroxisomal lumen in hypocotyls, we generated an Arabidopsis mutant defective in both PNC proteins. Previous studies described an ethanol-inducible RNA interference line deficient in PNC1 and PNC2 proteins, which leads to an inhibition of fatty acid breakdown, downstream pathways, such as the glyoxylate cycle and other β-oxidation reactions (Linka et al., 2008). It was demonstrated that ATP import mediated by PNC1 and PNC2 is essential for β-oxidation activity (Arai et al., 2008; Linka et al., 2008). In this study we established a double mutant (*pnc1/2*) by crossing homozygous T-DNA lines for PNC1 (SAIL_303H02, *pnc1*) and PNC2 (SALK_014579, *pnc2*) (Linka et al., 2008). RT-PCR analysis verified the absence of full-length *PNC* transcripts in single mutants (Fig. 12). Double mutants were generated and selected for homozygosity on MS medium supplemented with sucrose, kanamycin and glufosinate.

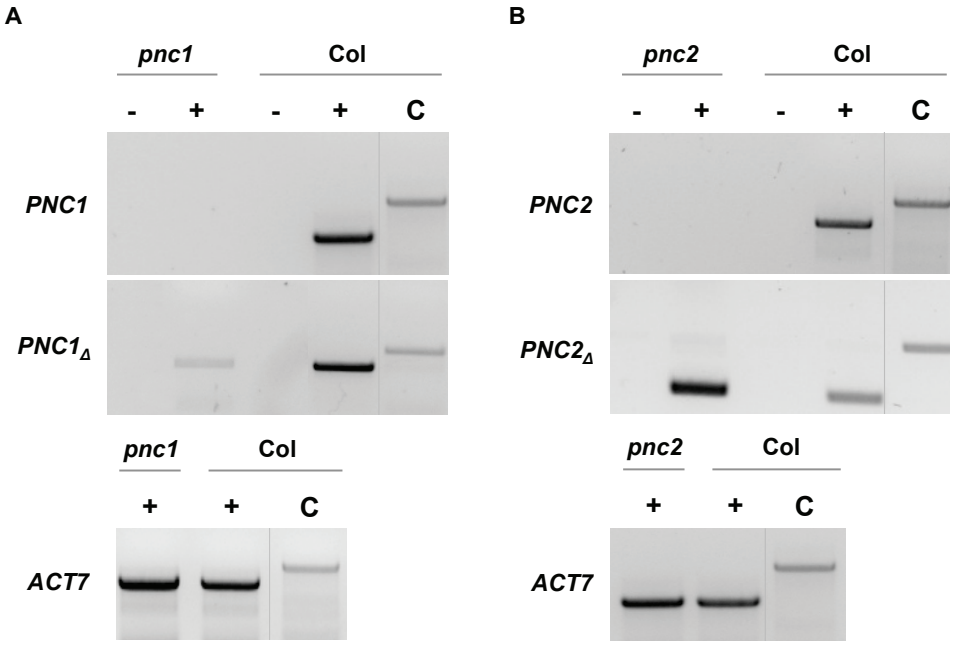

Fig. 12: Full-length transcripts are absent in *pnc1* and *pnc2* mutants.
To determine the expression of *PNC1*, *PNC2* and *ACT7* in mutant lines RT-PCR on cDNA was achieved. Two primer combinations were used. One primer pair was designed to yield a full-length transcript from 5'-UTR to 3'-UTR (PNC1: 1023 bp, PNC2: 1050 bp), the other primer combination amplified a product from 5'-UTR up to the T-DNA insertion site to yield putative truncated transcripts (PNC1: 613 bp, PNC2: 365 bp). As control (C) PCRs were additionally performed with wild-type genomic DNA (PNC1: 1486 bp, PNC2: 1581 bp). To verify the integrity of cDNAs PCRs were done amplifying the actin gene *ACT7* (cDNA: 734 bp, gDNA: 918 bp).

In this study we avoided the use of ethanol-inducible RNA interference lines repressing PNC1 and PNC2, as this system is less convenient to use than stable lines. In inducible approaches the reproducibility of gene repression may vary. In addition ethanol was shown to cause non-specific physiological affects and stress symptoms in plants (Roslan et al., 2001).

We expected the mutations in *pnc1/2* to cause severe phenotypic effects due to a constitutive disruption of peroxisomal ATP import. In multiple assays, including (i) sucrose-dependency, (ii) growth response to 2,4-DB, and (iii) Nile Red staining of oil bodies, the β-oxidation capacity of *pnc1/2* was tested.

Typical β-oxidation mutants fail to establish in the absence of exogenous sucrose, as they cannot derive energy from the degradation of storage reserves to fuel seedling growth (Graham, 2008; Quettier and Eastmond, 2009). Thus *pnc1*, *pnc2*, *pnc1/2* mutants, the respective wildtype and a positive control, the peroxisomal import mutant in PEROXIN14 (*pex14)* (Orth et al., 2007) were grown on MS agar plates in the absence or presence of sucrose. Seedling growth and hypocotyl lengths of etiolated seedlings were compared (Fig. 13).

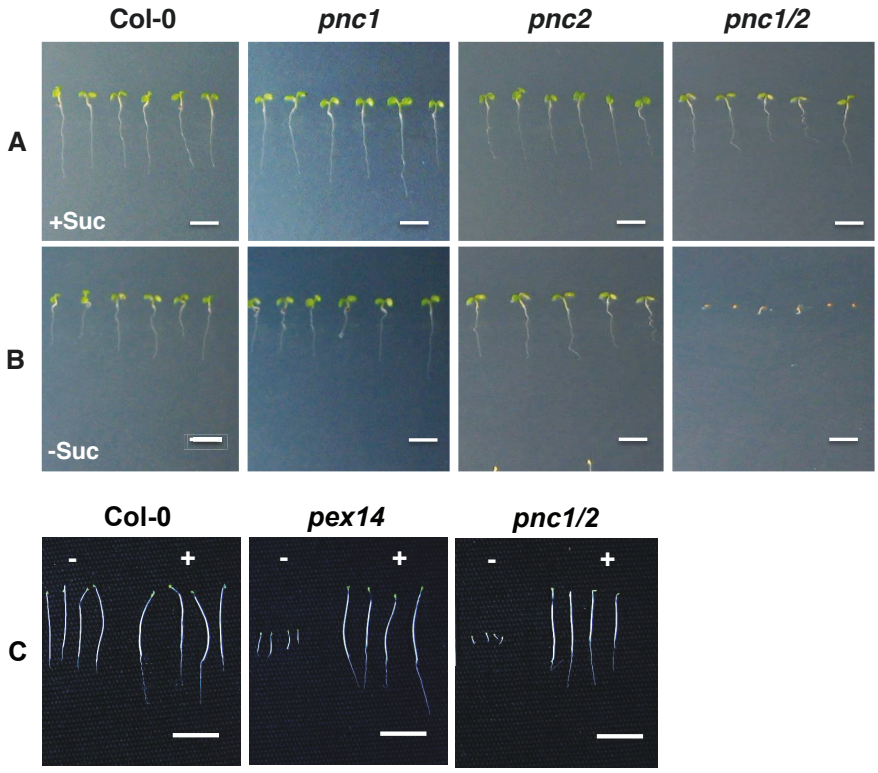

Fig. 13: In the absence of sucrose *pnc1/2* seedlings cannot establish.
To assess if *pnc1/2* mutants are able to establish in the absence of sucrose, seedling growth was observed (upper box, A and B) and hypocotyl lengths were monitored (lower box, C) for seedlings grown on medium with (+) or without sucrose (-). A, B: The single mutants, the double mutant and the wildtype were grown for 5 days in the presence (+Suc) or absence of sucrose (1%) (-Suc) in short-day conditions. C: To monitor hypocotyl growth *pnc1/2*, a positive control *pex14* and the wildtype were grown with (+) or without (-) sucrose in constant darkness for five days. Scale bars = 1 cm.

Experiments showed that in the absence of sucrose *pnc1* and *pnc2* seedlings developed wild-type-like. The *pnc1* and *pnc2* single mutants and wildtype did not depend on external sugar.

After five days of growth cotyledons were green and the primary roots were developed in wildtype and both single lines. On medium without sucrose the double mutant germinated, but failed to establish. Cotyledons and the primary root did not emerge (Fig. 13, B). An application of exogenous sucrose alleviated the block in β-oxidation and almost completely rescued the strong retardations of *pnc1/2* plants; seedlings grew as well as the wildtype (Fig. 13, A). Because a strong phenotype was observed for *pnc1/2* seedlings grown in continuous light, we cultivated the seedlings in continuous darkness to provoke skotomorphogenesis. Germinated on sucrose-less medium, the double mutant did not develop a primary root. The same observation was made for the positive control, the *pex14*. Supplied with sucrose *pnc1/2* and *pex14* seedlings grew like the wildtype and hypocotyl lengths did not differ to plants grown with sucrose (Fig. 13, C).

As a second assay to display defects in fatty acid degradation, growth responses to 2,4-DB, a synthetic auxin analog, were monitored (Estelle and Somerville, 1987). While in wildtype plants 2,4-DB is converted to the herbicide 2,4-D via peroxisomal β-oxidation, mutants in peroxisomal fatty acid degradation do not efficiently convert 2,4-DB to the toxic 2,4-D. In consequence, root growth and hypocotyl lengths are reduced in the wildtype, but not in β-oxidation mutants, which consequently do not display severe growth defects as they are resistant to 2,4-DB (Hayashi et al., 1998; Zolman et al., 2000). For this assay, *pnc1/2* double mutants and wildtype were grown in the presence of 2,4-DB (Fig. 14, grey bars), 2,4-D (Fig. 14, light grey bars), or ethanol as control (Fig. 14, dark grey bars). Our analysis revealed that in contrast to wildtype *pnc1/2* mutants were resistant to 2,4-DB (Fig. 14). Primary root growth and hypocotyl lengths were not diminished in *pnc1/2* in comparison to control conditions. Wildtype plants exhibited shorter primary roots and hypocotyls upon 2,4-DB treatment. 2,4-D treatment led to drastically decreased primary root growth and hypocotyl lengths in both *pnc1/2* and wildtype. Here, wildtype plants exhibited a hypocotyl growth reduction of 50%, hypocotyls of *pnc1/2* were reduced 60-70% compared to the negative control (EtOH) (Fig. 14).

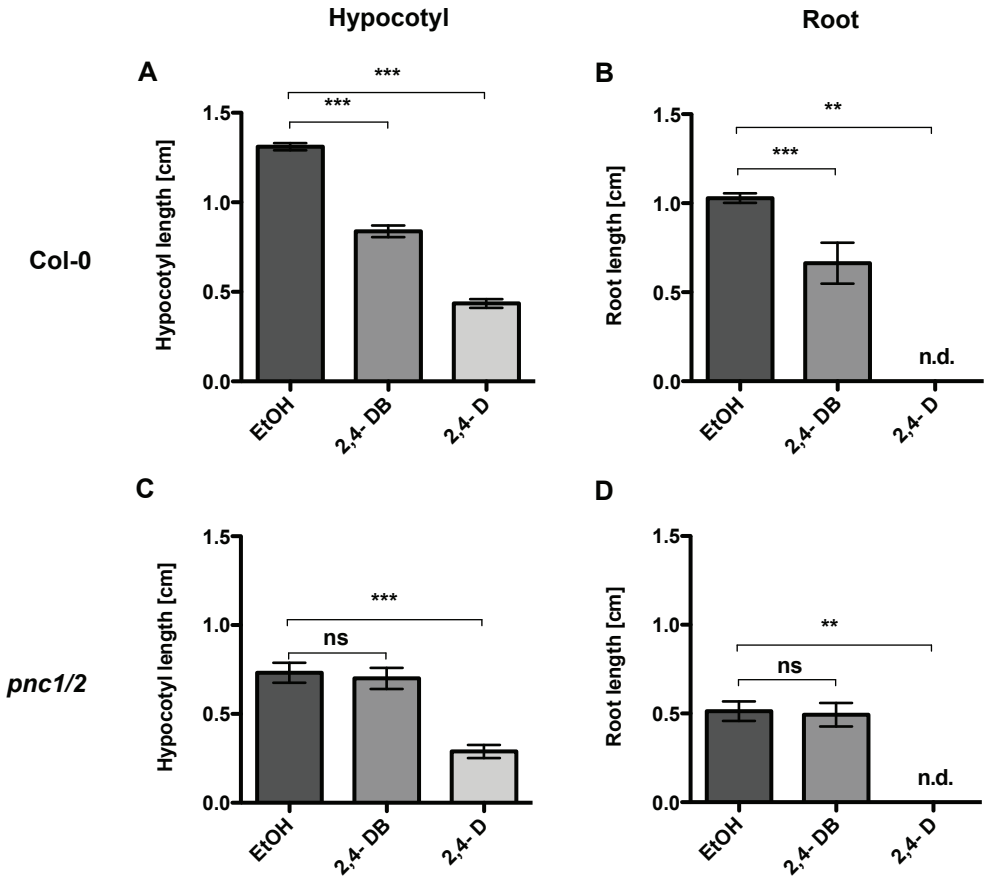

Fig. 14: Sensitivity of pnc1/2 to 2,4-dichlorophenoxybutyric acid (2,4-DB) is decreased.
The effect of 2,4-DB (0.8 µM) and 2,4-D (0.23 µM) on hypocotyl (left) and root length (right) in five-day old *pnc1/2* (C, D) and the wildtype (A, B) was analyzed. As negative control, plants were grown in the presence of 0.001% EtOH. Graphs show Means ± SEMs (N= 50), n.d. = not detectable. ***P < 0.0001; **P = 0.001-0.01; ns (not significant), P > 0.05. Scale bars = 1 cm.

Mutants compromised in the degradation of fatty acids retain oil bodies in their hypocotyls (Linka et al., 2008; Dietrich et al., 2009). The vital stain Nile Red was used for the intracellular detection of lipid droplets in 5-day old seedlings (Greenspan et al., 1985). Plants of the double mutant *pnc1/2*, the single lines *pnc1*, *pnc2*, and seedlings of the peroxisomal ABC transporter *pxa1-1* (positive control) were stained the lipophilic dye Nile Red (Fig. 15).

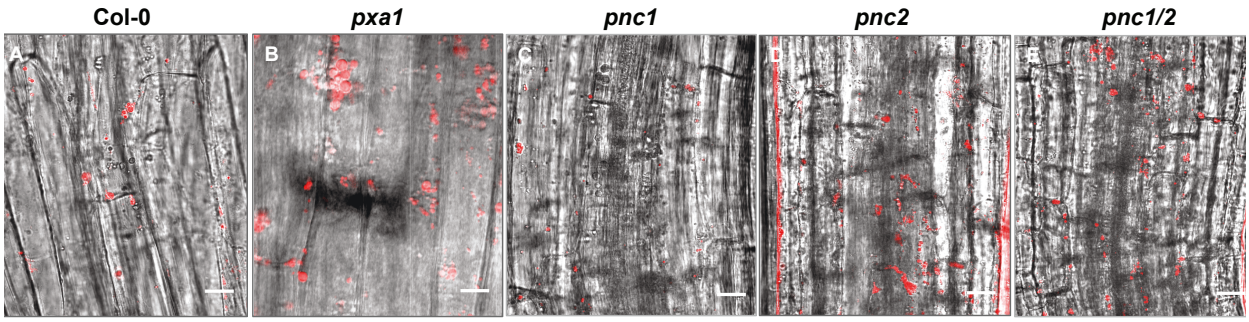

Fig. 15: Nile red staining reveals that lipid bodies are retained in *pnc1/2* hypocotyls.
5-day old *pnc1/2* and Col-0 etiolated seedlings were stained with the lipophilic dye Nile Red. The presence of oil bodies in the hypocotyl was examined using a laser-scanning microscope. Scale bars = 20 µM.

In hypocotyls of *pnc1*, *pnc2* and *pnc1/2* a significantly larger number of oil bodies were retained when compared to wildtype. In *pxa1-1* a comparably high number of oil bodies existed, which seemed to be slightly larger than in *pnc* lines and wildtype (Zolman et al., 2001; Bernhardt et al., 2012) (Fig. 15).

The experiments indicated that the absence of both peroxisomal ATP importers caused defects in seedling establishment in the absence of exogenous sucrose. Another evidence that fatty acid oxidation was strongly defective in *pnc1/2* was that 2,4-DB was not metabolized to 2,4-D. The lipid droplets retained in *pnc1/2* seedlings also implied that the rate of lipolysis was diminished due to a block in β-oxidation. Taken together, we concluded that β-oxidation was severely impaired in *pnc1/2* plants.

The pH in the peroxisome lumen of hypocotyls is not altered when β-oxidation is impaired

To understand if the acidic pH_{Per} observed in etiolated seedlings was a consequence of high levels of β-oxidation, pHGFP and pHGFP-SKL expressing plants derived from a cross of the peroxisomal and cytosolic marker lines with *pnc1/2* were examined. We examined the peroxisomal pH in hypocotyls of 30 plants lacking both PNC1 and PNC2 (Fig. 16). The cytosolic pH was determined as reference. The pH values measured were compared to wildtype pHGFP and pHGFP-SKL lines. Measurements revealed that in wildtype and *pnc1/2* mutants the peroxisomal pH was 6.2. Thus, the absence of adenine nucleotide carriers and the resulting block in β-oxidation did not alter the acidic pH in hypocotyl peroxisomes. The cytosolic pH of *pnc1/2* was 7.4±0.12, which did not significantly differ from the pH_{cyt} in wildtype.

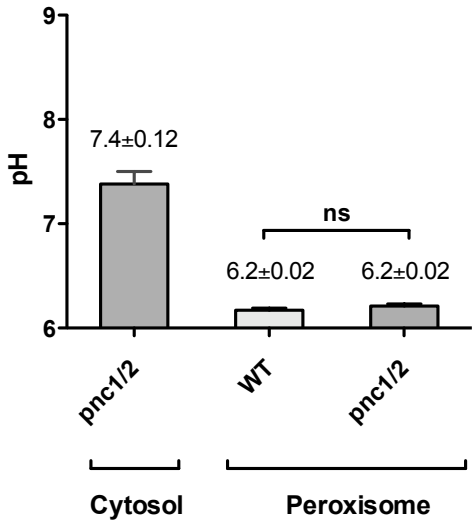

Fig. 16: Peroxisomal pH is not altered in *pnc1/2* mutants.
The pH of peroxisomes and cytosol was determined in *pnc1/2* mutant hypocotyls. For analysis plants were grown on ½ MS supplemented with sucrose for 5 d in complete darkness. Values are given as mean pH values. Error bars represent SEMs. $P = 0.2827$, ns.

We concluded that the loss of PNC1 and PNC2 and thus impaired β-oxidation and glyoxylate cycle levels did not directly influence the peroxisomal pH, because the peroxisomal pH of hypocotyls remained acidic in *pnc1/2* mutants.

Discussion

In this study, we demonstrated the expression of a pH-sensitive GFP in peroxisomes of stable transgenic *Arabidopsis* lines (Fig. 1). Construction of these transgenic lines enabled us to investigate the peroxisomal pH in roots and hypocotyls non-invasively and as naturally as possible (Fig. 2-6, Fig. 16, Tab. S2). Our study for the first time describes the peroxisomal pH of different Arabidopsis tissues, *i.e.* roots and hypocotyls. Using confocal laser scanning microscopy, we discovered the peroxisomal pH in root cells is alkaline with an average pH of 8.2 (Fig. 4). A similar plant-optimized ratiometric form of a pH-sensitive GFP was established transiently in Arabidopsis leaves, determining an alkaline lumen in leaf peroxisomes (Shen et al., 2013). Surprisingly, we found that the peroxisomal lumen of hypocotyls was acidic (pH 6.3, Fig. 5). In this study we addressed the question why the pH in hypocotyl peroxisomes is acidic.

Tissue-specific differences in the pH indicate that the pH is not static. Peroxisomes are highly dynamic in their metabolism (Hayashi and Nishimura, 2003). Enzymatic contents differ significantly between subtypes of peroxisomes depending on their distinct metabolic roles (Pracharoenwattana and Smith, 2008). The peroxisomal pH is a dynamic parameter reflecting physiological conditions and subsequent metabolic demands of the plant. Thus, the peroxisomal pH is regulated under varying conditions (Nishimura et al., 1996; Shen et al., 2013). We proposed that an acidification of peroxisomes in hypocotyls is linked to the degradation of fatty acids. Studies using a pHluorin-variant to examine the peroxisomal pH of Baker's yeast grown in medium with fatty acids as carbon source revealed a lower peroxisomal lumen pH compared to the cytosol (Lasorsa et al., 2004). An acidic peroxisomal pH in yeast is close to the average pH_{per} of 6.3, we detected in hypocotyl cells of *Arabidopsis*. We hypothesized that the consistency of pH_{per} in yeast and *Arabidopsis* might indicate a general mechanism underlying, which is putatively linked to β-oxidation.

It was reported that the yeast peroxisomal adenine nucleotide carrier Ant1p actively acidifies the peroxisomal matrix and thus generates a proton gradient across the peroxisomal membrane (Lasorsa et al., 2004). Ant1p catalyzes the import of $ATP(^{4-})$ in exchange with $ADP(^{3-})$ or $ADP(^{2-})$, resulting in an net transfer of negative charges. *In vitro* uptake studies using recombinant protein demonstrated that the yeast carrier compensates the adenine nucleotide exchange with protons, leading to an electroneutral transport (Lasorsa et al., 2004). Accordingly, we performed *in vitro* uptake experiments with recombinant PNC1 and PNC2 proteins reconstituted in liposomes. In contrast to the previous study in yeast, we showed that a pH gradient did not stimulate the uptake of adenine nucleotides mediated by PNC1 and PNC2, concluding that these carriers most likely do not

compensate the electrogenic exchange of adenine nucleotides by importing protons into the peroxisomal lumen.

To further elucidate the impact of β-oxidation and glyoxylate cycle on peroxisomal pH, we established a double mutant line devoid of PNC1 and PNC2 (*pnc1/2*). In various physiological experiments we have proven that β-oxidation is strongly impaired in *pnc1/2*. However, when measuring the peroxisomal pH in *pnc1/2*, we saw that a lack of PNC1 and PNC2 does not influence pH_{Per}. We concluded that an inhibition of β-oxidation and downstream metabolism affected on the level of ATP import does not directly influence the pH in peroxisomes.

Thus, we hypothesize that yet unknown mechanisms, such as proton pumps could exist, which are responsible for pH_{Per} homeostasis and would cause a strong acidification of the peroxisomal lumen. So far, proteomic studies of plant peroxisomes did not reveal strong evidences for the existence of peroxisomal proton pumps (Reumann et al., 2007; Eubel et al., 2008). However, ATPase subunits have been discovered in peroxisomes of the methylotropic yeast *Hansenula polymorpha* (Douma et al., 1987; Nicolay et al., 1987; Douma et al., 1990). There, peroxisomal proton-translocating ATPases transport protons either into or out of peroxisomes under ATP consumption. Since enrichment and purification of peroxisomes for proteomics is not trivial, peroxisomal fractions are often contaminated with high-abundance proteins of other organelles, such as mitochondria or chloroplasts. Among the proteins detected, were subunits of ATP synthase, such as the β-subunit of the ATP synthase complex (ATP2a), which is one of the most prominent mitochondrial enzymes (Reumann et al., 2007). Also other subunits, *e.g.* ATP1, ATP5, ATP7, or ATP16 were identified (Eubel et al., 2008). However, most of these proteins were regarded as contaminations. Nevertheless, it cannot be ruled out that proton pumps, such as ATPases exist in plant peroxisomes. Mathematical models predict that a small number of pumps is sufficient to acidify compartments, such as secretory or endocytic vesicles (Grabe and Oster, 2001; Dettmer et al., 2006). Hence, it is possible that because low abundance proteins are filtered out of the peroxisomal proteomics data or simply are below detection limit, relevant proton pumping enzymes are simply overlooked (Bussell et al., 2013).

Besides active proton pumping mechanisms, a pH gradient formation can be built-up in an energy-independent manner. One physical mechanism proposed is the Donnan equilibrium, which is predicted to occur at the outer mitochondrial and the lysosomal membrane (Henning, 1975; Moriyama et al., 1992; Porcelli et al., 2005). If the peroxisomal membrane was permeable to small ions, including OH^- and H^+, the solutes could balance the charges of matrix proteins, which are unable to pass the membrane. In case of an overall negative charge inside peroxisomes, protons are attracted, creating an inward-directed proton gradient that leads to an acidic lumen. If the peroxisomal pH was dominated mostly by positive charges on matrix proteins, OH^- molecules would be attracted and a pH gradient could form, resulting in a more alkaline pH inside (Stell and Joslin,

1986). However, it is highly questionable, whether the Donnan equilibrium alone would suffice to regulate peroxisomal pH.

In conclusion, we have shown that a proton gradient exists across the peroxisomal membrane. Ratiometric fluorescence imaging revealed an acidic luminal pH of peroxisomes involved in storage oil mobilization. Biochemical studies and pH imaging analyses revealed that the peroxisomal adenine nucleotide carriers PNC1 and PNC2 are not responsible for an acidification of the peroxisomal lumen in Arabidopsis hypocotyls. From our *in planta* studies we concluded that β-oxidation and glyoxylate cycle, both processes which release acids, do not directly influence the peroxisomal pH.

Supplemental material

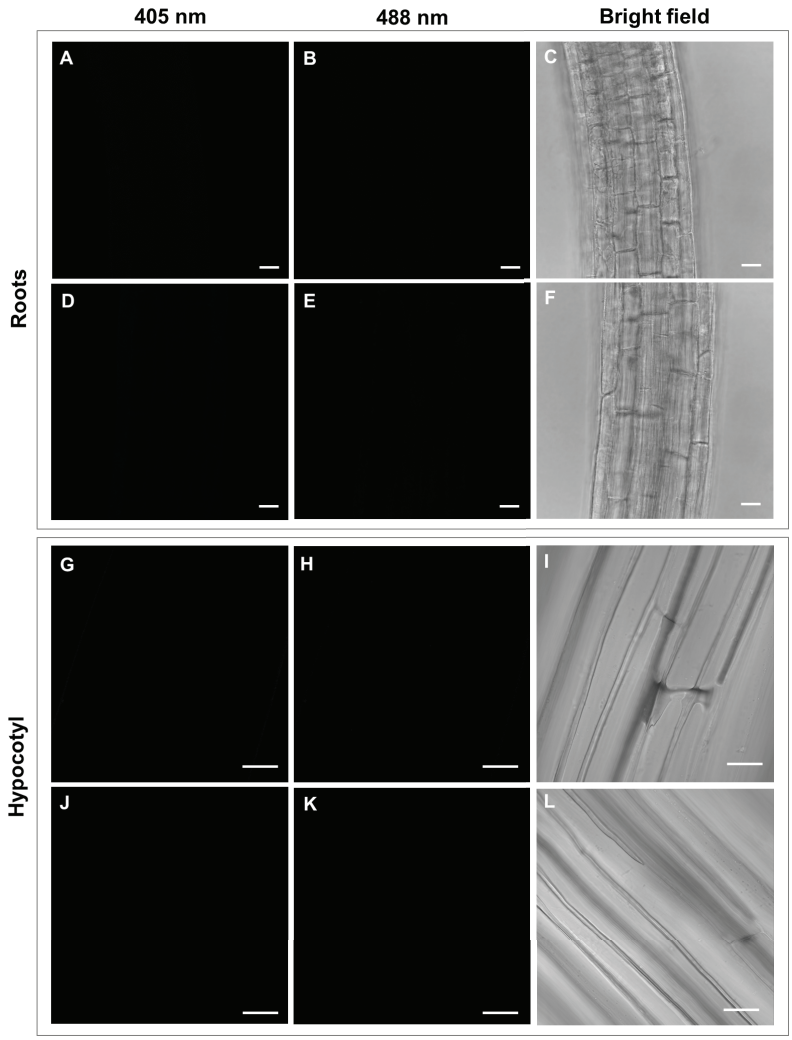

Fig. S1: Autofluorescence in Arabidopsis roots and etiolated hypocotyl.
The chlorophyll autofluorescence of Arabidopsis root (A-F) and hypocotyl tissue (G-L) was measured to optimize both pHGFP (A-C; G-I) and pHGFP-SKL (D-F; J-L) settings for confocal microscopy. The left column shows images taken with an excitation of 405 nm, the middle column shows pictures taken with an excitation of 488 nm. The right column shows the respective bright field images. Bars=20 µm. N = 10.

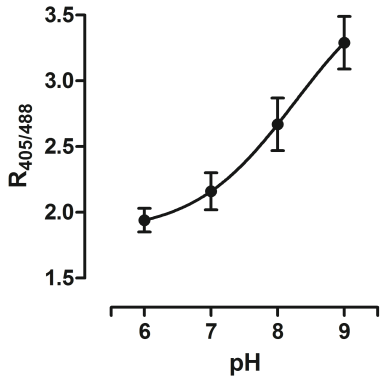

Fig. S2: *In situ* calibration curve with nigericin.
To validate calibrations, ammonium acetate was substituted with nigericin. A calibration curve was recorded for root peroxisomes. Data points are given as means ± SEM. N ≥ 15 per pH step.

Tab. S1: Comparison of root peroxisomal pH using nigericin or ammonium acetate for calibration.
The peroxisomal pH of roots was determined in four independent pHGFP-SKL lines (SKL1-1, SKL1-2, SKL1-3, SKL1-4). Calibration was performed with nigericin instead of ammonium acetate to equalize peroxisomal pH and pH buffer. The table compares the two different calibration methods. Data are means ± SEM of at least three independent experiments. T test of the pHGFP-SKL groups, $P < 0.05$, ns.

		Nigericin	Ammonium acetate
pHGFP-SKL	SKL1-1	8.04 ± 0.07	8.20 ± 0.06
	SKL1-2	8.23 ± 0.25	8.20 ± 0.10
	SKL1-3	8.27 ± 0.18	8.10 ± 0.05
	SKL1-4	8.15 ± 0.23	8.19 ± 0.06

Tab. S2: Peroxisomal and cytosolic pH in Arabidopsis roots and hypocotyls.
The peroxisomal and cytosolic pH values of roots and shoots were determined in four independent pHGFP-SKL lines (SKL1-1, SKL1-2, SKL1-3, SKL1-4) and three pHGFP lines (pHGFP1-1, pHGFP1-2, pHGFP1-3), respectively. Data are the means ± SEM of at least three independent experiments. ANOVA test of the pHGFP groups, $P < 0.05$, ns; ANOVA test of pHGFP-SKL groups, $P < 0.05$, ns.

		Root pH	Hypocotyl pH
pHGFP-SKL	SKL1-1	8.2 ± 0.06	6.3 ± 0.08
	SKL1-2	8.2 ± 0.10	6.3 ± 0.08
	SKL1-3	8.1 ± 0.05	6.3 ± 0.09
	SKL1-4	8.2 ± 0.06	6.4 ± 0.05
pHGFP	Cyt1-1	7.3 ± 0.03	7.3 ± 0.03
	Cyt1-2	7.4 ± 0.10	7.4 ± 0.07
	Cyt1-3	7.3 ± 0.03	7.3 ± 0.03

Acknowledgements

This project was funded by DFG-GRK 1525. We thank Dr. Melinda Frame at Michigan State University, as well as Dr. Stefanie Weidtkamp-Peters at Heinrich-Heine University for their expert assistance with CLSM microscopy. We thank Dr. Kristin Bernhardt, Hendrik Wolff, and Lennart Charton for their help with plant experiments and biochemical assays. We thank Kirsten Abel for technical assistance and Elisabeth Klemp and Katrin L. Weber GC-MS analysis support. We acknowledge Dr. Gaëlle Cassin-Ross for providing *pex14* seeds and Dr. Kyaw Aung for sharing YFP-PTS1 seeds. We thank Alisandra Denton and the reviewers for carefully reading this manuscript and constructive criticism.

References

Arai, Y., Hayashi, M., and Nishimura, M. (2008). Proteomic identification and characterization of a novel peroxisomal adenine nucleotide transporter supplying ATP for fatty acid beta-oxidation in soybean and Arabidopsis. Plant Cell **20,** 3227-3240.

Bernhardt, K., Wilkinson, S., Weber, A.P.M., and Linka, N. (2012). A peroxisomal carrier delivers NAD^+ and contributes to optimal fatty acid degradation during storage oil mobilization. Plant J **69,** 1-13.

Bethmann, B., Simonis, W., and Schönknecht, G. (1998). Light-induced changes of cytosolic pH in *Eremosphaera viridis*: recordings and kinetic analysis. J Exp Bot **49,** 1129-1137.

Bussell, J.D., Behrens, C., Ecke, W., and Eubel, H. (2013). Arabidopsis peroxisome proteomics. Front Plant Sci **4,** doi: 10.3389/fpls.2013.00101.

Dettmer, J., Hong-Hermesdorf, A., Stierhof, Y.-D., and Schumacher, K. (2006). Vacuolar H^+-ATPase Activity is required for endocytic and secretory trafficking in Arabidopsis. Plant Cell **18,** 715-730.

Dietrich, D., Schmuths, H., Lousa Cde, M., Baldwin, J.M., Baldwin, S.A., Baker, A., Theodoulou, F.L., and Holdsworth, M.J. (2009). Mutations in the Arabidopsis peroxisomal ABC transporter COMATOSE allow differentiation between multiple functions in planta: insights from an allelic series. Mol Biol Cell **20,** 530-543.

Douma, A., Veenhuis, M., Sulter, G., and Harder, W. (1987). A proton-translocating adenosine triphosphatase is associated with the peroxisomal membrane of yeasts. Arch Microbiol **147,** 42-47.

Douma, A., Veenhuis, M., Waterham, H., and Harder, W. (1990). Immunocytochemical demonstration of the peroxisomal ATPase of yeasts. Yeast **6,** 45-51.

Estelle, M.A., and Somerville, C. (1987). Auxin-resistant mutants of *Arabidopsis thaliana* with an altered morphology. Mol Gen Genet **206,** 200-206.

Eubel, H., Meyer, E.H., Taylor, N.L., Bussell, J.D., O'Toole, N., Heazlewood, J.L., Castleden, I., Small, I.D., Smith, S.M., and Millar, A.H. (2008). Novel proteins, putative membrane transporters, and an integrated metabolic network are revealed by quantitative proteomic analysis of Arabidopsis cell culture peroxisomes. Plant Physiol **148,** 1809-1829.

Fasano, J.M., Swanson, S.J., Blancaflor, E.B., Dowd, P.E., Kao, T.-h., and Gilroy, S. (2001). Changes in root cap pH are required for the gravity response of the Arabidopsis root. Plant Cell **13,** 907-921.

Gao, D., Knight, M.R., Trewavas, A.J., Sattelmacher, B., and Plieth, C. (2004). Self-reporting Arabidopsis expressing pH and $[Ca^{2+}]$ indicators unveil ion dynamics in the cytoplasm and in the apoplast under abiotic stress. Plant Physiol **134,** 898-908.

Geldner, N., Denervaud-Tendon, V., Hyman, D.L., Mayer, U., Stierhof, Y.D., and Chory, J. (2009). Rapid, combinatorial analysis of membrane compartments in intact plants with a multicolor marker set. Plant J **59,** 169-178.

Gendreau, E., Traas, J., Desnos, T., Grandjean, O., Caboche, M., and Hofte, H. (1997). Cellular basis of hypocotyl growth in *Arabidopsis thaliana*. Plant Physiol **114,** 295-305.

Gjetting, K.S.K., Ytting, C.K., Schulz, A., and Fuglsang, A.T. (2012). Live imaging of intra- and extracellular pH in plants using pHusion, a novel genetically encoded biosensor. J Exp Bot **63,** 3207-3218.

Gould, S.J., Keller, G.A., Hosken, N., Wilkinson, J., and Subramani, S. (1989). A conserved tripeptide sorts proteins to peroxisomes. J Cell Biol **108,** 1657-1664.

Grabe, M., and Oster, G. (2001). Regulation of organelle acidity. J Gen Physiol **117,** 329-344.

Graham, I.A. (2008). Seed storage oil mobilization. Annu Rev Plant Biol **59,** 115-142.

Greenspan, P., Mayer, E.P., and Fowler, S.D. (1985). Nile red: a selective fluorescent stain for intracellular lipid droplets. J Cell Biol **100,** 965-973.

Grefen, C., Donald, N., Hashimoto, K., Kudla, J., Schumacher, K., and Blatt, M.R. (2010). A ubiquitin-10 promoter-based vector set for fluorescent protein tagging facilitates temporal stability and native protein distribution in transient and stable expression studies. Plant J **64,** 355-365.

Guern, J., Felle, H., Mathieu, Y., and Kurkdjian, A. (1991). Regulation of intracellular pH in plant cells. Int Rev Cytol **127,** 1-1.

Hayashi, M., and Nishimura, M. (2003). Entering a new era of research on plant peroxisomes. Curr Opin Plant Biol **6,** 577-582.

Hayashi, M., Toriyama, K., Kondo, M., and Nishimura, M. (1998). 2,4-Dichlorophenoxybutyric acid-resistant mutants of Arabidopsis have defects in glyoxysomal fatty acid beta-oxidation. Plant Cell **10,** 183-195.

Henning, R. (1975). pH gradient across the lysosomal membrane generated by selective cation permeability and Donnan equilibrium. Biochim Biophys Acta **401,** 307-316.

Hu, J., Baker, A., Bartel, B., Linka, N., Mullen, R.T., Reumann, S., and Zolman, B.K. (2012). Plant peroxisomes: biogenesis and function. Plant Cell **24,** 2279-2303.

Kasahara, M., and Hinkle, P.C. (1976). Reconstitution of D-glucose transport catalyzed by a protein fraction from human erythrocytes in sonicated liposomes. Proc Natl Acad Sci U S A **73,** 396-400.

Kopriva, S. (2006). Regulation of sulfate assimilation in Arabidopsis and beyond. Ann Bot **97,** 479-495.

Krebs, M., Held, K., Binder, A., Hashimoto, K., Den Herder, G., Parniske, M., Kudla, J., and Schumacher, K. (2012). FRET-based genetically encoded sensors allow high-resolution live cell imaging of $Ca^{(2+)}$ dynamics. Plant J **69,** 181-192.

Lasorsa, F.M., Scarcia, P., Erdmann, R., Palmieri, F., Rottensteiner, H., and Palmieri, L. (2004). The yeast peroxisomal adenine nucleotide transporter: characterization of two transport modes and involvement in DeltapH formation across peroxisomal membranes. Biochem J **381,** 581-585.

Linka, N., and Esser, C. (2012). Transport proteins regulate the flux of metabolites and cofactors across the membrane of plant peroxisomes. Front Plant Sci **3,** doi: 10.3389/fpls.2012.00003.

Linka, N., Theodoulou, F.L., Haslam, R.P., Linka, M., Napier, J.A., Neuhaus, H.E., and Weber, A.P. (2008). Peroxisomal ATP import is essential for seedling development in *Arabidopsis thaliana*. Plant Cell **20,** 3241-3257.

Mano, S., Nakamori, C., Hayashi, M., Kato, A., Kondo, M., and Nishimura, M. (2002). Distribution and characterization of peroxisomes in Arabidopsis by Visualization with GFP: Dynamic morphology and actin-dependent movement. Plant Cell Physiol **43,** 331-341.

Martinoia, E., Maeshima, M., and Neuhaus, H.E. (2007). Vacuolar transporters and their essential role in plant metabolism. J Exp Bot **58,** 83-102.

Miesenbock, G., De Angelis, D.A., and Rothman, J.E. (1998). Visualizing secretion and synaptic transmission with pH-sensitive green fluorescent proteins. Nature **394,** 192-195.

Moriyama, Y., Maeda, M., and Futai, M. (1992). Involvement of a non-proton pump factor (possibly Donnan-type equilibrium) in maintenance of an acidic pH in lysosomes. FEBS Lett **302,** 18-20.

Moseyko, N., and Feldman, L.J. (2001). Expression of pH-sensitive green fluorescent protein in *Arabidopsis thaliana*. Plant Cell Environ **24,** 557-563.

Nagel, K.A., Schurr, U., and Walter, A. (2006). Dynamics of root growth stimulation in *Nicotiana tabacum* in increasing light intensity. Plant Cell Environ **29,** 1936-1945.

Nicolay, K., Veenhuis, M., Douma, A.C., and Harder, W. (1987). A ^{31}P NMR study of the internal pH of yeast peroxisomes. Arch Microbiol **147,** 37-41.

Nishimura, M., Hayashi, M., Kato, A., Yamaguchi, K., and Mano, S. (1996). Functional transformation of microbodies in higher plant cells. Cell Struct Funct **21,** 387-393.

Norris, S.R., Meyer, S.E., and Callis, J. (1993). The intron of *Arabidopsis thaliana* polyubiquitin genes is conserved in location and is a quantitative determinant of chimeric gene expression. Plant Mol Biol **21,** 895-906.

Nozawa, A., Nanamiya, H., Miyata, T., Linka, N., Endo, Y., Weber, A.P.M., and Tozawa, Y. (2007). A cell-free translation and proteoliposome reconstitution system for functional analysis of plant solute transporters. Plant Cell Phys **48,** 1815-1820.

Orij, R., Postmus, J., Ter Beek, A., Brul, S., and Smits, G.J. (2009). *In vivo* measurement of cytosolic and mitochondrial pH using a pH-sensitive GFP derivative in *Saccharomyces cerevisiae* reveals a relation between intracellular pH and growth. Microbiology **155,** 268-278.

Orth, T., Reumann, S., Zhang, X., Fan, J., Wenzel, D., Quan, S., and Hu, J. (2007). The PEROXIN11 protein family controls peroxisome proliferation in Arabidopsis. Plant Cell **19,** 333-350.

Overly, C.C., Lee, K.D., Berthiaume, E., and Hollenbeck, P.J. (1995). Quantitative measurement of intraorganelle pH in the endosomal-lysosomal pathway in neurons by using ratiometric imaging with pyranine. Proc Natl Acad Sci U S A **92,** 3156-3160.

Porcelli, A.M., Ghelli, A., Zanna, C., Pinton, P., Rizzuto, R., and Rugolo, M. (2005). pH difference across the outer mitochondrial membrane measured with a green fluorescent protein mutant. Mol Cell Biol Res Commun **326,** 799-804.

Pracharoenwattana, I., and Smith, S.M. (2008). When is a peroxisome not a peroxisome? Trends Plant Sci **13,** 522-525.

Quettier, A.L., and Eastmond, P.J. (2009). Storage oil hydrolysis during early seedling growth. Plant Physiol Biochem **47,** 485-490.

Reumann, S., and Weber, A.P. (2006). Plant peroxisomes respire in the light: some gaps of the photorespiratory C2 cycle have become filled- others remain. Biochim Biophys Acta **1763,** 1496-1510.

Reumann, S., Babujee, L., Ma, C., Wienkoop, S., Siemsen, T., Antonicelli, G.E., Rasche, N., Luder, F., Weckwerth, W., and Jahn, O. (2007). Proteome analysis of Arabidopsis leaf peroxisomes reveals novel targeting peptides, metabolic pathways, and defense mechanisms. Plant Cell **19,** 3170-3193.

Roberts, J.K., Ray, P.M., Wade-Jardetzky, N., and Jardetzky, O. (1980). Estimation of cytoplasmic and vacuolar pH in higher plant cells by ^{31}P NMR. Nature **283**, 870-872.

Rook, F., Corke, F., Card, R., Munz, G., Smith, C., and Bevan, M.W. (2001). Impaired sucrose−induction mutants reveal the modulation of sugar−induced starch biosynthetic gene expression by abscisic acid signalling. Plant J **26,** 421-433.

Roslan, H.A., Salter, M.G., Wood, C.D., White, M.R., Croft, K.P., Robson, F., Coupland, G., Doonan, J., Laufs, P., and Tomsett, A.B. (2001). Characterization of the ethanol−inducible alc gene−expression system in *Arabidopsis thaliana*. Plant J **28,** 225-235.

Rottensteiner, H., and Theodoulou, F.L. (2006). The ins and outs of peroxisomes: co-ordination of membrane transport and peroxisomal metabolism. Biochim Biophys Acta **1763,** 1527-1540.

Sambrook, J., Russell, D.W., and Russell, D.W. (1989). Molecular cloning: a laboratory manual, 3rd edn. (Cold Spring Harbor Laboratory Press).

Schulte, A., Lorenzen, I., Böttcher, M., and Plieth, C. (2006). A novel fluorescent pH probe for expression in plants. Plant Methods **2,** doi:10.1186/1746-4811-2-7.

Scott, A.C., and Allen, N.S. (1999). Changes in cytosolic pH within Arabidopsis root columella cells play a key role in the early signaling pathway for root gravitropism. Plant Physiol **121,** 1291-1298.

Sheen, J., Zhou, L., and Jang, J.-C. (1999). Sugars as signaling molecules. Curr Opin Plant Biol **2,** 410-418.

Shen, J., Zeng, Y., Zhuang, X., Sun, L., Yao, X., Pimpl, P., and Jiang, L. (2013). Organelle pH in the Arabidopsis endomembrane system. Mol Plant **6,** 1419-1437.

Zolman, B.K., Yoder, A., and Bartel, B. (2000). Genetic analysis of indole-3-butyric acid responses in *Arabidopsis thaliana* reveals four mutant classes. Genetics **156,** 1323-1337.

Zolman, B.K., Silva, I.D., and Bartel, B. (2001). The Arabidopsis *pxa1* mutant is defective in an ATP-binding cassette transporter-like protein required for peroxisomal fatty acid beta-oxidation. Plant Physiol **127,** 1266-1278.

Contribution of the authors to manuscript 3

S.K.-V. wrote the manuscript, performed all pH measurements and established the double mutant *pnc1/2*. **L.C.** performed protein expression studies, *in vitro* uptake experiments with recombinant protein and liposome floating experiments. **H.W.** performed parts of the physiological characterization of *pnc1/2*, including the 2,4-DB screen and Nile Red staining. **M.K.** and **K.S.** established the pH measurement setup. **N.L.**, **A.P.M.W.** and **J.H** assisted in drafting this manuscript. **N.L.** designed the research.

Outlook

Impact of β-oxidation on peroxisomal pH

We showed that β-oxidation, at least on the level of ATP import, does not affect peroxisomal pH. To make a general statement about the involvement of β-oxidation on peroxisomal pH, we crossed the pH-sensitive GFP sensors into an Arabidopsis line, which lacks the peroxisomal, a core enzyme of β-oxidation (*kat2*) (Germain et al., 2001; Footitt et al., 2007). We will investigate the peroxisomal pH in the *kat2* sensor line and compare it to the data previously obtained for *pnc1/2*.

Proton-pumping enzymes in peroxisomes

Although proteomic studies did not reveal any evidence for peroxisomal ATPases (Reumann et al., 2007; Eubel et al., 2008), we planned to investigate the existence of proton-pumping enzymes in peroxisomes. We will perform pH measurements in the presence of the ATPase inhibitors concanamycin A and *ortho*-vanadate in Arabidopsis lines expressing pHGFP-SKL (Dröse and Altendorf, 1997). Concanamycin A specifically inhibits vacuolar-type H(+)-ATPases, whereas vanadate inhibits P-type ATPases (Dröse and Altendorf, 1997; Axelsen and Palmgren, 2001; Huss and Wieczorek, 2009). We expect the peroxisomal pH to increase in the presence of vanadate or concanamycin, when ATPases are present and inhibited.

Discovering components of the pH-regulating system in Arabidopsis

The existence of a proton gradient across the peroxisomal membrane was established in our study and the work of Shen et al., 2013. To decipher which factors maintain this gradient, we plan to establish an ethyl methanesulfonate (EMS) mutagenesis population in Arabidopsis (Kim et al., 2006), which we screen for changes in peroxisomal pH in a large-scale experiment. As pH measurements can now be performed with a photometer (Dr. M. Krebs, pers. communication), we will cultivate Arabidopsis EMS mutants and screen them photometrically in 96-well plates. We will isolate those lines having an altered peroxisomal pH compared to wildtype. Following, we will map the locus involved in peroxisomal pH maintenance in the mutant population. In parallel, metabolite profiles of mutants could be analyzed.

As EMS mutagenesis is laborious, it could be considered to confirm the peroxisomal pH data, applying a second independent biosensor approach. Recently, a sensor named pHusion was developed, which is a ratiometric pH sensor and applies tandem fusion of GFP and mRFP (Gjetting et al., 2012). While GFP fluorescence is pH sensitive, the fluorescence of mRFP is not. Highest fluorescence of GFP can be observed at pH 7-8, whereas it gradually decreases at lower pH (pH 5-6). Especially at more acidic pH, as observed in hypocotyl peroxisomes, the tandem sensor it useful, because fluorescence of GFP and mRFP (internal control) can be compared to determine changes in intracellular pH. Due to constant mRFP fluorescence, pure quenching artifacts can be estimated. Secondly, the pKa of pHusion is low (pH 6), thus the sensor is well suited for acidic compartments (Gjetting et al., 2012).

References

Avnir, Y., and Barenholz, Y. (2005). pH determination by pyranine: medium-related artifacts and their correction. An Biochem **347,** 34-41.

Axelsen, K.B., and Palmgren, M.G. (2001). Inventory of the superfamily of P-type ion pumps in Arabidopsis. Plant Physiol **126,** 696-706.

Dröse, S., and Altendorf, K. (1997). Bafilomycins and concanamycins as inhibitors of V-ATPases and P-ATPases. J Exp Biol **200,** 1-8.

Eubel, H., Meyer, E.H., Taylor, N.L., Bussell, J.D., O'Toole, N., Heazlewood, J.L., Castleden, I., Small, I.D., Smith, S.M., and Millar, A.H. (2008). Novel proteins, putative membrane transporters, and an integrated metabolic network are revealed by quantitative proteomic analysis of Arabidopsis cell culture peroxisomes. Plant Physiol **148,** 1809-1829.

Footitt, S., Cornah, J.E., Pracharoenwattana, I., Bryce, J.H., and Smith, S.M. (2007). The Arabidopsis 3-ketoacyl-CoA thiolase-2 (*kat2-1*) mutant exhibits increased flowering but reduced reproductive success. J Exp Bot **58,** 2959-2968.

Germain, V., Rylott, E.L., Larson, T.R., Sherson, S.M., Bechtold, N., Carde, J.P., Bryce, J.H., Graham, I.A., and Smith, S.M. (2001). Requirement for 3-ketoacyl-CoA thiolase-2 in peroxisome development, fatty acid beta-oxidation and breakdown of triacylglycerol in lipid bodies of Arabidopsis seedlings. Plant J **28,** 1-12.

Gjetting, K.S.K., Ytting, C.K., Schulz, A., and Fuglsang, A.T. (2012). Live imaging of intra- and extracellular pH in plants using pHusion, a novel genetically encoded biosensor. J Exp Bot **63,** 3207-3218.

Huss, M., and Wieczorek, H. (2009). Inhibitors of V-ATPases: old and new players. J Exp Bot **212,** 341-346.

Kano, K., and Fendler, J.H. (1978). Pyranine as a sensitive pH probe for liposome interiors and surfaces. pH gradients across phospholipid vesicles. BBA Biomembranes **509,** 289-299.

Kim, Y., Schumaker, K.S., and Zhu, J.-K. (2006). EMS mutagenesis of Arabidopsis. In Arabidopsis Protocols (Springer), pp. 101-103.

Reumann, S., Babujee, L., Ma, C., Wienkoop, S., Siemsen, T., Antonicelli, G.E., Rasche, N., Luder, F., Weckwerth, W., and Jahn, O. (2007). Proteome analysis of Arabidopsis leaf peroxisomes reveals novel targeting peptides, metabolic pathways, and defense mechanisms. Plant Cell **19,** 3170-3193.

VI. ADDENDUM

Additional experiments

The *Addendum* contains experiments that were not presented previously. First, a study on the influence of ATPases on peroxisomal pH is presented (VI.1), which was conducted as follow-up experiment on the study of peroxisomal pH presented in *Manuscript 3*. As we found out that the peroxisomal pH is most likely neither depended on the peroxisomal adenine nucleotide carriers PNC1 and PNC2, nor on β-oxidation activity, we followed the hypothesis that proton-pumping enzymes, such as ATPases might be involved in peroxisomal pH maintenance. Secondly, an experiment is presented that examines the morphology of peroxisomes in *pnc1/2* (VI.2). We compared the shape of peroxisomes in *pnc1/2* that of the peroxisomal NAD carrier PXN, which is known to exhibit peroxisome morphology defects. These abnormalities are presumably caused by an accumulation of intermediates due to defective fatty acid degradation (Mano et al., 2012).

VI.1 On the impact of V-type and P-type ATPases on peroxisomal pH

Introduction

Compartmentation enables the simultaneous action of biochemical pathways in different reaction spaces. This necessitates the exchange of substrates by membrane transporters. A differential pH between compartments is a crucial parameter enabling secondary active transport (Axelsen and Palmgren, 2001). Compartments are acidified by vacuolar-type H^+-ATPases (V-ATPases) or by P-type ATPases (Schumacher, 2006). P-ATPases are named P-type, as they form a phosphorylated intermediate (Axelsen and Palmgren, 2001). V-ATPases are specifically inhibited by micromolar concentrations of concanamycin A, a macrolide antibiotic. P-ATPases are sensitive to *ortho*-vanadate, whereas V-ATPases are not (Dröse and Altendorf, 1997).

Although we and Shen et al., 2013 demonstrated that a proton ion gradient exists between cytosol and peroxisomes in *Arabidopsis*, the components responsible for peroxisomal pH maintenance remain unknown. Proteomic studies detected several subunits of ATP synthase (AtMg01190), such as the β subunit of the ATP synthase complex (ATP2a), or ATP1, ATP5, ATP7, and ATP16. However, these hits were regarded as contaminations (Reumann et al., 2007; Eubel et al., 2008). As modeling predicts that a very small number of pumps suffice to acidify compartments, it is likely that ATPases exist in plant peroxisomes (Grabe and Oster, 2001; Dettmer et al., 2006). To this end, organelle proteomics possibly did not detect peroxisomal ATPases as concentrations were below detection limit.

We measured the peroxisomal pH in *Arabidopsis* hypocotyl in the presence of either concanamycin A, vanadate, or without treatment, to discover if pH changes upon treatment.

We hypothesized that the peroxisomal pH would approximate to the cytosolic pH when ATPases are effectively inhibited.

Experimental procedures

Plant material and growth conditions

The establishment of *Arabidopsis* wildtype plants stably transformed with pHGFP-SKL is described in *Manuscript 3*. Etiolated seedlings were grown on 0.5x MS in the presence of 1% (w/v) sucrose (pH 5.8), solidified with 0.45% (w/v) phyto agar for 5 d at 22°C in constant darkness, covering the plates with aluminum foil. A 12 h light pulse was given to induce germination.

Confocal laser scanning microscopy

The pH of peroxisomes was examined with a Fluoview 1000 Confocal Laser Scanning Microscope (Olympus). The microscope was equipped with a 63x/1.2 W Korr UPLSAPO objective. The GFP sensor was sequentially excited at 405 nm (10%) and 488 nm (20%). The emitted light was detected at 500 nm to 520 nm. In addition a bright field image was taken. The detection pinhole size was set to 152 µm in all experiments.

In situ calibration and intracellular pH measurements

Calibration and calculation of pH was performed as presented in *Manuscript 3*.

ATPase inhibition assay and pH imaging

Etiolated seedlings were grown as described above. Plant material was incubated in liquid 0.5x MS, 1% (w/v) sucrose (pH 5.8) supplemented with (i) 1 µM Concanamycin A dissolved in DMSO (stock 1 mM), (ii) 500 µM Vanadate dissolved in water (stock 5 mM) (Gordon, 1991), or (iii) 0.1% DMSO (v/v, neg. control) over night. The pH of the inhibitor stocks was adjusted to pH 7. Imaging of the peroxisomal pH was performed as presented in *Manuscript 3*.

Results

Vanadate, not Concanamycin A influences the peroxisomal pH

To examine whether peroxisomes contain an ATPase-type proton pump, we performed pH studies in the presence of specific ATPase inhibitors, which allowed distinguishing between V-type and P-type ATPases. To accurately determine the peroxisomal pH, we performed an *in situ* sensor calibration first (Fig. 1A). The pH-sensitive GFP was sequentially excited at 405 nm and 488 nm. Fluorescence emission was detected at 500 nm to 520 nm. Ratio values ($R_{405/488}$) of calculated and plotted against the calibration buffer pH.

The measurements of the peroxisomal pH revealed that the pH was not altered in the presence of DMSO as negative control. As reported previously, an acidic peroxisomal pH of 6.1 ± 0.01 was measured in *Arabidopsis* hypocotyls. When treated with the V-ATPase inhibitor concanamycin A, the pH of peroxisomes increased slightly to 6.15 ± 0.01. In the presence of vanadate, the

peroxisomal pH increased to almost wild-type level (pH 7.3, *Manuscript 3*). The peroxisomal pH was 7.22 ± 0.02 in these samples.

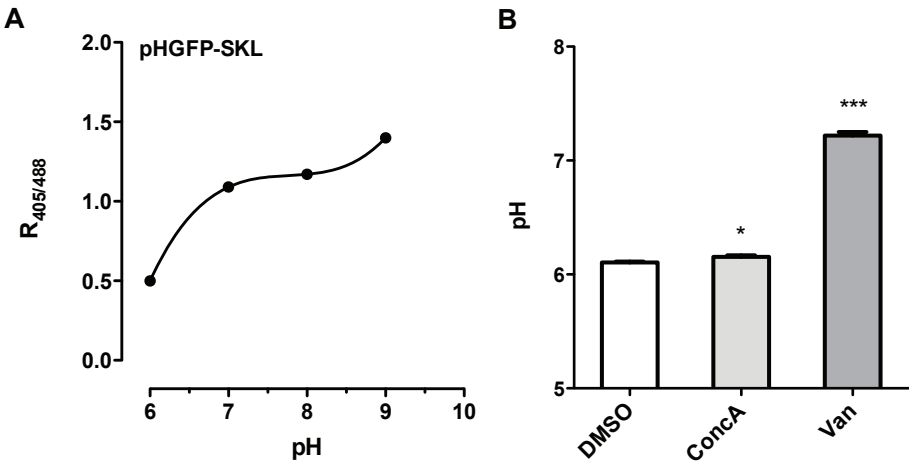

Fig. 1: Determination of the peroxisomal pH in the presence of Concanamycin A and Vanadate.
A: *In situ* calibration curve were recorded shoots of *Arabidopsis* seedlings expressing the peroxisomal GFP sensor pHGFP-SKL. Data points are given as means ± SEM. N ≥ 15 per pH step. B: Measurement of the peroxisomal pH in one pHGFP-SKL *Arabidopsis* line. For pH analysis plants were grown on ½ MS supplemented with sucrose for 5 d in constant darkness. Plants were either treated with DMSO (white) as negative control, concanamycin A (grey), or vanadate (dark grey) over night. Values are given as mean pH values. Error bars represent SEMs. **P* = 0.0112, ****P* < 0.0001.

Based on our inhibitor studies, we conclude that the peroxisomal pH might be maintained by P-type ATPase activity in peroxisomal membrane.

Discussion and Outlook

Our experiments revealed an effect of vanadate on the peroxisomal pH, leading to the assumption that a P-type ATPase regulates peroxisomal pH, as vanadate specifically inhibits these proton pumps. However, we cannot exclude that the increase in peroxisomal pH we observed is a secondary effect, because the impact of vanadate on pH is more complex.

For example, vanadate is also known to inhibit serine/threonine kinases in animals (Morioka et al., 1998). Although some kinases are present in peroxisomes, serine/threonine kinases have not been discovered in *Arabidopsis* peroxisomes (Dammann et al., 2003; Fukao et al., 2003; Reumann et al., 2004; Reumann et al., 2007; Reumann et al., 2009). Furthermore, vanadate is known to impact extraperoxisomal malate synthesis in *Elodea densa* (Beffagna et al., 1993). Peroxisomes contain malate, which is associated with the peroxisomal isoform of malate dehydrogenase and is involved in the peroxisomal malate/oxaloacetate redox shuttle (Reumann and Weber, 2006). In case of vanadate-inhibited malate synthesis, the peroxisomal malate levels might be reduced and thus affect pH inside peroxisomes. To investigate the impact of malate levels on peroxisomal pH, it would be required to determine the peroxisomal pH in *Arabidopsis* mutants, lacking malate synthase (At5g03860) (Cornah et al., 2004). The peroxisomal pH can then be investigated in the absence of presence of vanadate.

To identify factors or components involved in peroxisomal pH homeostasis, an ethyl methanesulfonate (EMS) mutagenesis population of transgenic *Arabidopsis* expressing a peroxisome-targeted pH-sensitive GFP can be performed (Kim et al., 2006). Large-scale pH measurements can be perfomed with a 96-well format compatible fluorimeter (Dr. M. Krebs, pers. communication). *Arabidopsis* mutants exhibiting an altered peroxisomal pH will be isolated and affected gene loci will be mapped.

References

Axelsen, K.B., and Palmgren, M.G. (2001). Inventory of the superfamily of P-type ion pumps in Arabidopsis. Plant Physiol **126,** 696-706.

Beffagna, N., Romani, G., and Lovadina, S. (1993). Inhibition of malate synthesis by vanadate: Implications for the cytosolic alkalinization induced by vanadate concentrations partially inhibiting the plasmalemma H^+ pump. J Exp Bot **44,** 1535-1542.

Cornah, J.E., Germain, V., Ward, J.L., Beale, M.H., and Smith, S.M. (2004). Lipid utilization, gluconeogenesis, and seedling growth in Arabidopsis mutants lacking the glyoxylate cycle enzyme malate synthase. J Biol Chem **279,** 42916-42923.

Dammann, C., Ichida, A., Hong, B., Romanowsky, S.M., Hrabak, E.M., Harmon, A.C., Pickard, B.G., and Harper, J.F. (2003). Subcellular targeting of nine calcium-dependent protein kinase isoforms from Arabidopsis. Plant Physiol **132,** 1840-1848.

Dettmer, J., Hong-Hermesdorf, A., Stierhof, Y.-D., and Schumacher, K. (2006). Vacuolar H+-ATPase Activity is required for endocytic and secretory trafficking in Arabidopsis. Plant Cell **18,** 715-730.

Dröse, S., and Altendorf, K. (1997). Bafilomycins and concanamycins as inhibitors of V-ATPases and P-ATPases. J Exp Biol **200,** 1-8.

Eubel, H., Meyer, E.H., Taylor, N.L., Bussell, J.D., O'Toole, N., Heazlewood, J.L., Castleden, I., Small, I.D., Smith, S.M., and Millar, A.H. (2008). Novel proteins, putative membrane transporters, and an integrated metabolic network are revealed by quantitative proteomic analysis of Arabidopsis cell culture peroxisomes. Plant Physiol **148,** 1809-1829.

Fukao, Y., Hayashi, M., Hara-Nishimura, I., and Nishimura, M. (2003). Novel glyoxysomal protein kinase, GPK1, identified by proteomic analysis of glyoxysomes in etiolated cotyledons of *Arabidopsis thaliana*. Plant Cell Physiol **44,** 1002-1012.

Gordon, J.A. (1991). Use of vanadate as protein-phosphotyrosine phosphatase inhibitor. Methods in enzymology **201,** 477-482.

Grabe, M., and Oster, G. (2001). Regulation of Organelle Acidity. J Gen Physiol **117,** 329-344.

Kim, Y., Schumaker, K.S., and Zhu, J.-K. (2006). EMS mutagenesis of Arabidopsis. Methods Mol Biol **323,** 101-103.

Morioka, M., Fukunaga, K., Kawano, T., Hasegawa, S., Korematsu, K., Kai, Y., Hamada, J.-i., Miyamoto, E., and Ushio, Y. (1998). Serine/threonine phosphatase activity of calcineurin is inhibited by sodium orthovanadate and dithiothreitol reverses the inhibitory effect. Biochem Biophys Res Commun **253,** 342-345.

Reumann, S., and Weber, A.P. (2006). Plant peroxisomes respire in the light: some gaps of the photorespiratory C2 cycle have become filled- others remain. Biochim Biophys Acta **1763,** 1496-1510.

Reumann, S., Ma, C., Lemke, S., and Babujee, L. (2004). AraPerox. A database of putative Arabidopsis proteins from plant peroxisomes. Plant Physiol **136,** 2587-2608.

Reumann, S., Babujee, L., Ma, C., Wienkoop, S., Siemsen, T., Antonicelli, G.E., Rasche, N., Luder, F., Weckwerth, W., and Jahn, O. (2007). Proteome analysis of Arabidopsis leaf peroxisomes reveals novel targeting peptides, metabolic pathways, and defense mechanisms. Plant Cell **19,** 3170-3193.

Reumann, S., Quan, S., Aung, K., Yang, P.F., Manandhar-Shrestha, K., Holbrook, D., Linka, N., Switzenberg, R., Wilkerson, C.G., Weber, A.P.M., Olsen, L.J., and Hu, J.P. (2009). In-depth proteome analysis of Arabidopsis leaf peroxisomes combined with *in vivo* subcellular targeting verification indicates novel metabolic and regulatory functions of peroxisomes. Plant Physiol **150,** 125-143.

Schumacher, K. (2006). Endomembrane proton pumps: connecting membrane and vesicle transport. Curr Opin Plant Biol **9,** 595-600.

Shen, J., Zeng, Y., Zhuang, X., Sun, L., Yao, X., Pimpl, P., and Jiang, L. (2013). Organelle pH in the Arabidopsis endomembrane system. Mol Plant **6,** 1419-1437.

VI.2 Peroxisomes are elongated in *pnc1/2* mutants

Introduction

Defects in single enzymes of fatty acid oxidation can lead to aberrant peroxisome morphologies (Funato et al., 2006; Mano et al., 2011). It was shown that a mutation in acyl-CoA oxidase (ACX), a core enzyme of peroxisomal β-oxidation, causes a reduced number and enlargement of peroxisomes in human fibroblasts (Funato et al., 2006). A comparable study was conducted in plants, examining the morphology of peroxisomes in a peroxisomal NAD/CoA carrier loss-of-function mutant (*pxn*). There, also a reduced number and enlargement of peroxisomes was observed (Mano et al., 2011). Abnormal peroxisome morphologies in plants were also observed for other β-oxidation mutants, namely the *kat* mutant, which is deficient in 3-ketoacyl-CoA thiolase activities (Germain et al., 2001; Hayashi et al., 2001; Hayashi et al., 2002) and the *mfp2* mutant, lacking the multifunctional protein (Rylott et al., 2006). It was suggested that accumulating intermediates of β-oxidation influence peroxisome size and abundance (Mano et al., 2011). However, a direct connection of peroxisomal metabolism with morphology and abundance of these organelles was not shown.

Hence, we examined the morphology of peroxisomes in *pnc1/2* mutants (*Manuscript 3*). The peroxisomal adenine nucleotide carriers PNC1 and PNC2 are essential for β-oxidation, supplying ATP for the activation of fatty acids, which is a prerequisite to subsequent degradation (Linka et al., 2008). Double mutants devoid of PNCs were crossed into a marker line expressing YFP with a C-terminal SKL tripeptide, which enables fluorescence tagging of peroxisomes (Fan et al., 2005). As positive control we included the *pxn1* mutant (Bernhardt et al., 2012) crossed to the YFP-PTS1 marker line described above.

Experimental procedures

Plant material and growth conditions

To obtain mutants expressing the peroxisomal fluorescence marker, homozygous *pnc1/2* and *pxn1* mutants were crossed to Arabidopsis lines, which stably express a Type 1 Peroxisomal Targeting Signal (PTS1), which was C-terminally fused to a yellow fluorescent protein (YFP) (Fan et al., 2005). The three amino acids serine (S), lysine (K), and leucine (L) direct the YFP to peroxisomes (Gould et al., 1989). Mutants were selected on kanamycin (*pnc2*, YFP-PTS1), glufosinate (*pnc1*), sulfadiazine (*pxn1*) and according to respective fluorescence intensities.

Seeds were surface-sterilized and stratified for 2 d at 4°C. Seedlings were grown on 0.5x MS in the presence of 1% (w/v) sucrose (pH 5.8), solidified with 0.45% (w/v) phyto agar for 5 d at 22°C, 70% humidity under constant illumination (100 µmol m^{-2} s^{-1}, plates were covered with one layer of mesh). When seedlings exhibited first true leaves, they were transferred to soil. Plants were cultivated under long-day conditions (8h-light/16h-dark regime, 100 µmol m^{-2} s^{-1}, day temperature 22°C, night temperature 20°C).

Confocal laser scanning microscopy

Adult plants of lines expressing the fluorescent organelle marker were observed in confocal laser scanning microscopy. YFP was excited with a 514-nm laser line; chlorophyll was excited with 633-nm lasers. For emission detection a 530-nm to 600-nm band pass was chosen for YFP. Fluorescence signal for chlorophyll was detected using a 650-nm long pass filter.

Results

Peroxisome morphologies in mature *pnc1/2* Arabidopsis plants were examined in confocal laser scanning microscopy (Fig. 1). We found that compared to *pxn* mutants, which were examined as positive control, peroxisomes were not enlarged in *pnc1/2* lines. We observed that as expected from experiments of Mano et al., 2011, *pxn* plants exhibited peroxisomes three to four times larger than wildtype. When comparing the shape of *pnc1/2* organelles to peroxisomes of the wildtype, we observed that peroxisomes were frequently elongated in mesophyll cells (Fig. 1).

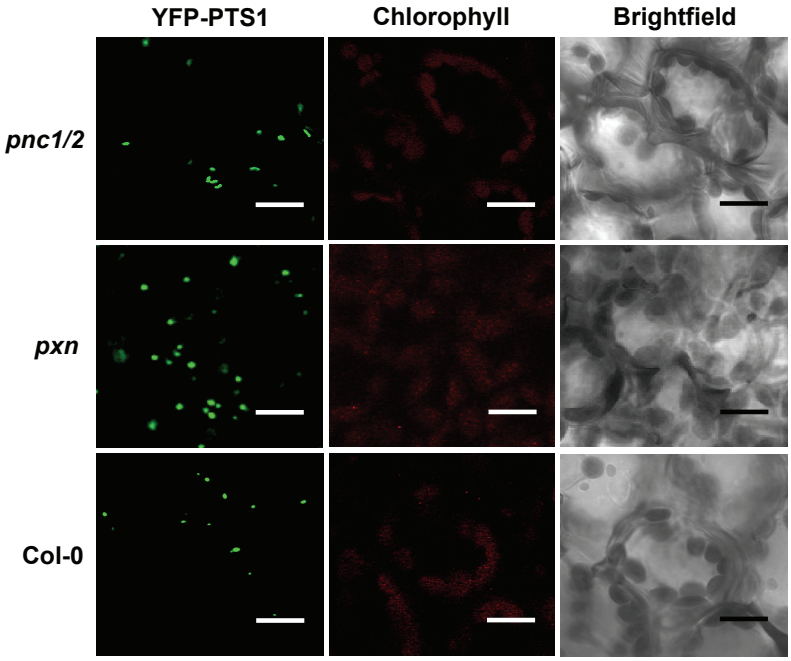

Fig. 1: Peroxisomes are slightly elongated in leaves of the *pnc1/2* mutant.
Peroxisome morphology was observed in adult *pnc1/2* mutants, expressing a stable peroxisomal marker line (YFP-PTS1, upper panel) and the respective wildtype Col-0 (lower panel). A mutant of the peroxisomal NAD/CoA carrier *pxn* expressing YFP-PTS1 was included, as this mutant is known to have aberrant peroxisome morphology. To verify intactness of plant material chlorophyll autofluorescence (middle) and brightfield images (right) were taken. Scale bars = 10 µM.

Discussion and Outlook

Our experiments revealed that a defect in peroxisomal ATP import does not cause enlarged, but elongated peroxisomes in Arabidopsis. At first this seems counterintuitive, as one would expect that fatty acids, which cannot be degraded because they are not activated due to a lack of PNC1 and PNC2, accumulate and hence would cause an enlargement of peroxisomes, as observed for *pxn*, *kat* and and *mfp* mutants (Germain et al., 2001; Hayashi et al., 2001; Hayashi et al., 2002; Rylott et al., 2006; Mano et al., 2011). However, we assume that in *pnc* mutants peroxisomes are elongated,

because peroxisome fission is defective. Elongated peroxisomes were observed in Arabidopsis *pdd2* mutants defective in one allele of the Dynamin-Related Protein 3 (DRP3A) (Aung and Hu, 2009). DRP3A is a dynamin-related GTPase shared by the fission machineries of Arabidopsis peroxisomes and mitochondria (Fujimoto et al., 2009). Already Linka et al., 2008 suggests that PNC1 and PNC2 might exhibit other functions in peroxisomes in addition to storage oil mobilization. Hence, we assume that PNC proteins might supply energy for the fission of peroxisomes. Additional experiments need to be performed to unravel the putative role of PNC1 and PNC2 in the multiplication of peroxisomes.

References

Aung, K., and Hu, J. (2009). The Arabidopsis peroxisome division mutant *pdd2* is defective in the DYNAMIN-RELATED PROTEIN3A (DRP3A) gene. Plant Signal Behav **4,** 542-544.

Bernhardt, K., Wilkinson, S., Weber, A.P.M., and Linka, N. (2012). A peroxisomal carrier delivers NAD($^+$) and contributes to optimal fatty acid degradation during storage oil mobilization. Plant J **69,** 1-13.

Fan, J., Quan, S., Orth, T., Awai, C., Chory, J., and Hu, J. (2005). The Arabidopsis PEX12 gene is required for peroxisome biogenesis and is essential for development. Plant Physiol **139,** 231-239.

Fujimoto, M., Arimura, S., Mano, S., Kondo, M., Saito, C., Ueda, T., Nakazono, M., Nakano, A., Nishimura, M., and Tsutsumi, N. (2009). Arabidopsis dynamin-related proteins DRP3A and DRP3B are functionally redundant in mitochondrial fission, but have distinct roles in peroxisomal fission. Plant J **58,** 388-400.

Funato, M., Shimozawa, N., Nagase, T., Takemoto, Y., Suzuki, Y., Imamura, Y., Matsumoto, T., Tsukamoto, T., Kojidani, T., and Osumi, T. (2006). Aberrant peroxisome morphology in peroxisomal beta-oxidation enzyme deficiencies. Brain Dev **28,** 287-292.

Germain, V., Rylott, E.L., Larson, T.R., Sherson, S.M., Bechtold, N., Carde, J.P., Bryce, J.H., Graham, I.A., and Smith, S.M. (2001). Requirement for 3-ketoacyl-CoA thiolase-2 in peroxisome development, fatty acid beta-oxidation and breakdown of triacylglycerol in lipid bodies of Arabidopsis seedlings. Plant J **28,** 1-12.

Gould, S.J., Keller, G.A., Hosken, N., Wilkinson, J., and Subramani, S. (1989). A conserved tripeptide sorts proteins to peroxisomes. J Cell Biol **108,** 1657-1664.

Hayashi, M., Nito, K., Takei-Hoshi, R., Yagi, M., Kondo, M., Suenaga, A., Yamaya, T., and Nishimura, M. (2002). Ped3p is a peroxisomal ATP-binding cassette transporter that might supply substrates for fatty acid beta-oxidation. Plant Cell Physiol **43,** 1-11.

Hayashi, Y., Hayashi, M., Hayashi, H., Hara-Nishimura, I., and Nishimura, M. (2001). Direct interaction between glyoxysomes and lipid bodies in cotyledons of the *Arabidopsis thaliana ped1* mutant. Protoplasma **218,** 83-94.

Linka, N., Theodoulou, F.L., Haslam, R.P., Linka, M., Napier, J.A., Neuhaus, H.E., and Weber, A.P.M. (2008). Peroxisomal ATP import is essential for seedling development in *Arabidopsis thaliana*. Plant Cell **20,** 3241-3257.

Mano, S., Nakamori, C., Fukao, Y., Araki, M., Matsuda, A., Kondo, M., and Nishimura, M. (2011). A defect of peroxisomal membrane protein 38 causes enlargement of peroxisomes. Plant Cell Physiol **52,** 2157-2172.

Rylott, E.L., Eastmond, P.J., Gilday, A.D., Slocombe, S.P., Larson, T.R., Baker, A., and Graham, I.A. (2006). The *Arabidopsis thaliana* multifunctional protein gene (MFP2) of peroxisomal beta-oxidation is essential for seedling establishment. Plant J **45,** 930-941.

VII. CONCLUDING REMARKS

A long-term goal of metabolite transporter research is to understand the metabolic network of plants. Transporters are 'gatekeepers' at the membrane of organelles and thus are switches that regulate the flux of energy, metabolic precursors, and end products across compartments up to the organismal level (Lunn, 2007). In this perspective, transport proteins are targets for rational metabolic engineering (Weber and Bräutigam, 2012). The main goals of plant metabolic engineering are to improve biomass yield, producing high quality valuable goods (Capell and Christou, 2004), and increasing plant resource-use efficiency to optimize plant growth under conditions of limited water, fertilizer or land (Weber and Bräutigam, 2012).

So far, the importance of modulating transport capacities at cellular membranes has been underestimated in metabolic engineering (Weber and Bräutigam, 2012). This is most likely due to limited biochemical and structural information on transporters; compared to soluble proteins, the characterization of membrane proteins is challenging (Xie, 2008).

This thesis extended the inventory of MCF carriers in plants, screening 20 plant proteomes for MCF carriers (*Manuscript 1*). MCFs were clustered in orthologous groups, assigning their putative transport functions. Interestingly, we identified an orthologous MCF group, which against previous expectations (Picault et al., 2004) was split into two subclasses, (i) PHT3;1/PHT3;2 and (ii) PHT3;3. Further investigations revealed that these subclasses indeed resembled different transport functions. In conclusion, we established a new workflow that proved effective at identifying and characterizing new MCF carriers in plants. Our workflow was advantageous, since computational costs of multiple sequence alignments and construction of phylogenetic trees exclude a phylogenetic approach for whole-genome comparisons in eukaryotes, or at least make it very difficult (Li et al., 2003). The identification of MCF carriers in various plant proteomes generated a candidate list of MCF carriers that can be characterized in many aspects in the future.

The analysis of the mitochondrial carrier PHT3;3 revealed a new transport function for this carrier in mitochondrial sulfate import (*Manuscript 2*). The carrier was named SIT1 according to its transport function. This thesis describes the first carrier belonging to the MCF that specifically transports sulfate. Other MCF carriers exist, which *in vitro* exchange sulfate, but non-specifically. For example dicarboxylate carriers transport sulfate, but also accept oxaloacetate, succinate, phosphate, and thiosulfate (Palmieri et al., 2008). Based on this thesis, we postulated that SIT1 might contribute to maintain a functional metabolic network driving the replenishment of the TCA cycle with dicarboxylic acids. Anapleurosis of the TCA cycle is fundamental to maintain a steady-state metabolic network (Sweetlove et al., 2010). The TCA cycle does not only serve to generate ATP, but feeds in a wider metabolic network. It provides carbon skeletons for nitrogen assimilation, is involved in generating turgor for cell expansion, charge balancing or pH homeostasis (Sweetlove et al., 2010). In conclusion, this thesis demonstrated that sulfate is imported into plant mitochondria.

The import of sulfate was not expected from previous data, which elucidated that only sulfide and cysteine traverse the mitochondrial membrane for the assimilation of sulfur in cysteine biosynthesis (Hell et al., 2002), or sulfide and cyanide detoxification (Alvarez et al., 2012; Birke et al., 2012). However, this thesis demonstrated the existence of a sulfate carrier in mitochondria, which is presumably not involved in any aforementioned process, besides energy metabolism. Future studies are dedicated to investigate the role of SIT1 in plants.

Intracellular pH regulation is essential to maintain enzymatic pathways and metabolism, which widely depend on specific pH conditions (Pittman, 2012). Distinct pH conditions are maintained in various plant cell compartments, such as the cytosol, vacuole, endomembrane system, plastids, or mitochondria (Pittman, 2012). However, the mechanism of peroxisomal pH regulation is a long-standing matter of debate (Rottensteiner and Theodoulou, 2006). In this thesis we showed that the peroxisomal pH changes in respect to different types of peroxisomes (*Manuscript 3*). Peroxisomes in leaves are mainly involved in photorespiratory glycolate metabolism, whereas peroxisomes in etiolated plant tissues serve to degrade fatty acids to form sucrose (Hayashi and Nishimura, 2003). At present, the functions of peroxisomes in roots are not fully understood (Kamada-Nobusada et al., 2008). We discovered an acidic pH in peroxisomes in etiolated hypocotyl, a tissue that is mainly involved in lipid turnover. Root peroxisomes displayed an alkaline pH. One explanation could be that the specific metabolism of peroxisomes from different cell types influences peroxisomal pH (Rottensteiner and Theodoulou, 2006). One can hypothesize that root peroxisomes are metabolically more similar to unspecialized peroxisomes of leaves than to etiolated tissue peroxisomes (Olsen et al., 1993). This explains why we observed an alkaline pH in root peroxisomes, which is analogous to observations made in Arabidopsis leaf peroxisomes (Shen et al., 2013). In the case of peroxisomes involved in storage oil mobilization, we predicted that the peroxisomal ATP carrier is responsible for the acidification of peroxisomes, co-importing protons into the matrix, as described for yeast. Our studies, however, did not support this hypothesis. An impaired ATP import into peroxisomes and thus concomitantly reduced levels of fatty acid degradation did not affect peroxisomal pH, as shown for the yeast homolog Ant1p previously (Lasorsa et al., 2004). Concluding, this thesis described the existence of tissue-specific pH conditions in plant peroxisomes, acidic in fatty acid degrading tissue. Different proton ion concentrations in peroxisomes versus cytosol were also observed in yeast, but not in human peroxisomes. In yeast, peroxisomes, which are specifically involved in fatty acid oxidation, exhibit either an alkaline or acidic pH in peroxisomes (Lasorsa et al., 2004; van Roermund et al., 2004). In human fibroblasts and Chinese hamster ovary cells, the peroxisomal pH adapts to the cytosolic pH and thus is near neutral (Jankowski et al., 2001).

The question that arises is, how a pH gradient across the peroxisomal membrane is generated and maintained. It is plausible to assume that peroxisomes, which connect many metabolic pathways in plants (Erdmann et al., 1997), possess their own pH regulating system that

controls transport of solutes, ion trapping and in consequence, metabolism. Hence, we tested whether ATPase proton pumps are involved in peroxisomal pH homeostasis. As it is possible that the endoplasmatic reticulum (ER) brings together peroxisomes and ATPases, we assumed that proton pumps might be involved. ATPases are synthesized at the ER and then leave the organelle via the secretory pathway (Sze et al., 1999). Also peroxisomes derive from the ER (Mullen and Trelease, 2006). Hence, peroxisomes could acquire ATPases before they bud off the ER. The yeast *Hansenula polymorpha* presumably possesses proton-translocation ATPases residing in the peroxisomal membrane (Douma et al., 1987).

Here, preliminary data showed that vanadate, a specific P-ATPase inhibitor, altered the peroxisomal pH, indicating that P-ATPase-type proton pumps might contribute to peroxisomal pH maintenance. Further detailed investigations will reveal if ATPases are present in peroxisomes of plants.

References

Alvarez, C., García, I., Romero, L.C., and Gotor, C. (2012). Mitochondrial sulfide detoxification requires a functional isoform O-acetylserine(thiol)lyase C in *Arabidopsis thaliana*. Mol Plant **5,** 1217-1226.

Birke, H., Haas, F., Luit, J., Wirtz, M., and Hell, R. (2012). Cysteine biosynthesis, in concert with a novel mechanism, contributes to sulfide detoxification in mitochondria of *Arabidopsis thaliana*. Biochemical J **445,** 275-283.

Capell, T., and Christou, P. (2004). Progress in plant metabolic engineering. Curr Opin Biotech **15,** 148-154.

Douma, A.C., Veenhuis, M., Sulter, G.J., and Harder, W. (1987). A proton-translocating adenosine triphosphatase is associated with the peroxisomal membrane of yeasts. Arch Microbiol **147,** 42-47.

Erdmann, R., Veenhuis, M., and Kunau, W.H. (1997). Peroxisomes: Organelles at the crossroads. Trends Cell Biol **7,** 400-407.

Hayashi, M., and Nishimura, M. (2003). Entering a new era of research on plant peroxisomes. Curr Opin Plant Biol **6,** 577-582.

Hell, R., Jost, R., Berkowitz, O., and Wirtz, M. (2002). Molecular and biochemical analysis of the enzymes of cysteine biosynthesis in the plant *Arabidopsis thaliana*. Amino Acids **22,** 245-257.

Kamada-Nobusada, T., Hayashi, M., Fukazawa, M., Sakakibara, H., and Nishimura, M. (2008). A putative peroxisomal polyamine oxidase, AtPAO4, is involved in polyamine catabolism *in Arabidopsis thaliana*. Plant Cell Physiol **49,** 1272-1282.

Lasorsa, F.M., Scarcia, P., Erdmann, R., Palmieri, F., Rottensteiner, H., and Palmieri, L. (2004). The yeast peroxisomal adenine nucleotide transporter: characterization of two transport modes and involvement in DeltapH formation across peroxisomal membranes. Biochemical J **381,** 581-585.

Li, L., Stoeckert, C.J., and Roos, D.S. (2003). OrthoMCL: identification of ortholog groups for eukaryotic genomes. Genome Res **13,** 2178-2189.

Lunn, J.E. (2007). Compartmentation in plant metabolism. J Exp Bot **58,** 35-47.

Mullen, R.T., and Trelease, R.N. (2006). The ER-peroxisome connection in plants: development of the ER semi-autonomous peroxisome maturation and replication model for plant peroxisome biogenesis. Biochim Biophys Acta **1763,** 1655-1668.

Olsen, L.J., Ettinger, W.F., Damsz, B., Matsudaira, K., Webb, M.A., and Harada, J.J. (1993). Targeting of glyoxysomal proteins to peroxisomes in leaves and roots of a higher plant. Plant Cell **5,** 941-952.

Palmieri, L., Picault, N., Arrigoni, R., Besin, E., Palmieri, F., and Hodges, M. (2008). Molecular identification of three *Arabidopsis thaliana* mitochondrial dicarboxylate carrier isoforms: organ distribution, bacterial expression, reconstitution into liposomes and functional characterization. Biochemical J **410,** 621-629.

Picault, N., Hodges, M., Palmieri, L., and Palmieri, F. (2004). The growing family of mitochondrial carriers in Arabidopsis. Trends Plant Sci **9,** 138-146.

Pittman, J.K. (2012). Multiple transport pathways for mediating intracellular pH homeostasis: The contribution of H^+/ion exchangers. Frontiers in Plant Science **3,** doi: 10.3389/fpls.2012.00011.

Rottensteiner, H., and Theodoulou, F.L. (2006). The ins and outs of peroxisomes: co-ordination of membrane transport and peroxisomal metabolism. Biochim Biophys Acta **1763,** 1527-1540.

Shen, J., Zeng, Y., Zhuang, X., Sun, L., Yao, X., Pimpl, P., and Jiang, L. (2013). Organelle pH in the Arabidopsis endomembrane system. Mol Plant **6,** 1419-1437.

Sweetlove, L.J., Beard, K.F., Nunes-Nesi, A., Fernie, A.R., and Ratcliffe, R.G. (2010). Not just a circle: flux modes in the plant TCA cycle. Trends Plant Sci **15,** 462-470.

Sze, H., Li, X., and Palmgren, M.G. (1999). Energization of plant cell membranes by H^+-pumping ATPases: regulation and biosynthesis. Plant Cell **11,** 677-689.

Takahashi, H., Kopriva, S., Giordano, M., Saito, K., and Hell, R. (2011). Sulfur assimilation in photosynthetic organisms: molecular functions and regulations of transporters and assimilatory enzymes. Ann Rev Plant Biol **62,** 157-184.

van Roermund, C.W., de Jong, M., L, I.J., van Marle, J., Dansen, T.B., Wanders, R.J., and Waterham, H.R. (2004). The peroxisomal lumen in *Saccharomyces cerevisiae* is alkaline. J Cell Sci **117,** 4231-4237.

Weber, A.P., and Bräutigam, A. (2012). The role of membrane transport in metabolic engineering of plant primary metabolism. Curr Opin Biotechnol **24,** 256-262.

Xie, H. (2008). Activity assay of membrane transport proteins. Acta Biochim Biophys Sin **40,** 269-277.

VIII. PUBLISHED MANUSCRIPTS

Manuscript 4

An engineered plant peroxisome and its application in biotechnology

Sarah K. Kessel-Vigelius[1a *], Jan Wiese[1*], Martin G. Schroers[1*], Thomas J. Wrobel[1*], Florian Hahn[1], and Nicole Linka[1a]

[1]Institute of Plant Biochemistry, Heinrich-Heine University Düsseldorf, 40225 Düsseldorf, Germany

*First author

[a]Corresponding author

Plant Science 210 (2013) 232–240

Contents lists available at SciVerse ScienceDirect

Plant Science

journal homepage: www.elsevier.com/locate/plantsci

Review

An engineered plant peroxisome and its application in biotechnology☆

Sarah K. Kessel-Vigelius[1], Jan Wiese[1], Martin G. Schroers[1], Thomas J. Wrobel[1], Florian Hahn, Nicole Linka*

Heinrich-Heine University, Plant Biochemistry, Universitätsstrasse 1, Building 26.03.01, D-40225 Düsseldorf, Germany

ARTICLE INFO

Article history:
Received 20 March 2013
Received in revised form 8 June 2013
Accepted 10 June 2013
Available online 17 June 2013

Keywords:
Peroxisome
Biotechnology
Genetic engineering
Metabolism
Stress tolerance

ABSTRACT

Plant metabolic engineering is a promising tool for biotechnological applications. Major goals include enhancing plant fitness for an increased product yield and improving or introducing novel pathways to synthesize industrially relevant products. Plant peroxisomes are favorable targets for metabolic engineering, because they are involved in diverse functions, including primary and secondary metabolism, development, abiotic stress response, and pathogen defense. This review discusses targets for manipulating endogenous peroxisomal pathways, such as fatty acid β-oxidation, or introducing novel pathways, such as the synthesis of biodegradable polymers. Furthermore, strategies to bypass peroxisomal pathways for improved energy efficiency and detoxification of environmental pollutants are discussed. In sum, we highlight the biotechnological potential of plant peroxisomes and indicate future perspectives to exploit peroxisomes as biofactories.

Contents

1. Introduction

Plants have evolved the ability to produce a wide range of molecules. Many of these compounds are of biotechnological importance, as they serve as food, colorants, flavors, fragrances, traditional medicines, pharmaceuticals, cosmetics, and renewable fuels [1]. Their chemical synthesis is often difficult and expensive, thus genetic engineering is an alternative approach to optimize the production of desired metabolites in plants.

In plants, biochemical pathways are compartmentalized and individual steps of a particular pathway are distributed over

Abbreviations: H_2O_2, hydrogen peroxide; JA, jasmonic acid; PHA, polyhydroxyalkanoate; ROS, reactive oxygen species.

* Corresponding author. Tel.: +49 0211 81 10412.
E-mail addresses: Sarah.Vigelius@hhu.de (S.K. Kessel-Vigelius), Jan.Wiese@hhu.de (J. Wiese), Martin.Schroers@hhu.de (M.G. Schroers), Thomas.Jan.Wrobel@hhu.de (T.J. Wrobel), Florian.Hahn@hhu.de (F. Hahn), Nicole.Linka@hhu.de (N. Linka).
[1] Co-first authors.

0168-9452/$ – see front matter © 2013 The Authors. Published by Elsevier Ireland Ltd. All rights reserved.
http://dx.doi.org/10.1016/j.plantsci.2013.06.005

different compartments. In this context, peroxisomes, which are subcellular organelles 1 μm in diameter [2], represent as organelles at a metabolic crossroads [3,4], because they participate in one or more steps in many significant metabolic reactions, including primary carbon metabolism (e.g. beta-oxidation of fatty acids and photorespiration), secondary metabolism (e.g. production of glucosinolates), development (e.g. synthesis of plant hormones), abiotic stress response, and pathogen defense [4].

Thus, peroxisomes are an attractive target for metabolic engineering, to increase yield and quality of plant products. Manipulation of peroxisomal scavenging systems for reactive oxygen species (ROS) might enhance plant fitness under environmental stress conditions [5]. Besides altering peroxisomal functions, novel pathways can be implemented in peroxisomes, enabling the synthesis of desired metabolites or degradation of toxic molecules. The following characteristics illustrate why peroxisomes are well suited for biotechnological purposes:

(i) Peroxisomes are surrounded by a single lipid bilayer membrane [4]. Novel reactions can be compartmentalized within peroxisomes. A peroxisomal compartmentation is favorable because end products or intermediates can be toxic for the cell. As peroxisomes are equipped with efficient ROS-detoxifying systems [6], ROS-producing reactions can be introduced in peroxisomes without deleterious effects.
(ii) Peroxisomes allow an efficient targeting of heterologous proteins, since protein-targeting signals for the peroxisome are well established. Soluble, nuclear-encoded proteins are targeted to peroxisomes by two different targeting signals, which direct soluble proteins to peroxisomes. Most proteins use the Type 1 Peroxisomal Targeting Signal (PTS1) to enter peroxisomes, which consists of three amino acids at the carboxyl terminus (SKL, or a conserved variant) [7,8]. The Type 2 Peroxisomal Targeting Signal (PTS2) is a conserved nonapeptide (9 amino acids), which is attached to the amino terminus of peroxisomal proteins [9]. Fusion of either signal peptide to a heterologous protein results in direct targeting to peroxisomes. Thus, the enzymatic content of peroxisomes can be easily modified. In contrast to plastids and mitochondria, the peroxisomal protein import machinery is able to import fully folded proteins and stable protein complexes in a receptor-independent fashion [4]. The import of heterologous protein complexes into peroxisomes depends on a mechanism called piggybacking, where a protein without a peroxisomal targeting signal uses a PTS-carrying protein as shuttle [10,11]. Therefore, coupling of a shuttle protein to other proteins might enable the targeting of even larger protein complexes to peroxisomes without modifying the import receptor machinery.
(iii) Peroxisomes are highly dynamic organelles, which are able to adjust size and number [12]. They multiply by fission and proliferation [4]. Latter is induced by various environmental, developmental and metabolic cues and is controlled by the PEROXIN11 protein family and several transcription factors [13,14]. A rapid increase in peroxisome number allows an accumulation of substances produced in peroxisomes [2].

In recent years, major progress has been made in genomics and proteomics, revealing the diversity of peroxisomal metabolism [4,15]. However, mechanisms to exploit plant peroxisomes for optimizing metabolism or modifying metabolic fluxes toward compounds of interest are not well studied. Here, we present recent pioneering approaches to produce plant peroxisome biofactories. Moreover, we indicate putative targets and possible strategies that in the future could be exploited to engineer peroxisomes for biotechnological purposes.

2. Improving seed oil yield and quality

One of the major goals of agricultural biotechnology is to increase the content and/or improve the value of oils in oilseed plants, including sunflower, soybean, palm, oilseed rape, and maize crops [16]. Oilseed crops are not only important for human nutrition [17], but can also be used for a variety of chemical applications.

Plants are able to produce a wide range of different fatty acids, whereas the number of fatty acids shared between plant species is relatively low. All conventional crops contain palmitic acid, stearic acid, oleic acid, linoleic acid, and linolenic acid. These are termed "usual" fatty acids. Fatty acids, which in their chemical structures differ from usual fatty acids, are referred to as "unusual" fatty acids. Unusual fatty acids, exhibiting hydroxylations or acetylations, are of major industrial interest, as they provide raw materials for the generation of biopolymers or fuels [18].

Vegetable oils, for example, serve as a sustainable replacement of petroleum-based chemicals [16]. One appealing method to produce high-value oils is the genetic engineering of plants accumulating ricinoleic acid, which serves as precursor for economically-viable products, such as ink, lubricants, varnishes, emulsifiers, nylon, or biodiesel [18,19].

The bottleneck for increased oilseed content and the production of 'designer oils' is the channeling of fatty acids into storage oil. Inefficient integration arises either by enhanced biosynthesis of native fatty acids or by the low affinity of acyltransferases to unusual fatty acids [20,21]. As a consequence, accumulated fatty acids are degraded via peroxisomal beta-oxidation, which simultaneously operates during lipid synthesis (Fig. 1).

Inactivating peroxisomal beta-oxidation enzymes by using specific promoters only active during seed filling could minimize such futile cycling. Another strategy is to produce the desired oil in a specific plant tissue with low beta-oxidation activity (e.g. leaves). Leaf-specific oil production might be favorable if the accumulation of industrial-valuable oil in seeds affected germination or seedling establishment [22].

3. Plant peroxisomes confer stress tolerance

Various abiotic and biotic stress conditions, such as salinity, heat, cold, drought, and pathogen infection induce oxidative stress in plants. This results in overproduction of ROS in chloroplasts, mitochondria, and peroxisomes, with highly oxidative metabolism [23,24]. Plants are unable to escape exposure to environmental stresses, thus they have developed a complex antioxidant defense system to control ROS levels and protect cells from oxidative injury [6]. Here, we present several strategies to improve stress tolerance in plants through modified peroxisomal metabolism circumventing oxidative stress and thereby increasing fitness [25].

3.1. Increasing the peroxisome population

Plant peroxisomes multiply under stress conditions. In plants the PEROXIN11 family, which consist of five isoforms (a–e), controls proliferation of peroxisomes. When overexpressed, the number of peroxisomes increases. Conversely, reducing the expression of PEX11 genes results in decreased peroxisome abundance [26]. The expression of PEX11b is controlled through a phytochrome A-dependent pathway, involving the far-red light photoreceptor phyA and the bZIP transcription factor HY5 homolog [13,27].

Additionally, peroxisomal proliferation is induced by environmental stimuli and various stresses, such as high light intensities, H_2O_2, ozone, xenobiotics, cadmium, salt, pathogens, and senescence. However, little is known about the principal molecular mechanisms [28–33]. Stress-induced peroxisome proliferation

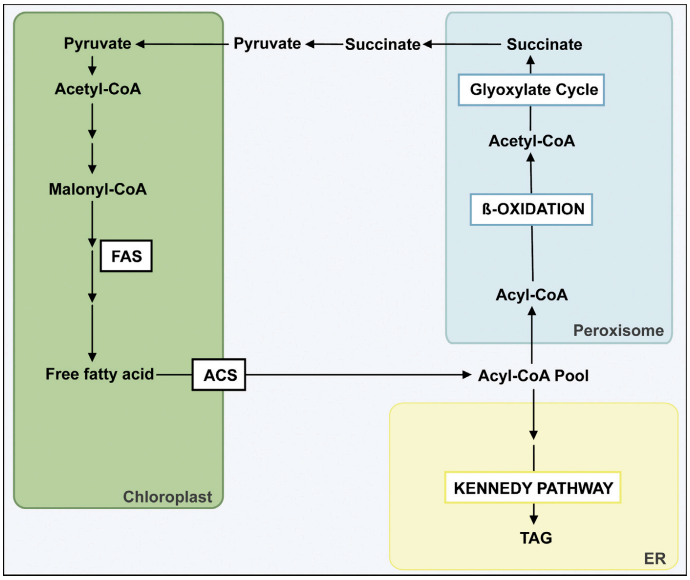

Fig. 1. Fatty acids synthesis and catabolism take place simultaneously in plant cells. In chloroplasts fatty acids (FAs) are generated from acyl-CoA and pyruvate via the fatty acid synthesis complex and are then released into the cytosol. FAs are either catabolized via peroxisomal β-oxidation or incorporated into triacylglycerols via the Kennedy pathway in the ER. CoA, coenzyme A; FAS, fatty acid synthesis complex; ACS, acyl CoA synthetase; ER, endoplasmic reticulum; TAG, triacylglycerol.

may reflect the ability to cope with oxidative damage. Consequently, controlling the peroxisomal population is a promising strategy to enhance stress tolerance in plants.

Introduction of a peroxisome proliferator-activated receptor from *Xenopus laevis* in tobacco plants leads to increased peroxisome number in transgenic tobacco plants [34]. Expression of this regulatory complex increases peroxisome number in transgenic tobacco plants, as it was previously reported for animal tissues [35]. The activity of peroxisomal enzymes involved in ROS-scavenging is increased, leading to potentially improved resistance to oxidative stress [36]. The induced peroxisome proliferation disrupts the plant's redox state, leading to modified salicylic acid levels and altered expression patterns of jasmonic acid and ethylene biosynthesis genes. These changes positively affect pathogen resistance [36].

In an independent approach, an enlarged peroxisome population was produced by up-regulation of the *Arabidopsis* peroxisome biogenesis gene PEX11, the regulator of peroxisome proliferation [13]. However, increasing the peroxisome number did not result in elevated salt tolerance in *Arabidopsis* seedlings and older plants [37]. Future studies need to elucidate if manipulating peroxisome biogenesis can be a strategy to alter stress tolerance. However, understanding regulation and all possible side-effects is crucial when increasing the peroxisomal population.

3.2. Improving peroxisomal ROS-scavenging systems

Under non-stress conditions ROS produced by peroxisomal metabolism are scavenged by the simultaneous action of the peroxisomal antioxidant systems catalase, ascorbate peroxidase and the ascorbate–glutathione cycle [38]. However, under oxidative stress conditions peroxisomal ROS generation is enhanced and ROS scavenging is insufficient [38]. The ability to cope with an increased ROS production is correlated with upregulation of peroxisomal antioxidant systems in natural stress-tolerant plant species [39,40]. One goal for engineering plants with wide-ranging stress resistance would be improving the peroxisomal ROS scavenging machinery (i.e. modulate the gene expression and enzymatic activity).

Catalase as a prominent H_2O_2 scavenger is an important target. It is highly abundant in plant peroxisomes but has a low substrate affinity [41]. Modulation of its catalytic activity might be a starting-point to overcome this drawback, leading to more efficient ROS detoxification in plant peroxisomes. Because bacterial catalases offer higher H_2O_2 affinity, several studies have ectopically expressed the *Escherichia coli* catalase in plant species such as tobacco, tomato, and rice [42–44]. The resulting transgenic plants displayed an increased protection against oxidative stress. The same outcome was achieved by overexpression of the peroxisomal ascorbate peroxidase (APX), which acts in tandem with catalase to degrade H_2O_2 [45,46]. Alternatively, an enhanced ascorbate–glutathione cycle in the peroxisomal matrix could reduce plant stress [38]. To accomplish this task various modifications are required simultaneously: (i) enlarging the peroxisomal glutathione and ascorbate pool by stimulating biosynthesis and uptake into peroxisomes, (ii) increasing the NADPH levels in peroxisomes by over-expressing the peroxisomal NAD kinase for NADPH production [47], and (iii) constitutive peroxisomal targeting of glutathione reductase, which carries a weak peroxisomal targeting signal and is located in the cytosol and peroxisomes [48]. Previous studies have successfully induced the biosynthesis of glutathione and ascorbate, resulting in higher glutathione and ascorbate levels in the cytosol [49,50]. To increase peroxisomal import of glutathione and ascorbate, specific peroxisomal transport proteins remain to be identified. To date, modifying the redox state of peroxisomal ascorbate and glutathione pools is feasible [47,48]. Enhancing glutathione and ascorbate uptake remains to be achieved in future, since corresponding peroxisomal transporters have not been identified thus far.

3.3. Improved pest and pathogen resistance

Plants suffer from infections caused by fungi, bacteria, viruses and nematodes. Peroxisomes play a substantial role in disease resistance and are targets for genetic improvement to confer pathogen tolerance in plants [4].

The phytohormone jasmonic acid (JA) is a lipid-derived signaling molecule that induces plant defense mechanisms [51]. Its production is triggered in response to tissue injury (wounding) caused by herbivore attack. The last steps of JA biosynthesis occur in peroxisomes [51]. The JA precursor 12-oxo-phytodienoic acid (OPDA) is imported into peroxisomes and is subsequently reduced to OPC8:0 (3-oxo-2-(2′[Z]-pentenyl)-cyclopentan-1-octanoic acid), In three rounds of peroxisomal beta-oxidation activated OPC8:0 is converted to JA [52]. Overexpression of the transcription factor WRKY30 in rice resulted in a constitutive expression of plastidic JA biosynthesis genes. This was associated with increased endogenous JA accumulation and enhanced tolerance against fungal pathogens [53]. As JA biosynthetic enzymes locate to companion cells and sieve elements of the vascular bundle [54], it might be beneficial to not only improve biosynthesis, but extend JA production to other tissues to prime plants against herbivore attack. This involves exploiting a natural peroxisomal function.

Plant peroxisomes contribute to extracellular defense mechanisms against fungi by preventing colonization. Upon fungal invasion peroxisomes migrate toward the site of invasion [55]. Under these conditions the myrosinase PEN2, which is bound to the peroxisomal membrane, hydrolyzes indolic glucosinolates to antifungal defense compounds protecting plants against fungal entry [56]. Furthermore, certain benzylglucosinolates play a role in pathogen defense and are found in developing seeds and germinating seedlings [57]. These active defense molecules are synthesized in the cytosol by transferring a benzoyl moiety from benzoyl-CoA to a hydroxylated aliphatic glucosinolate, though the precursor benzoyl-CoA is primarily produced from cinnamic acid via peroxisomal beta-oxidation [58–60].

Engineering levels of these defense compounds might enhance plant immunity against pathogens. This can be achieved by targeting either biosynthetic or regulatory genes of glucosinolate biosynthesis [58,61]. Glucosinolates are naturally found in crucifers, including oilseed rape and *Arabidopsis*, but their production could be successfully implemented in non-cruciferous plants, such as tobacco [62]. However, cruciferous crop seeds with high glucosinolate content are unwanted as primary food source for animals or humans, because these metabolites have a bitter taste [63]. An agricultural challenge for the future is to eliminate glucosinolates from edible parts of crops, but retain their synthesis in source tissues for protection against pathogen attack. Specific expression and suppression of peroxisomal modules involved in benzylglucosinolate production might be a promising approach to solve this problem.

3.4. Peroxisomal small heat shock proteins for enhanced stress tolerance

Small heat-shock proteins are induced in response to various stresses. They act as molecular chaperones preventing the aggregation of nascent and stress-accumulated misfolded proteins [64,65]. Two peroxisome-located small heat-shock proteins called AtAcd31.2 and AtHsp15.7 were identified in *Arabidopsis* [66]. AtAcd31.2 is constitutively expressed, whereas AtHsp15.7 expression is strongly induced by heat and oxidative stress [66], suggesting that peroxisomal small heat-shock proteins play a role in protecting proteins under both physiological and stress conditions [67]. The overexpression of small heat-shock proteins might be a useful strategy to produce plants with enhanced tolerance against different stresses. Previous studies have demonstrated that substantial tolerance to salt, drought and high light can be achieved by over-expressing cytosolic or plastidic heat-shock proteins [67–69].

4. Modulating auxin synthesis in peroxisomes

Peroxisomes are involved in biogenesis of the auxin indole-3-acetic acid. Indole-3-butyric acid is metabolized to the active form indole-3-acetic acid by removing two side-chain methylene units in a process similar to fatty acid beta-oxidation [70,71]. It has been shown that indole-3-butyric acid-derived auxin influences cell expansion in certain cell types, resulting in elongated root hairs and enlarged cotyledons [72]. Elongation of root hairs by stimulating auxin production is a promising approach to enlarge root surface area and thereby enhance water and nutrient uptake [73]. Whether this goal can be accomplished without major drawbacks on plant development remains to be shown.

5. Implementation of artificial metabolic pathways to gain novel peroxisomal functions

Besides optimizing peroxisomal metabolism, metabolic engineering can achieve novel peroxisomal functions. The goal is to introduce artificial pathways into plant peroxisomes for either producing novel substances or improving efficiency of peroxisomal pathways degrading toxic compounds.

5.1. Production of biodegradable polymers in plant peroxisomes

Plant peroxisomes are attractive factories for biodegradable polymers, such as polyhydroxyalkanoates (PHA). Renewable bioplastics are sustainable and have the potential to replace conventional mineral oil-based plastics [74].

PHAs are a group of polyesters, which are naturally formed and deposited as inclusion bodies in many bacterial genera. They are not produced in eukaryotes [75]. PHAs can incorporate more than one hundred different hydroxyacids, mainly varying in functional groups of side chains and chain length [76]. Thus, physical properties of PHA range from glues to brittle plastics, depending on the composition [77]. The biosynthesis pathway of the most common type of PHAs, the homopolymer poly-3-hydroxybutyrate (PHB), was discovered first in *Ralstonia eutropha*, where it serves as a carbon sink [78,79]. Its synthesis pathway has been successfully introduced into different microorganisms, which naturally do not produce these polymers [80]. To increase substrate availability for PHA biosynthesis, overproduction of the starting substrate acetyl-CoA was induced, which led to an improved PHA production in these organisms [81].

However, PHA production in microorganisms is not economical because of expensive bacterial feedstock, such as glucose [82]. To address economic inefficiency, plants producing high amounts of PHA were designed. Plants are well suited, as water, light, CO_2, and a few minerals suffice to produce high amounts of biomass. Moreover, plants are unable to degrade PHAs and thus can accumulate these polymers in high amounts. For successful PHA production in plants three prerequisites are needed: (i) the bacterial three-gene pathway consisting of a 3-ketothiolase (*pha*A), an acetoacetyl-CoA reductase (*pha*B) and a PHA synthase (*pha*C), (ii) a large acetyl-CoA pool, and (iii) reducing power [83].

PHA production was first achieved in the cytosol of Arabidopsis and tobacco, because only two additional enzymes had to be introduced, *pha*B and *pha*C, as plants endogenously possess a cytosolic form of *pha*A as part of the mevalonate pathway (Fig. 2A). The production of PHA led to a strong reduction of plant growth, resulting from depletion of cytoplasmic acetyl-CoA, inhibiting

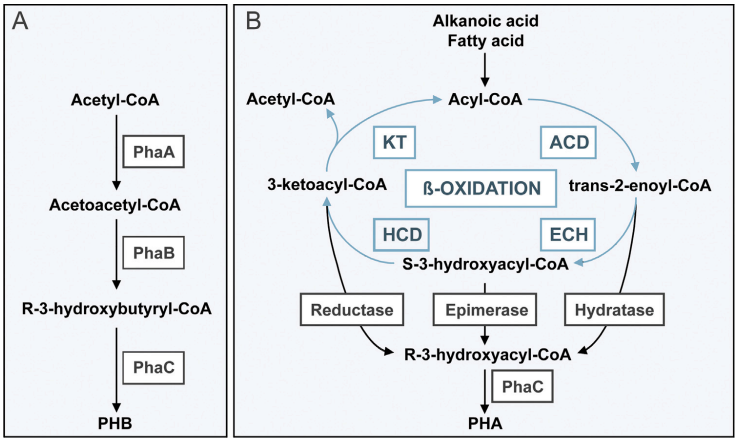

Fig. 2. (A) PHB synthesis in *Ralstonia eutropha*. Bacterial pathway of PHB production in *R. eutropha*. *pha*A, 3-ketothiolase; *pha*B, acetoacetyl-CoA reductase; *pha*C, PHA synthase. (B) PHA synthesis in plants can be implemented into the beta-oxidation cycle. Intermediates of the beta-oxidation can be used for PHA synthesis. Either an epimerase, a hydratase, or a reductase is necessary to convert cycle intermediates into substrates for *pha*C. The beta-oxidation core reactions are depicted in blue. KT, 3-ketothiolase; ACD, acyl-CoA dehydrogenase; ECH, enoyl-CoA hydratase I; HCD, S-3 hydroxyacyl-CoA dehydrogenase.

isoprenoid and flavonoid biosynthesis [75,84]. To achieve higher PHA levels, with less deleterious effects, production was targeted to chloroplasts of numerous plant species. PHA yield was predicted to increase, as plastids have a high flux of acetyl-CoA, which is required for fatty acid biosynthesis. In transgenic plant lines accumulating high amounts of PHA in their chloroplasts, growth was reduced, plants were chlorotic, and sometimes fertility was impacted. The reasons for the strong phenotype have not been clearly determined [85–87].

To minimize plant growth defects, PHA synthesis was targeted to plant peroxisomes (Fig. 2B) exploiting peroxisomal carbon flux through beta-oxidation for synthesis [88–91]. A peroxisomal targeting signal was fused to the bacterial *pha*A, *pha*B, and *pha*C genes. Peroxisomes of PHA-producing plants are significantly enlarged. This reflects that these organelles have the capability to increase their size to accommodate large volumes of PHA granules [91]. Studies with the C4-grass sugarcane, a high biomass crop, showed that peroxisomal PHA biosynthesis significantly contributes to PHA production levels of commercial interest in crop plants, without interfering with plant growth [91].

5.2. Peroxisomal bypass pathways to reduce photorespiration

A central function of plant peroxisomes is their contribution to photorespiration (Fig. 3) [4]. This light-dependent pathway is linked to photosynthesis by the dual function of plastidic RubisCO. Low carbon dioxide concentrations favor the oxygenase reaction of RubisCO leading to an accumulation of toxic 2-phosphoglycolate [92]. This compound is efficiently degraded via the photorespiratory C2 cycle, converting 2-phosphoglycolate to 3-phosphoglycerate, which re-enters the Calvin–Benson cycle. CO_2 and ammonia (NH_3) are released. Substantial energy costs are required for re-assimilation (Fig. 3) [92]. The goal is to optimize plant metabolism and to increase biomass production by minimizing energy losses in photorespiration. As photorespiration is required in all photosynthetic organisms, it cannot be eliminated completely, but bypassed [93]. So far, three reactions have been tested in plants circumventing energy loss from photorespiration [94]. A reduction of the RubisCO oxygenase reaction was attempted by increasing CO_2 levels inside chloroplasts, utilizing carbon derived from 2-phosphogycolate (Fig. 3, blue pathway) [95]. Secondly, an alternative plastidic conversion route for 2-phosphoglycolate has been reported (Fig. 3, red pathway) [96]. Both approaches bypassing the mitochondrial CO_2 release led to an increase in biomass production under ambient CO_2 conditions [95,96].

To avoid mitochondrial NH_3 production a short-circuit pathway of the photorespiratory nitrogen cycle was implemented into peroxisomes [97]. Glyoxylate carboligase (GCL) and hydroxypyruvate isomerase (HYI) from *E. coli* were introduced into peroxisomes of transgenic tobacco leaves resulting in a peroxisomal conversion of glyoxylate to hydroxypyruvate (Fig. 3, green pathway). Unfortunately, this bypass did not show the benefits expected for biomass production [97]. Instead, leaves of transgenic tobacco displayed chlorotic lesions under ambient CO_2 levels. Detailed analyses revealed that the GCL/HYI pathway introduced was not fully operating, due to silencing of the bacterial hydroxypyruvate isomerase gene [97]. Thus, the functionality of this proposed pathway remains to be demonstrated. The use of RNA-silencing tobacco mutants might overcome this obstacle [98]. It might enable further analyses studying peroxisomes as tools to bypass photorespiration [97].

5.3. Peroxisomal degradation pathways for pollutants

Genetically modified plants can help to reduce environmental pollution by degradation of long-persisting chemical compounds in contaminated soil or ground water. The implementation of catabolic pathways from various bacterial and fungal organisms into plants allows detoxification of certain organic pollutants [99].

For example, tobacco plants have been developed which degrade the halogenated aliphatic compound 1,2-dichloroethane, a carcinogenic chemical of high stability. In these plants, two enzymes from *Xanthobacter autotrophicus* were expressed that catabolize 1,2-dichloroethane to glycolate in combination with endogenous enzymes [100]. High accumulation of the resulted end product glycolate is toxic for the plant cell and needs to be directly metabolized. In particular for the root tissue, it might be to ectopically introduce the photorespiratory enzyme glycolate oxidase in root cells for the conversion of glycolate to glyoxylate.

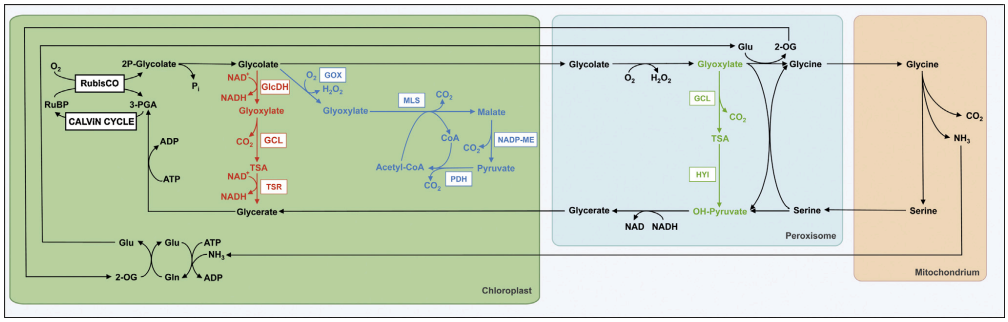

Fig. 3. The loss of ammonia during photorespiration can be bypassed. Ammonia and CO_2 are released in mitochondria during the conversion of glycine to serine. Ammonia can be re-assimilated in chloroplasts. The ammonia-consuming reactions can be bypassed by a photorespiratory short-circuit in peroxisomes (shown in green) by introducing two bacterial enzymes GCL and HYI. The plastidic bypasses introduced by Maier et al. [95] and Kebeish et al. [96] are presented in blue and red, respectively. RuBP, ribulose-1,5-bisphosphate; PGA, phosphoglycerate; Glu, glutamate; Gln, glutamine; 2-OG, 2-oxoglutarate; ATP, adenosine triphosphate; ADP, adenosine diphosphate; NAD(H), nicotinamide adenine dinucleotide; TSA, tartronic semialdehyde; GCL, glyoxylate carbolyase; HYI, hydroxypyruvate isomerase.

Sulfur dioxide is a major air pollutant emitted by industrial processes. SO_2 adversely affects growth and development of crop species, causing chlorosis, necrosis and long-term yield reduction [101–103]. It enters plant tissues as gas, where it is transformed to sulfite. Excess amounts of sulfite are toxic to the plant cell. Peroxisomal catalase activity is sensitive to sulfite, resulting in high H_2O_2 levels upon sulfite stress [104]. The key enzyme to protect plants against sulfite toxicity is the peroxisomal sulfite oxidase, catalyzing the oxidation of sulfite to sulfate. To improve sulfite detoxification, the peroxisomal sulfite oxidase from maize was overexpressed in plants [105,106]. Transgenic lines exhibiting elevated sulfite oxidase levels confer enhanced tolerance to excess sulfite, which is indicated by lower H_2O_2 and higher catalase levels. Hence, the overexpression of sulfite oxidase may protect peroxisomal catalase from inhibition by sulfite [106].

6. Concluding remarks

Besides recent progress in the field of peroxisome engineering, the emerging potential of plant peroxisomes for green biotechnology is described in this review. Strategies are presented which either (i) manipulate peroxisomal pathways to alter oilseed quantity and quality, or (ii) improve tolerance toward abiotic and biotic stresses. Further, approaches are shown which involve (iii) implementing new pathways in peroxisomes, such as the production of biodegradable polymers, (iv) bypassing peroxisomal pathways for a better energy-cost efficiency, and (v) detoxifying pollutants from contaminated soil, water and air.

However, several limitations have to be considered when modifying or introducing pathways to peroxisomes. If fluxes through endogenous peroxisomal pathways are changed, overall cellular metabolism and substrate homeostasis could be negatively influenced. For example, changes in peroxisomal contributions to auxin synthesis or photorespiration were reported to create substantial reductions in fitness [107,108]. In order to estimate the biotechnological potential of plant peroxisomes, it is necessary to understand how peroxisomal metabolism is regulated and coordinated.

When implementing novel pathways, the pH optimum inside peroxisomes needs to be considered, because newly introduced enzymes with a strict cofactor- and pH-dependency might be impaired. The pH of plant peroxisomes has not yet been determined. Reports for other eukaryotic organisms, including yeast and mammals, indicated contradictory results the peroxisomal matrix is either acidic or alkaline [109–112]. In addition, cofactors need to be available in peroxisomes, when implementing certain enzymatic reactions. Peroxisomes are capable of importing fully folded proteins, which have already bound their cofactor in the cytosol [113]. For ATP, NAD and CoA transporters have been identified importing these cofactors into peroxisomes [114–116]. Further, the level of peroxide radicals could interfere with enzyme activities, since peroxisomes exhibit an oxidative metabolism producing ROS.

Successful engineering of plant peroxisomal metabolism requires insights into the complete protein inventory. To date, proteome analyses identified more than 100 peroxisomal proteins in plants. However, further enzymes are necessary to fulfill proposed or described metabolic functions [117]. In this context, a major obstacle is the missing comprehensive knowledge about metabolite transport proteins, mediating the flux of solutes across the peroxisomal membrane [118]. Although many peroxisomal transport steps are hypothesized in plants, the corresponding transporter genes have not yet been assigned. Besides the three cofactor carriers mentioned earlier, only the carrier importing fatty acids has been identified so far [114–116,118–120]. With regard to metabolite transport, biotechnological implementations have to be considered carefully, because the prospective substrates and products need to be shuttled in and out of peroxisomes.

As very little is know about endogenous export from peroxisomes, secretion of substances produced in peroxisomes might even be a favorable trait for biotechnological production, as it is known for algae [121]. Such a process protects the cell from potential toxic effects of compounds created in this organelle. On the other hand, secretion of products can be favorable to avoid expensive downstream processing after biotechnological production. In a process called peroxicretion, subsequent excretion of peroxisomal products from cells was achieved by fusing the soluble domain of a Golgi-derived v-SNARE to a peroxisomal membrane protein used as an anchor. Fusion of peroxisomes with the plasma membrane was induced and products were released into the extracellular space [122]. This artificial secretion pathway, coupled to an inducible promoter controlling the time point of product release, might raise the utility of engineered production in plant peroxisomes for industrial biotechnology.

A long-term goal of engineering plant peroxisomes is the construction of synthetic peroxisomes in plants or other eukaryotic organisms, such as yeast. First steps toward this goal have been taken recently, when in a human cell line two antioxidant enzymes, a Cu/Zn-superoxide dismutase and a catalase isoform, were expressed in polymer vesicles, which have a membrane made

permeable by insertion of channel proteins. In this artificial peroxisome superoxide radicals and H_2O_2 detoxification was functional [123].

Acknowledgements

This work was supported by the DFG-grant 1781/1-1, 1781/2-1 and GRK 1525. The authors thank Andreas P.M. Weber for helpful discussion and P.K. Lundqvist for reading the manuscript.

References

[1] J.M. Hibberd, A.P.M. Weber, Plant metabolism and physiology, Curr. Opin. Plant Biol. 15 (2012) 225–227.
[2] M. Hayashi, M. Nishimura, Entering a new era of research on plant peroxisomes, Curr. Opin. Plant Biol. 6 (2003) 577–582.
[3] R. Erdmann, M. Veenhuis, W.H. Kunau, Peroxisomes: organelles at the crossroads, Trends Cell Biol. 7 (1997) 400–407.
[4] J. Hu, et al., Plant peroxisomes: biogenesis and function, Plant Cell 24 (2012) 2279–2303.
[5] J. Nielsen, Metabolic engineering: techniques for analysis of targets for genetic manipulations, Biotechnol. Bioeng. 58 (1998) 125–132.
[6] J.M. Palma, et al., Antioxidative enzymes from chloroplasts, mitochondria, and peroxisomes during leaf senescence of nodulated pea plants, J. Exp. Bot. 57 (2006) 1747–1758.
[7] S.J. Gould, G.A. Keller, N. Hosken, J. Wilkinson, S. Subramani, A conserved tripeptide sorts proteins to peroxisomes, J. Cell Biol. 108 (1989) 1657–1664.
[8] C. Ma, S. Reumann, Improved prediction of peroxisomal PTS1 proteins from genome sequences based on experimental subcellular targeting analyses as exemplified for protein kinases from Arabidopsis, J. Exp. Bot. 59 (2008) 3767–3779.
[9] B.W. Swinkels, S.J. Gould, A.G. Bodnar, R.A. Rachubinski, S. Subramani, A novel, cleavable peroxisomal targeting signal at the amino-terminus of the rat 3-ketoacyl-CoA thiolase, EMBO J. 10 (1991) 3255–3262.
[10] M.S. Lee, R.T. Mullen, R.N. Trelease, Oilseed isocitrate lyases lacking their essential type 1 peroxisomal targeting signal are piggybacked to glyoxysomes, Plant Cell 9 (1997) 185–197.
[11] T. Meyer, C. Holscher, C. Schwoppe, A. von Schaewen, Alternative targeting of *Arabidopsis* plastidic glucose-6-phosphate dehydrogenase G6PD1 involves cysteine-dependent interaction with G6PD4 in the cytosol, Plant J. 66 (2011) 745–758.
[12] M. Schrader, N.A. Bonekamp, M. Islinger, Fission and proliferation of peroxisomes, Biochim. Biophys. Acta 1822 (2011) 1343–1357.
[13] T. Orth, et al., The PEROXIN11 protein family controls peroxisome proliferation in Arabidopsis, Plant cell 19 (2007) 333–350.
[14] M. Yan, N. Rayapuram, S. Subramani, The control of peroxisome number and size during division and proliferation, Curr. Opin. Cell Biol. 17 (2005) 376–383.
[15] M. Islinger, S. Grille, H.D. Fahimi, M. Schrader, The peroxisome: an update on mysteries, Histochem. Cell Biol. 137 (2012) 547–574.
[16] J.A. Napier, I.A. Graham, Tailoring plant lipid composition: designer oilseeds come of age, Curr. Opin. Plant Biol. 13 (2010) 330–337.
[17] N. Ruiz-Lopez, O. Sayanova, J.A. Napier, R.P. Haslam, Metabolic engineering of the omega-3 long chain polyunsaturated fatty acid biosynthetic pathway into transgenic plants, J. Exp. Bot. 63 (2012) 2397–2410.
[18] J.A. Napier, The production of unusual fatty acids in transgenic plants, Annu. Rev. Plant Biol. 58 (2007) 295–319.
[19] J. Jaworski, E.B. Cahoon, Industrial oils from transgenic plants, Curr. Opin. Plant Biol. 6 (2003) 178–184.
[20] V. Eccleston, J. Ohlrogge, Expression of lauroyl-acyl carrier protein thioesterase in *Brassica napus* seeds induces pathways for both fatty acid oxidation and biosynthesis and implies a set point for triacylglycerol accumulation, Plant Cell 10 (1998) 613–622.
[21] L. Moire, E. Rezzonico, S. Goepfert, Y. Poirier, Impact of unusual fatty acid synthesis on futile cycling through beta-oxidation and on gene expression in transgenic plants, Plant Physiol. 134 (2004) 432–442.
[22] S.P. Slocombe, et al., Oil accumulation in leaves directed by modification of fatty acid breakdown and lipid synthesis pathways, Plant Biotechnol. J. 7 (2009) 694–703.
[23] B. Halliwell, Reactive species and antioxidants. Redox biology is a fundamental theme of aerobic life, Plant Physiol. 141 (2006) 312–322.
[24] R. Mittler, Oxidative stress, antioxidants and stress tolerance, Trends Plant Sci. 7 (2002) 405–410.
[25] W. Wang, B. Vinocur, A. Altman, Plant responses to drought, salinity and extreme temperatures: towards genetic engineering for stress tolerance, Planta 218 (2003) 1–14.
[26] N. Kaur, J. Hu, Dynamics of peroxisome abundance: a tale of division and proliferation, Curr. Opin. Plant Biol. 78 (2009) 781–788.
[27] M. Desai, J. Hu, Light induces peroxisome proliferation in Arabidopsis seedlings through the photoreceptor phytochrome A, the transcription factor HY5 HOMOLOG, and the peroxisomal protein PEROXIN11b, Plant Physiol. 146 (2008) 1117–1127.
[28] M.C. Castillo, L.M. Sandalio, L.A. del Rio, J. Leon, Peroxisome proliferation, wound-activated responses and expression of peroxisome-associated genes are cross-regulated but uncoupled in *Arabidopsis thaliana*, Plant Cell Environ. 31 (2008) 492–505.
[29] E. Lopez-Huertas, W.L. Charlton, B. Johnson, I.A. Graham, A. Baker, Stress induces peroxisome biogenesis genes, EMBO J. 19 (2000) 6770–6777.
[30] D.J. Morre, et al., Peroxisome proliferation in Norway spruce induced by ozone, Protoplasma 155 (1990) 58–65.
[31] J.M. Palma, M. Garrido, M.I. Rodriguez-Garcia, L.A. del Rio, Peroxisome proliferation and oxidative stress mediated by activated oxygen species in plant peroxisomes, Arch Biochem. Biophys. 287 (1991) 68–74.
[32] G.M. Pastori, L.A. del Rio, An activated-oxygen-mediated role for peroxisomes in the mechanism of senescence of *Pisum sativum* leaves, Planta 193 (1994) 385–391.
[33] M.C. Romero-Puertas, et al., Cadmium toxicity and oxidative metabolism of pea leaf peroxisomes, Free Radic. Res. 31 (Suppl) (1999) S25–S31.
[34] A.G. Nila, et al., Expression of a peroxisome proliferator-activated receptor gene (xPPARalpha) from *Xenopus laevis* in tobacco (*Nicotiana tabacum*) plants, Planta 224 (2006) 569–581.
[35] I. Isemann, S. Green, Activation of a member of the steroid hormone receptor superfamily by peroxisome proliferators, Nature 347 (1990) 645–650.
[36] J.H. Valenzuela-Soto, et al., Transformed tobacco (*Nicotiana tabacum*) plants over-expressing a peroxisome proliferator-activated receptor gene from *Xenopus laevis* (xPPARα) show increased susceptibility to infection by virulent *Pseudomonas syringae* pathogens, Planta 233 (2011) 507–521.
[37] S. Mitsuya, et al., Salt stress causes peroxisome proliferation, but inducing peroxisome proliferation does not improve NaCl tolerance in *Arabidopsis thaliana*, PLoS One 5 (2010) e9408.
[38] L.A. del Rio, et al., Reactive oxygen species, antioxidant systems and nitric oxide in peroxisomes, J. Exp. Bot. 53 (2002) 1255–1272.
[39] V. Mittova, M. Guy, M. Tal, M. Volokita, Salinity up-regulates the antioxidative system in root mitochondria and peroxisomes of the wild salt-tolerant tomato species *Lycopersicon pennellii*, J. Exp. Bot. 55 (2004) 1105–1113.
[40] V. Mittova, M. Tal, M. Volokita, M. Guy, Up-regulation of the leaf mitochondrial and peroxisomal antioxidative systems in response to salt-induced oxidative stress in the wild salt-tolerant tomato species *Lycopersicon pennellii*, Plant Cell Environ. 26 (2003) 845–856.
[41] A. Mhamdi, G. Noctor, A. Baker, Plant catalases: peroxisomal redox guardians, Arch. Biochem. Biophys. 61 (2012) 4197–4220.
[42] E.A. Mohamed, et al., Overexpression of bacterial catalase in tomato leaf chloroplasts enhances photo-oxidative stress tolerance, Plant Cell Environ. 26 (2003) 2037–2046.
[43] T. Moriwaki, et al., Overexpression of the *Escherichia coli* catalase gene, katE, enhances tolerance to salinity stress in the transgenic indica rice cultivar, BR5, Plant Biotechnol. Rep. 2 (2008) 41–46.
[44] T. Shikanai, et al., Inhibition of ascorbate peroxidase under oxidative stress in tobacco having bacterial catalase in chloroplasts, FEBS Lett. 428 (1998) 47–51.
[45] Y.-J. Li, R.-L. Hai, X.-H. Du, X.-N. Jiang, H. Lu, Over-expression of a Populus peroxisomal ascorbate peroxidase (PpAPX) gene in tobacco plants enhances stress tolerance, Plant Breeding 128 (2009) 404–410.
[46] J. Wang, H. Zhang, R.D. Allen, Overexpression of an Arabidopsis peroxisomal ascorbate peroxidase gene in tobacco increases protection against oxidative stress, Plant Cell Physiol. 40 (1999) 725–732.
[47] J.C. Waller, P.K. Dhanoa, U. Schumann, R.T. Mullen, W.A. Snedden, Subcellular and tissue localization of NAD kinases from Arabidopsis: compartmentalization of *de novo* NADP biosynthesis, Planta 231 (2010) 305–317.
[48] A.R. Kataya, S. Reumann, Arabidopsis glutathione reductase 1 is dually targeted to peroxisomes and the cytosol, Plant Signal. Behav. 5 (2010).
[49] Z. Chen, T.E. Young, J. Ling, S.C. Chang, D.R. Gallie, Increasing vitamin C content of plants through enhanced ascorbate recycling, Proc. Natl. Acad. Sci. USA 100 (2003) 3525–3530.
[50] C.H. Foyer, et al., Overexpression of glutathione-reductase but not glutathione synthase leads to increases in antioxidant capacity and resistance to photoinhibition in poplar trees, Plant Physiol. 109 (1995) 1047–1057.
[51] I.F. Acosta, E.E. Farmer, Jasmonates, The *Arabidopsis* Book, vol. 8, 2010, pp. e0129.
[52] C. Wasternack, E. Kombrink, Jasmonates: structural requirements for lipid-derived signals active in plant stress responses and development, ACS Chem. Biol. 5 (2010) 63–77.
[53] X. Peng, et al., Constitutive expression of rice WRKY30 gene increases the endogenous jasmonic acid accumulation, PR gene expression and resistance to fungal pathogens in rice, Planta 236 (2012) 1485–1498.
[54] B. Hause, G. Hause, C. Kutter, O. Miersch, C. Wasternack, Enzymes of jasmonate biosynthesis occur in tomato sieve elements, Plant Cell Physiol. 44 (2003) 643–648.
[55] V. Lipka, et al., Pre- and postinvasion defenses both contribute to nonhost resistance in Arabidopsis, Science 310 (2005) 1180–1183.
[56] P. Bednarek, et al., A glucosinolate metabolism pathway in living plant cells mediates broad-spectrum antifungal defense, Science 323 (2009) 101–106.
[57] G. Graser, N.J. Oldham, P.D. Brown, U. Temp, J. Gershenzon, The biosynthesis of benzoic acid glucosinolate esters in *Arabidopsis thaliana*, Phytochemistry 57 (2001) 23–32.
[58] V. Baskar, M.A. Gururani, J.W. Yu, S.W. Park, Engineering glucosinolates in plants: current knowledge and potential uses, Appl. Biochem. Biotechnol. 168 (2012) 1694–1717.

[59] S. Lee, et al., Benzoylation and sinapoylation of glucosinolate R-groups in Arabidopsis, Plant J. 72 (2012) 411–422.
[60] A.V. Qualley, J.R. Widhalm, F. Adebesin, C.M. Kish, N. Dudareva, Completion of the core β-oxidative pathway of benzoic acid biosynthesis in plants, Proc. Natl. Acad. Sci. U.S.A. 109 (2012) 16383–16388.
[61] F. Geu-Flores, C.E. Olsen, B.A. Halkier, Towards engineering glucosinolates into non-cruciferous plants, Planta 229 (2009) 261–270.
[62] M.E. Møldrup, et al., Engineering of benzylglucosinolate in tobacco provides proof-of-concept for dead-end trap crops genetically modified to attract *Plutella xylostella* (diamondback moth), Plant Biotechnol. J. 10 (2012) 435–442.
[63] N. Nesi, R. Delourme, M. Brégeon, C. Falentin, M. Renard, Genetic molecular approaches to improve nutritional value of *Brassica napus* L. seed, C. R. Biol. 331 (2008) 763–771.
[64] W. Wang, B. Vinocur, O. Shoseyov, A. Altman, Role of plant heat-shock proteins and molecular chaperones in the abiotic stress response, Trends Plant Sci. 9 (2004) 244–252.
[65] J.C. Young, J.M. Barral, F. Ulrich Hartl, More than folding: localized functions of cytosolic chaperones, Trends Biochem. Sci. 28 (2003) 541–547.
[66] C. Ma, M. Haslbeck, L. Babujee, O. Jahn, S. Reumann, Identification and characterization of a stress-inducible and a constitutive small heat-shock protein targeted to the matrix of plant peroxisomes, Plant physiol. 141 (2006) 47–60.
[67] H. Chauhan, N. Khurana, A. Nijhavan, J.P. Khurana, P. Khurana, The wheat chloroplastic small heat shock protein (sHSP26) is involved in seed maturation and germination and imparts tolerance to heat stress, Plant Cell Environ. 35 (2012) 1912–1931.
[68] Y. Sato, S. Yokoya, Enhanced tolerance to drought stress in transgenic rice plants overexpressing a small heat-shock protein, sHSP17.7, Plant Cell Rep. 27 (2008) 329–334.
[69] J. Zou, C. Liu, A. Liu, D. Zou, X. Chen, Overexpression of OsHsp17.0 and OsHsp23.7 enhances drought and salt tolerance in rice, J. Plant Physiol. 169 (2012) 628–635.
[70] L.C. Strader, A.H. Culler, J.D. Cohen, B. Bartel, Conversion of endogenous indole-3-butyric acid to indole-3-acetic acid drives cell expansion in Arabidopsis seedlings, Plant Physiol. 153 (2010) 1577–1586.
[71] B.K. Zolman, N. Martinez, A. Millius, A.R. Adham, B. Bartel, Identification and characterization of Arabidopsis indole-3-butyric acid response mutants defective in novel peroxisomal enzymes, Genetics 180 (2008) 237–251.
[72] L.C. Strader, B. Bartel, The Arabidopsis PLEIOTROPIC DRUG RESISTANCE8/ABCG36 ATP binding cassette transporter modulates sensitivity to the auxin precursor indole-3-butyric acid, Plant Cell 21 (2009) 1992–2007.
[73] A.P. Wasson, et al., Traits and selection strategies to improve root systems and water uptake in water-limited wheat crops, J. Exp. Bot. 63 (2012) 3485–3498.
[74] K. Sudesh, H. Abe, Y. Doi, Synthesis, structure and properties of polyhydroxyalkanoates: biological polyesters, Prog. Polym. Sci. 25 (2000) 1503–1555.
[75] Y. Poirier, D.E. Dennis, K. Klomparens, C. Somerville, Polyhydroxybutyrate, a biodegradable thermoplastic, produced in transgenic plants, Science 256 (1992) 520–523.
[76] A. Steinbüchel, et al., Considerations on the structure and biochemistry of bacterial polyhydroxyalkanoic acid inclusions, Can. J. Microbiol. 41 (1995) 94–105.
[77] Q. Ren, N. Sierro, M. Kellerhals, B. Kessler, B. Witholt, Properties of engineered poly-3-hydroxyalkanoates produced in recombinant *Escherichia coli* strains, Appl. Environ. Microbiol. 66 (2000) 1311–1320.
[78] Y. Poirier, Polyhydroxyalknoate synthesis in plants as a tool for biotechnology and basic studies of lipid metabolism, Prog. Lipid Res. 41 (2002) 131–155.
[79] A. Steinbüchel, S. Hein, in: W. Babel, A. Steinbüchel (Eds.), Biopolyesters, vol. 71, Springer, Berlin, Heidelberg, 2001, pp. 81–123.
[80] Y. Poirier, N. Erard, J. MacDonald-Comber Petetot, Synthesis of polyhydroxyalkanoate in the peroxisome of *Pichia pastoris*, FEMS Microbiol. Lett. 207 (2002) 97–102.
[81] K. Kocharin, Y. Chen, V. Siewers, J. Nielsen, Engineering of acetyl-CoA metabolism for the improved production of polyhydroxybutyrate in *Saccharomyces cerevisiae*, AMB Express 2 (2012) 52.
[82] Y. Poirier, Polyhydroxyalkanoate synthesis in plants as a tool for biotechnology and basic studies of lipid metabolism, Prog. Lipid Res. 41 (2002) 131–155.
[83] K. Tilbrook, L. Gebbie, P.M. Schenk, Y. Poirier, S.M. Brumbley, Peroxisomal polyhydroxyalkanoate biosynthesis is a promising strategy for bioplastic production in high biomass crops, Plant Biotechnol. J. 9 (2011) 958–969.
[84] H. Nakashita, et al., Production of biodegradable polyester by a transgenic tobacco, Biosci. Biotechnol. Biochem. 63 (1999) 870–874.
[85] K. Bohmert, et al., Transgenic *Arabidopsis* plants can accumulate polyhydroxybutyrate to up to 4% of their fresh weight, Planta 211 (2000) 841–845.
[86] L.A. Petrasovits, et al., Enhanced polyhydroxybutyrate production in transgenic sugarcane, Plant Biotechnol. J. 10 (2012) 569–578.
[87] Y. Poirier, C. Nawrath, C. Somerville, Production of polyhydroxyalkanoates, a family of biodegradable plastics and elastomers, in bacteria and plants, Biotechnology 13 (1995) 142–150.
[88] Y. Arai, et al., Synthesis of a novel class of polyhydroxyalkanoates in Arabidopsis peroxisomes, and their use in monitoring short-chain-length intermediates of beta-oxidation, Plant Cell Physiol. 43 (2002) 555–562.
[89] J.J. Hahn, A.C. Eschenlauer, U.B. Sleytr, D.A. Somers, F. Srienc, Peroxisomes as sites for synthesis of polyhydroxyalkanoates in transgenic plants, Biotechnol. Prog. 15 (1999) 1053–1057.
[90] V. Mittendorf, et al., Polyhydroxyalkanoate synthesis in transgenic plants as a new tool to study carbon flow through beta-oxidation, Plant J. 20 (1999) 45–55.
[91] V. Mittendorf, et al., Synthesis of medium-chain-length polyhydroxyalkanoates in *Arabidopsis thaliana* using intermediates of peroxisomal fatty acid beta-oxidation, Proc. Natl. Acad. Sci. USA 95 (1998) 13397–13402.
[92] S. Reumann, A.P. Weber, Plant peroxisomes respire in the light: some gaps of the photorespiratory C2 cycle have become filled – others remain, Biochim. Biophys. Acta 1763 (2006) 1496–1510.
[93] V.G. Maurino, C. Peterhansel, Photorespiration: current status and approaches for metabolic engineering, Curr. Opin. Plant Biol. 2010 (2010) 23.
[94] C. Peterhansel, C. Blume, S. Offermann, Photorespiratory bypasses: how can they work? J. Exp. Bot. 64 (2013) 709–715.
[95] A. Maier, et al., Transgenic introduction of a glycolate oxidative cycle into *A. thaliana* chloroplasts leads to growth improvement, Front. Plant Sci. 3 (2012) 38.
[96] R. Kebeish, et al., Chloroplastic photorespiratory bypass increases photosynthesis and biomass production in *Arabidopsis thaliana*, Nat. Biotechnol. 25 (2007) 593–599.
[97] J.d.F.C. Carvalho, et al., An engineered pathway for glyoxylate metabolism in tobacco plants aimed to avoid the release of ammonia in photorespiration, BMC Biotechnol. 11 (2011) 111.
[98] O. Voinnet, S. Rivas, P. Mestre, D. Baulcombe, An enhanced transient expression system in plants based on suppression of gene silencing by the p19 protein of tomato bushy stunt virus, Plant J. 33 (2003) 949–956.
[99] B. Van Aken, Transgenic plants for phytoremediation: helping nature to clean up environmental pollution, Trends Biotechnol. 26 (2008) 225–227.
[100] G.L. Mena-Benitez, et al., Engineering a catabolic pathway in plants for the degradation of 1,2-dichloroethane, Plant Physiol. 147 (2008) 1192–1198.
[101] H.A. Menser, H. He, Ozone and sulfur dioxide synergism—injury to tobacco plants, Science 153 (1966) 424–425.
[102] M. Noji, et al., Cysteine synthase overexpression in tobacco confers tolerance to sulfur-containing environmental pollutants, Plant Physiol. 126 (2001) 973–980.
[103] T. van der Kooij, L.J. DeKok, S. Haneklaus, E. Schnug, Uptake and metabolism of sulphur dioxide by *Arabidopsis thaliana*, New Phytol. 135 (1997) 101–107.
[104] S. Veljovic-Jovanovic, L. Milovanovic, T. Oniki, U. Takahama, Inhibition of catalase by sulfite and oxidation of sulfite by H_2O_2 cooperating with ascorbic acid, Free Radic. Res. 31 (Suppl) (1999) S51–S57.
[105] G. Brychkova, et al., Sulfite oxidase protects plants against sulfur dioxide toxicity, Plant J. 50 (2007) 696–709.
[106] Z. Xia, et al., Overexpression of a maize sulfite oxidase gene in tobacco enhances tolerance to sulfite stress via sulfite oxidation and CAT-mediated H_2O_2 scavenging, PLoS ONE 7 (2012) e37383.
[107] D. Igarashi, et al., Identification of photorespiratory glutamate:glyoxylate aminotransferase (GGAT) gene in Arabidopsis, Plant J. 33 (2003) 975–987.
[108] B.K. Zolman, A. Yoder, B. Bartel, Genetic analysis of indole-3-butyric acid responses in *Arabidopsis thaliana* reveals four mutant classes, Genetics 156 (2000) 1323–1337.
[109] T.B. Dansen, K.W. Wirtz, R.J. Wanders, E.H. Pap, Peroxisomes in human fibroblasts have a basic pH, Nat. Cell Biol. 2 (2000) 51–53.
[110] A. Jankowski, et al., In situ measurements of the pH of mammalian peroxisomes using the fluorescent protein pHluorin, J. Biol. Chem. 276 (2001) 48748–48753.
[111] F.M. Lasorsa, et al., The yeast peroxisomal adenine nucleotide transporter: characterization of two transport modes and involvement in deltapH formation across peroxisomal membranes, Biochem J. 381 (2004) 581–585.
[112] C.W. van Roermund, et al., The peroxisomal lumen in *Saccharomyces cerevisiae* is alkaline, J Cell Sci. 117 (2004) 4231–4237.
[113] T. Lanyon-Hogg, S.L. Warriner, A. Baker, Getting a camel through the eye of a needle: the import of folded proteins by peroxisomes, Biol. Cell 102 (2010) 245–263.
[114] Y. Arai, M. Hayashi, M. Nishimura, Proteomic identification and characterization of a novel peroxisomal adenine nucleotide transporter supplying ATP for fatty acid beta-oxidation in soybean and Arabidopsis, Plant Cell 20 (2008) 3227–3240.
[115] K. Bernhardt, S. Wilkinson, A.P.M. Weber, N. Linka, A peroxisomal carrier delivers NAD(+) and contributes to optimal fatty acid degradation during storage oil mobilization, Plant J. 69 (2012) 1–13.
[116] N. Linka, et al., Peroxisomal ATP import is essential for seedling development in *Arabidopsis thaliana*, Plant Cell 20 (2008) 3241–3257.
[117] S. Reumann, Toward a definition of the complete proteome of plant peroxisomes: Where experimental proteomics must be complemented by bioinformatics, Proteomics 11 (2011) 1764–1779.
[118] N. Linka, C. Esser, Transport proteins regulate the flux of metabolites and cofactors across the membrane of plant peroxisomes, Front. Plant Sci. 3 (2012) 3.
[119] S. Footitt, et al., Control of germination and lipid mobilization by COMATOSE, the Arabidopsis homologue of human ALDP, EMBO J. 21 (2002) 2912–2922.

[120] M. Hayashi, et al., Ped3p is a peroxisomal ATP-binding cassette transporter that might supply substrates for fatty acid beta-oxidation, Plant Cell Physiol. 43 (2002) 1–11.
[121] R. Radakovits, R.E. Jinkerson, A. Darzins, M.C. Posewitz, Genetic engineering of algae for enhanced biofuel production, Eukaryot. Cell 9 (2010) 486–501.
[122] C.M. Sagt, et al., Peroxicretion: a novel secretion pathway in the eukaryotic cell, BMC Biotechnol. 9 (2009) 48.
[123] P. Tanner, V. Balasubramanian, C.G. Palivan, Aiding nature's organelles: artificial peroxisomes play their role, Nano Lett. (2013), http://dx.doi.org/10.1021/nl401215n.

Contribution of the authors to manuscript 4

S.K.-V., **M.G.S.**, **T.J.W.** and **J.W.** wrote the manuscript as co-authors. **S.K.-V.** managed the revision and final decisions and correspondence on the manuscript in agreement with **N.L.**. **A.P.M.W.** assisted in drafting this manuscript. **F.H.** assisted with figure layouts.

Manuscript 5

Agrobacterium-mediated *Arabidopsis thaliana* transformation: an overview of T-DNA binary vectors, floral dip and screening for homozygous lines

Sarah K. Kessel-Vigelius[1*], Kristin Bernhardt[1*], Jan Wiese[1*], Nicole Linka[1], and Andreas P. M. Weber[1a]

[1]Institute of Plant Biochemistry, Heinrich-Heine University Düsseldorf, 40225 Düsseldorf Germany

*First author

[a]Corresponding author

Journal of Endocytobiosis and Cell Research (2012) 19-28 | International Society of Endocytobiology
zs.thulb.uni-jena.de/content/main/journals/ecb/info.xml

Journal of Endocytobiosis and Cell Research

Technical note

Agrobacterium-mediated *Arabidopsis thaliana* transformation: an overview of T-DNA binary vectors, floral dip and screening for homozygous lines

Kristin Bernhardt[1], Sarah K. Vigelius[1], Jan Wiese[1], Nicole Linka, and Andreas P.M. Weber[2, *]

[1,2] Institute of Plant Biochemistry, Heinrich-Heine University Düsseldorf, 40225 Düsseldorf, Germany; [1] First authors; these authors contributed equally to this manuscript. [2] Correspondence to: andreas.weber@uni-duesseldorf.de

For more than two decades Agrobacterium-mediated stable genetic transformation of plant cells is a routine laboratory method to generate transgenic plants. The natural capability of *Agrobacterium tumefaciens* to infect plants is thereby exploited for transferring foreign genes into plant cells. During stable transformation engineered DNA fragments are integrated into the plant genome and can be passed on to the next generations. The host specificity of Agrobacteria to plant species is limited and the genetic mechanisms underlying host specificity are complex. Besides *Arabidopsis thaliana*, *Agrobacterium tumefaciens* is also capable of successfully transforming a large variety of other plant species, such as maize or rice.

Using Agrobacteria to transform Arabidopsis is straightforward, requiring only standard laboratory equipment. Transformation by floral dip is easy and can be performed by non-specialists. Due to its small size, short generation time, high seed production and easy handling, Arabidopsis, which has emerged as model organism for plant biology research, is frequently chosen to generate transgenic plants.

This review focuses on the generation of transgenic Arabidopsis plants by Agrobacteria using the floral dip method. Besides a simplified protocol for the Agrobacterium-mediated transformation, we here describe common Agrobacterium strains and suitable binary T-DNA vectors. Further, we focus on plant selection to finally isolate homozygous transgenic mutant lines.

Journal of Endocytobiosis and Cell Research (2012) 19-28
Category: technical notes
Keywords: Transgenic plant, transformation technology, Agrobacteria, Arabidopsis, floral dip method, binary vectors

Received: 20 February 2012; Accepted: 09 March 2012

Introduction

An important step in plant science was taken when Marc van Montagu and Jeff Schell discovered the genetic transfer mechanism between Agrobacteria and plants (Van Larebeke et al. 1974). Later, this finding enabled researchers to perform controlled expression of transgenes in plants. In early experiments tissue cultures were transformed, though regenerating plant tissue is difficult and laborious (Lloyd et al. 1986; Valvekens et al. 1988). In 1987, Marks and Feldman established a technique, which did not require tissue culture. Instead, transgenic plants were generated by co-cultivation of Arabidopsis seeds with Agrobacteria (Feldman and Marks 1987). However, the reproducibility of this method proved difficult and generation of transgenic lines took several years. Plant transformation was improved when Pelletier and colleagues succeeded in transforming Arabidopsis plants by vacuum infiltration (Bechtold et al. 1993). In the late 1990s protocols were further simplified. Transgenic plants were gained by dipping inflorescences into Agrobacteria solution (Clough and Bent 1998). Although other transformation methods, like particle bombardment, protoplast bombardment or direct gene transfer into protoplasts (Negrutiu et al. 1987) are available, Agrobacterium-mediated plant transformation remains the most frequently used method (Vain 2007).

Genetically altered plants are important experimental tools to both basic and applied molecular research, allowing the investigation of functions of a gene-of interest (GOI) *in planta* by either silencing or mis-expression. Loss-of-function can be accomplished by creating hairpin RNA molecules, which evoke the formation of small interfering RNAs (siRNAs). These molecules were shown to down-regulate gene functions (Smith et al. 2000; Small 2007). Today, artificial micro RNAs (amiRNAs) are more commonly used to silence genes. This is because amiRNAs, generated from endogenous precursors, do more specifically hit target genes than siRNAs (Schwab et al. 2005; Alvarez et al. 2006; Schwab et al. 2006). Ectopic over-expression of genes is achieved by placing the GOI downstream of a strong heterologous promoter, like the cauliflower mosaic virus 35S promoter (p35S) or the ubiquitin10 promoter (pUB10). To determine its subcellular localisation or to purify the GOI, it can be translationally fused to a fluorescent protein or purification tag, either controlled by its endogenous or a heterologous promoter (Karimi et al. 2007). The activity of a promoter can be analyzed by cloning its sequence upstream of a reporter gene, such as β-glucuronidase (GUS) (Jefferson et al. 1987). Further applications of transgenic plants in basic research are for example mapping of genes (Clough et al. 2000) or genetic screening for desired phenotypes (Bent 2000). In applied agronomical and horticultural research, plant genetic engineer-

ing is used to generate useful plant phenotypes, which are unachievable by conventional plant breeding (Vain 2007). In the following chapters we describe different Agrobacteria strains, which can be used for transformation, we show binary vectors that can be used for different purposes (Table 1) and we provide a simplified floral dip protocol (Box). Furthermore we delineate the selection of transgenic plants to gain homozygous mutants for phenotypic analyses. In Figure 2 we sum up all steps from the preparation to the homozygous mutant plants.

The Method

Agrobacteria strains

Agrobacteria are soil-dwelling plant pathogens that integrate bacterial transfer DNA (T-DNA) into the plant genome (Chilton et al. 1977). The T-DNA is transferred to plant cells, transported to the nucleus and expressed when inserted in the host's nuclear genome. The T-DNA encodes for enzymes that either induce tumor formation or produce opines. These nitrogen-rich molecules serve as energy source for the Agrobacteria, but cannot be metabolized by the plant (McCullen and Binns 2006).

The tumor-inducing plasmid (Ti-plasmid) encodes for the T-DNA and virulence effector (vir) proteins, which are important for targeting the plant cell and integrating into the genome. For plant transformation disarmed Ti-plasmids are used, which enable transfer function, but do not induce tumor formation due to the removal of oncogenes and opine synthases from the wild-type T-DNA (Bevan et al. 1983; Fraley et al. 1983; Herrera-Estrella et al. 1983).

The commonly used Agrobacteria strains are C58 with the disarmed Ti-plasmid pTiC58 (Wood et al. 2001) and the C58-derivatives GV3101::pMP90 and GV3101::pMP90RK (Koncz and Schell 1986). These strains confer resistance to rifampicin due to pTiC58. The strain GV3101::pMP90 carries an additional resistance to gentamycin.

T-DNA Binary Vector Systems

The finding that the T-DNA region and the vir genes of a Ti-plasmid can reside on different replicons led to the development of binary vector system (Hoekema et al. 1983; de Framond et al. 1983). These plasmids facilitated genetic engineering for many laboratories, because the recombination of foreign DNA with the Ti-plasmid is not required anymore and the cloning procedure became less difficult. In addition, binary vectors yield more DNA than the initial large T-DNA vectors, due to an increased copy number in *Escherichia coli* (Lee and Gelvin 2008).

The T-DNA binary vector system is composed of two vectors, a T-DNA binary vector and a second disarmed Ti-plasmid called vir helper plasmid. The binary vector harbors the GOI within the T-DNA region. In this region, which is delimited by left (LB) and right border (RB), the transfer of T-DNA into the plant genome is induced. The T-DNA vector also contains a marker for selection and maintenance in both *E. coli* and Agrobacteria, and a selectable marker for plants. The vir helper plasmid, such as pTiC58, pMK90 or pMK90RK, is harbored in the Agrobacterium strain. It only carries the virulence effector proteins and a selection marker.

Over the past years binary vectors have become more sophisticated and suitable for genetic engineering. Table 1 summarizes many commonly used conventional or Gateway® compatible vector series.

The first T-DNA binary vectors were still large in size, thus plasmid size was progressively reduced and this led to minimal vectors, such as the pPZP or pGREEN plasmids. These plasmids have a more reduced *ori* than for example vectors of the pBIN series (Bevan 1984; Frisch et al. 1995). The integration of T-DNA into the plant genome is polar from RB to LB (Sheng and Citovsky 1996). Early binary T-DNA vectors, such as the pBIN19 (Bevan 1984; Frisch et al. 1995) harbor the resistance cassette close to the RB resulting in false positive transformants only containing the resistance marker, but not the GOI. The resistance cassette in pPZP, pGTPV and pGREEN series is located close to the LB (Table 1). This improvement reduces the number of false positives, because the insertion of the GOI precedes the selection marker (extensively reviewed in Hellens et al. 2000a).

In this review we focus on vector series, which often provide different promoter versions, selectable markers or fusion tags on the same vector backbone, so that it is possible to use vectors of the same series for multiple purposes (Table 1).

Principle of floral dip method

The transformation of Arabidopsis is an essential tool to study GOI function. This review describes Agrobacterium-mediated transformation of Arabidopsis using the floral dip method (Box). It can be performed within a short time without using special equipment and with high yield of transformants in every laboratory. Most Arabidopsis ecotypes, such as Col-0, Ws-0, Nd-0 and No-0 can be transformed with this method, whereas Ler-0 appears to be less efficient (Clough and Bent 1998). Optimal transformation efficiency is yielded when healthy plants are used having around 10 cm high bolts and flowers containing several unopened floral buds. With plants in the ideal status a transformation efficiency of 2-3% can be achieved (Martinez-Trujillo 2004).

To perform the floral dip method, Arabidopsis plants are grown on soil simultaneously to cloning and Agrobacteria transformation procedure. If the cloning procedure takes longer then expected, first bolts could be cut to keep plants in the right developmental stage. Secondary bolts will proliferate. Before dipping, an Agrobacteria over night culture is resuspended in 5% (w/v) sucrose solution to remove corresponding selective agents and other potentially harmful growth media components. The surfactant Silwet L-77 is added to the solution favoring plant transformation by reducing surface tension and promoting agrobacterial adhesion to the plant tissue. Silwet L-77 can be substituted by less-expensive surfactants, such as Tween-20, which is as efficient as Silwet L-77 (Das and Joshi 2011). Transformation of female gametes is achieved by dipping Arabidopsis plants into Agrobacteria solution (Desfeux et al. 2000; Bechthold et al. 2003). Dipped plants are covered with a plastic dome or a layer of saran wrap for one day and placed to low light conditions (50 µmol m^{-2} s^{-1}

Table 1: Overview of restriction-enzyme and Gateway® compatible binary T-DNA vector series

Vector	Application category	BSM	PSM	Ref
Vector series for restriction-enzyme cloning				
pGPTV series	Constitutive transgene expression; promoter studies (GUS)	Kan	HygB, Kan, Gluf, Ble, Mtx	1
pGreen/pGreenII series	Constitutive transgene expression; promoter studies (GUS, GFP, LUC,)	Kan	HygB, Kan, Gluf, Sul	2
pCAMBIA series	Constitutive transgene expression; promoter studies (GUS and GFP),	Kan, Clm	HygB, Kan, Gluf	3
pPZP series	Constitutive transgene expression	Spec, Clm	Kan, Gent	4
pORE series	Constitutive transgene expression; promoter studies and reporter gene assays (GUS, GFP)	Kan	Kan, Gluf	5
Gateway compatible vector series				
pMDC series	Constitutive/inducible expression; promoter studies (GUS and GFP), promoterless variants; various tags (6x His)	Kan, Spec*	HygB, Kan, Bar	6
pGWB series	Inducible expression; promoter studies (GUS, GFP, EYFP, ECFP, RFP), promoterless variants; various tags (6x His, 4x/10x Myc, FLAG, 3x HA, T7, TAP)	Kan, Spec*	Kan, HygB, Gluf	7, 8
GATEWAY destination vectors	Constitutive transgene expression; promoter studies (GUS, GFP); gene silencing (hairpin RNAi)	Spec*	HygB, Kan, Gluf	9
pHELLSGATE	Gene silencing (hairpin RNAi)	Spec	Kan	10, 11
pAGRIKOLA	Gene silencing (hairpin RNAi)	Kan	Kan, Gluf	12

* Gateway vector presented carries a chloramphenicol resistance, which can be used to maintain the Gateway cassette;
References (Ref) are: 1: (Becker 1990; Becker et al. 1992) 2: (Hellens et al. 2000b), 3: www.cambia.org, 4: (Hajdukiewicz et al. 1994), 5: (Coutu et al. 2007), 6: (Curtis and Grossniklaus 2003), 7: (Nakagawa et al. 2007), 8: (Nakamura et al. 2010), 9: (Karimi et al. 2002), 10: (Wesley et al. 2001), 11: (Helliwell and Waterhouse 2003), 12: (Hilson et al. 2004);
Abbreviations: BSM: Bacterial selection marker, PSM: Plant selection marker, Ble: Bleomycin, Clm: Chloramphenicol, Gent: Gentamycin, Gluf: Glufosinate ammonium (Basta), HygB: Hygromycin B, Kan: Kanamycin, Mtx: Methotrexate, Spec: Spectinomycin, Sul: Sulfonamides, CFP: Cyan fluorescent protein, EYFP: Enhanced yellow fluorescent protein, GFP: Green Fluorescent Protein, GUS: β-glucuronidase, LUC: Luciferase, RFP: Red fluorescent protein, TAP: Tandem affinity purification; Useful weblinks: http://www.pgreen.ac.uk/; http://www.cambia.org; http://www.psb.ugent.be/gateway/; antibiotics are dissolved in water, except HygB, which is dissolved in HEPES, ampicillin (dissolved in 50% ethanol) and chloramphenicol (dissolved in 100% ethanol).

light intensity), and moderate temperature (20°C). This retains humidity and favors both Agrobacteria and Arabidopsis growth to enhance transformation efficiency. After ripening, T_0 seeds are harvested for selection (Figure 1).

Screening for transgenic Arabidopsis plants

T_0 seeds are surface sterilized by chlorine gas or ethanol for selection (Clough and Bent 1998; Chang and Pikaard 2005). Several thousands of seeds are sufficient to identify positive transformants. Sterilized seeds are spread on half-strength MS medium (Murashige and Skoog 1962) including the according selective agent (Table 1 and 2). Depending on the selective agent, non-transformed plants are impaired in growth. In most cases sensitive seedlings are pale and arrested in development at the cotyledon stage. Milder selective agents retard growth. Surviving seedlings can be distinguished in early seedling establishment. There they show longer roots and true leaves emerge. Wild-type seedlings should always be included as negative control to monitor the appearance of non-transformed lines on the particular batch of selection media. At least 15 candidate seedlings are transferred to soil. Alternatively, the selection procedure can be accomplished without sterile culture as described in Davis et al. (2009).

The successful integration of the transgene into plant genomic DNA is verified by PCR analysis. Genomic DNA is isolated from a rosette leaf. A fast method for isolation of genomic DNA is presented in Berendzen et al. (2005). The preparation according to Edwards et al. (1991) is advisable for long-term storage of DNA. The choice of appropriate oligonucleotides for PCR amplification depends on the GOI. Vector specific primers binding to promoter and terminator are conceivable, but also a combination of T-DNA border specific and transgene specific primers. Genomic DNA from wild-type plants should be used as negative control, while vector DNA is the corresponding positive control.

Table 2: Genetic markers and selective agents for plant transformation

Gene, Enzyme, Source	PSM	Conc	Ref
aac3, Aminoglycoside-N-Acetyltransferase, *Serratia marcescens*	Gent	50 µg/mL	1
aadA, Amino-glycoside-3″-adenyltransferase, *Shigella sp.*	Spec	100 µg/mL	2
bar, Phosphinotricin acetyl transferase, *Streptomyces hygroskopicus*	Gluf	7.5 µg/mL	3
dhfr, Dihydrofolate reductase, *M. musculus*	Mtx	100 µg/mL	4
hph, Hygromycin phosphotransferase, *E. coli*	HygB	30 µg/mL	5
nptII, Neomycin Phosphotransferase II, *E. coli* Tn5	Kan	50 µg/mL	6, 7
sulI, Dihydropteroate synthase, *E. coli* pR46	Sul	7.5 µg/mL	8

References (Ref) are: 1: (Hayford et al. 1988) 2: (Svab and Maliga 1993), 3: (De Block et al. 1989), 4: (Kemper et al. 1992), 5: (Waldron et al. 1985) 6: (Bevan et al. 1983), 7: (Fraley et al. 1983), 8: (Guerineau et al. 1990). Selectable marker genes are extensively reviewed in: (Sundar and Sakthivel 2008).
Abbreviations: Conc: Concentration of selective agent in the medium; PSM: Plant selection marker; Gent: Gentamycin, Gluf: Glufosinate ammonium (Basta), HygB: Hygromycin B, Kan: Kanamycin, Mtx: Methotrexate, Spec: Spectinomycin, Sul: Sulfonamides; antibiotics are dissolved in water, except HygB, which is dissolved in HEPES, ampicillin (dissolved in 50% ethanol) and chloramphenicol (dissolved in 100% ethanol).

Besides PCR screening using gDNA, protein or mRNA expression can be directly analyzed by immunoblot or RT-PCR, respectively. In case of an RNA interference (RNAi) approach, the down-regulation of the target transcript should be verified by qRT-PCR (Udvardi et al. 2008).

The progeny of confirmed T_0 plants is further analyzed (Figure 1). Seeds are again spread on half-strength MS medium with selective agent, and T_1 plants are verified via PCR. A T_1 plant with a single T-DNA insertion is considered homozygous when all descendants survive the marker screen. In the case of a heterozygous T_1, plant, the offspring will segregate 1:2:1. Consequently a quarter of the seedlings will show compromised growth during the screen (Figure 1). In the case of multiple insertions it is possible that all descendants of the T_1 generation survive the marker screen even though the T-DNA insertion is not homozygous for the GOI. Physiological experiments can be started with T_2 seeds, produced from homozygous T_1 seedlings.

Agrobacterium-mediated plant transformation may give rise to phenotypes independent of the GOI, such as embryo-lethality if the T-DNA disrupts essential genes (homozygous seeds will not germinate). T-DNA insertion is minimally biased (Alonso and Stepanova 2003), thus assumed to occur largely random (Ostergaard and Yanofsky, 2004). Analysis of more than several independent transgenic lines (multiple alleles) is required to preclude off-target effects.

Multiple T-DNA insertions can be detected by Southern blotting. The genomic DNA is restricted with a single endonuclease featuring a single restriction site in the T-DNA and using a T-DNA specific probe next to this site for hybridization. Multiple T-DNA insertions are expected to result in several bands (Southern 1975; Logemann et al. 2006). Multiple insertions can also be identified by T-DNA mapping (Liu et al. 1995) which additionally gives information about the place of insertion. The biochemical and physiological characterization of transgenic plants can begin as soon as the genetic analysis (Meinke et al. 1998) has been successfully finished.

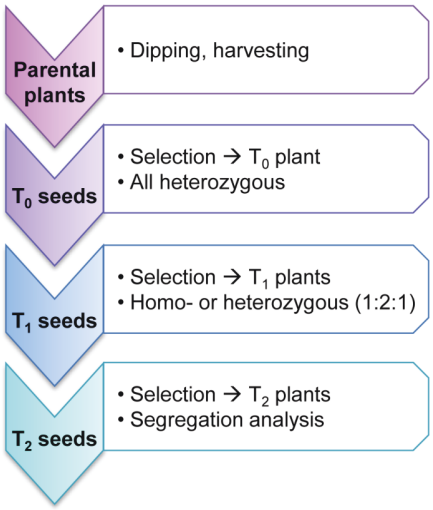

Figure 1: Selection of transgenic plants
This figure displays the selection process from dipped plants to homozygous seeds, which can be used in physiological experiments.

Final remarks

The transformation of Arabidopsis is a multi-step process. The procedure from preparation to selection of homozygous lines is time-consuming, thus proper planning is necessary. Figure 2 sums up the key steps for Arabidopsis transformation. The successful transformation starts with the choice of an appropriate vector system (Gateway® or conventional), promoter and fusion tag. Attention has to be paid to the selective markers depending on the number of transgenes, which will be transformed into one plant line. The selection cassette might be present in a parental mu-

tant line. If it is intended to cross transgenic individuals, care should be taken to employ different selection markers.

Following the described scheme, transgenic Arabidopsis lines ready to be analyzed can be generated in six to eight months.

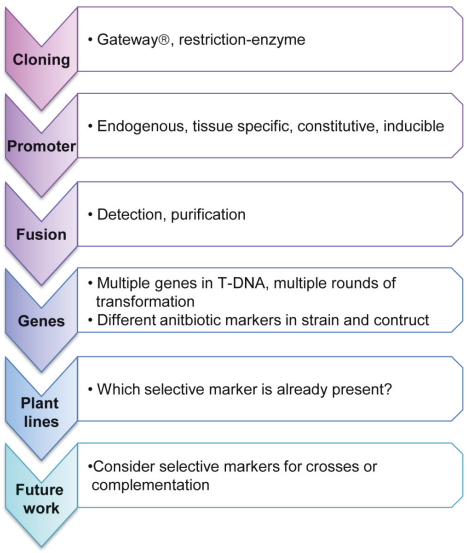

Figure 2: Key steps of Agrobacterium-mediated plant transformation procedure
In this scheme the main steps from cloning to future experiments with homozygous plants are explained.

References

Alonso JM, Stepanova AN (2003) T-DNA mutagenesis in Arabidopsis. *Methods Mol Biol.* 236:177-188.

Alvarez JP, Pekker I, Goldshmidt A, Blum E, Amsellem Z, Eshed Y. (2006) Endogenous and synthetic microRNAs stimulate simultaneous, efficient, and localized regulation of multiple targets in diverse species. *Plant Cell*. 18:1134-1151.

Bechtold N, Ellis J, Pelletier G. (1993) In planta Agrobacterium mediated gene transfer by infiltration of adult *Arabidopsis thaliana* plants. *C R Acad Sci Paris Life Sciences*. 316:1194-1199.

Bechtold N, Jolivent S, Voisin R, Pelletier G. (2003) The endosperm and the embryo of *Arabidopsis thaliana* are independently transformed through infiltration by *Agrobacterium tumefaciens*. *Transgenic Res*. 12:509-517

Becker D. (1990) Binary vectors which allow the exchange of plant selectable markers and reporter genes. *Nucleic Acids Res*. 18:203.

Becker D, Kemper E, Schell J, Masterson R. (1992) New plant binary vectors with selectable markers located proximal to the left T-DNA border. *Plant Mol Biol.* 20:1195-1197.

Bent AF. (2000) Arabidopsis in planta transformation. Uses, mechanisms, and prospects for transformation of other species. *Plant Physiol*. 124:1540-1547.

Berendzen K, Searle I, Ravenscroft D, Koncz C, Batschauer A, Coupland G, Somssich IE, Ulker B. (2005) A rapid and versatile combined DNA/RNA extraction protocol and its application to the analysis of a novel DNA marker set polymorphic between *Arabidopsis thaliana* ecotypes Col-0 and Landsberg erecta. *Plant Methods*. 1:4.

Bevan M. (1984) Binary Agrobacterium vectors for plant transformation. *Nucleic Acids Res*. 12:8711-8721.

Bevan M, Barnes WM, Chilton MD. (1983) Structure and transcription of the nopaline synthase gene region of T-DNA. *Nucleic Acids Res*. 11:369-385.

Chang S, Pikaard CS. (2005) Transcript profiling in Arabidopsis reveals complex responses to global inhibition of DNA methylation and histone deacetylation. *J Biol Chem*. 280:796-804.

Chilton MD, Drummond MH, Merio DJ, Sciaky D, Montoya AL, Gordon MP, Nester EW. (1977) Stable incorporation of plasmid DNA into higher plant cells: the molecular basis of crown gall tumorigenesis. *Cell.* 11:263-271.

Clough SJ, Bent AF. (1998) Floral dip: a simplified method for Agrobacterium-mediated transformation of *Arabidopsis thaliana*. *Plant J*. 16:735-743.

Clough SJ, Fengler KA, Yu IC, Lippok B, Smith RK Jr, Bent AF. (2000) The Arabidopsis dnd1 "defense, no death" gene encodes a mutated cyclic nucleotide-gated ion channel. *Proc Natl Acad Sci USA.* 97:9323-9328.

Coutu C, Brandle J, Brown D, Brown K, Miki B, Simmonds J, Hegedus DD. (2007) pORE: a modular binary vector series suited for both monocot and dicot plant transformation. *Transgenic Res*. 16:771-781.

Curtis MD, Grossniklaus U. (2003) A gateway cloning vector set for high-throughput functional analysis of genes in planta. *Plant Physiol*. 133:462-469.

Das P, Joshi NC. (2011) Minor modifications in obtainable Arabidopsis floral dip method enhances transformation efficiency and production of homozygous transgenic lines harboring a single copy of transgene. *ABB*. 2:59-67.

Davis AM, Hall A, Millar AJ, Darrah C, Davis SJ. (2009) Protocol: Streamlined sub-protocols for floral-dip transformation and selection of transformants in *Arabidopsis thaliana*. *Plant Methods*. 5:3.

De Block M, De Brouwer D, Tenning P. (1989) Transformation of *Brassica napus* and *Brassica oleracea* using *Agrobacterium tumefaciens* and the expression of the bar and neo genes in the transgenic plants. *Plant Physiol*. 91:694-701.

de Framond AJ, Barton KA, Chilton M-D. (1983) Mini-Ti: A new vector strategy for plant genetic engineering. *Nat Biotech.* 1:262-269.

Desfeux C, Clough SJ, Bent AF. (2000) Female reproductive tissues are the primary target of Agrobacterium-mediated transformation by the Arabidopsis floral-dip method. *Plant Physiol*. 123:895-904.

Edwards K, Johnstone C, Thompson C. (1991) A simple and rapid method for the preparation of plant genomic DNA for PCR analysis. *Nucleic Acids Res*. 19:1349.

Feldman KA, Marks DM. (1987) Agrobacterium mediated transformation of germinating seeds of *Arabidopsis thaliana*: A non-tissue culture approach. *Mol Gen Genet*. 208:1-9.

Fraley RT, Rogers SG, Horsch RB, Sanders PR, Flick JS, Adams SP, Bittner ML, Brand LA, Fink CL, Fry JS, Galluppi GR, Goldberg SB, Hoffmann NL, Woo SC. (1983) Expression of bacterial genes in plant cells. *Proc Natl Acad Sci USA*. 80:4803-4807.

Frisch DA, Harris-Haller LW, Yokubaitis NT, Thomas TL, Hardin SH, Hall TC. (1995) Complete sequence of the binary vector Bin 19. *Plant Mol Biol.* 27:405-409.

Guerineau F, Brooks L, Meadows J, Lucy A, Robinson C, Mullineaux P. (1990) Sulfonamide resistance gene for plant transformation. *Plant Mol Biol*. 15:127-136.

Hajdukiewicz P, Svab Z, Maliga P. (1994) The small, versatile pPZP family of Agrobacterium binary vectors for plant transformation. *Plant Mol Biol*. 25:989-994.

Hayford MB, Medford JI, Hoffman NL, Rogers SG, Klee HJ. (1988) Development of a plant transformation selection system based on expression of genes encoding gentamicin acetyltransferases. *Plant Physiol*. 86:1216-1222.

Hellens R, Mullineaux P, Klee H. (2000a) Technical focus:a guide to Agrobacterium binary Ti vectors. *Trends Plant Sci*. 5:446-451.

Hellens RP, Edwards EA, Leyland NR, Bean S, Mullineaux PM. (2000b) pGreen: a versatile and flexible binary Ti vector for Agrobacterium-mediated plant transformation. *Plant Mol Biol*. 42:819-832.

Helliwell C, Waterhouse P. (2003) Constructs and methods for high-throughput gene silencing in plants. *Methods*. 30:289-295.

Herrera-Estrella L, Block MD, Messens E, Hernalsteens JP, Montagu MV, Schell J. (1983) Chimeric genes as dominant selectable markers in plant cells. *EMBO J.* 2:987-995.

Hilson P, Allemeersch J, Altmann T, Aubourg S, Avon A, Beynon J, Bhalerao RP, Bitton F, Caboche M, Cannoot B, Chardakov V, Cognet-Holliger C, Colot V, Crowe M, Darimont C, Durinck S, Eickhoff H, de Longevialle AF, Farmer EE, Grant M, Kuiper MT, Lehrach H, Leon C, Leyva A, Lundeberg J, Lurin C, Moreau Y, Nietfeld W, Paz-Ares J, Reymond P, Rouze P, Sandberg G, Segura MD, Serizet C, Tabrett A, Taconnat L, Thareau V, Van Hummelen P, Vercruysse S, Vuylsteke M, Weingartner M, Weisbeek PJ, Wirta V, Wittink FR, Zabeau M, Small I. (2004) Versatile gene-specific sequence tags for Arabidopsis functional genomics: transcript profiling and reverse genetics applications. *Genome Res*. 14:2176-2189.

Hoekema A, Hirsch PR, Hooykaas PJJ, Schilperoort RA. (1983) A binary plant vector strategy based on separation of vir- and T-region of the *Agrobacterium tumefaciens* Ti-plasmid. *Nature.* 303:179-180.

Hofgen R, Willmitzer L. (1988) Storage of competent cells for Agrobacterium transformation. *Nucleic Acids Res*. 16:9877.

Jefferson RA, Kavanagh TA, Bevan MW. (1987) GUS fusions: beta-glucuronidase as a sensitive and versatile gene fusion marker in higher plants. *EMBO J.* 6:3901-3907.

Karimi M, Inze D, Depicker A. (2002) GATEWAY vectors for Agrobacterium-mediated plant transformation. *Trends Plant Sci*. 7:193-195.

Karimi M, Depicker A, Hilson P. (2007) Recombinational cloning with plant gateway vectors. *Plant Physiol*. 145:1144-1154.

Kemper E, Grevelding C, Schell J, Masterson R. (1992) Improved method for the transformation of *Arabidopsis thaliana* with chimeric dihydrofolate reductase constructs which confer methotrexate resistance. *Plant Cell Rep*. 11:118-121.

Koncz C, Schell J. (1986) The promoter of the TL-DNA gene 5 controls the tissue-specific expression of chimeric genes carried by a novel type of Agrobacterium binary vector. *Mol Gen Genet*. 204:383–396.

Lee LY, Gelvin SB. (2008) T-DNA binary vectors and systems. *Plant Physiol.* 146:325-332.

Liu YG, Mitsukawa N, Oosumi T, Whittier RF. (1995) Efficient isolation and mapping of *Arabidopsis thaliana* T-DNA insert junctions by thermal asymmetric interlaced PCR. *Plant J.* 8:457-463.

Lloyd AM, Barnason AR, Rogers SG, Byrne MC, Fraley RT, Horsch RB. (1986) Transformation of *Arabidopsis thaliana* with *Agrobacterium tumefaciens*. *Science.* 234:464-466.

Logemann E, Birkenbihl RP, Ulker B, Somssich IE. (2006) An improved method for preparing Agrobacterium cells that simplifies the Arabidopsis transformation protocol. *Plant Methods*. 2:16.

Martinez-Trujillo ML-B, Cabrera-Ponce V, Luis J, Herrera-Estrella, L. (2004) Improving transformation efficiency of *Arabidopsis thaliana* by modifying the floral dip method. *Plant Mol Biol Rep*. 22:7.

McCullen CA, Binns AN. (2006) *Agrobacterium tumefaciens* and plant cell interactions and activities required for interkingdom macromolecular transfer. *Annu Rev Cell Dev Biol.* 22:101-127.

Meinke DW, Cherry JM, Dean C, Rounsley SD, Koornneef M. (1998) *Arabidopsis thaliana*: A model plant for genome analysis. *Science.* 282:662-682.

Mersereau M, Pazour GJ, Das A. (1990) Efficient transformation of *Agrobacterium tumefaciens* by electroporation. *Gene.* 90:149-151.

Murashige T, Skoog F. (1962) A revised medium for rapid growth and bio assays with tobacco tissue cultures. *Physiol Plant*. 15:14.

Nakagawa T, Kurose T, Hino T, Tanaka K, Kawamukai M, Niwa Y, Toyooka K, Matsuoka K, Jinbo T, Kimura T. (2007) Development of series of gateway binary vectors, pGWBs, for realizing efficient construction of fusion genes for plant transformation. *J Biosci Bioeng*. 104:34-41.

Nakamura S, Mano S, Tanaka Y, Ohnishi M, Nakamori C, Araki M, Niwa T, Nishimura M, Kaminaka H, Nakagawa T, Sato Y, Ishiguro S. (2010) Gateway binary vectors with the bialaphos resistance gene, bar, as a selection marker for plant transformation. *Biosci Biotechnol Biochem*. 74:1315-1319.

Negrutiu I, Shillito RD, Potryskus I, Biasini G, Sala F. (1987) Hybrid genes in the analysis of transformation conditions. I. Setting up a simple method for direct gene transfer in plant protoplasts. *Plant Mol Biol.* 8:363-373.

Ostergaard L, Yanofsky MF. (2004) Establishing gene function by mutagenesis in *Arabidopsis thaliana*. *Plant J.* 39:682-696.

Sambrook JR, Russel DW. (2001) Molecular Cloning: A Laboratory Manual (Third Edition), CSHL Press.

Schwab R, Ossowski S, Riester M, Warthmann N, Weigel D. (2006) Highly specific gene silencing by artificial microRNAs in Arabidopsis. *Plant Cell*. 18:1121-1133.

Schwab R, Palatnik JF, Riester M, Schommer C, Schmid M, Weigel D. (2005) Specific effects of microRNAs on the plant transcriptome. *Dev Cell*. 8:517-527.

Sheng J, Citovsky V. (1996) Agrobacterium-plant cell DNA transport: have virulence proteins, will travel. *Plant Cell*. 8:1699-1710.

Small I. (2007) RNAi for revealing and engineering plant gene functions. *Curr Opin Biotechnol*. 18:148-153.

Smith NA, Singh SP, Wang MB, Stoutjesdijk PA, Green AG, Waterhouse PM. (2000) Total silencing by intron-spliced hairpin RNAs. *Nature.* 407:319-320.

Southern EM. (1975) Detection of specific sequences among DNA fragments separated by gel electrophoresis. *J Mol Biol*. 98:503-517.

Sundar IK, Sakthivel N. (2008) Advances in selectable marker genes for plant transformation. *J Plant Physiol*. 165:1698-1716.

Svab Z, Maliga P. (1993) High-frequency plastid transformation in tobacco by selection for a chimeric aadA gene. *Proc Natl Acad Sci USA*. 90:913-917.

Udvardi MK, Czechowski T, Scheible WR. (2008) Eleven golden rules of quantitative RT-PCR. *Plant Cell*. 20:1736-1737.

Vain P. (2007) Thirty years of plant transformation technology development. *Plant Biotech J.* 5:221-229.

Valvekens D, Montagu MV, Van Lijsebettens M. (1988) *Agrobacterium tumefaciens* mediated transformation of *Arabidopsis thaliana* root explants by using kanamycin selection. *Proc Natl Acad Sci USA.* 85:5536-5540.

Van Larebeke N, Engler G, Holsters M, Van den Elsacker S, Zaenen I, Schilperoort RA, Schell J. (1974) Large plasmid in *Agrobacterium tumefaciens* essential for crown gall-inducing ability. *Nature.* 252:169-170.

Waldron C, Murphy EB, Roberts JL, Gustafson GD, Armour SL, Malcolm SK. (1985) Resistance to hygromycin B. *Plant Mol Biol*. 5:103-108.

Wesley SV, Helliwell CA, Smith NA, Wang MB, Rouse DT, Liu Q, Gooding PS, Singh SP, Abbott D, Stoutjesdijk PA, Robinson SP, Gleave AP, Green AG, Waterhouse PM. (2001) Construct design for efficient, effective and high-throughput gene silencing in plants. *Plant J*. 27:581-590.

Wood DW, Setubal JC, Kaul R, Monks DE, Kitajima JP, Okura VK, Zhou Y, Chen L, Wood GE, Almeida NF Jr, Woo L, Chen Y, Paulsen IT, Eisen JA, Karp PD, Bovee D Sr, Chapman P, Clendenning J, Deatherage G, Gillet W, Grant C, Kutyavin T, Levy R, Li MJ, McClelland E, Palmieri A, Raymond C, Rouse G, Saenphimmachak C, Wu Z, Romero P, Gordon D, Zhang S, Yoo H, Tao Y, Biddle P, Jung M, Krespan W, Perry M, Gordon-Kamm B, Liao L, Kim S, Hendrick C, Zhao ZY, Dolan M, Chumley F, Tingey SV, Tomb JF, Gordon MP, Olson MV, Nester EW. (2001) The genome of the natural genetic engineer *Agrobacterium tumefaciens* C58. *Science.* 294:2317-2323.

BOX - Plant transformation method

Step 1 Cloning
Clone the GOI in an appropriate binary vector (Table 1). Consider features like promoter, fusion tag and selection cassette (Table 1 and 2). Isolate 1 µg of plasmid DNA of the final construct for transformation into Agrobacteria (Sambrook 2001).

Step 2 Plant growth
Sow Arabidopsis seeds on well-watered soil and stratify at 4°C in the dark for two days. Germinate seeds and grow the seedlings under long day conditions (16 h light/8 h darkness, 100 µmol m^{-2} s^{-1} light intensity, 20°C/18°C) for three weeks. Transfer five plants to a fresh pot filled with watered soil. Grow the plants under long day conditions for three to four weeks until they begin to bolt. Prepare four pots with five plants per construct (Figure 3A).

Step 3 Competent Agrobacteria
Produce competent Agrobacteria by inoculating 200 mL LB medium with 2 mL of an agrobacterium over-night culture. Incubate main culture aerobically at 28°C for 6 h to grow the cells to OD_{600} 0.5-0.8. At this OD the transition to the log-phase begins. Centrifuge the culture at 4,500 g at 4°C for 10 min. Wash the pellet in 10 mL ice-cold TE-buffer. Resuspend the pellet in 20 mL LB medium. Aliquot 500 µL fractions in microcentrifuge tubes. Shock-freeze in liquid nitrogen and store at -80°C (Hofgen and Willmitzer 1988).

Step 4 Agrobacteria transformation using the freeze-thaw method
Transform the construct with the GOI into Agrobacteria.
Thaw one aliquot of competent cells per construct on ice. Add 1 µg plasmid DNA and keep the mixture on ice for 5 min. Freeze it in liquid nitrogen for 5 min. Heat-shock the mixture for 5 min at 37°C. Add 0.8 mL LB medium and incubate on a rocker at 28°C for 2-4 h. Centrifuge for 2 min at 3,000 g. Discard the supernatant, resuspend the pellet in 100 µL LB, and spread the Agrobacteria suspension on YEP-plates with appropriate antibiotics. Incubate the plates at 28°C for two days. Re-streak four single colonies on a new plate and incubate these plates at 28°C for one to two days (Hofgen and Willmitzer 1988). To verify the presence of the construct perform a colony PCR (Sambrook 2001). Consider that larger constructs (>20 kb) might require electro-transformation (Mersereau et al. 1990).

Step 5 Plant status optimal for transformation
Grow plants until bolts reach 10 cm height. The plants should have several unopened floral buds and a low number of siliques. When the plants get the first bolts, but the cloning is not yet finished, they can be removed. Cutting first bolts allows proliferation of secondary inflorescences from axillary buds.

Step 6 Agrobacteria culture for dipping
Inoculate a 5 mL liquid culture of Agrobacteria in LB medium supplied with antibiotics that select for both the *vir* helper plasmid and T-DNA binary vector two days prior to plant transformation. Incubate it aerobically at 28°C over night.
Inoculate 250 mL of YEP medium with 1 mL of the pre-culture and incubate under the same conditions for 16-24 h (OD_{600} = 1.5 – 2). Measure the OD_{600} of your Agrobacteria culture.
Sediment the cells at 5,500 g for 10 min at room temperature (note that the pellet is pink). Resuspend it in 5 % (w/v) sucrose solution to a final OD_{600} of 0.8. Add 0.02 % (v/v) Silwet L-77 or 0.07 % (v/v) Tween-20. Note that high concentrations of surfactant are toxic. For transformation of varying T-DNA binary vectors with different selection markers, mix equal volumes of the Agrobacteria strains resuspended in sucrose solution. Nest a tall 250 mL beaker in a 600 mL beaker to easily dip the plants overhead. This minimizes the contamination of Agrobacterium solution with soil. Transfer the Agrobacteria suspension to the 250 mL beaker.

Step 7 Preparation of plants
Remove already developed siliques from the plants to minimize the number of non-transformed seeds in your batch, which increases the ratio of transformed to untransformed seeds. This step might be time consuming.

Step 8 Dipping – Plant transformation

Prepare two stripes of aluminum foil to cover the rosette leaves and the soil, leaving a gap for the inflorescences (Figure 3B). This prevents loss of soil and contamination of leaves with Agrobacteria suspension. Dip the inflorescences into the Agrobacteria suspension by inverting the plants. Allow soaking for 1 min (Figure 3B). The same suspension can be used for ten or more pots and for different plants. To prevent damage of the flower buds, remove excess liquid by draining plants for a few seconds. Staking bolts facilitates harvesting of seeds.

Step 9 Plant handling after transformation

Place pots on their sides in a plastic tray lined with humid paper. Cover the trays with a dome or saran wrap maintaining humidity. Keep the plants in low light (50 µmol m^{-2} s^{-1} light) for one day (Figure 3C). Put the plants upright and return them to normal growth conditions the next day. Grow the transformed plants for further 3-4 weeks until the first siliques become brown. Stop watering and let the siliques ripen.

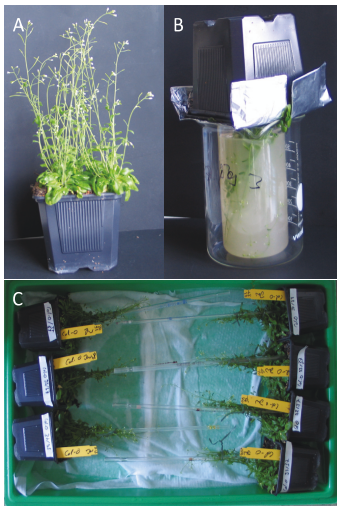

Figure 3: Floral dip procedure
(A) Arabidopsis plants with 10 cm high bolts. Flowers containing several unopened floral buds should be used for optimal transformation efficiencies. (B) Arabidopsis plants, prepared for transformation, are dipped in Agrobacteria solution. (C) After dipping the plants are placed horizontally in a tray with humid paper and covered with transparent foil to maintain humidity.

Step 10 Collection of seeds

Harvest dried seeds with a mesh sieve and pool the T_0 seeds of plants transformed with the same construct.

Step 11 Seed surface sterilization

Seeds can be surface sterilized either by chlorine gas (A), or ethanol (B).

A) **Chlorine gas method**

Fill one spatula tip of seeds (around 20 µL volume) in one microcentrifuge tube and place it opened into a desiccator jar under a fume hood. Sterilize four to six seed aliquots per seed pool. Store non-sterilized seeds of the original seed batch. Storage of sterilized seeds decreases germination efficiency.

Place a beaker containing 100 mL of sodium hypochlorite (13% of active chlorine) next to the seeds in the desiccator. Add 3 mL of concentrated hydrochloric acid to initiate chlorine gas formation. Immediately close the desiccator to prevent gas emission. Expose the seeds for 2 h, release the gas and close the tubes quickly to prevent contamination. Open the microcentrifuge tubes under a sterile laminar flow hood and let remaining chlorine gas evaporate for 30 min (Clough and Bent 1998).

B) **Ethanol liquid method**

Fill up to 50 µl seeds in a microcentrifuge tube (three aliquots per seed batch) and add 500 µL of 70% ethanol. Shake the seeds continuously for 5-10 min. Remove the liquid and let the seeds dry in the microcentrifuge tube under the laminar flow hood (~ 30 min-1 h). Sterile seeds can alternatively be poured on a sterile filter paper for drying (~ 15 min). Sterilization by this method does not allow longer-term seed storage (modified after Chang and Pikaard 2005).

Step 12 Selection of primary transformants

Spread the seeds of one seed pool on four to eight half-strength MS plates with the appropriate selection agents (Table 1 and 2). Stratify the seeds at 4°C in the dark for two days. Grow the seedlings for up to three weeks under long day conditions (16 h light/8 h darkness, 20°C). Transformed plants are easily distinguishable from non-transformed seedlings. They are greener, have longer roots, and produce true leaves. Non-resistant seeds germinate, but appear yellowish. In most cases growth is arrested at the cotyledon stage. Transfer resistant seedlings to new pots filled with watered soil. Grow plants under long day conditions and harvest T_1 seeds.

Step 13 gDNA isolation using sucrose buffer

To test if resistant plants carry the T-DNA, gDNA from leaves is isolated. Cut one leave disc with a microcentrifuge tube cap and store it on ice until extraction. Add 200 µL sucrose buffer and grind the tissue with a blue pipette tip at room temperature until the solution becomes greenish and the tissue appears macerated. Boil the sample at 100°C for 10 min. Centrifuge for 5 seconds. Place the samples on ice. Perform a 20 µL PCR reaction with 1 µL of the supernatant, containing the genomic DNA. Store the samples at 4°C over night or at -20°C for long-term storage (Berendzen et al. 2005)

Step 14 Segregation analysis

T_2 plants are verified by growth on selective medium and PCR. Segregation analysis will reveal whether the ancestor is a homo-, or heterozygous plant. The offspring of homozygous plants survives the marker screen to 100% and can be used for physiological experiments. Southern Blotting is only performed when no independent lines are available.

Equipment and reagents

Equipment
Pots, VQB 9 x 9 x 8 cm, TEKU, Germany
Aluminum foil, Carl Roth, Germany
Plastic tray and dome or plastic film
Sticks for plant staking
Mesh sieve, 450 µm, Retsch, Germany
Scissors
Jeweler's forceps (Dumont type 5)
Microcentrifuge tubes, 1.5 mL, Sarstedt, Germany
Pipette tips, Sarstedt, Germany
Erlenmeyer flasks for Agrobacteria cultivation, VWR, Germany
Tall 250 mL beaker and a 600 mL beaker for dipping
Desiccator jar
BioPhotometer, Eppendorf, Germany
Centrifuge J2-21, Rotor JA-10, Beckman, USA
Centrifuge 5424, Eppendorf, Germany
Veriti 96-Well Thermal Cycler, Applied Biosystems, USA
Thermomixer comfort, Eppendorf, Germany
Incubator shakers, Innova 44, New Brunswick scientific, USA
Growth chamber, Model AR-66C and CU-36C, Percival scientific, USA
Fume hood
Sterile laminar flow hood

Reagents
Buffers and solutions:
TE-buffer:
10 mM Tris-HCl, pH 7.5; 0.1 mM EDTA
Sucrose solution:
5% (w/v) sucrose in water
Sucrose buffer for gDNA isolation:
50 mM Tris-HCl, pH 7.5; 300 mM sodium chloride; 300 mM sucrose
Media:
Luria-Bertani medium (LB):
1% (w/v) Tryptone; 0.5% (w/v) Yeast extract; 1% (w/v) Sodium chloride; 1.5% (w/v) Agar for plates
YEP medium:
1% (w/v) yeast extract; 1% (w/v) peptone; 0.5% (w/v) sodium chloride; 1.5% (w/v) Agar for plates
Half-strength MS medium:
0.44% (w/v) MS salts, including vitamins; 0.05% (w/v) MES, pH 5.7 (KOH); 0.8% (w/v) phytoagar for plates
Soil:
2/3 Top soil; 1/3 Vermiculite

Other chemicals:
Liquid nitrogen
Silwet L-77 or Tween-20
Sodium hypochlorite (13% of active chlorine)
Concentrated hydrochloric acid (HCl)
Sterile 70% ethanol and 100% ethanol
Selection agents

Contribution of the authors to manuscript 5

S.V., **K.B.** and **J.W.** wrote the manuscript as co-authors with equal contribution. **N.L.** and **A.P.M.W.** assisted in drafting and submitting this manuscript.

IX. ACKNOWLEDGEMENTS

Ich möchte von Herzen danken:

Dr. Nicole Linka für die wundervolle Betreuung während meiner Diplom- und Doktorarbeit. Du hast mich wirklich immer unterstützt, mir sehr viel Selbstvertrauen gegeben und an mich geglaubt. Du hast nie versucht mich zu ändern, sondern hast mir Freiheit gegeben meine Themen und Experimente zu entwickeln, aber hast mich dabei optimal gefördert. Danke besonders für deine Unterstützung als ich in die USA gegangen bin. Du hast mir den Start dort sehr einfach gemacht und mich während der ganzen Zeit via Skype betreut. Du bist eine wirklich tolle Chefin und ich werde dich in Zukunft vermissen!

Prof. Dr. Andreas Weber für die Bereitschaft mich für die Diplom- und Doktorarbeit in seinem Institut aufzunehmen. Ich bin ihnen sehr dankbar für das umfangreiche Wissen, dass ich in den letzten Jahren erlernen durfte. Ich danke ihnen, dass sie es mir ermöglicht haben an die Michigan State University zu gehen. Der Aufenthalt dort hat mich enorm weitergebracht. Sie haben mich stets unterstützt und meine Projekte mit guten Ideen weitergebracht.

Prof. Dr. Michael Feldbrügge für die Unterstützung als Zweitgutachter dieser Arbeit. Danke, dass du mir besonders in unseren Committee Meetings neue Denkanstöße gegeben hast und durch deine Sichtweise dazu beigetragen hast, meine Projekte voranzubringen und diese auch aus einer „Nicht-Pflanzen-Perspektive“ zu betrachten.

Prof. Dr. Jianping Hu and the Hu lab for the wonderful time I had at Michigan State. You gave me the opportunity to work in your lab and learn some peroxisome cell biology. Thanks to my lab mates Gaëlle, Navneet, Kyaw, Ronghui and Jiying for supporting me and letting me be a full Hu lab member.

Prof. Dr. Barb Sears for enormous support during my stay at Michigan State. Thanks for your support, your trust in me, and thanks for giving me “George”. You made my life there so much easier. Go Green, Go White!

Dr. Sigrun Wegener-Feldbrügge für die tolle Unterstützung als Koordinatorin des iGRAD-Plant. Du hast uns durch deine tolle Organisation des Programms das Doktorandenleben sehr erleichtert.

Dr. Ilka Haferkamp für die Unterstützung meiner Arbeit. Du hast mir durch deine Kreativität, dein umfangreiches Wissen über die MCF Familie und das Korrekturlesen meiner Manuskripte sehr geholfen.

Prof. Dr. Martin Lercher und Prof. Dr. Rüdiger Simon für die Unterstützung während meiner Labrotations.

Dr. Anna Kersting und Dr. Christian Eßer für eine tolle Zeit in der Bioinformatik. Ihr habt mir den Einstieg in die Informatik sehr erleichtert und habt mir stets, auch über meine Labrotation hinaus, mit meinen Projekten geholfen. `print "Hello, World!"`

Dr. Kristin Bernhardt, **Dr. Christian Rosar**, **Dr. Frederique Breuers** für eure äußerste Hilfsbereitschaft, Unterstützung und Freundschaft. Ihr allesamt habt mich als meine ehemaligen Laborkollegen fast die ganzen Jahre über begleitet. Ich vermisse euch.

Der **Peroxisomengruppe** für eure Hilfsbereitschaft und Kollegialität. Ich danke euch für spannende Diskussionen und tolle Dinnerabende. Ihr wart tolle Kollegen und seid super Freunde.

Canan Külahoglu, Dr. Thea Pick, Manuel Sommer, Dominik Brilhaus, Nadine Hocken, Ali Denton, Simon Schliesky, Jan Wiese, Martin Schroers, Thomas Wrobel und **Sam Kurz** für die tolle Zeit und lustige Mittagspausen. Ihr wart super Kollegen. Ich werde euch vermissen.

Dem **Weberlab** für die Unterstützung und eine super Zeit mit euch. Ihr seid ein tolles Team!

Alisandra Denton, **Jan Wiese** und **Peter Lundquist** für das Korrekturlesen meiner Manuskripte.

Allen, die an meinen Manuskripten beteiligt waren. Danke jenen, die ich an dieser Stelle vergessen habe oder namentlich nicht einzeln erwähnen konnte.

Meinem Mann **Dennis Keßel** für seine Liebe und stetes Verständnis.

Meinen Eltern und **meiner Familie** für die Unterstützung im Studium und der Dissertation.

Der **Deutschen Forschungsgemeinschaft** und dem **iGRAD-Plant** für das Stipendium.